NOVEL AND SUSTAINABLE METHODS TO DEVELOP GREENER POLYMERS

MARIANA D’ALMEIDA GAMEIRO, BSc, MSc

Thesis submitted to the University of Nottingham
for the degree of Doctor of Philosophy

September 2018

EPSRC
Engineering and Physical Sciences
Research Council

University of Nottingham
UK | CHINA | MALAYSIA

DECLARATION

All work presented in this Thesis is the original work of the author, with the exception of results referenced to other sources. It has not been submitted as part of any other degree or professional qualification.

Date:……………………………. Signed: …………………………….

Mariana D'Almeida Gameiro

ACKNOWLEDGMENTS

First of all, I would like to express my sincere gratitude to my supervisor Professor Steve Howdle for the opportunity to undertake my PhD in his laboratory, for the continuous guidance, support, motivation, immense knowledge, patience and for being my “African father” along the way. I could not have imagined having a better supervisor for my PhD. Listening to his sentence “*keep smiling*”, was certainly one of my boosts to carry on. For all the travels, conferences, “percebes”, meetings, chats and for inspiring me, thank you Steve! I would also like to thank my co-supervisor Dr. Derek Irvine, for sharing his knowledge along the way.

My sincere thanks also go to Professor Peter Licence and Professor Chris Moody, who provided me the opportunity to start this PhD as part of the Centre of Doctoral Training (CDT) in Sustainable Chemistry in Nottingham. I must thank them for their trust, guidance and advice along the way and for the opportunities they offered me along these 4 years. Thank you so much!

I must also thank Professor Yonas Chebude, not just for this amazing collaboration, but also for his friendship, support, patience, and for believing and giving me the opportunity to visit Addis Ababa. በጣም አመሰግናለሁ!

I must also express my gratitude to Professor Martyn Poliakoff for his support and encouragement. Words cannot express how grateful I am to Professor Martyn Poliakoff for his support on the difficult times during my PhD.

I want to say thank you to Ray Marriot from Suprex for sharing his expertise and for the opportunity to use Suprex facilities in Bangor. I should also thank everyone from Croda, especially Amy Goddard, Adeline Coulson (and her team) and Grant Mitchell for the opportunity to undertake a placement at Cowick.

I must say a big thank you to Peri Williams, Helen Carson and Mandy Broniewski for their support, patience, for the organisation of travels, for the endless emails I sent to them and for the smile that was always waiting for me when I came in to their offices. Thank you so much!

I want to thank everyone in the workshop for their technical support throughout these years. Also, I need to thank Mick Cooper and Ben Gleadhill for their amazing help, patience and support with MALDI technique. Thank you all!

I also need to thank Dominika Regentova for the guidance and support to start my "organic chemistry life" and Tom Ward for his help in synthesising my monomers.

A big thanks to everyone in B10 for their help, patience, scientific and non-scientific discussions and for the amazing atmosphere we had in the lab! A special thanks to (in alphabetical order… please don't be mad at Polly!): Alice Haddleton, Andrea Hufendiek, Katie Pepper, Liv Monaghan, Sam Irving, Silvio Curia, Simon Basset and Tom Bennett. Without their advice and support in the lab and during the writing process, it would have not been the same! Thank you so much!

Finally, I want to thank all my family and friends who have been a strong support for me during these past 4 years. To my mum, dad, sister and Quiqui for all their support, friendship, and for always encouraging and believing in me. Their love, memorable journeys and amazing lunch/dinners have kept me smiling and motivated until the end. Thank you to Ana and Joaquim, for all their love and support throughout these years! Also, I would like to thank my grandparents for all their support, specially to my grandfather Joaquim who has been my inspiration and to whom this Thesis is dedicated.

Last, but definitely not least, I must thank Duarte for all his support, love, patience, friendship and prudence. His passion and inspiration kept me motivated to always try to be the best and helped me to be the person I am today. Without him, all this adventure in the UK would have not been possible.

Thank you all *Obrigada a todos*

ABSTRACT

This Thesis reports the development of green approaches towards the synthesis of novel polyesters. Generally, polyesters are synthesised using harsh conditions (such as high temperatures) and rely upon petrochemical-derived building blocks. By using biomass, more specifically plant oil derived sources, such as glycerol and vernolic acid (fatty acid, FA), we will explore a more renewable approach. In addition, $scCO_2$ will be explored as a novel solvent and processing aid and also, immobilised enzymes will be used as biocatalysts.

Chapter 1 has introduced the essential background of green chemistry and the importance of using biomass in the production of polymers. In addition, it also presents the fundamentals of polymer synthesis, with an emphasis on polyesters (linear and branched). A general introduction of enzymes and their use in polymer chemistry is given. Since the main aim of this thesis is to synthesise greener polyesters, the impact of using alternative solvents, such as $scCO_2$, is well described, not only in polymerisations but also in the extraction of valuable compounds from biomass.

Chapter 2 provides a detailed description of the high-pressure equipment, the standard operating procedures, analytical techniques and methods used to synthesis and characterise throughout this thesis.

Chapter 3 explores the use of glycerol, which is a by-product from biodiesel production, to synthesise linear polyesters through polycondensation with bio-based succinic acid. Bulk polycondensations (120 – 140 ºC), with no catalyst and using stannous octanoate ($Sn(Oct)_2$), as a non-selective metal catalyst produced branched poly(glycerol succinate) (PGLSA). By combining $scCO_2$ and enzyme catalysis (*Candida antarctica* lipase B, CaLB), it was possible to decrease the temperature of this process to as low as 40 ºC, and produced linear PGLSA.

Chapter 4 investigates the synthesis of water soluble glycerol-based surfactants. Using the methodology developed in Chapter 3, PGLSA was used

as a main block for the synthesis of potential surfactants. Therefore, with specific molar ratios, PGLSA was functionalised with lauric acid or methoxy poly(ethylene glycol) (with a molecular weight of 350 Da), using $scCO_2$ and CaLB. The evaluation of the performance as surfactants was assessed and it was demonstrated that linear PGLSA-based polymers are interesting candidates as surface-active agents. A comparison with commercial available surfactants is made.

Chapter 5 exploits oil obtained from nature to develop greener polyesters. Ironweed is a prolifically growing natural plant in East Africa and is one of the few plants containing naturally occurring epoxy oils in its seeds – 40% of vernonia oil (VO) by weight of the seed. In this work, VO was extracted using $scCO_2$, which offers several advantages, such as its environmental compatibility, its selectivity towards the lipid part of the seeds and allows the oil extraction at low temperatures (60 ºC). One of the main components of VO is vernolic acid, which accounts for 80 wt.% of the oil. The epoxy groups and double bonds from the triglyceride of VA offer great opportunities for modification. Therefore, VA was isolated from the oil and converted into new monomers for polyesters. Four different potential monomers were synthesised, a hydroxy and dihydroxy acids (13-hydroxyoctadeca-9,11-dienoic acid (HA) and 12,13-dihydroxyoctadec-9-enoic acid (DHA), respectively) a diacid (dodec-2-enedioic acid) and diol (dodec-2-ene-1,12-diol, (DED)).

Chapter 6 investigates the synthesis of the vernolic acid-based polyesters from the monomers synthesised in Chapter 5, through polycondensation. The condensation of AB_2 and A_2 + B_2 monomers is normally performed under harsh conditions (> 200 ºC). In this work, polycondensation reactions of HA (AB monomer), DHA (AB_2 monomer) and DED (A_2 monomer) with azelaic acid (AB_2 commercially available monomer) were performed in bulk (at 100 – 140 ºC) and under supercritical conditions. Using $scCO_2$ allowed the decrease of the reaction temperature (35 – 95 ºC) which is desirable from a sustainable perspective.

Chapter 7 sums up the overall conclusions achieved from this work and summaries possible opportunities for future research in this field.

In summary, the methodologies described in this Thesis, using biomass derived building blocks, such as glycerol and vernolic acid, and combining the use of $scCO_2$ and CaLB (when possible), allowed the syntheses of greener polyesters. These approaches are an important step towards the development of the next generation of biorenewable and biodegradable polymers.

ABBREVIATIONS

1,3-PDO	1,3-Propanediol
1,4-BD	1,4-Butanediol
AA	Adipic acid
AcC	Acetyl cellulose
AZ	Azelaic acid
BGA	German Federal Health Department (from Bundesgesundheitsamt)
$Bi(OTf)_3$	Bismuth (III) trifluoromethanesulfonate
Bu_2SnO	Dibutyltin(IV) oxide
CaLB	Candida antarctica lipase B
CMC	Critical micelle concentration
CO2	Carbon dioxide
Đ	Dispersity
Da	Daltons
DBN	1,5-Diazabicyclo- [5.4.0]undec-5-ene
DBTO	Dibutyltin(IV) oxide
DBU	1,8-Diazabicycloundec-7-ene
DCTB	Trans-2-[3-(4-tert-Butylphenyl)-2-methyl-2-propenylidene]malononitrile
DED	Dodec-2-ene-1,12-diol
DHA	12,13-Dihydroxyoctadec-9-enoic acid
DLS	Dynamic light scattering
DMA	Dynamic mechanical analysis
DMF	Dimethyl formamide
DMSO	Dimethyl sulfoxide
DP	Degree of polymerisation
DSC	Differential scanning calorimetry
EC	European Commission
EE	Extraction efficiency
EINECS	European Inventory of existing chemical substances
ELO	Epoxidised linseed oil
EO	Epoxidised oil
EPDM	Ethylene propylene diene monomer
ESI	Electrospray ionisation mass spectrometry
ESO	Epoxidised soybean oil

EU	European Union
ε-CL	ε-Caprolactone
FA	Fatty acid
FAME	Fatty acid methyl ester
FDA	Food and drug administration
FFA	Free fatty acid
FP	Framework programme
FTIR	Fourier-transform infrared spectroscopy
GC	Gas chromatography
GeO	Germanium oxide
GPC	Gel permeation chromatography
H_5IO_6	Metaperiodic acid
HA	13-Hydroxyoctadeca-9,11-dienoic acid
HIO_4	Periodic acid
LA	Lactic acid
LDA	Lithium diisopropylamide
$LiAlH_4$	Lithium aluminium hydride
m-PDA	*m*-Phenylenediamine
M-PEG	Poly(ethylene glycol) methyl ether
m/z	Mass-to-charge ratio
MALDI	Matrix assisted laser desorption/ionisation
MALLS	Multiangle laser light scattering
M_n	Number-average molecular weight
mN/m	Millinewtons per meter
M_n^{theo}	Theoretical molecular weight of compound
MS	Mass spectrometry
M_w	Weight-average molecular weight
$NaBH_4$	Sodium borohydride
NatraGem^{TM} E145	Polyglycerol succinate laurate
NMR	Nuclear magnetic resonance spectroscopy
Novozyme$^{®}$ 435	CaLB immobilised on cross-linked acrylic resin beads
NY11	Nylon 11
p-TsOH	*p*-Toluenesulfonic acid
PBAT	Poly(butylene adipate-co-terephthalate)
PBS	Poly(butylene succinate)

PBSA	Poly(butylene succinate adipate)
PBT	Poly(butylene terephthalate)
p_c	Critical pressure
PCL	Poly(e-caprolactone)
PE	Polyethylene
PEF	Poly(ethylene furanoate)
PEG	Poly(ethylene glycol), same as PEO
PEO	Poly(ethylene oxide), same as PEG
PES	Poly(ethylene succinate)
PET	Poly(ethylene terephthalate)
PGLSA	Poly(glycerol succinate)
PHA	Poly(hydroxyalkanoate)
PHB	Poly(hydroxybutyrate)
PLA	Polylactide / Poly(lactic acid)
PLGA	Poly(lactic-co-glycolic acid)
PP	Polypropylene
PS	Polystyrene
Psi	Pounds-per-square-inch
PTSA	p-Toluenesulfonic acid
PTT	Poly(trimethylene terephthalate)
PVC	Poly(vinyl chloride)
Q_{CO2}	CO2 flow rate
REACH	Registration, Evaluation and Restriction of Chemicals
RI	Refractive index
ROP	Ring-opening polymerisation
RT	Room temperature (~ 24 ºC)
SA	Succinic acid
$Sc(OTf)_3$	Scandium(III) triflate
$scCO_2$	Supercritical carbon dioxide
SCF	Supercritical fluid
SFE	Supercritical fluid extraction
SFT	Surface tension
$Sn(Oct)_2$	Stannous (or Tin) 2-ethylhexanoate
$SnCl_2$	Stannous (or Tin) chloride
TBD	1,5,7-Triazabicyclo[4.4.0]dec-5-ene
T_c	Critical temperature

TCA	Tricarboxylic acid cycle
T_g	Glass transition temperature
TG	Triglycerides
THF	Tetrahydrofuran
$Ti(OBu)_4$	Titanium (IV) butoxide
$Ti(O\textit{i}Pr_4)$	Titanium isopropoxide
T_m	Melting temperature
TMSI	Iodotrimethylsilane
ToF	Time of flight
TTIP	Titanium isopropoxide
Tween^{TM} 20	PEG20-sorbitan laurate
v/v	Percent volume to volume
VA	Vernolic acid
VO	Vernonia oil
wt.%	Weight percentage in relation to volume
δ	Chemical shift
θ	Contact angle or wetting angle
σ	Surface tension

CONTENTS

Valeu a pena?
Tudo vale a pena
Se a alma não é pequena.

Was it worthwhile?
Everything is worthwhile
if the soul is not small.

(Fernando Pessoa, in *Mensagem*)

To my grandparents,

Joaquim and Maria

CHAPTER 1. INTRODUCTION

1.1. Overview

The aim of this chapter is to deliver the essential background for the main themes of this Thesis:

a) Emphasis will be placed on green chemistry,
b) general aspects of polymer chemistry and an
c) introduction to supercritical carbon dioxide as a clean, inexpensive and green alternative to conventional solvents for oil extraction and polymer synthesis

Finally, the general aims of this work will also described.

1.2. The importance of green and sustainable chemistry

In the 1980's society became more concerned with regards to the generation of waste and the use of hazardous and toxic compounds in the fine chemical industries.[1] The world is currently facing several challenges regarding the exponential increase of the world population and the effect of society on the ecosystems (biodiversity, climate change, natural media, etc.).[2-3] For a sustainable world, several sciences must be involved, including chemistry, biology, engineering, physics and social sciences, to name a few.[4] Nevertheless, chemistry is the science which plays a more dominant role in this context, since it produces molecules, materials and compounds essential for society development (*e.g.* synthesis of new pharmaceutical compounds, formation of textiles, development of batteries, synthesis of polymers or creating substances essential for food).[5]

It was in the early 1990's that Sheldon [6] first introduced the concept of the *E* factor: the mass ratio of waste to the desired product. This invention was triggered by the mass formation of waste in the manufacture of chemicals in various industry segments (Table 1.1).

Table 1.1 – *E* factors in the manufacture of chemicals in different industry segments.[6]

Industry sector	Annual production (ton)	*E* factor ($kg_{waste}/kg_{product}$)
Oil refining	$10^6 – 10^8$	< 0.1
Bulk chemicals	$10^4 – 10^6$	<1-5
Fine chemicals	$10^2 – 10^4$	5 to > 50
Pharmaceuticals	$10 – 10^3$	25 to > 100

Another concept used to measure the conversion efficiency and selectivity in organic synthesis, atom economy, was proposed by Barry Trost.[7] Using this concept it is possible to assess the mass of waste produced in a particular synthesis route. The atom economy is calculated by dividing the molecular weight of the desired product by the sum of the molecular weights of all reactants, and it is expressed as a percentage.

These two concepts ('green metrics') contributed to the development of the *Twelve Principles of Green Chemistry*, in 1998, by Paul Anastas and John Warner.[8] The use of renewable resources as starting materials along with green procedures are two of the most important challenges for the production of a variety of materials. The proposed principles are:[8]

1. Prevention: It is better to prevent waste than to treat or clean up waste after it has been created.
2. Atom Economy: Synthetic methods should be designed to maximise the incorporation of all materials used in the process into the final product.
3. Less Hazardous Chemical Syntheses: Wherever practicable, synthetic methods should be designed to use and generate substances that possess little or no toxicity to human health and the environment.
4. Designing Safer Chemicals: Chemical products should be designed to affect their desired function while minimising their toxicity.
5. Safer Solvents and Auxiliaries: The use of auxiliary substances (*e.g.*, solvents, separation agents, etc.) should be made unnecessary wherever possible and innocuous when used.
6. Design for Energy Efficiency: Energy requirements of chemical processes should be recognised for their environmental and economic

impacts and should be minimised. If possible, synthetic methods should be conducted at ambient temperature and pressure.

7. Use of Renewable Feedstocks: A raw material or feedstock should be renewable rather than depleting whenever technically and economically practicable.
8. Reduce Derivatives: Unnecessary derivatization (use of blocking groups, protection/ deprotection, temporary modification of physical/chemical processes) should be minimised or avoided if possible, because such steps require additional reagents and can generate waste.
9. Catalysis: Catalytic reagents (as selective as possible) are superior to stoichiometric reagents.
10. Design for Degradation: Chemical products should be designed so that at the end of their function they break down into innocuous degradation products and do not persist in the environment.
11. Real-time analysis for Pollution Prevention: Analytical methodologies need to be further developed to allow for real-time, in-process monitoring and control prior to the formation of hazardous substances.
12. Inherently Safer Chemistry for Accident Prevention: Substances and the form of a substance used in a chemical process should be chosen to minimise the potential for chemical accidents, including releases, explosions, and fires.

Thus, in 2000, Roger Sheldon defined Green Chemistry as follows:[9]

> *"Green chemistry efficiently utilises (preferably renewable) raw materials, eliminates waste and avoids the use of toxic and/or hazardous reagents and solvents in the manufacture and application of chemical products."*

However, Green Chemistry does not consider either the economic or social perspective. A sustainable improvement involves the so-called three pillars of sustainability (or three Ps): people (social), planet (environment) and profit (economic elements) (Figure 1.1).[10-12] The concept of sustainable development was first introduced in 1987 as follows:[13]

> *"(…) development that meets the needs of the present generation without compromising the ability of future generations to meet their own needs."*

For a synthetic process to be both green and sustainable, it needs not only to take into consideration the *12 Principles of Green Chemistry*, it must also consider societal and economic concerns.[14] A balance between socio-economic, eco-efficiency and socio-ecological metrics corresponds to all the aspects of sustainability.

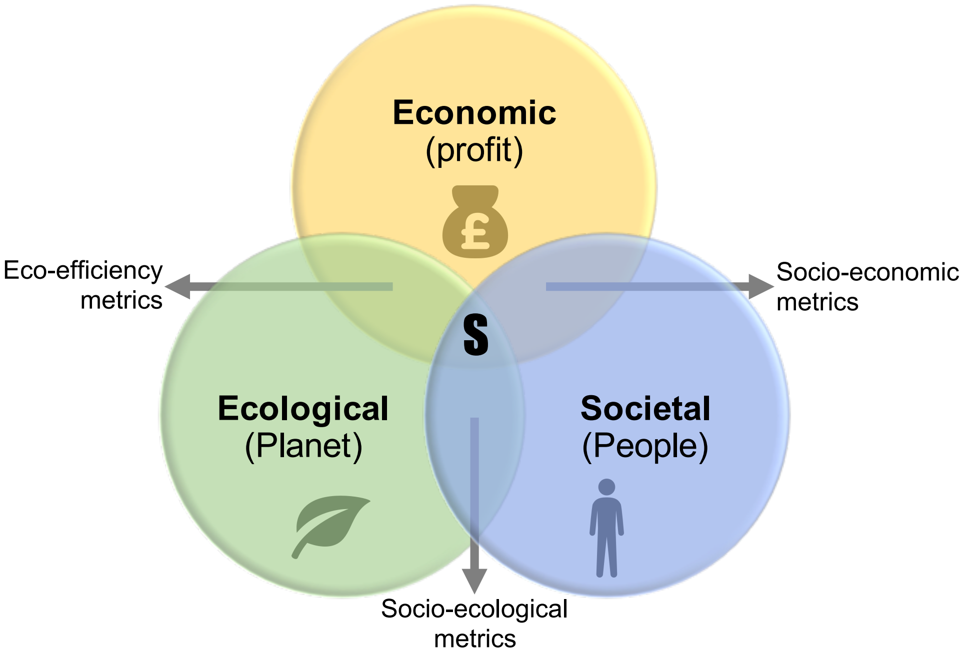

Figure 1.1 – Sustainability metrics Venn Diagram. The overlapping region of these three circles (**S**) corresponds to all three aspects of sustainability being fulfilled.

In the late 20th century, awareness of the environmental degradation, concerns for human health and the possible depletion of fossil fuels caused by its large consumption for energy,[15] lead to an increased interest in using renewable resources (Figure 1.2).

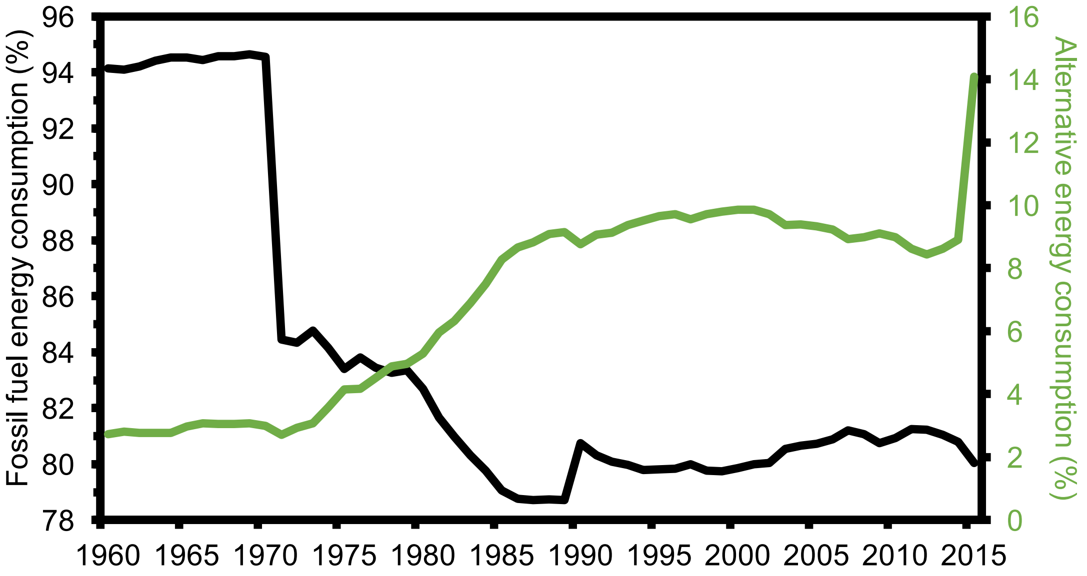

Figure 1.2 – Global energy consumption from fossil fuels (— black line, based on coal, oil, petroleum and natural gas products) and alternative sources (— green line, based on non-carbohydrate clean energy, based on hydropower, nuclear, geothermal and solar power). (data obtained from IEA Statistics[16-17])

Most of the non-renewable resources are used for the production of fuels, useful for transportation (diesel, gasoline and kerosene). A minor portion of these non-renewable feedstocks are also used for the production of economically important chemicals, such as plastics.[18-19] The "plastic age" started at the beginning of 1900's and is still present today (Figure 1.3).[20] At the time, due to the vast availability of cheap fossil fuels appropriate for the production of a variety of materials, Yarsley & Couzens (1945) stated that *"the possible applications* [of plastics] *are almost inexhaustible*" and this has turned out to be very true.[21]

The global production of plastics has reached 335 million tonnes (2016)[22] per year and more than 98% comes from petrochemical starting materials.[23] This represents 6% of global oil consumption.[24] Therefore, there has been also an increased interest in the production of materials from renewable sources and that plastics never became a waste.[24-25]

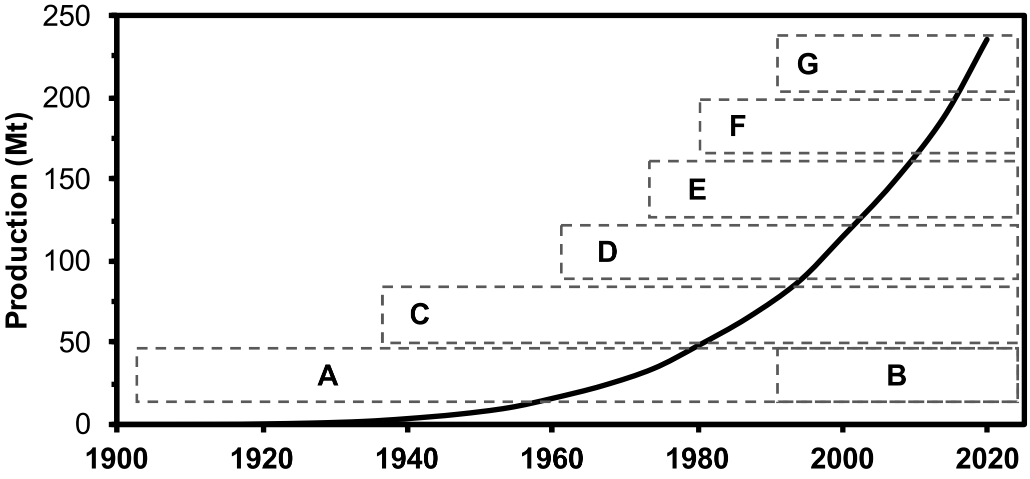

Figure 1.3 – Plastic production in million tonnes, Mt, since 1900. *Note*: A) polymer invention and development (until today), B) biopolymers, C) product/usage diversification, D) accumulation in natural habits, E) concerns for wildlife, F) concerns for human health, G) legislation. (adapted from Thompson*, et al.* [20])

1.3. The bioeconomy challenge

Political considerations have been applied worldwide regarding these issues, in particular the importance of recycling. The postconsumer plastic waste regeneration in Europe, from 2006 to 2014, was 25 million tonnes (annual average).[26] In the beginning of 2018, Plastics Europe (Association of Plastics Manufacturers) released figures regarding the yearly amount of plastics waste that had been collected, recycled, used for energy recovery or sent to landfill (Figure 1.4).[27] From 2006 to 2016, the volumes of plastic waste recycled increased almost 80% and the amount sent to landfill decreased by 43%. Ideally, landfill should eventually reach 0 t. Energy recovery (increased by 61%) using waste as a starting material, combined with heat, is a very important and viable alternative for plastic waste which cannot be recycled (some materials cannot be recycled due to contamination and product quality).

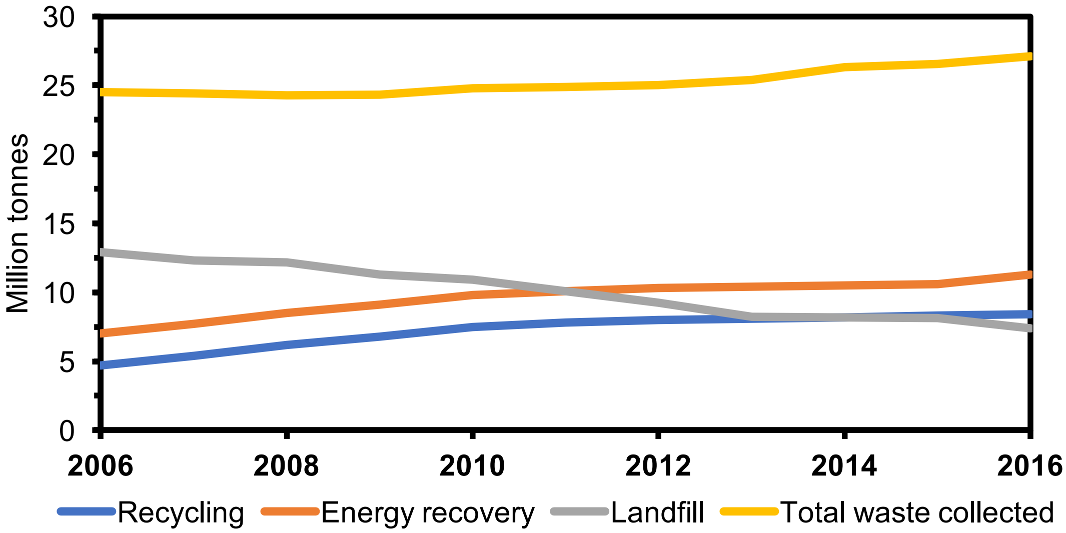

Figure 1.4 – Total plastics waste recycled (blue line), energy recovery (orange line), landfill (grey line) and collected (yellow line). (Adapted from Plastics [27])

In December 2015, the European Commission (EC) adopted an EU Action Plan for a circular economy – an economy in which plastics never become waste. Two years later, in 2017, the EC revealed another goal, confirming that it will work towards plastic production and use, ensuring that all plastic used for packaging will be recyclable by 2030.[28] An overview of the global flow of plastics used for packaging, in 2013, is showed below (Figure 1.5)[24]. 40% of these plastics are landfilled and 32% "lost", either in the collection system or is illegally dumped or mismanaged. 14% is sent to incinerators and/or converted into energy. Nevertheless, only 14% is collected for recycling.

To successfully meet all these targets (where plastics never become waste), the EC has implemented a framework programme (FP), started in 1983, to support and foster research in the European Research Area.[29]

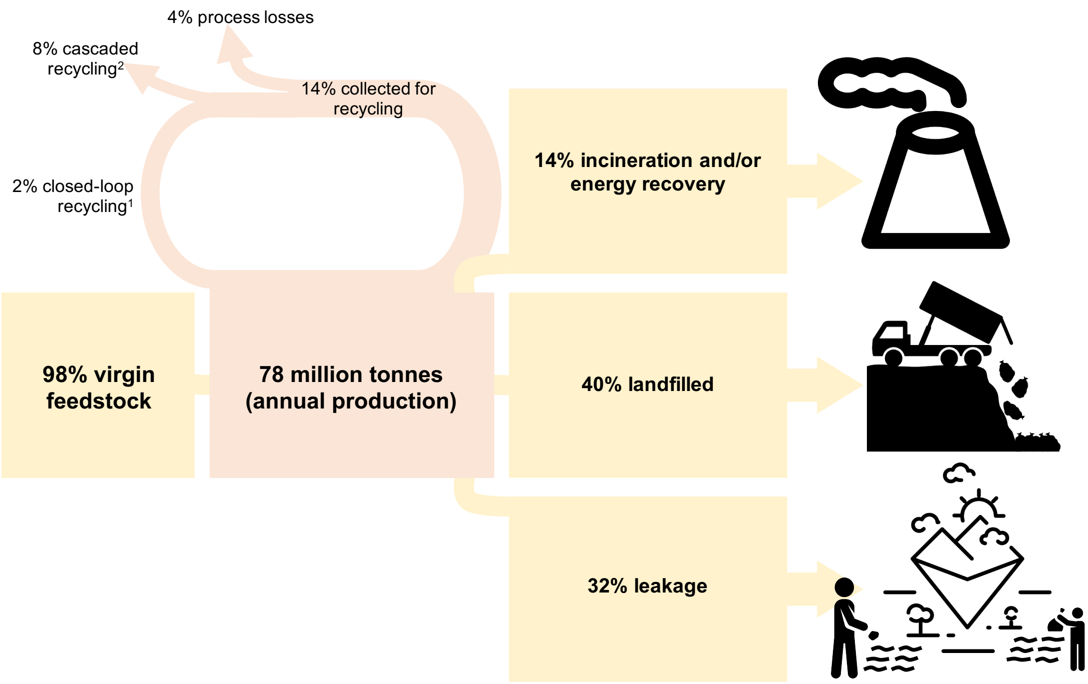

Figure 1.5 – Global flow of plastics for packing using, in 2013. *Note*: [1] Closed-loop recycling: recycling of plastics into the same or similar-quality applications; [2] cascaded recycling: recycling of plastics into other, lower-value applications. (Adapted from World Economic Forum and Foundation [24]).

1.3.1. The importance of using biomass

The 7th principle of Green Chemistry is to "use renewable feedstocks" rather than fossil resources. The fast-growing world population is leading to an increased demand for energy, resources, and the consumption and production of different materials, such as plastics.[30] All of which are depleting fossil feedstocks. For this reason, the introduction of renewable carbon resources, such as biomass and waste, into synthetic procedures is of high interest. Biomass refers to "any organic matter that is available on a renewable or recurring basis including dedicated energy crops and trees, agricultural food and feed crop residues, aquatic plants, wood and wood residues, animal wastes, and other waste materials".[31] Such examples are: industrial and public wastes, agricultural residues, organic household, various wood and energy crops (*e.g.* oilseed crops). The main components of biomass include; carbohydrates (cellulose, lignocellulose crops, starch and sugar crops), lipids (fats, waxes and oils), proteins, aromatic compounds – lignin, and ash (non-carbon minerals, *e.g.* calcium, phosphorous, potassium, etc.). In theory, using biomass as a raw material could provide an estimated volume of 1.7–2.0x10^{11}

tons per year at world level yet, only 3% is currently used for food and non-food applications (*e.g.* chemical industry and biomaterials).[30]

The plastic industry is one of the largest users of fossil fuels and the price of these plastics materials is critically dependent on the price and availability of petrochemical feedstocks.[26] Therefore, alternative routes need to be investigated in order to produce new materials not dependent on non-renewable resources.

1.3.2. Monomers and polymers from oxygen and hydrocarbon-rich biomass

One of the major aims in the polymer industry is to develop polymers that replace fossil fuel based materials. Polymers have a wide range of applications. One example is as packaging materials, which represents the largest market share of plastic resins.[32] Although inexpensive, useful and durable, fossil-based plastics can cause severe environmental problems due to their disposal, since they do not biodegrade.[33] A good alternative feedstock to these non-renewable resources for the production of polymers can be biomass.

Monomers and their subsequent polymers derived from biomass can be classified based on their origins:[34]

1. Oxygen-rich biomass: such as carboxylic acid (*e.g.* succinic acid, lactic acid), polyols (*e.g.* glycerol and sorbitol) and furan
2. Hydrocarbon-rich biomass: such as vegetable oils (*e.g.* vernonia oil), fatty acids (e.g. *vernolic acid)* and terpenes

This Thesis focuses on succinic acid, glycerol and vernonia oil as potential biomass sources. Therefore, in this section, a more detail description about these compounds will be given.

1.3.2.1. Polymers from oxygen-rich biomass

Succinic acid (SA, butanedioic acid) is an intermediate of tricarboxylic acid cycle (TCA, known as Krebs cycle) and also an end product of anaerobic fermentation.[35] Due to growing environmental concerns, the demand for the production of bio-based SA has increased (Figure 1.6).

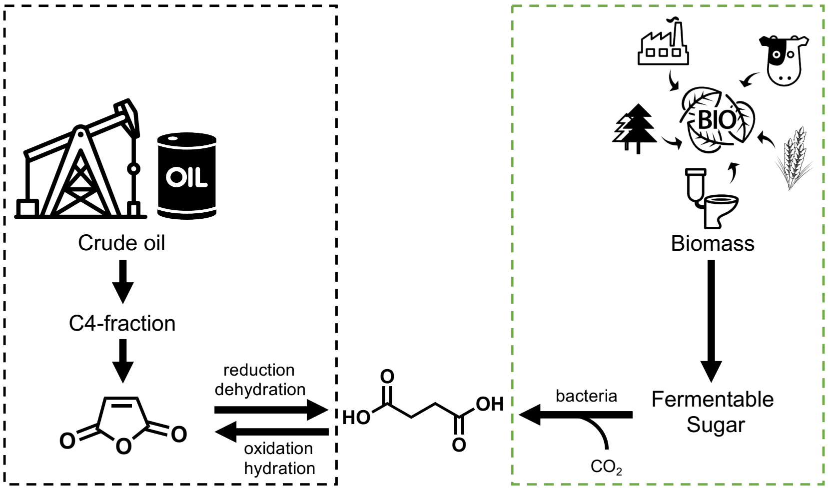

Figure 1.6 – Schematic representation of the possible pathways for succinic acid (SA) production. *Note:* the synthetic route using petrochemical resources is highlighted through the dashed black box (left); the bio-based SA is highlighted through the dashed green box (right). (adapted and modified from Bechthold*, et al.* [36])

Succinic acid has been used industrially for the production of copolyesters.[37-39] Poly(butylene succinate) (PBS), under the trade name BioPBS™, was developed by Mitsubishi Chemical Corporation.[37] This polymer results from the polycondensation of bio-based SA and 1,4-butanediol (1,4-BD) and it is used in food packaging (Figure 1.7). Showa Denko, from 1993-2016 produced PBS biodegradable polymer, under the trade name Bionalle®, using SA, 1,4-BD and ethylene glycol as building blocks.[38-39] However, in 2016-2017 the production of Bionalle® was terminated due to “the delay in permeation of environmental regulations on plastic shopping bags and a fall in market prices of biodegradable plastics”.[40]

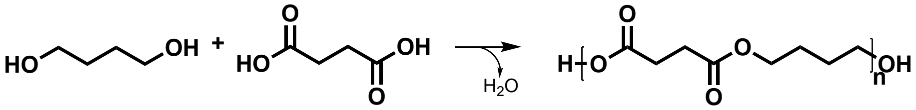

Figure 1.7 – Schematic representation for the synthesis of poly(butylene succinate) through the polycondensation of succinic acid and 1,4-butanediol.

Glycerol (1,2,3-propanetriol, also known commercially as glycerine) occurs in nature as a product of fat hydrolysis but it can also be obtained as a by-product of biodiesel production (Figure 1.8). Currently, glycerol is mainly obtained industrially from biodiesel (60-70%, in 2015), the rest from fatty acid (FA) and fatty alcohol production, and a minor fraction is obtained from soap making.[41]

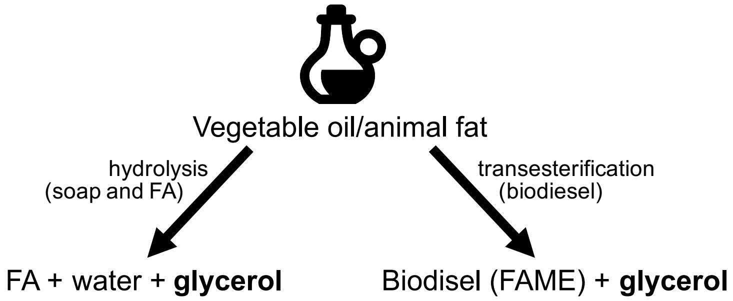

Figure 1.8 – Schematic representation of the possible pathways for glycerol production. *Note:* FA = fatty acids; FAME = fatty acid methyl ester.

After more than 20 years of commercial used in Europe, biodiesel has proven to be a good alternative fuel[42] and the continuing biodiesel production is leading to large surpluses of glycerol. Generally, 10-20% of the total volume of biodiesel produced is made up of crude glycerol as a waste product.[43] Most of the biodiesel production uses homogeneous catalysts resulting in crude glycerol containing methanol, soap, water, glycerides and ash , causing it to have few direct uses without purification.[41] The glycerol obtained from biodiesel production needs to be purified to at least 99.5 wt.% and the process requires high-temperature and vacuum distillation. Nevertheless, Benefuel, a new biodiesel plant, is using a heterogeneous catalyst in which glycerol is obtained with high purity (>98%) as a by-product.[44] This will allow its direct conversion into other commercially attractive chemicals.

The glycerol price is inversely proportional to biodiesel production.[43] This means that a high production of biodiesel results in increasing quantities of glycerol and consequently its price falls (Figure 1.9).

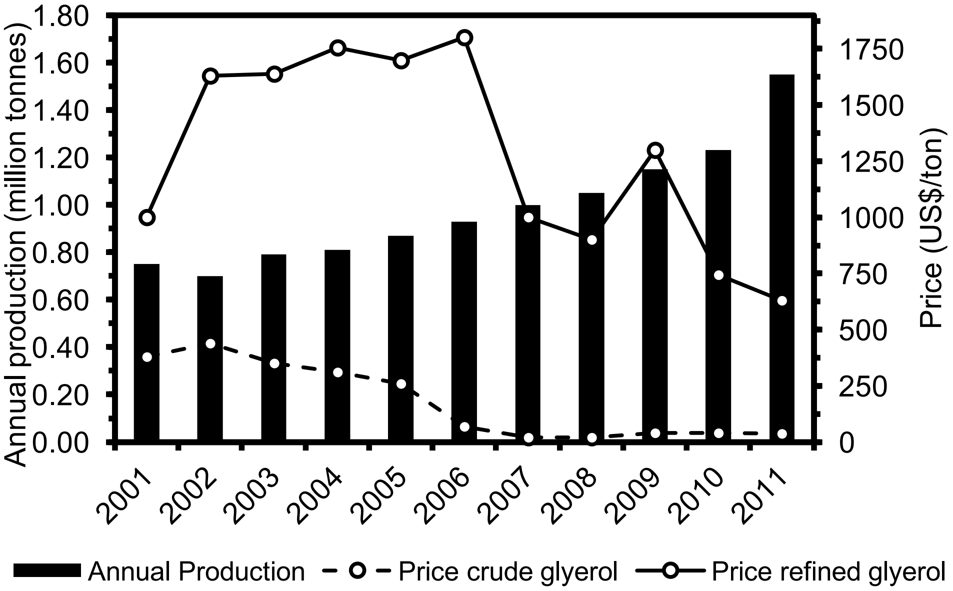

Figure 1.9 – Projection of global annual production and price of glycerol.[43]

Therefore, glycerol offers great opportunities in the development of new chemicals and compounds. The polycondensation of glycerol with dicarboxylic acids (azelaic, glutaric, iminodiacetic, sebacic and succinic acid, to name a few)[45-50] has been studied recently and it is an example of using this valuable by-product from biodiesel production.

The polycondensation of glycerol with succinic acid will be the main focus in Chapter 3.

1.3.2.2. Polymers from hydrocarbon-rich biomass

Vegetable oils represent another possible alternative feedstock for the synthesis of new chemicals and materials and its production has recently increased (Figure 1.10). Most vegetable oils have several applications, for example as food (65%), biofuels (20%) and chemical feedstocks (15%).[51]

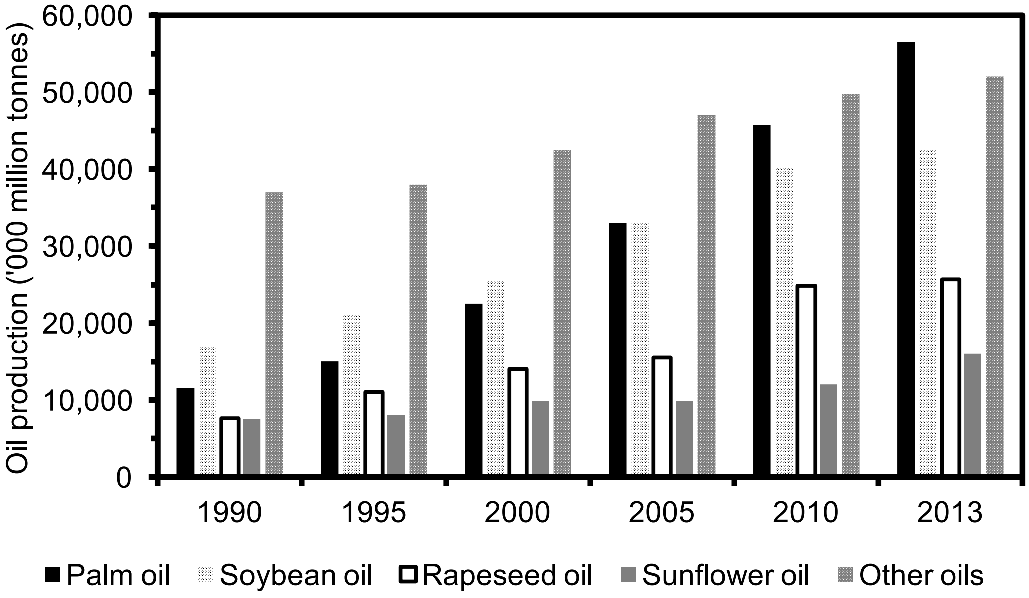

Figure 1.10 – Global oil production between 1999-2013.[52]

Palm oil is the most produced oil worldwide and is one of the cheapest. It is mainly used in the food and cosmetic industries. The direct use of unmodified vegetable oils is limited due to their low oxidative stability.[53] The *bis*-allyl hydrogens present are susceptible to free radical attack, hence undergoing oxidative degradation to form polar oxy compounds (lipid peroxidation, Figure 1.11).[54-55] Therefore, taking advantage of the C=C double bonds in the FA chains, allowed the addition of functional groups such as an oxirane ring. However, the epoxidation process used to add the ring involves the use of volatile solvents, which is not ideal from a sustainable point of view (see section 5.2.2. of this Thesis).

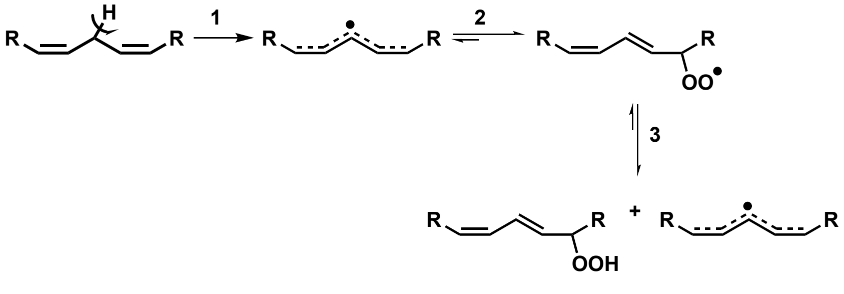

Figure 1.11 – Schematic representation of lipid peroxidation. *Note*: the hydrogen abstraction occurs in the methylene group in between the two C-C double bonds, in the presence of atmospheric triplet oxygen ($^3O_2$) giving a radical (step 1); the addition of oxygen is a fast step (step 2, β-fragmentation), this step is reversible; competing with β-fragmentation is the trapping of the peroxyl radical (hydroperoxide) by transfer of a hydrogen atom from an available *bis*-allylic methylene group (step 3 – slowest step)[56]

Natural epoxy vegetable oils, such as vernonia oil, offer a great opportunity for the synthesis of epoxy coatings,[57] thermoplastics[58] and biodegradable polymers.[59] In addition, since they naturally contain a oxirane rings, the drawbacks associated with the synthetic epoxidation process can be avoided.

Carlson*, et al.* [57] used vernonia oil (extracted from *Vernonia galamensis* grown in Kenya and Puerto Rico, using *n*-hexane) to synthesised epoxy coatings by applying high temperatures (150 – 200 ºC) for 10 to 120 min. The synthesised materials gave good adhesion and flexibility properties. Depending on the baking temperature the vernonia-based coatings HAD different colours. At 150 ºC the coating material was colourless while at 200 ºC it was golden yellow. The synthesis of vernonia-based cross-linked rubber-like elastomers was accomplished by reacting vernonia oil with the aromatic diamine m-phenylenediamine (m-PDA) and stearic acid (as catalyst), resulting in a thermoresistant elastomer (Figure 1.12).[60]

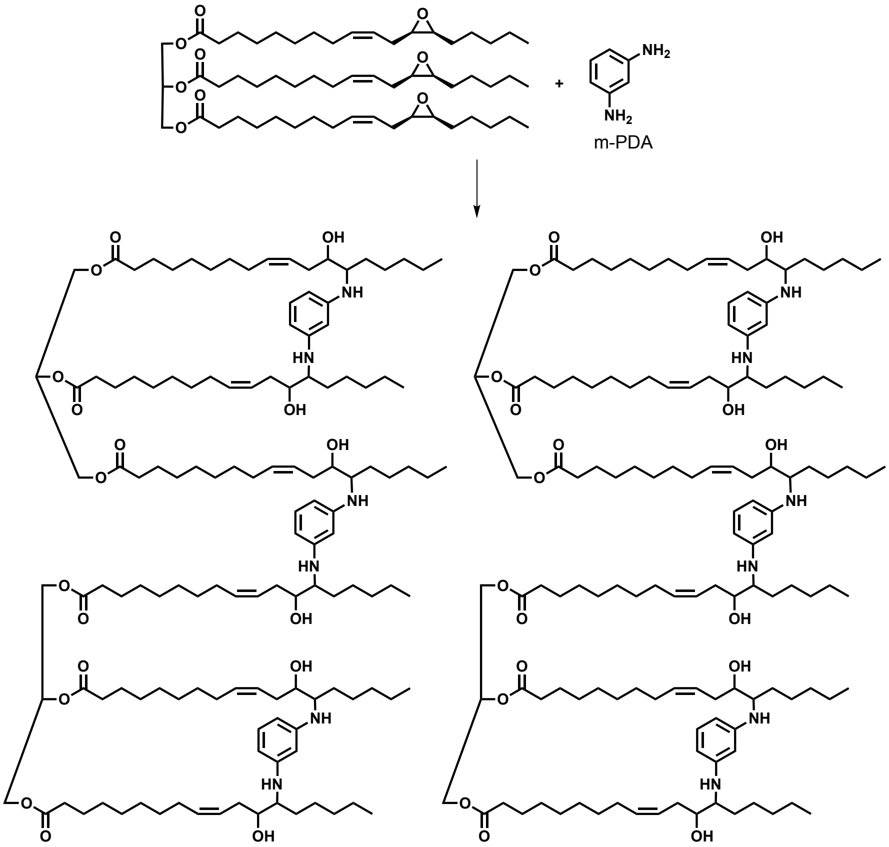

Figure 1.12 – Schematic representation for the synthesis of vernonia-based cross-linked rubber-like elastomers.

Polymer syntheses using monomers derived from vernonia oil are reported in this Thesis, in both Chapter 5 and 6.

1.3.3. Renewable and biodegradable polymers

According to green and sustainable development, the desire to obtain polymers from renewable feedstocks, with optimal properties for applications (like drug delivery, gene therapy, cosmetic, tissue engineering, implantation devices and construction materials), has grown in the last two decades.[61-62]

There are two main drivers for the developing interest in bioplastics: their synthetic route and their disposal (Figure 1.13).

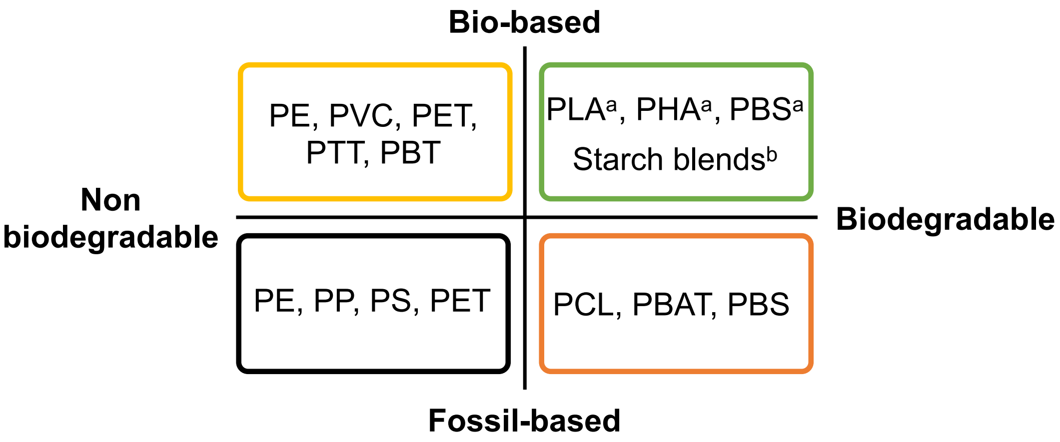

Figure 1.13 – Representation of commercial plastic materials based on the synthesis method and their disposal. *Note*: a) biodegradable polymers synthesised from bio-based intermediates; b) naturally occurring biodegradable polymers; PE = polyethylene; PVC = poly(vinyl chloride); PET = poly(ethylene terephthalate); PTT = poly(trimethylene terephthalate); PBT = poly(butylene terephthalate); PLA = polylactide; PHA = poly(hydroxyalkanoate); PBS = poly(butylene succinate); PP = polypropylene; PS = polystyrene; PCL = poly (ε-caprolactone); PBAT = poly(butylene adipate-*co*-terephthalate). (adapted from Ross*, et al.* [26])

Useful bio-based polymers such as polyethylene terephthalate (PET), polyethylene (PE), poly(vinyl chloride) (PVC) and poly(butylene terephthalate) (PBT) are non-biodegradable. By contrast, poly (ε-caprolactone) (PCL) although biodegradable, is produced from fossil feedstocks. Biodegradable and bio-based (biorenewable), although often used in conjunction with one another, have two different meanings. A biodegradable polymer is a material that can break down into smaller units easily. If something is biorenewable it means that comes from renewable resources, which is a very important requirement for green and sustainable polymers.

1.3.3.1. Commercial polyesters

Among the biodegradable and biorenewable polymers, polylactide (PLA) is the most studied due to its wide range of applications including agricultural films,[63] food packaging,[63] drug delivery system[64] and biomedical devices.[65] PLA can be obtained by the condensation of lactic acid (LA) or by the ring-opening (ROP) of lactide. It is commercially produced through ROP of lactide, using corn as feedstock (Figure 1.14).

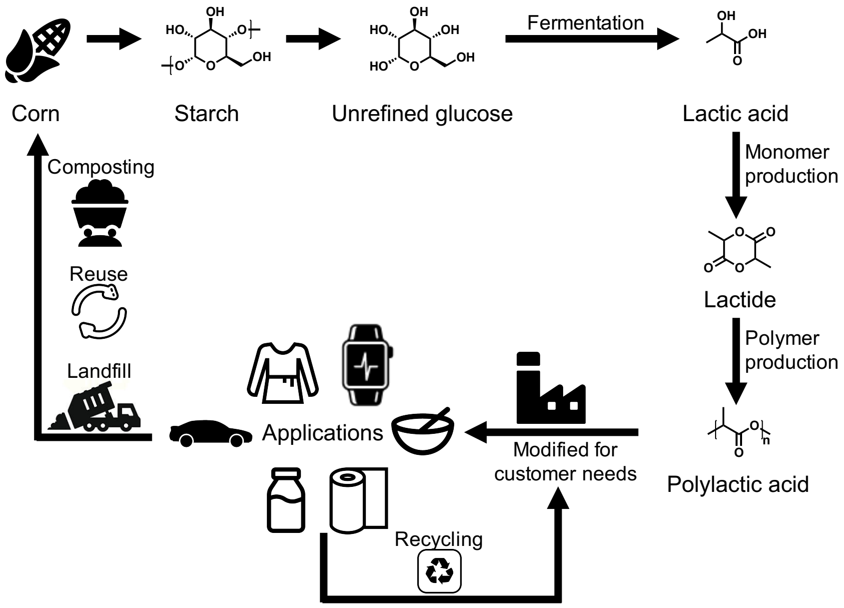

Figure 1.14 – Commercial production of PLA (adapted from Castro-Aguirre, *et al.* [66]).

Polyhydroxyalkanoates (PHAs) are another extensively studied polymer.[67-70] Similar to PLA, PHA is connected to a carbon-neutral footprint meaning its degradation does not increase atmospheric CO_2 levels.[71] PHA is produced by microorganisms and biodegradable through enzymatic degradation. There are different types of PHA: polyhydroxybutyrate (PHB), polyhydroxyvalerate (PHV), polyhydroxyhexanoate (PHH) and polyhydroxyoctanoate (PHO).[67] PHB, under the trade name Biopol, is produced through the fermentation of plants and sugars and has similar properties to polypropylene (PP).[72] Since PHAs are biodegradable, biocompatible and biorenewable, they have been used in several industry sectors, such as in tissue engineering and drug delivery.[73]

PCL is a hydrophobic aliphatic polyester composed of hexanoate units. PCL can be obtained by either ROP of ε-caprolactone[74] or condensation of 6-hydroxyhexanoic acid[75] (Figure 1.15). Industrially, ε-caprolactone is synthesised from the oxidation of cyclohexanone by peracetic acid.[76] Tissue engineering, drug delivery, medical devices and packaging are the industrial sectors where PCL is applied, due to its biodegradability and biocompatibility.[77]

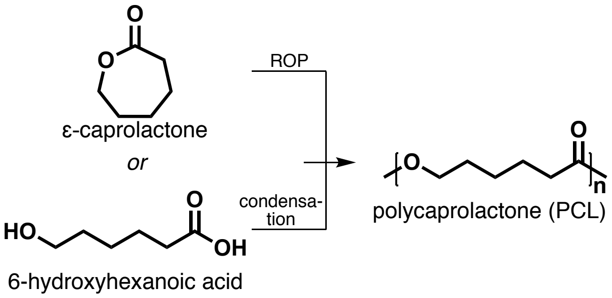

Figure 1.15 – Polycondensation of polycaprolactone (PCL) *via* ROP of ε-caprolactone or polycondensation of 6-hydroxyhexanoic acid.

1.3.3.2. Biodegradation

These aliphatic polyesters, PBS, vernonia-based polyesters, PLA, PHA, PCL and PBS all have a characteristic ester linkage present in their backbone. This bond can be easily hydrolysed in acidic or basic medium (Figure 1.16). In addition, these polymers can also biodegradable enzymatically.[78] The degradation process depends on the degree of crystallinity (X_c), chain flexibility, macroscopic structure (surface area) and molecular weight.[79-80] For example, a polymer with a higher chain flexibility will be easier to degrade enzymatically (hydrolases and lipases) since more sites will be accessible to water for hydrolysis. Increased flexibility will also allow the polymer chain to fit better into the active site of enzymes. Therefore, increasing chain flexibility increases the degradation rate. In addition, water does not diffuse in crystalline polymers.[80] Hence, amorphous polymer regions will degrade faster than crystalline regions. A further factor that influences degradation rate is the melting point. The higher the melting temperature of the polymer, the lower the degradation rate will be due to the chain mobility.[81]

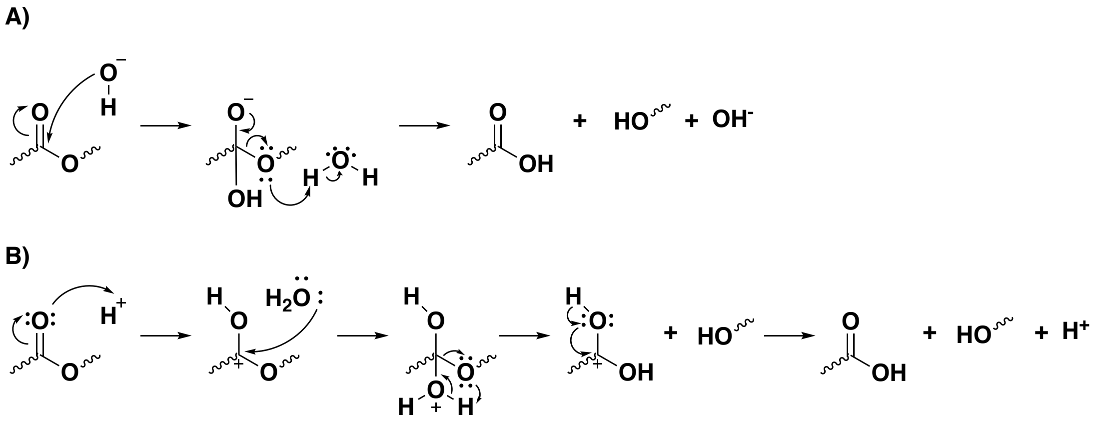

Figure 1.16 – Schematic representation of the hydrolysis of polyesters by A) basic and B) acidic catalysis. *Note*: the wavy lines corresponds to the polymer chain.

1.4. Polymers

The synthesis of polyesters *via* polycondensation will be the main focus of the Thesis. Hence, a detailed description of the synthesis procedures of polyesters is presented in this section.

1.4.1. Introduction to polymers

There are two main processes used to synthesise polymers: step growth and chain-growth polymerisations (Figure 1.17).

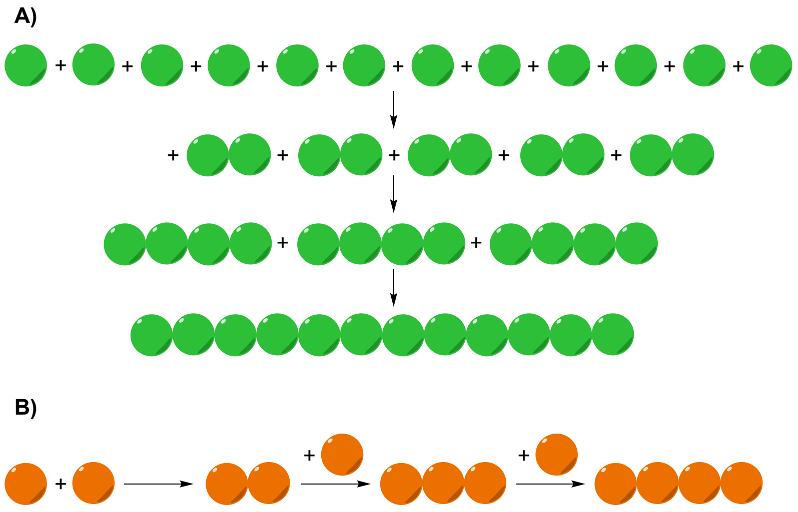

Figure 1.17 – Schematic representation of the two main polymerisation processes, A) step-growth and B) chain-growth polymerisation.

In step-growth polymerisation, each monomer unit reacts with another monomer unit leading to the formation of dimers, trimers and oligomers. These will react together to form the polymer chain (Figure 1.17 A)). Hence, the polymer chain grows in steps. An example of a step growth polymerisation is the polycondensation of bifunctional monomers (Figure 1.18 A)).

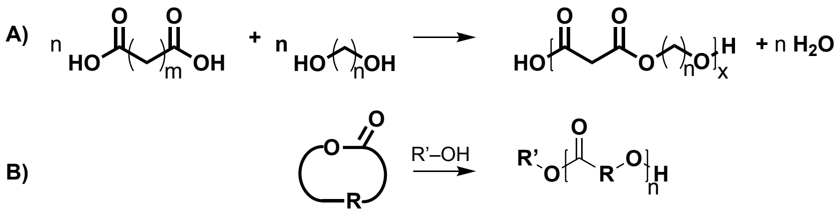

Figure 1.18 – Schematic representation of the synthesis of polyesters through A) polycondensation of bifunctional monomers and B) ROP of cyclic esters.

In chain-growth polymerisation the polymer chain grows by addition of 1 monomer unit at a time(Figure 1.17 B)). An example is the ROP of cyclic esters (Figure 1.18 B)).

An important parameter is molecular weight (as this gives information about the size of the polymer). It can be expressed as the number-average (M_n, Equation 1.1) or as the weight-average (M_w, Equation 1.2). The ratio between these averages measures the distribution of the molecular weight of the polymer, and it is denominated as dispersity ($Đ$, Equation 1.3). A monodispersed polymer containing only a single molecular weight will have M_n equivalent to M_w, where $Đ$ is equal to 1.

$$M_n=\frac{\text{total weight of sample}}{\text{number of molecules of } \mathrm{N_i}}=\frac{\sum \mathrm{N_i M_i}}{\sum \mathrm{N_i}}$$

Equation 1.1 – Determination of the number-average molecular weight (M_n). *Note:* $\mathrm{N_i}$ = total number of chains with degree of polymerisation of *i*; $\mathrm{M_i}$ = molecular weight of chain with a degree of polymerisation *i*.

$$M_w=\frac{\sum \mathrm{N_i M_i^2}}{\sum \mathrm{N_i\, M_i}}$$

Equation 1.2 – Determination of the weight-average molecular weight (M_n). *Note:* $\mathrm{N_i}$ = total number of chains with degree of polymerisation of *i*; $\mathrm{M_i}$ = molecular weight of chain with a degree of polymerisation *i*.

$$Đ=\frac{\mathrm{M_w}}{\mathrm{M_n}}$$

Equation 1.3 – Determination of the polymer dispersity ($Đ$).

1.4.1.1. Synthesis of polyesters *via* polycondensation

The polycondensation of bifunctional monomers is accompanied by the formation of a small molecular weight molecule, a by-product. For example, when dicarboxylic acids react with diols, the product will be water whilst the condensation between dimethyl ester and diols, yields methanol. The elimination of the by-product is crucial for a successful formation of polymer. Esterifications are equilibrium reactions. Removal of the by-product condensate (water) will avoid depolymerisation and will shift the reaction towards the formation of high molecular weight polymer according to the principle of *Le Chatelier*.[82] The removal of water can be accomplished by heat, high energy vacuum or by a flow of argon or nitrogen.[82] All of these techniques aid mass-transfer, making it more favourable for the by-product in the reaction medium to be transferred to the vapour phase, thus driving the reaction forward. As an alternative, molecular sieves can be used to absorb the low molecular weight by-product.

There are other factors that might influence the synthesis of high molecular weight polymers in polycondensation reactions. For example, side-reactions might occur such as intramolecular ring closure (cyclisation), hydrolysis, inter-chain transesterification and reaction with mono-functional impurities.[83] In addition, the stoichiometric balance between the functional groups is also crucial to obtain high molecular weight polymers (*e.g.* the ratio between hydroxy groups and carboxy groups). An imbalance (even small) in the monomer feed will affect the degree of polymerisation (DP) (see section 3.2.2.1 from this Thesis). All these factors could significantly affect the molecular weight of the desired polymer.

Useful polyesters are currently produced industrially through polycondensation such as PET (Figure 1.19 A)) and PBS (PGA, Figure 1.19 B)). Both plastics are used for the production of bottles and packaging. Generally in industry, one of the monomers (carboxylic acid or diol) is used in excess to allow for losses.[84] When either monomer has a low melting point, applying vacuum or azeotropic conditions (needed to remove the by-products of the reaction, *e.g.* water), can lead to monomer loss.

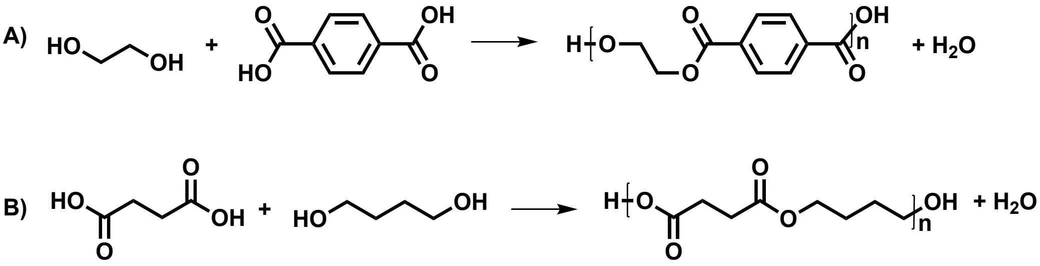

Figure 1.19 – Commercial polyesters A) poly(ethylene terephthalate) (PET) and B) poly(buthylene succinate) (PBS).

In general, polycondensations are considered to be slow reactions and to obtain high molecular weight polymers high temperatures are required. It is important to control the stoichiometric balance between functional groups and to remove the by-product of the polycondensation reaction. Due to the formation of a by-product, condensation reactions have a low atom economy.

1.4.1.1.1. Linear polyesters

Linear polyesters can be obtained by the condensation of two monomers (dicarboxylic acid and diol, Figure 1.20 A)) or by the self-condensation of a hydroxy acid (Figure 1.20 B)). For the latter, the monomer must contain both hydroxyl and acid functionalities. These reactions have been performed using organic acid (*e.g. p*-toluenesulfonic acid, PTSA[85]) or metal catalysts (such as titanium (IV) isopropoxide, TTIP[86]) at high temperatures.

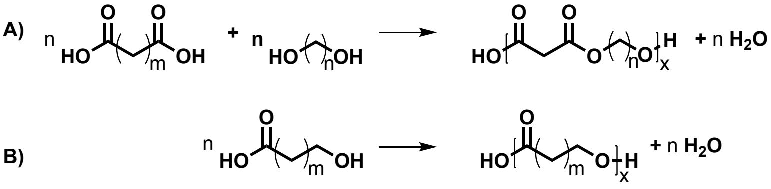

Figure 1.20 – Schematic representation of A) polycondensation of two monomers, dicarboxylic acid and diol and B) self-condensation of a hydroxy acid.

As mentioned, high temperatures are needed for polycondensations (> 150 ºC), this is to guarantee that the monomers are in the melt phase, to successfully remove the by-product of the reaction and to also overcome issues associated with viscosity increases as the polymer grows[87] As an example, Debuissy*, et al.* [86] performed the polycondensation of succinic acid (SA) and/or adipic acid (AA) and 1,3-propanediol (1,3-PDO) applying a two-stage melt condensation (Figure 1.21). In the first stage, the reagents were heated to 190 ºC for three hours in order to synthesise oligomers. To remove the by-product of water, vacuum (200 mbar) was applied to the system. The catalyst (0.1 mol% relative to the amount of diacid) was added into the system such as dry toluene. In the second stage, the reaction temperature was increased to 230 ºC and the pressure was decreased to 1-3 mbar. After 4 hours, polymers with a molecular weight of 24,000-38,200 Da (1.7< *Đ* < 1.9) were obtained.

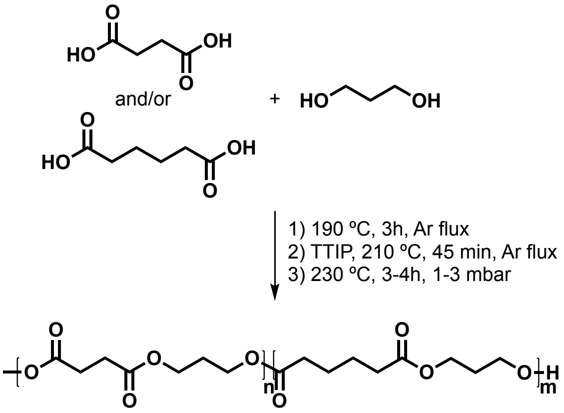

Figure 1.21 – Schematic representation of the two stage polycondensation synthesis of 1,3-propylene succinate-ran-1,3-propylene adipate) (PPSA) copolyesters, using succinic acid (SA) and/or adipic acid (AA) and 1,3-propanediol (1,3-PDO) as monomers.[86]

1.4.1.1.2. Polyesters from multifunctional monomers

The combination of A_n and B_m or AB monomers where n and/or m > 2, the resulted polymers can be branched or cross-linked.[88] As an example, the polycondensation of glycerol with diacids has been studied in detail and using metal catalysts, branching is expected (Figure 1.22). The main reason for this branching is that these types of catalyst do not show any regioselectivity towards primary *versus* secondary hydroxy groups and hence, a polymeric network is formed. A more detailed description of branched polymers can be found in section 3.2.2.1.

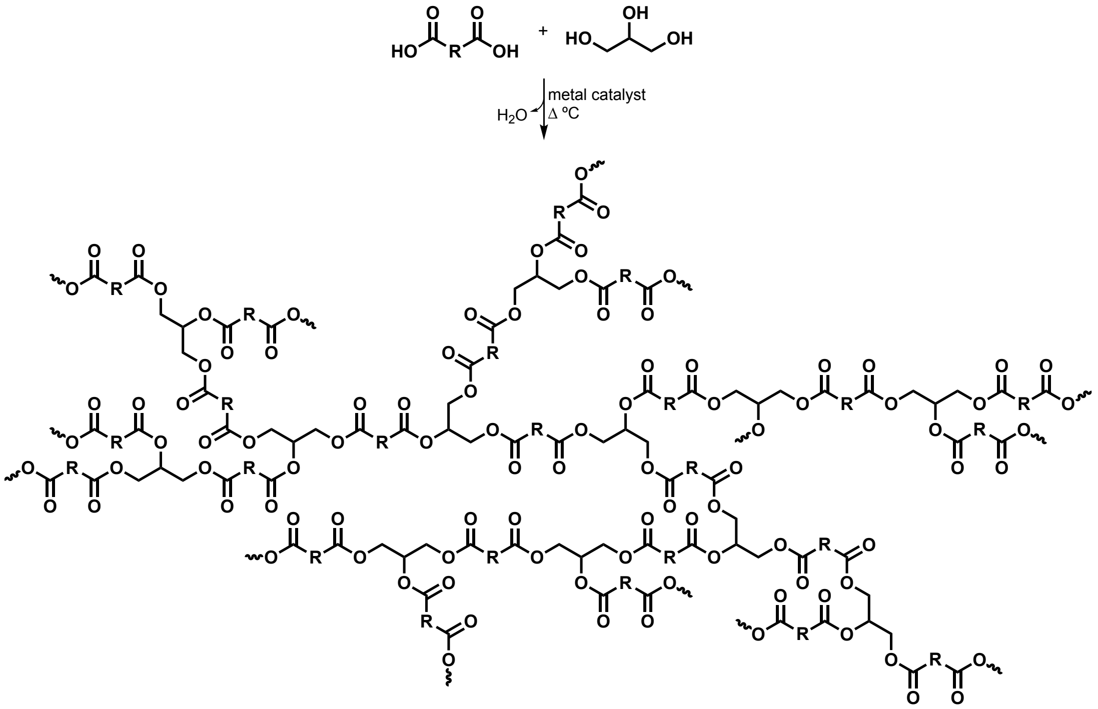

Figure 1.22 – Schematic representation of a cross-linked material resulting from the polycondensation of glycerol and a dicarboxylic acid.

1.5. Enzymatic polycondensations

1.5.1. Introduction

Over the last two decades, the field of enzyme-catalysed polycondensations, especially lipase-catalysed, has developed rapidly and become an important route to synthesise polymeric materials. Using enzymes as catalysts has several advantages, such as high efficiency, recyclability (when immobilised), the ability to operate under mild conditions and a low environmental impact.[89] Additionally, enzymes can be chemo-, regio- and enantioselective.[90] However, there are some drawbacks to using enzymes. “Free”-enzymes are sensitive to the environment but, when immobilised, enzymes can tolerate harsh environments including temperatures higher than 100 ºC and pressures above 100 bar.[90] “Free”-enzymes are expensive but, if immobilised, they can be reused; and due to the rapid development in molecular biology, the cost of enzyme production is constantly dropping.[91]

Enzymes are proteins which can have high catalytic activity and specificity towards certain chemical reactions.[92] Enzymes are divided into six main classes, on the basis of the reaction they catalyse (Table 1.2).[93]

Table 1.2 – The six main classes of enzymes established by the International Union of Biochemistry in 1955.[93]

Enzyme class	Type of reaction catalyzed
Oxidoreductases	Oxidation/reduction reactions
Transferases	Transfer an atom or group between two molecules
Hydrolases	Hydrolysis reactions
Lyases	Removal of a group from substrate (not by hydrolysis)
Isomerases	Isomerisation reactions
Ligases	The synthetic joining of two molecules, forming a new chemical bond

1.5.2. Lipases

Hydrolases are responsible for the breaking of chemical bonds by hydrolysis. Lipase is an example of an enzyme that falls in to the hydrolase category and it can be used in polymer chemistry.[89] *Candida antarctica* Lipase B (CaLB) is widely used in the hydrolysis and synthesis of esters.[94] CaLB immobilised on macroporous resin – Novozyme® 435 (10% by weight of lipase), is the most common enzyme used for polymerisation reactions.[95] The active site of this protein is located in the core of the protein (Figure 1.23), at the bottom of a funnel-like structure which has a highly hydrophobic surface. The limited available space and hydrophobicity in the active site explains its high selectivity.[96] The catalytic triad of CaLB is composed of serine-histidine-aspartate (Ser^{105}, His^{224} and Asp^{187}).[96] The catalytic mechanism is well understand (Figure 1.24). Li*, et al.* [96] evaluated the conformational stability of this lipase in the presence of both polar and nonpolar solvents. The authors determined that there is an intensive interaction between the active site and polar solvents, such as methanol, which might destroy the hydrogen bond between Ser^{105} and His^{224}. Moreover, CaLB gave higher activity in hydrophobic solvents such as hexane, toluene and diphenylether.[97]

CaLB can also catalyse the hydrolysis of polyesters. Therefore, the removal of the by-products is important during poly-esterifications to drive the equilibrium towards product formation. It is important to mention that ester bonds in the polymer backbone can undergo nucleophilic attack by the Ser^{105} (catalytic triad) of the lipase resulting in polymer chain breaking.[98]

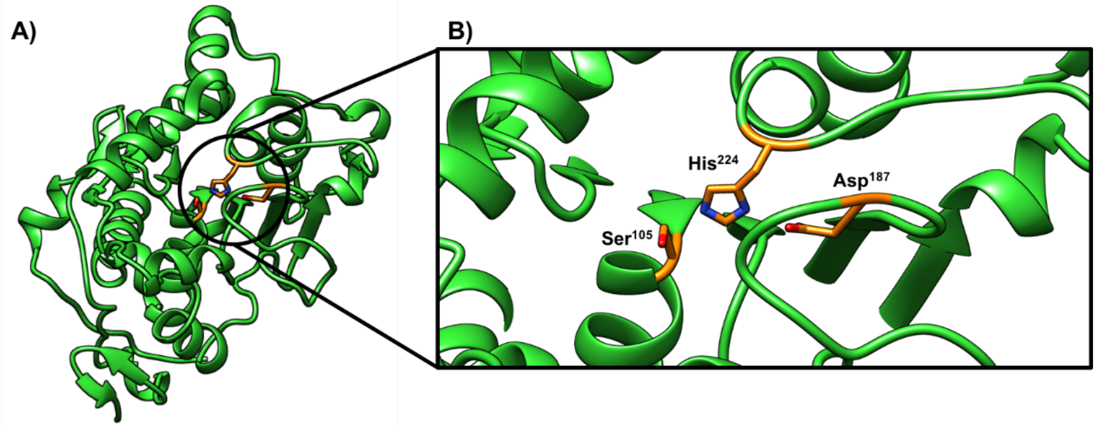

Figure 1.23 – Representation of the A) *Candida antarctica* lipase B and its B) active site, showing the catalytic triad serine-histidine-aspartate. (Images obtained using UCSF Chimera software[99])

The optimum temperature range for Novozyme® 435 is 30-60 ºC (declared by the supplier). However, this enzyme has shown good activity at higher temperatures (100 ºC).[100] Yet, in the presence of toluene at 80 ºC for 24 h, a swelling of the macroporous acrylic resin has been observed, which was found to reduce the catalytic activity of this enzyme.[101]

1.5.3. Enzymatic production of polyesters

There are several studies where researchers investigated different enzymes (lipases) at varying concentrations to explore the effect on the molecular weight of polymers synthesised through polycondensation. As an example, Uyama *et al.* performed the polycondensation of 1,4-butanediol (BDO) and sebacid acid (SbA) at 60 ºC (8 hours reaction) using different lipases: *Candida antarctica* lipase B (CaLB), *Mucor miehei* lipase (MmL), *Pseudomonas cepacia* lipase (PcL), Pseudomonas fluoroscens lipase (PfL) and *Porcine pancreatic* lipase (PpL).[102] Only CaLB, after an 8 hours reaction, obtained a polymer with a molecular weight of 3,800 Da ($Đ$ = 1.3) in a bulk system. In the presence of diisopropyl ether, only CaLB (8h) and MmL (48h) obtained polymers with a molecular weight of 2,000 ($Đ$ = 1.3) and 2,700 ($Đ$ = 1.4), respectively. Increasing the CaLB catalysed reaction time to 48h, resulted in a polymer with higher molecular weight (6,700 Da, $Đ$ = 1.6).

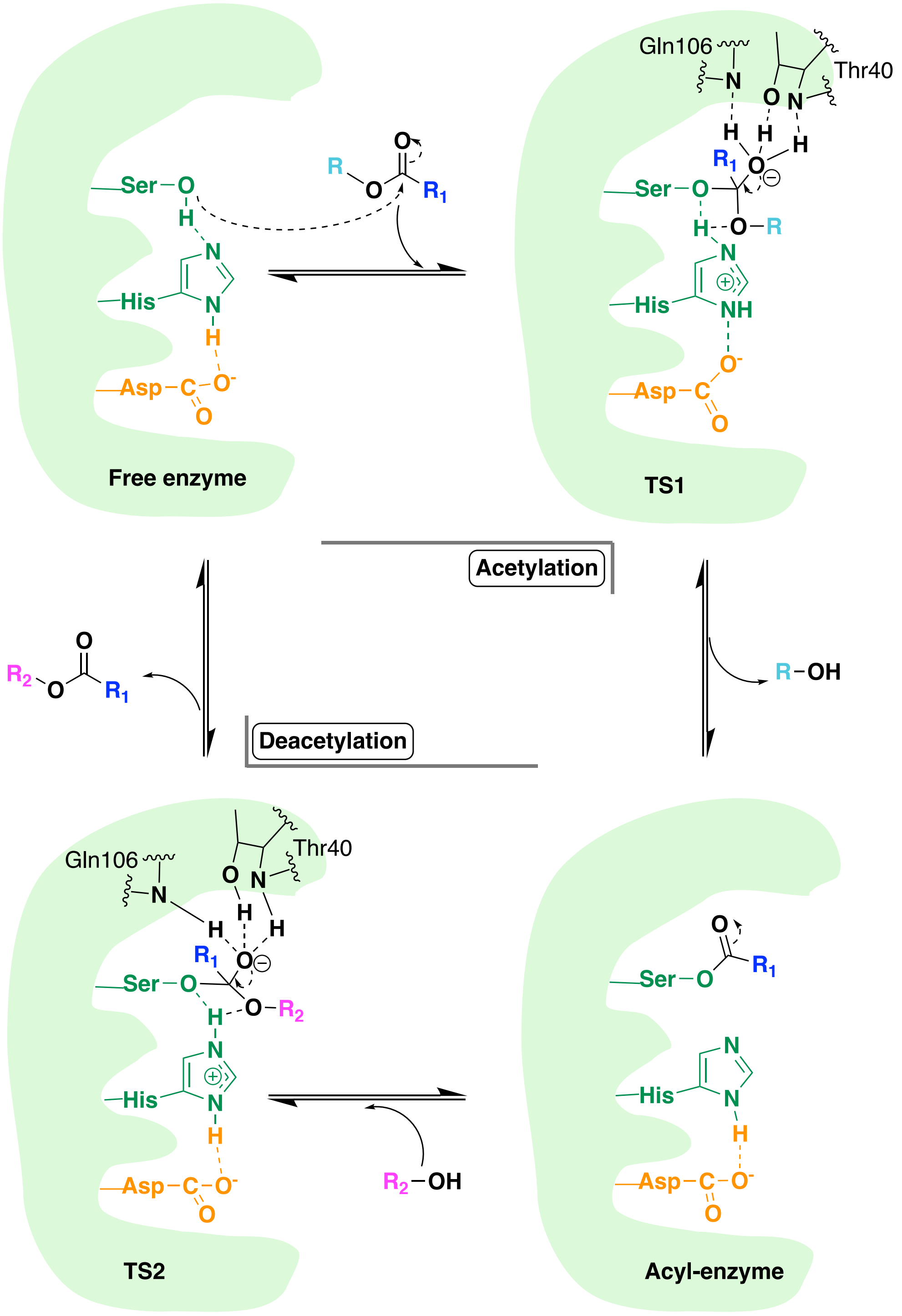

Figure 1.24 – Catalytic mechanism of CaLB for hydrolysis or transesterification. In the first step, Ser^{105} (nucleophile) attacks one ester group of the substrate (*e.g.* diacid or diester). The substrate acts as the acyl donor and the first transition state (TS1) is formed. The negatively charged part of TS1 is stabilised by three hydrogen bonds (represented by dashed lines) within the oxyanion hole – pocket in the active site formed by two aminoacids that can stabilised negative charges. The positive charge on His^{224} is stabilised by interaction with Asp^{187}. A proton transfer from the His^{224} to the alkyl oxygen of the substrate takes place and the leaving group is released (*e.g.* H_2O when the substrate is a diacid, or an alcohol when the substrate is a diester) leading to the formation of the acyl-enzyme complex. Afterwards, this complex reacts with the incoming nucleophile (*e.g.* diol). A proton is transferred from the diol to the His^{224} residue and a second transition state (TS2) is formed which is stabilised by hydrogen bond interaction with the oxyanion hole. Finally, in a last step, the enzyme is de-acylated to form the ester, which is then released, leaving the free enzyme ready for a new catalytic cycle. (Adapted from Veld and Palmans [103])

Other examples of enzymatic production of polyesters can be found in section 3.2.3.2 of this Thesis.

1.6. Sustainable reaction media – alternative solvents

The sustainability of a synthetic process and the techniques used are also important towards the formation of green products. Avoiding using volatile organic solvents (bulk system) might be the answer. Nevertheless, in polymer chemistry, avoiding organic solvents would not be enough. To decrease the viscosity of the polymer, high temperatures (> 150 ºC) are required.

Supercritical fluids (SCFs) have received a lot of attention as alternative green and sustainable solvents.[104-110]

A SCF can be defined as any substance, above its critical pressure (p_c) and critical temperature (T_c) (Figure 1.25). Once the compound, or mixture, is above the critical points, it exists in only one phase (Figure 1.25 A)). Supercritical fluids are neither a liquid nor a gas (Table 1.3). They can have gas-like diffusivities and low viscosity – which is exceptional for mass transfer properties, and also liquid-like densities – which allow the solvation of many compounds.[111]

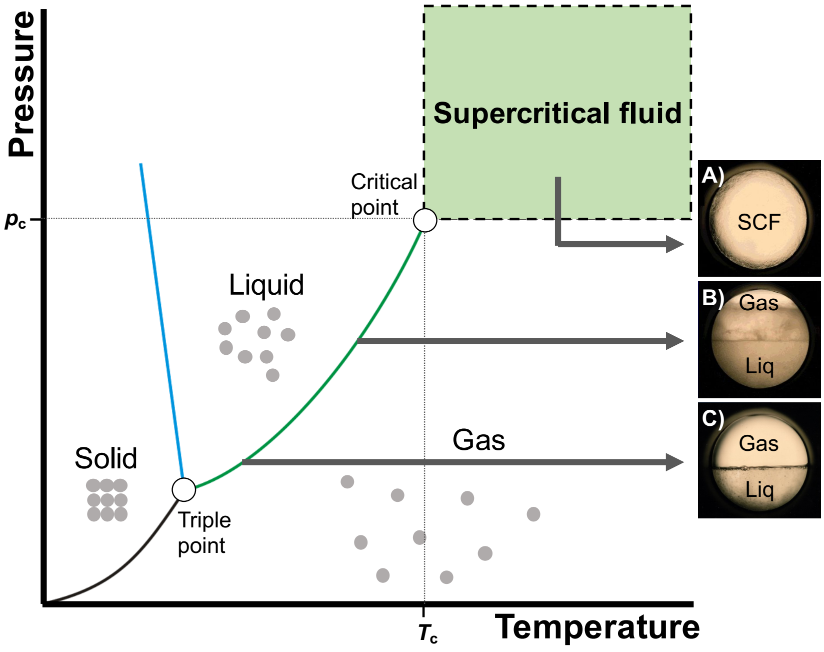

Figure 1.25 – Phase diagram of a SCF, illustrating the temperature-pressure relationship between solid, liquid, gas and supercritical phases. *Note*: p_c = critical pressure and T_c = critical temperature.

Table 1.3 – Comparison of the physical properties of gases, supercritical fluids and liquids.[111]

	Density (ρ, kg m^{-3})	Viscosity (η, Pa s)	Diffusion effect (D, m^2 s^{-1})
Gas	1	10^{-2}	10^{-5}
SCF	100-800	0.005-0.01	10^{-7}
Liquid	10^3	0.05-0.1	10^{-9}

Small changes in the temperature will significantly influence the density of the fluid (Figure 1.26). These tuneable characteristic of SCFs make them interesting reaction media and they have been used in several different fields, such as biodiesel production[110], extractions[104], polymer synthesis[112] and even decaffeination of coffee[107].

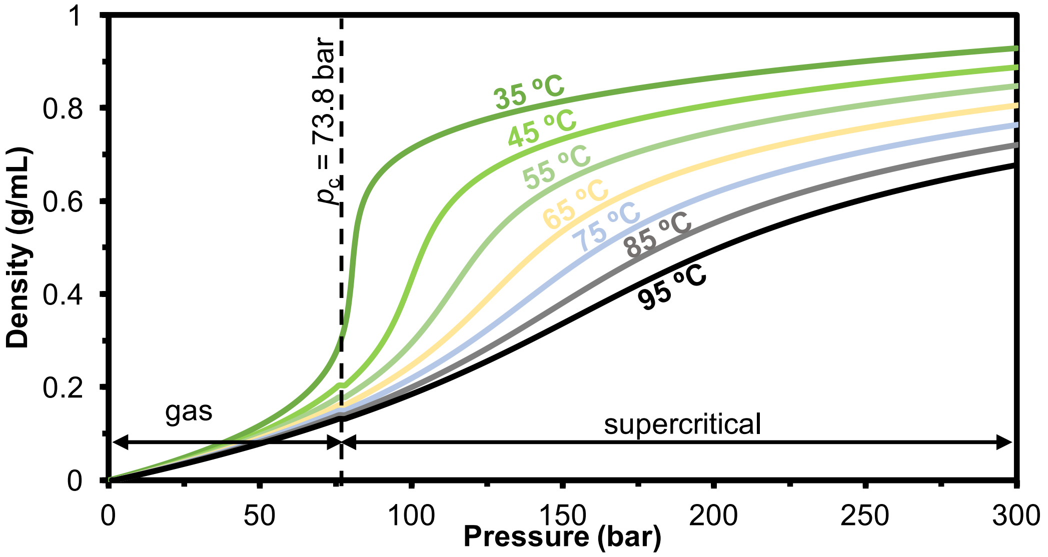

Figure 1.26 – Isothermal change in CO_2 density, increasing the pressure from 0 to 300 bar, at different temperatures. *Note*: the data was obtained from the National Institute of Standards and Technology (NIST).[113]

1.6.1. Supercritical carbon dioxide

With regards to environmental concerns, supercritical carbon dioxide ($scCO_2$) represents an environmentally friendly alternative to traditional solvents. CO_2 is naturally abundant with high purity. Moreover, it is generated in industrial plants (such as ammonia, hydrogen and ethanol plants and in electrical power generation stations), offering opportunities to recycle and reuse it. CO_2 has relatively low critical parameters: p_c = 73.8 bar and T_c = 31.1 ºC. Using $scCO_2$ has several advantages:[114]

1. It is inexpensive

2. Is non-flammable
3. It has low toxicity
4. It is relatively inert
5. It has high mass transfer and diffusivity
6. It generally has the ability to lower the viscosity of reaction media
7. Its density can be easily tuned from gas to liquid values merely by changing the pressure and/or temperature of the fluid[108]
8. It is characterised by a low dielectric constant ($\varepsilon \approx 2$), which make it a good solvent to non-polar molecules with low molecular weight
9. Leaves a clean, dry and solventless product

Moreover, it fulfils several of the 12 principles of green chemistry: 1) prevention, 4) safer chemicals, 5) safer solvents, 7) the use of renewable feedstocks.

Nevertheless, there are certain challenges when integrating $scCO_2$ industrially, including the relatively higher capital cost compared to traditional solvents.[115] Some reactions required polar solvents. Since CO_2 is non-polar and has poor solvent power. Solubility in $scCO_2$ can require much higher pressures for certain classes of solutes when compared with other compressed solvents with higher dielectric constants. However, the polarity of the $scCO_2$ can be increased with the addition of a co-solvent.

1.6.1.1. Extraction of oils using alternative solvents: supercritical carbon dioxide

Since ancient times humans have unconsciously consumed fats and oils through their food *via* plants, fish and meat. The oil was extracted by grinding, bruising or pressing techniques; later these techniques shifted to squeezing/press machines.[116] In the 19th century, Franz Von Soxhlet invented the automated solvent extraction system: Soxhlet extractor (in 1879).[117] In a normal liquid-solid extraction, a sample is placed in a cellulose thimble and positioned in the Soxhlet apparatus, where boiling solvent passes through. After several cycles over many hours, the apparatus is dismantled and the solvent, now containing the extract (*e.g.* oil), is evaporated off, leaving the desired product. Although this technique is still widely used for the extraction of oil from seeds, it has some drawbacks which are not desirable from a sustainable point of view, such as:

a) The use of volatile solvents (for example: *n*-hexane for oil extraction; acetone or methanol for the extraction of polar components; ethyl acetate for the extraction of phenolic compounds, to name a few)
b) The need to use high temperatures
c) It has no selectivity towards triglycerides (when extracting oil). In other words, it extracts everything that is soluble in the solvent used; thus, extra steps would be required to obtained pure oil (triglycerides fraction)

Therefore, a greener more sustainable approach to perform the extraction of oil would be desirable.

Supercritical fluid extraction (SFE) consists of two steps:

i. extraction of compounds soluble in the SCF
ii. separation/fractionation of the extracted solutes from the SCF

Essentially, there are two kinds of extractions, depending on the experiment purpose:[118]

i. Carrier material separator: where the raw material becomes the final product, without the components that are not desirable. An example of this is the decaffeination process of green tea.[119]
ii. Extract material separation: consists of the removal of desirable compounds, from the initial residue. Examples of this extraction technique are the oil (lipids)[120] or antioxidants extraction.[121]

In the first instance, removal of oil with this technology does not appear economical, due to the cost of high-pressure batch processes. However, SFE has been used in the extraction of high-value oils for food, pharmaceutical and cosmetic applications.[122] In fact, SFE of lipids has shown to be an ideal method for extracting certain lipids as an alternative to organic solvent extraction.[123]

When performing an extraction or separation process the most important parameters are the solubility and phase equilibrium of the systems. $scCO_2$ offers unusual possibilities for the selective extraction, fractionation and purification of natural components. It is possible to separate compounds that are soluble in $scCO_2$ by modifying the properties of the solvent. The solvation power of a SCF can be manipulated using pressure and temperature. For example, decreasing the pressure will lead to a reduction in the fluid density and, consequently, a reduction of the solvating power. Increasing temperature will decrease the CO_2 density, leading to a lower solvating power, hence reducing the solute solubility. However, the vapour pressure of the solute is increased with increasing temperature which, in turn increases the solvating power of the $scCO_2$ and also the solute solubility. When extracting an oil, a mixture of fatty acids (FAs) is achieved. The ideal separation process would be by fractionation, based on the different compounds' solubility in $scCO_2$, *i.e.* the desirable compounds should be insoluble and the others compounds soluble in $scCO_2$. Thus, having multiple separators would be ideal to collect the desired product. In 1992, Hartel *et al.*[124] studied the solubility of fatty acids in $scCO_2$ and the possibility of fractionating the FAs in this medium. The authors studied the effect of temperature and pressure on solubility of the following FAs: lauric, linoleic, myristic, oleic, palmitic and stearic acid.

1.6.1.2. Supercritical carbon dioxide polymerisations

In the field of polymer synthesis, $scCO_2$ is used as a solvent not just from environmental incentive, it has many other benefits. For example, as CO_2 is a gas at ambient conditions, by simply depressurising the system a dry, solvent free polymer is obtained. This removes the need for post polymerisation drying steps.[125] A further advantage of using $scCO_2$ is that it can decrease the viscosity of a system, removing the need for high temperature usually needed to reduce viscosity in traditional polymerisation.[126] Both of these advantages decrease energy-intensive procedures that can be associated with polymerisation and thus result in a reduction of potential cost.[114]

Under $scCO_2$ conditions, the most important effects on polymerisation reactions include the reduction of the glass transition temperature (T_g) of glassy polymers (plasticisation) allowing changes in polymer processing: physical properties (viscosity reduction), morphologies and subsequently permeable membrane.[108] Moreover, in certain polymerisation reactions, such as condensation reactions, by-products, like water and hydrochloric acid, can be removed easily using $scCO_2$, which will promote the reaction towards product formation.[109, 127-128]

1.6.1.3. Interaction of supercritical carbon dioxide with polymers

With the exception of fluorinated, silicone and a few vinyl polymers, $scCO_2$ is a poor solvent for the most polymeric chains since they are partially or completely insoluble.[115, 129-131] However, CO_2 interacts with carbonyl and ether oxygens in esters and polyesters (Figure 1.27). Depending on the steric hindrance in the polyester chain the magnitude of attractive energy will be different.[132] These interactions are crucial for the synthesis of polymers using $scCO_2$. As aforementioned, $scCO_2$ is very effective at penetrating between the polymeric chains, plasticising and liquefying several polymers, below their T_g.[108] This occurs due to the interaction of CO_2 and the polymer backbone and is a very important feature to process polymers. When using $scCO_2$, the need to use high temperatures to decrease the viscosity of the polymer can be avoided. The increasing of the space and the free volume fraction between the polymeric chains in the presence of $scCO_2$, allows them to slide past each other. Hence, CO_2 act as plasticiser (*e.g.* decreases the viscosity).[133]

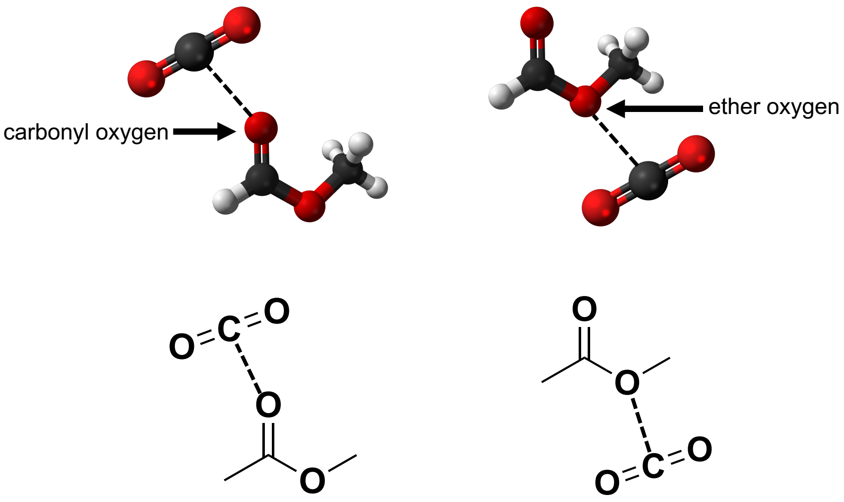

Figure 1.27 – Schematic representation of the interaction between carbonyl and ether oxygens with CO_2. *Note*: red, dark grey and white spheres represents oxygen, carbon and hydrogen atoms, respectively. (adapted from Kajiya*, et al.* [132])

1.6.1.4. Supercritical carbon dioxide enzymatic polymerisations

As mentioned before, as well as the fact that enzymes are environmentally acceptable, they can also be highly active and selective and they can mediate polymerisations. A combination of enzymatic polymerisations using $scCO_2$ as an alternative solvent is a method that has been actively studied over recent years.[134] Lopez-Luna*, et al.* [135] performed the synthesis of polyester (poly(δ-valerolactone)) using CaLB (10 wt.%) and $scCO_2$. A polymer with a maximum M_n of 28,000 Da with a PDI of 1.6 was obtained at 65 °C, 300 bar for 72 hours. A conversion of 68% was achieved.

The inherent gas-like low viscosity and high diffusivities of SCFs increases the rate of mass transfer of the substrates to the enzyme. Moreover, the liquid-like densities of SCFs result in higher dissolution.

The stability and activity of enzymes under $scCO_2$ conditions depends on the type of enzyme, the amount of water and the conditions applied into the system. Additionally, the depressurisation step is important as it could lead to a decrease in enzyme activity.[114]

1.7. Research aims

The key aim of this Thesis is to synthesise polyesters using greener approaches, focusing on the use of enzyme catalysis (CaLB) and supercritical carbon dioxide as the reaction medium.

Initially, this Thesis will focus on the use of glycerol to synthesise linear glycerol-based polyesters with a more sustainable approach. In the literature, the polycondensation of glycerol with diacids is often done at high temperatures (> 150 ºC), resulting in branched or cross-linked polymers. In addition, for the production of linear polyol-based polyesters, additional protection and deprotection steps are required, which in terms of green and sustainable chemistry is not ideal. Therefore, in this work, different catalysts are assessed (metal and bio-catalysts), at milder conditions than the ones stated in the literature (bulk reactions at < 140 ºC; $scCO_2$ reactions at 40, 50 and 60 ºC) to test the hypothesis that it is possible to obtained linear polyol-based polyester at near ambient temperatures with similar properties. The studies were supported by ^{1}H-NMR, ^{13}C-NMR, GPC, MALDI, FTIR and DSC.

Afterwards, we will focus in the conversion of poly(glycerol succinate) into a biorenewable and biodegradable surfactant at milder conditions than the ones indicated in the literature (> 200 ºC). Using $scCO_2$ and CaLB, we will focus on the functionalisation of PGLSA with lauric acid or methoxy poly(ethylene glycol). Application testing is carried out to test the proposition that PGLSA can be converted into a biodegradable surfactant, confirming its surface active properties (*via* several experiments).

Finally, this Thesis also investigates the synthesis of new building blocks from vernolic acid, a fatty acid present in ironweed (*Vernonia galamensis* sp.). Literature lacks demonstrable evidence of using natural epoxy oil to synthesise valuable building blocks for the production of polyesters. Therefore, this work will focus on the green extraction of vernonia oil from ironweed using $scCO_2$. Upon isolation of the vernolic acid, the synthesis of novel AB_2 and A_2 type monomers, valuable for polycondensation, is evaluated. Subsequently, the synthesis of the vernolic acid-based polyesters will be considered, through polycondensation. The condensation of AB_2 and A_2 + B_2 monomers is normally performed under harsh conditions (> 200 ºC). In this work, we will focus on using $scCO_2$ as reaction medium to do the polycondensations. The studies were supported by ^{1}H-NMR, GPC, and DMA.

CHAPTER 2. EXPERIMENTAL AND ANALYTICAL METHODS

2.1. Overview

This chapter describes in detail the experimental high pressure apparatus and the analytical techniques used to characterise the products obtained throughout the Thesis.

Firstly, the general high pressure setup used for polymerisations (Chapter 3, Chapter 4 and Chapter 6) is here described. Information on the specific equipment used to carry out polymerisations and the standard operating procedures are given. The following equipment was used:

A. Fixed volume view cell: to study the behaviour of samples in carbon dioxide, which is achieved using an in-house built stainless steel view cell equipped with sapphire windows.
B. Autoclave: the in-house built clamp-sealed stainless steel autoclave used for polymerisations.

Also in this chapter, the following analytical techniques, which were used throughout the projects are described: nuclear magnetic resonance spectroscopy (NMR), electrospray ionisation time-of-flight mass spectrometry (ESI-TOF), matrix assisted laser desorption/ionisation time-of-flight mass spectrometry (MALDI-TOF), gas chromatography (GC), gel permeation chromatography (GPC), fourier-transform infrared spectroscopy (FTIR), differential scanning calorimetry (DSC) and dynamic mechanical analysis (DMA). The analytical methods used to assess the performance of synthesised polymers as surfactant are also described in detail; the surface tension was measured by the Wilhelmy plate method and bubble pressure tensiometer. To analyse the size of the potential surfactant particles, dynamic light scattering (DLS) was used.

Information regarding the reactants, solvents, reaction conditions and reaction procedures can be found in the experimental part of the individual chapters.

2.2. High pressure equipment

2.1.1. High pressure setup for polymerisation

2.1.1.1. Carbon dioxide pump

For all high pressure experiments, pressurised CO_2 (BOC, 99.99%) was delivered to the autoclave using PM-101 SFE Pickel pump (New Ways of Analytics, Germany). The pump is composed of a gas input, a refrigerator unit for gas liquefaction and an outlet. The pump draws gaseous CO_2 from a CO_2 cylinder (at a pressure of ~55 bar) and the gas is condensed into liquid by the pump refrigerator (Figure 2.1). Compressed air at 3-5 bar (supplied by an external compressor) is used to compress the liquefied CO_2 and achieve the desire output pressure (200 – 300 bar) which can be set *via* an external knob on the pump.

Swagelok® high pressure stainless steel tubing was used to transport the liquefied CO_2 to the autoclaves. Manual HiP valves (High Pressure Equipment Company, USA) were employed to control the CO_2 inlet and outlet flows when filling the autoclaves and, at the end of the reactions, venting the system. Non-return valves (NRV) were also employed before each autoclave, to prevent backflow and hence avoid contamination of the CO_2 supply line and pump.

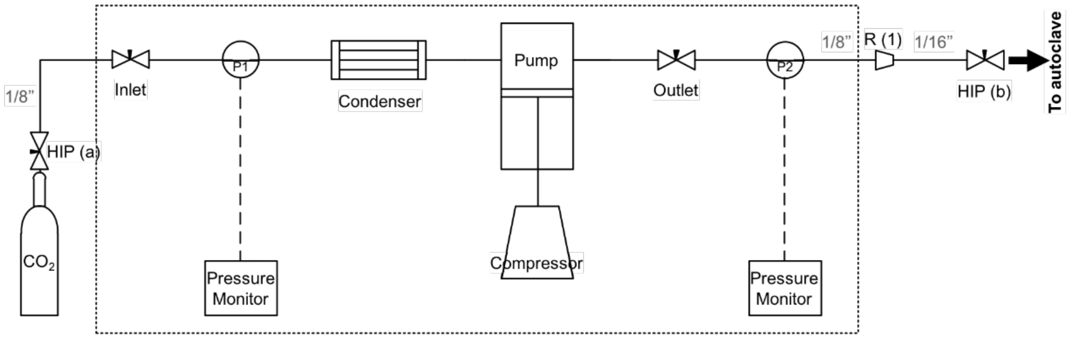

Figure 2.1 – Scheme of the high pressure pump (PM-101 SFE Pickel pump). *Note*: HIP = Manual HiP valves; P1/2 = pressure transducer 1/2; 1/8'' = pipe with a diameter of 1/8''; 1/16'' = pipe with a diameter of 1/16''; R (1) = reduction union 1.

2.1.1.2. High pressure clamp seal autoclave

All polymerisations performed under supercritical conditions were conducted using a 20 or 60 mL stainless steel high pressure reactor (autoclave). These autoclaves were design and built at the University of Nottingham.

The autoclave consists of two parts: the top (or head) and the base (or body) (Figure 2.2 and Figure 2.3). The head (Figure 2.3 c)) is attached to the body (Figure 2.3 d)) with a stainless-steel clamp (Figure 2.3 e)). To create a seal between the autoclave head and base, an O-ring, made of ethylene propylene diene monomer rubber (EPDM), is used. The clamp, which holds the head and base together secured by a screw mechanism is tightened with a distinctive key (Figure 2.3 i)). The safety-needle and torque thumbwheel are unique for each clamp and, therefore, to each autoclave. In addition, this key is used as a safety needle assembly (Figure 2.2 f) and Figure 2.3 f)), which is screwed into the autoclave head to create a seal before pressurising. The maximum working conditions of the autoclave is 300 bar and 300 ºC.

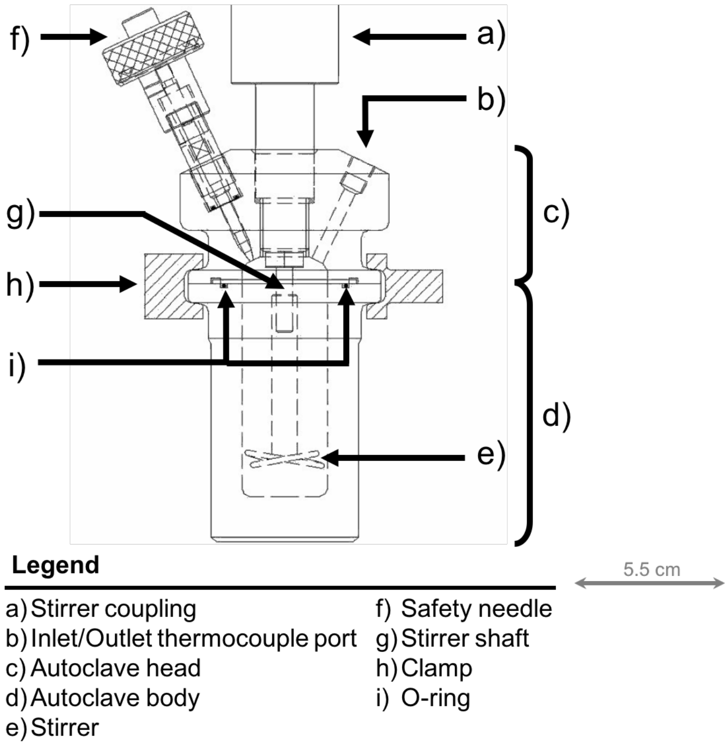

Figure 2.2 – Cross-section view of the stainless steel high pressure reactor (autoclave). *Note*: the inlet port fittings have been omitted to simplify the cross-section view.

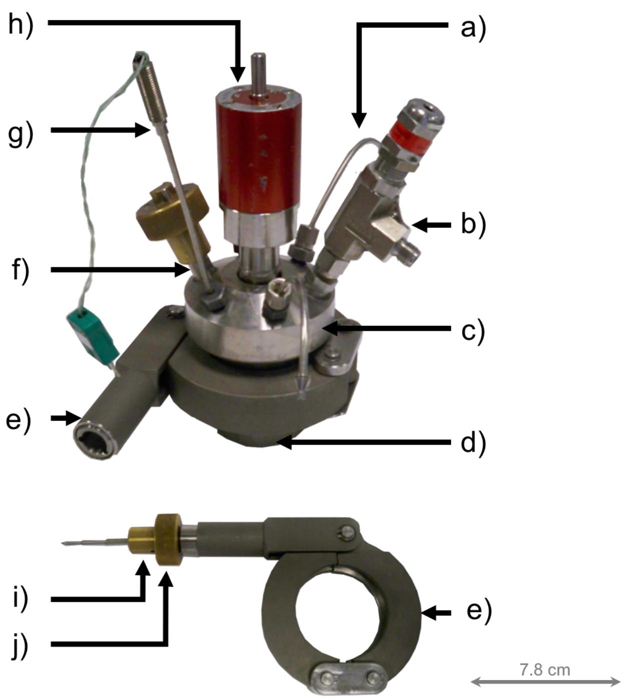

Legend

a) 1/8” inlet/outlet pipe
b) Spring loaded pressure relief valve
c) Head
d) Base
e) Clamp
f) Screw insert
g) Thermocouple
h) Magnetically coupled overhead stirrer
i) Safety needle
j) Torque thumbwheel

Figure 2.3 – Stainless steel autoclave with a 20 mL base.

The autoclave was designed to include various safety features:

a) The clamp cannot be unscrewed while the autoclave is under pressure. Nevertheless, in the case of valve blocking, or pipe blocking, during the venting process, the key can be loosened slowly, to allow residual pressure to be released *via* its vent hole
b) The temperature and pressure monitors are connected to a trip box. To avoid overpressure, this trip is set to a maximum of 130 ºC and 300 bar.

The temperature inside the autoclave is monitored using a thermocouple (chromel-alumel) (RS Instruments, type-K) (Figure 2.3 g)) which is connected to a digital heating controller (made in-house), which is linked to an external heating jacket (Watlow, UK) attached around the base of the autoclave. This allows the autoclave to be heated to the desired reaction temperature. The pressure is monitored using a quartz piezoelectric transducer (RDP Electronics, UK), which emits an electrical current when the quartz crystal experiences strain under pressure. The transducer is connected to a digital controller (University of Nottingham) which shows the pressure in pounds-per-square-inch (PSI; 1 bar = 14.5 PSI) (Figure 2.4 T1). A calibration is performed by the manufacturer, allowing precise and reproducible readouts. If the reaction overpressures (> 300 bar), the trip box would cut the power to the heating jacket (Figure 2.4). Therefore, the temperature will decrease and consequently, the pressure. The spring loaded pressure relief valve (SS-4R3A, Swagelok®) is integrated in the head of the autoclave as a further safety feature to prevent the system exceeding safe working pressures (> 345 bar) (Figure 2.3 b)). For a normal reaction, a plate seals this valve, held tight by the spring of pre-set tension. In the event of over pressure, this plate and spring will drive back to reveal an exit route for the pressure, venting the system and, therefore, decreasing the pressure. All reactions were stirred using a magnetic coupled overhead stirrer, linked to a motor (IKA Works GmbH, Germany), typically set to 150 rpm (Figure 2.3 h)). All the pipes used in the set-up are from Swagelok®. 1/8’’ inlet and outlet tubing (SS316, Swagelok®) are connected directly to the autoclave. Reducing unions (Figure 2.4 R(1), R(2) and R(3)) are used to connect the set-up to the associated pipe work.

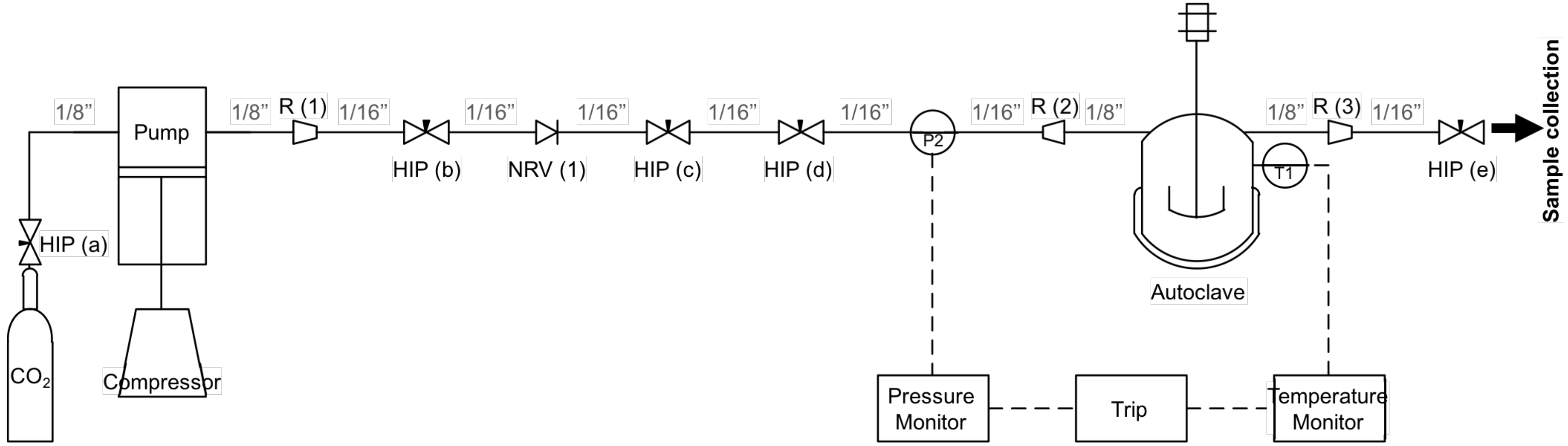

Figure 2.4 – Scheme of the individual high pressure set-up. *Note*: HIP = Manual HiP valves; 1/8’’ = pipe with a diameter of 1/8’’; 1/16’’ = pipe with a diameter of 1/16’’; P1/2 = pressure transducer 1/2; R (1/3) = reduction union 1/3; R (2) = increasing union 2. T1 = thermocouple 1.

2.1.1.2.1. Standard operation procedure

Before conducting any experiment using $scCO_2$, the equipment set-up must be leak tested:

A. Leak testing

1. The autoclave was fully assembled by placing an EPDM O-ring between the head and body of the autoclave. The two parts were then clamped together. The clamp was tightened using the safety key, which was then screwed into the head. The inlet and outlet pipes were connected and the Swagelok® fittings tightened, then the heating jacket was secured around the body.
2. The thermocouple was connected to the control box to monitor the internal temperature of the autoclave.
3. The set-up was leak tested by pressurising to ~50 bar (with CO_2) at room temperature. All fittings were checked with a leak detecting fluid called Snoop®.
4. If a leak was detected, the autoclave was vented to ambient pressure through the outlet HiP tap (Figure 2.4 HIP (e)) and any leaking fittings were tightened. Fittings were never tightened under pressure.
5. Steps 3 and 4 were repeated until no leaks persisted.
6. Residual pressure from the leak test was vented until the autoclave was at atmospheric pressure.

Following the leak test and to minimise risks and increase safety of the high pressure polymerisations, the following standard operation procedure (SOP) was followed:

B. Polymerisation using supercritical carbon dioxide

7. The vessel was opened and the appropriate amount of reactants, catalyst and molecular sieves were added to the base (of the autoclave).
8. The autoclave was once again clamped together and purged, through the key hole, with a flow of CO_2 (2 bar) for five minutes to flush out residual air from the system.

9. After this time, the safety key was screwed into the head to seal the vessel.
10. The stirrer was switched on (150 rpm) and the vessel pressurised to around 50 bar.
11. The heating jacket was connected to the control box and the temperature set to the desired value with the pressure monitored throughout the heating process.
12. The autoclave was allowed to reach its final temperature and the pressure was increased to the desired value, if necessary, by slow addition of CO_2.
13. After the desired time, the reactions were stopped setting the temperature controller to 0 ºC and removing the heating jacket before, placing the vessel in a water/ice bath (0 °C).
14. Once the pressure was below 20 bar, the CO_2 was vented by opening the outlet HiP tap (Figure 2.4 HIP (e)). Generally, this would take 20 minutes.
15. Once at ambient temperature and pressure, the safety key was removed from the head of the autoclave and the Swagelok® fittings undone.
16. Finally, the clamp was opened and the product collected.

2.1.2. High pressure fixed volume view cell

To study the behaviour of samples under $scCO_2$ conditions, a fixed volume (100 mL) view cell was used (Figure 2.5**,** Figure 2.6 and Figure 2.7). The fixed volume view cell was built at the University of Nottingham and is similar to the autoclave (described above, Figure 2.2). It consists of a body, heated by internal cartridges (Watlow, UK), attached to two heads each containing a sapphire window, using the same key and clamp system. The autoclave is kept horizontal, on a purpose-built stand, and secured in a place using a clamp system. The maximum operating condition for the system is 100 ºC and 300 bar.

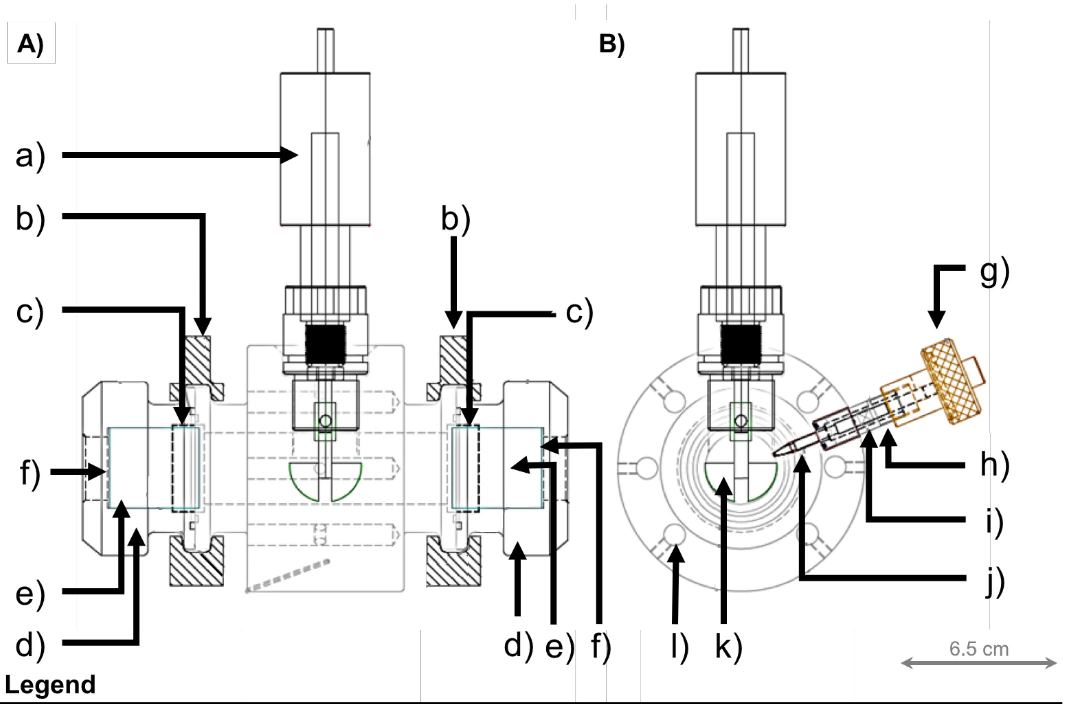

Legend

a) Magnetically coupled overhead stirrer
b) Front/back clamp
c) O-Ring
d) Head
e) Sapphire window
f) Teflon spacer
g) Torque thumbwheel
h) Vent hole
i) Screw insert
j) Safety needle
k) Stirrer blade
l) Heating cartridges

Figure 2.5 – Schematic of the 100 mL clamp-sealed stainless steel autoclave with two view ports; A) side view and B) front-end view of the view cell.

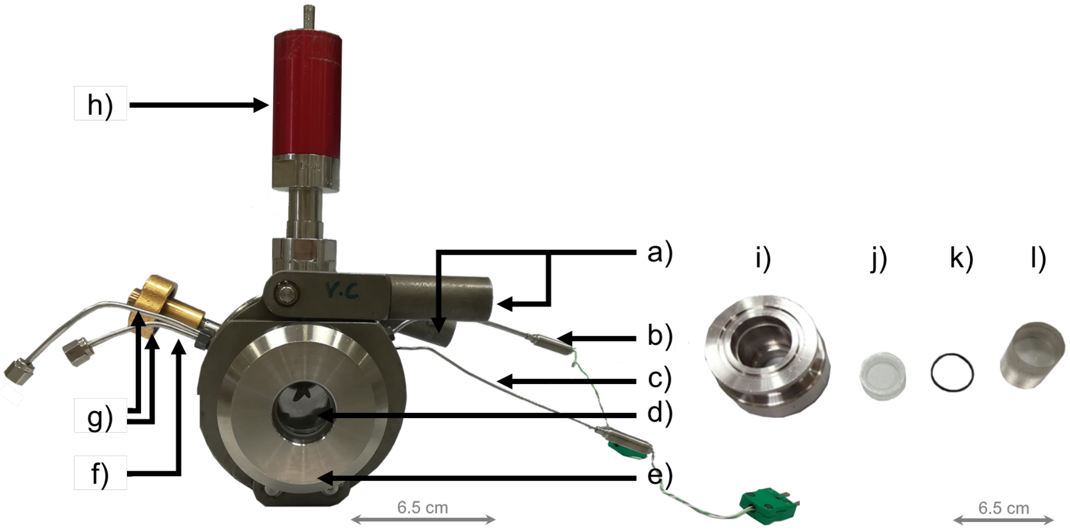

Legend

a) Back/front clamps
b) Internal thermocouple
c) External thermocouple
d) Sapphire window
e) Head
f) Safety key
g) Inlet/outlet pipes
h) Magnetically coupled overhead stirrer
i) Head
j) *Teflon* spacer
k) O-Ring
l) Sapphire window

Figure 2.6 – Fixed volume view cell (100 mL) demonstrating the autoclave set-up (left) and the i) head, j) *Teflon* spacer, k) O-ring and l) sapphire window (right)

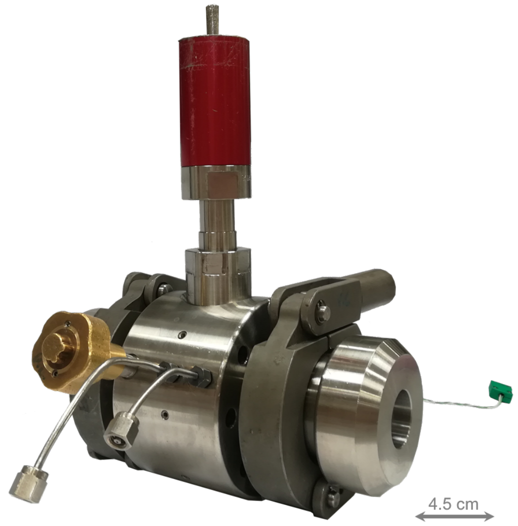

Figure 2.7 – Side view of the fixed volume view cell (100 mL).

The body of the view cell contains a CO_2 inlet and a CO_2 outlet pipe. The autoclave temperature (internal and external) is monitored by two thermocouples type-K (chromel-alumel, RS Components, UK), which are connected to a digital heating controller CAL-3300 (CAL Controls, USA). A transducer is placed close to the inlet pipe, in order to monitor the system pressure. For safety purposes, a trip switch (connected to the pressure box and temperature monitor) is included in the system. The presence of a magnetically coupled overhead stirrer allows the possibility to stir constantly, if needed. Nevertheless, in this Thesis, this was not used.

2.1.2.1. Standard operation procedure

The standard operation procedure (SOP) for the high pressure fixed volume autoclave was as follow:

1. The view cell was fully assembled:
    a. EPDM O-rings were fitted around each sapphire window;
    b. *Teflon* spacers were put between the windows and the relative heads (to ensure the sapphire windows were pressing against a soft surface and also to create a seal);
    c. The head was laid onto a level surface and the sapphire windows were fully inserted;

   d. An EPDM O-ring was placed in the rear end of the autoclave body, then the back head and body were clamped together (tightening the clamp with the safety key). The body was positioned on a purpose-built stand and secured in place in the fume hood. The inlet and outlet pipes were attached and the Swagelok® fittings tightened;
   e. The heating cartridges were inserted into the body, then an EPDM O-ring was placed in the front end of the body and then the front head was clamped to the body. The clamp was tightened using the safety key, which was then screwed into the body of the autoclave.
2. The internal and external thermocouples were connected to the control box.
3. A polycarbonate safety screen was positioned in front of the autoclave. This was only removed when the autoclave was at ambient pressure.
4. The set-up was leak tested by pressurising to ~40 bar (using CO_2). All fittings were checked for leaks with a leak detecting fluid called Snoop®.
5. If required, the autoclave was vented to ambient pressure through the outlet HiP tap and any leaking fittings were tightened.
6. Steps 4 and 5 were repeated until no leaks remained.
7. Residual pressure from the leak test was vented until the autoclave was at atmospheric pressure. The key was removed and the front end of the autoclave was opened. The solid materials (polymer or monomer) contained in an open glass vial (the vial was kept in place by using Blue-Tack) were placed inside. The front end was then re-sealed.
8. The safety screen was positioned again in front of the window.
9. The pressure was increased to ~50 bar.
10. The control box was set to heat to the desired temperature with the pressure monitored throughout. Typically, a difference of 2–3 °C was observed between the internal and external thermocouple. This is due to the thickness of the autoclave walls.
11. When the temperature reached the set value, the pressure was increased to the experimental desired value by slow addition of CO_2.
12. At the end of the experiment, the heating cartridges were switched off allowing the temperature of the autoclave to drop to room temperature.

13. The CO_2 was vented into the fume hood by opening outlet HiP tap. This was done slowly (over a 45 minute period) to avoid excessive foaming of the polymer and to reduce stress on the sapphire windows.
14. Once at ambient temperature and pressure, the safety key was removed, and the front-end clamp opened, to retrieve the sample.

2.3. Analytical methods

This section will include the techniques used to characterise the products throughout the project.

2.1.3. Nuclear magnetic resonance spectroscopy

Nuclear magnetic resonance (NMR) is a common technique used to confirm the identity of compounds, containing a NMR active nuclei.[136] In this Thesis ^1H and ^{13}C were performed, with a nuclear spin quantum number of ½.

All the spectra were recorded on a Bruker Advance III HD 400MHz or Bruker Advance 400MHz, with chemical shifts, in ppm, referenced relative to a deuterated solvent (normally chloroform-d_1 (7.26 ppm), acetone-d_6 (2.05 ppm) or methanol-d_3 (3.31 ppm)). Sample concentration was 7 mg/mL. Mestrelab MNova software was used for analysis.

2.1.4. Mass spectrometry

2.1.4.1. Electrospray ionisation time-of-flight mass spectrometry

A Bruker microToF LC-MS spectrometer was employed for the characterisation of compounds, with 1 mg/mL, dissolved in 50:50 MeOH:H_2O (v/v) or 60:40 EtOH:H_2O (v/v). Spectra were analysed using Compass DataAnalysis software.

2.1.4.2. Matrix assisted laser desorption/ionisation-time of flight mass spectrometry

A Bruker Ultraflex III spectrometer was used for the analysis of the glycerol-based polymers. The spectra were collected in reflection mode and analysed using FlexAnalysis software. For the sample preparation, 20 µL of a polymeric solution in methanol (10 mg/mL) was mixed with 20 µL of a solution of matrix *trans*–2–[3–(4–*tert*–butylphenyl)–2–methyl–2–propenylidene] malononitrile (DCTB) (1 mg/mL) in acetonitrile. 1 µL of this mixture was spotted on the target plate (designated for polymer samples) and allowed to air dry before the plate was inserted into the instrument for analysis. In matrix assisted laser desorption/ionisation mass spectrometry (MALDI MS), a laser vaporizes the sample which is associated with the matrix compound to minimize fragmentation. Ions are separated using time of flight mass spectrometry (TOF MS), which is well adapted for the detection of low and high M_n polymer species.

2.1.5. Gas chromatography

Gas chromatography was performed on an Agilent 6890 GC coupled to Agilent 5973 MS (EI detector) instrument equipped with a Zebron ZB5-MS column (30m x 0.25mm x 0.25 µm). The temperature program used was from 60 ºC (1 min hold) and 60 ºC/min to 300 ºC (10 min hold); the injection temperature was at 250 ºC with 50:1 split ratio; the carrier gas was helium. For the analysis of lipids, the oil needs to be derivatise, including hydrolysis and methylation. Therefore, on a typical procedure, 100 mg oil was dissolved in 10 mL hexane.100 µL of 2 N potassium hydroxide in methanol (11.2 g in 100 mL methanol) was added to the solution. The mixture was submitted to vortex for 30 seconds and the clear supernatant was transferred into a 2 mL autosampler vial.

2.1.6. Gel permeation chromatography

Gel permeation chromatography (GPC) is an essential technique for polymer analysis. It separates polymer samples by weight fractions to determine M_n, M_w and Đ, based on the polymers hydrodynamic volume in solution.[137] In this Thesis, this information was obtained using an Agilent 1260 infinity multidetector GPC/SEC (size exclusion chromatography) system with a Wyatt Optilab light scattering detector. The GPC was equipped with two columns; an Agilent PLGEL 5 µm Mixed D (7.5 mm X 300 mm) and a PLGEL 5 µm guard column (7.5 mm X 50 mm). THF was used as the eluent at a flow rate of 1 mL/min and the following differential index of refraction values (dn/dc) were used for evaluation: for glycerol-based polymers 0.0304 mL/g and for vernonia-based polymers 0.1133 mL/g. The samples to be analysed (10 mg/mL) were passed through a syringe filters (Whatman, 25 mm, 0.2 µm) prior to analysis. The software used for analysis was Astra® 6 (Wyatt).

2.1.7. Fourier-transform infrared spectroscopy

Fourier-transform infrared spectroscopy (FTIR) is a valuable analytical technique for identification of functional groups in polymeric samples. In this Thesis, FTIR analyses were carried out using a Bruker Alpha Platinum-ATR, allowing the possibility of analysing solid samples in the absence of solvents. This instrument was equipped with a RockSolid™ interferometer. All experiments were run in attenuated total reflection (ATR) mode using a platinum ATR single reflection diamond. The spectra were acquired with a resolution of 4 cm^{-1}, in the range 4,000–400 cm^{-1} by recording 36 interferograms. The software used for analysis was OPUS Spectroscopy.

2.1.8. Differential scanning calorimetry

The thermal properties of the synthesised polymers were investigated using differential scanning calorimetry (DSC). This technique monitors the different in heat flow rate between a sample and a reference while both are subjected to a controlled temperature set-up programme. This technique gives the valuable information regarding the melting points (T_m) and glass transition temperatures (T_g) of the polymers.

The DSC used was a TA Instruments Q2000, equipped with an auto-sampler, suitable for use from -90 to 300 ºC, using indium and sapphire standards. Tzero aluminium pan (TA instruments) were used for all samples and pressed prior to use. In a normal experiment, a polymeric sample (*ca.* 2 mg) was cooled to -90 ºC (10 ºC/min) and then heated to 200 ºC (10 ºC/min). Afterwards, the sample was cooled again to -90 ºC (10 ºC/min) and then heated up to 200 ºC (10 ºC/min). The first heating cycle was used to remove the thermal history of the sample and the T_m and T_g were recorded from the second heating cycle. The experiments were carried out under a N_2 flow (50 mL/min). All the data were analysed using the Universal Analysis software.

2.1.9. Dynamic mechanical analysis

The glass transition (T_g) of the synthesised polymers was also investigated using dynamic mechanical analysis (DMA). Measurements were performed on a Triton Technologies DMA (now Mettler Toledo DMA1), using the powder pocket accessory. 5 mg of sample was weighed into a powder pocket and measured at 1 and 10 Hz in single cantilever bending geometry between -100 – 250 °C. The determined value of T_g was taken as the maximum peak of the tan delta (tan δ) curve, at a frequency of 1 Hz.

2.1.10. Surfactant performance assessment

In order to evaluate the surfactant performance of the synthesised polymers, several analysis techniques were performed to determine the surface tension, critical micelle concentration, size of micelles and also the contact angle.

2.1.10.1. Tensiometry

2.1.10.1.1. Static: Wilhelmy plate method

The Wilhelmy plate tensiometer was used to measure the static surface tension of water, upon addition of potential surfactants. A flat platinum plate is dipped into the aqueous solution and slowly pulled back and held within 1 µm of the surface position. The surface is allowed to relax and reach an equilibrium with the plate present. Afterwards, the force on the plate is measured and surface tension (mN/m) determined from the force (F) and the contact angle formed (θ) (Equation 2.1). If the potential surfactant has good surface active agent properties, the surface tension of the aqueous solutions will be lower than ~72 mN/m, which is the surface tension of pure water.

$$\mathrm{SFT} = \frac{F}{L \cdot \cos(\theta)}$$

Equation 2.1 – Equation to determine the static surface tension (SFT) through the Wilhelmy plate method. *Note*: F = force applied to the flat platinum plate; L = wetted length of the plate, which corresponds to its perimeter; θ = contact angle.

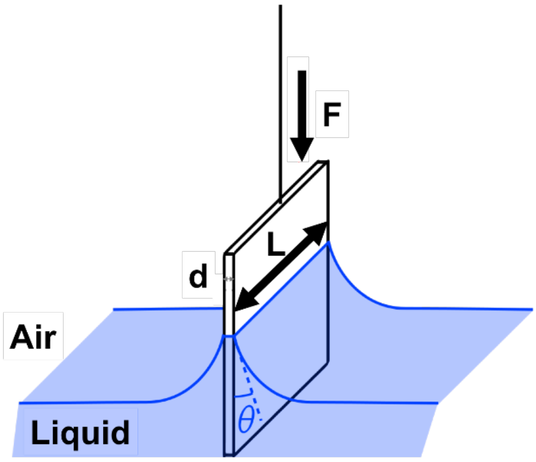

Figure 2.8 – Schematic representation of the Wilhelmy plate method. *Note*: F = force applied to the flat platinum plate; L = wetted length of the plate, which corresponds to its perimeter; θ = contact angle; d = diameter of the plate. This image was adapted from KRÜSS GmbH.[138]

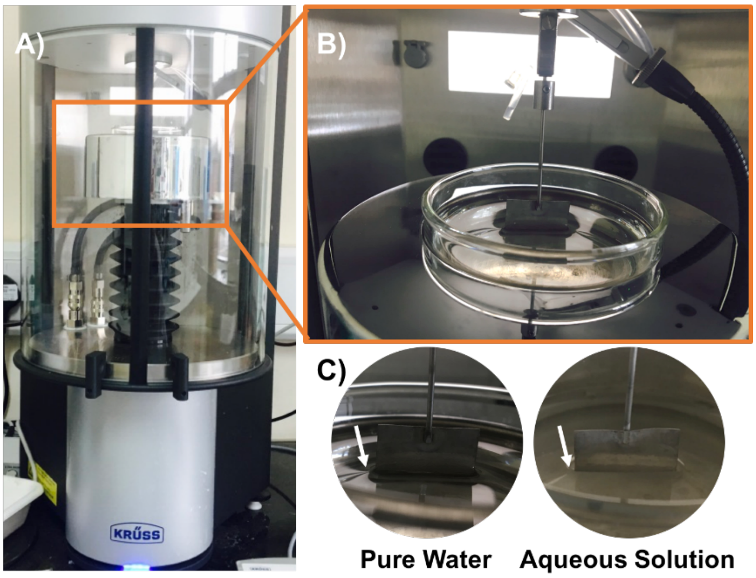

Figure 2.9 – Images of the instrument used to measure the static surface tension. A) Wilhelmy plate tensiometer, Krüss. B) Image highlighting the flat platinum plate submerging a liquid. C) Images showing before (pure water) and after (aqueous solution) the addition of surface active agents. Image C shows that the pure water sample has a higher surface tension, indicated by the contact angle compared to the aqueous solution containing surfactant.

The analyses were performed using a Krüss Tensiometer K100 (KRÜSS GmbH). Mili-Q water was used for the aqueous solutions of surfactant (typically 1 wt.%). The surface tension values were determined by the automatic dilution of the stock solutions using a Metrohm 700 Dosino. Before each experiment, the platinum plate was rinsed with Milli-Q water and flamed afterwards to dry it and remove any potential impurities. In a typical experiment, a sample is automatically diluted, and a measurement of the surface tension is recorded at every 3 minutes. All measurements were performed at ambient temperature (~ 20 ºC). The range of the equipment was 1–300 mN/m at a resolution of ± 0.01 mN/m. Each recorded value was an average of ~ 10 runs, until a standard deviation of ≤ 0.1 mN/m was obtained. Measurements were made in duplicate.

2.1.10.1.2. Dynamic: bubble pressure tensiometry

The bubble pressure tensiometer measures the dynamic surface tension before equilibrium is reached (Figure 2.10 and Figure 2.11). In the method used, a capillary tube (Figure 2.11 a)) is submerged in an aqueous solution.[139] From this tube, bubbles of air are periodically released (at increasing rates). The pressure within the tube changes continuously as the radius of the bubble

(r_B) changes. When the radius of the capillary tube (r_{cap}) and the radius of the bubble curvature (r_B) are equal, the maximum pressure is reached (Figure 2.10 B). The pressure drops rapidly as the bubble expands beyond r_{cap} (Figure 2.10 C).

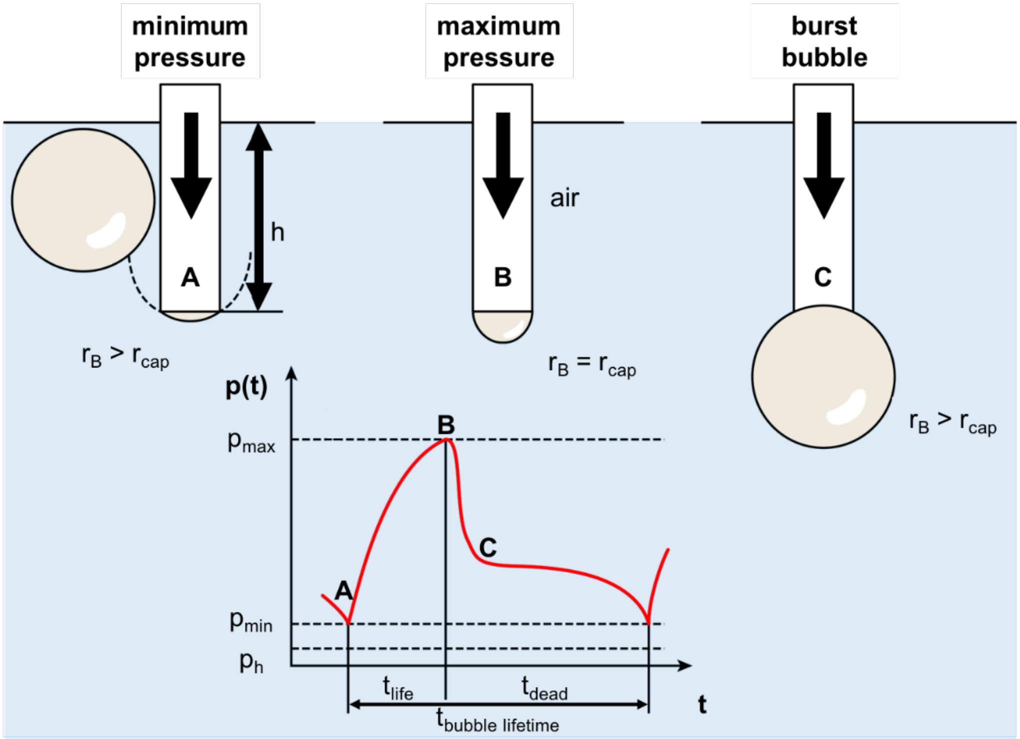

Figure 2.10 – Schematic representation of the bubble pressure during surface tension measurements. *Note*: r_B = radius of bubble; r_{cap} = radius of capillary; $t_{bubble\ lifetime}$ = life time of the bubble, in seconds; p_{max} = maximum bubble pressure measured; p_{min} = minimum bubble pressure measured. This image was adapted from SITA®.[140]

The surface tension value was calculated from the deviation between the pressure maximum and minimum (Equation 2.2). Before each measurement, the instrument was calibrated with pure water. Therefore, the instrument will take into consideration the radius of the capillary tube.

$$SFT=k \cdot (p_{max} - p_{min})$$

Equation 2.2 – Surface tension (SFT) determined using the bubble pressure method. *Note*: k = calibration factor (m), determined automatically in pure water (typically equal to the radius of the capillary tube divided by two; p_{max} = maximum bubble pressure measured (N/m^2); p_{min} = minimum bubble pressure measured (N/m^2).

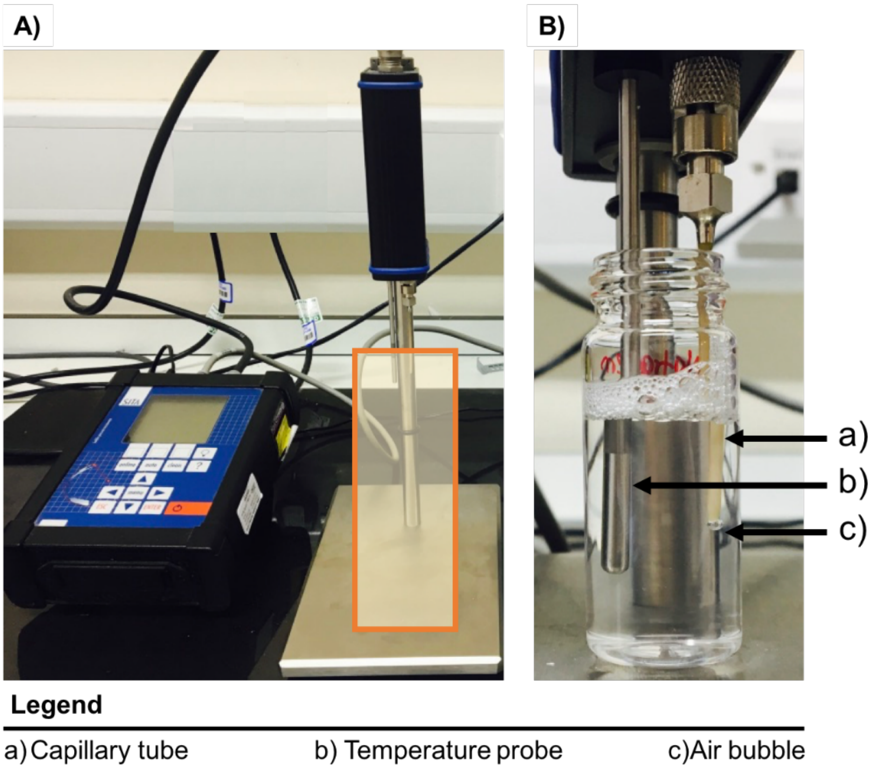

Figure 2.11 – Bubble pressure tensiometer apparatus. A) Image showing the SITA t100 bubble pressure tensiometer; the highlighted area denotes where the aqueous solution to be analysed is placed. B) Image showing the capillary tube (a), the temperature probe (b) and the formation of the air bubble (c).

For each SFT sample measurement, aqueous solutions with typically 0.1, 0.5 and 1 wt.% of surfactant were tested using a SITA® t100 Bubble Pressure tensiometer (Figure 2.11). This instrument can measure SFT ranging from 10–100 mN/m ± 0.1 mN/m.

2.1.10.1. Dynamic light scattering

Dynamic light scattering (DLS) analyses were performed using a Malvern Zetasizer Nano ZS system in order to determine the hydrodynamic diameter of the polymeric particles in water. Polystyrene disposable cuvettes were used and the samples were not filtered to retain information on the possible presence of microscopic aggregates. The analyses were performed at ambient temperature (~ 20 °C) on a 1 mL sample, collecting the scattered light at 173°. Typically, three separate experiments of 10-15 runs (chosen by the instrument depending on the optical quality of the dispersions) were performed for each sample to check upon significance and reliability.

CHAPTER 3. THE GLYCEROL OPPORTUNITY

3.1. Overview

The global production of polymeric materials has reached 335 million tons per year, and more than 98% comes from petroleum-based resources.[23, 141-143] These materials are widely used in large quantities in several industrial applications including fabrics, pharmaceuticals, cosmetics and food.[143-147] Several factors, such as depletion of fossil resources, poor degradability, environmental accumulation and customer awareness have increased the interest to drive the research towards more sustainable and environmentally friendly alternatives to synthesise polymeric materials.[148] The synthesis of polyol-based polyesters has been studied in the literature, [45, 112, 149-151] and these can be used as the main blocks to synthesise surfactants which will be discussed later in Chapter 4. Their synthesis can be achieved by the polycondensation of bio-sourced glycerol and succinic acid. The synthesis of glycerol-based polymers (through polycondensation) is normally achieved using toxic catalysts, solvents and high temperatures (>120 ºC), which is not ideal in terms of green and sustainable chemistry.[49, 152-154]

This chapter focuses on a greener synthesis of linear poly(glycerol-succinate), trying to address all of these issues. Combining enzymes and supercritical carbon dioxide opens the possibility for a green and solvent-free polycondensation route. Nevertheless, some challenges need to be met when synthesising linear polyesters from glycerol *via* polycondensation: (1) controlling possible hyperbranching through the secondary alcohol functional group (2) removal of the condensate (water) to drive the reaction towards the formation of the product and (3) decreasing the polymerisation temperature. To assess the properties and the efficiency of the synthesis of glycerol-based polyesters, several analytical methods are used to characterise the polyesters: ^{1}H-NMR, ^{13}C-NMR, MALDI-TOF, GPC, FT-IR and DSC.

Consequently, this chapter explores the possibility of a greener enzymatic synthesis of glycerol-based polyesters, by exploiting the unique properties of supercritical carbon dioxide.

3.2. Introduction

3.2.1. Renewable polymers

The fast-growing world population will lead to a drastically increased demand for energy and resources, accompanied by massive consumption and production of products from fossil fuels. Despite the discovery of new oil reserves, these will be depleted, and the exploration of oil will become economically unviable.[2-3] Therefore, the need to find solutions to overcome this dependence upon fossil resources, will increase continuously. In recent decades, alternative and renewable feedstocks for the synthesis of polymeric materials have received a lot of attention. [155-160] The possible applications of greener polymers range from medical and tissue engineering, food packaging, and coatings to cosmetics, to name a few.[161]

Glycerol (1,2,3-propanetriol) is a well-known organic molecule and it is the simplest polyol with more than two hydroxy groups. Glycerol is a by-product of biodiesel production. The hydrolysis of triglycerides from biomass (such as palm oil, sunflower oil or rapeseed oil) results in methyl esters and glycerol. This reaction (direct transesterification) has been well known for more than 20 years in the production of biodiesel of high quality.[43] Three moles of methyl ester and one mole of glycerol are obtained for every mole of triglyceride feed. The glycerol is considered to be a valuable by-product since methyl esters are the target product. According to European statistics (Eurostat),[162] between 2007 and 2016, biodiesel production has increased by 83% in the European Union. Thus, considering these data, glycerol is becoming widely available and because it is an unwanted by-product, its price is inversely proportional to the increase in biodiesel production.[163] Additionally, glycerol can be also found naturally in triglycerides and it is commercially produced by the fermentation of sugar (glucose and fructose) either directly, or as a by-product of the industrial conversion of lignocellulose into ethanol.[164]

The polycondensation of glycerol with dicarboxylic acids (azelaic, glutaric, iminodiacetic, sebacic and succinic acid, to name a few) has been studied recently (Figure 3.1).[45-50] Wyatt*, et al.* [50], Agach*, et al.* [45] and Somisetti*, et al.* [49]

have synthesised glycerol-diacid polyesters, at high temperatures and in the presence of acid catalysts (stannous chloride – $SnCl_2$, sulfuric acid – H_2SO_4 and titanium (IV) butoxide – $Ti(OBu)_4$, to name a few), obtaining linear and/or branched polyesters.

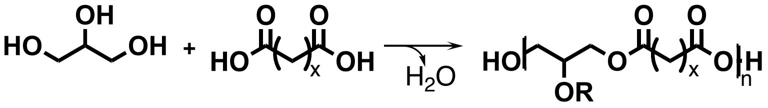

Figure 3.1 – Polycondensation of glycerol with dicarboxylic acids. Depending on the conditions applied, a linear polyester (R = H) or a branched material (R = polyester unit) can be obtained.

Previously, most dicarboxylic acids have been produced from petrochemical feedstocks but, due to sustainability awareness in industrial and academic organisations, there has been a drive to produce them from more environmentally friendly starting materials.[165-166] Succinic acid (SA) has been shown to be an attractive platform for different applications in surfactant, food and pharmaceutical industries.[167] Presently, SA is industrially produced mostly from petrochemical feedstocks, but because of environmental considerations (see above) there has been a trend towards to the production of bio-based SA from biomass (*e.g.* sucrose and glycerol).[166, 168-169]

Dicarboxylic acids normally have higher melting points than the respective monoacids of the same molecular weight.[170] Thus, when performing polycondensation with dicarboxylic acids, high temperatures are required to melt it. Later in this chapter, we will demonstrate a new approach that leads to the possibility of using near-room temperatures to perform polycondensation of glycerol and succinic acid.

Within the current consciousness about the need to create ‘*greener’* polymers, the synthesis of polyesters from bio-sourced glycerol and succinic acid offers a good alternative to fossil-based materials. Bio-based poly(glycerol-succinate) (PGLSA) could be a suitable renewable, water-soluble and biodegradable ingredient to synthesise for a surfactant. The condensation of glycerol and succinic acid has been studied previously but usually involves energy intensive processes (high heat, high vacuum), toxic solvents and/or catalysts.[46-47, 147, 153-154, 171] Wyatt*, et al.* [172] successfully obtained a linear and branched PGLSA with a molecular weight of 2000 Da and a narrow dispersity

(1.06). Since these polyesters were soluble in polar solvents, such as dimethylformamide (DMF), the authors suggest that crosslinking was avoided, or present in negligible quantities, within 24 hours at 150 ºC. Agach*, et al.* [171] synthesised branched PGLSA, obtaining polymers with molecular weights up to 1,100 Da in the absence of solvents but at a temperature of 190 ºC. In this study, they also evaluated the influence of the ratio between glycerol and succinic acid on the molecular weight and degree of branching; the higher the ratio of Gly:SA, the lower the branching obtained, and the lower the molecular weight of the obtained PGLSA.

Biodegradable and biorenewable, although often used in conjunction with one another, have two different meanings. A biodegradable polymer is a material that can biodegrade easily; although, it does not mean that it comes from renewable resources, which is a very important requirement for ‘greener’ polymers. The relationship between biorenewable and biodegradable polymers is shown in Figure 3.2. Polycaprolactone (PCL), poly(butylene succinate adipate) (PBSA), poly(ethylene succinate) (PES) and poly(butylene succinate) (PBS) are petroleum based, but they can be degraded by microorganisms or enzymes.[173-176] However, polyethylene (PE), Nylon 11 (NY11) and acetyl cellulose (AcC) can be produced from renewable resources, but they do not biodegrade. Poly(hydroxybutyrate) (PHB), poly(lactide) (PLA), starch blends (Starch) and poly(glycerol-succinate) (PGLSA) are produced from renewable resources and are biodegradable as well.

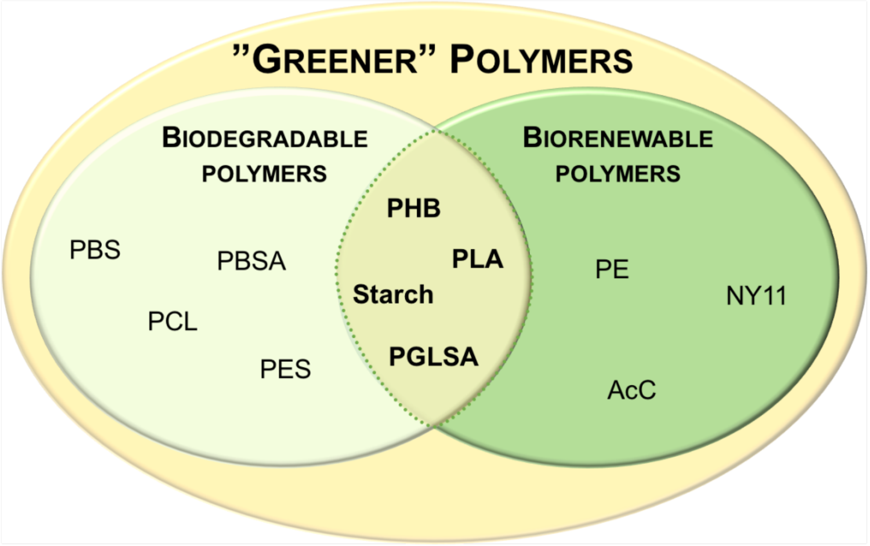

Figure 3.2 – "Greener" polymers definition: combination of biodegradable and biorenewable polymers. Biodegradable polymers can be degraded by microorganisms but that does not mean that they come from renewable feedstocks; Biorenewable polymers come from renewable sources but are necessarily biodegradable. Polymers which are both biodegradable and biorenewable are called "greener" polymers, such as PHB (poly(hydroxyburate)), PLA (poly(lactide)), starch and PGLSA (poly(glycerol-succinate)). (adapted from Tokiwa*, et al.* [177])

A study of the biodegradability of poly(glycerol-succinate) showed that the biodegradation of PGLSA (with different Gly:SA molar ratios: 1.33, 1.5, 1.7 and 1.9) reaches 60% degradation after 10 days, and 90% degradation after 28 days. These data confirm that poly(glycerol-succinate) can be considered readily biodegradable.[171] Also, the branching and size of the polymer does not influence the biodegradability.

3.2.2. Condensation polymerisation

Condensation polymerisation proceeds *via* a step-growth polymerisation mechanism normally resulting broad dispersities (> 2). To obtain high molecular weight polymers, high conversions need to be achieved (Figure 3.3). Contrariwise, in chain-growth polymers, even at low monomer conversion, it is expected to obtain high molecular weight polymers. This Thesis will investigate polycondensation, which is a step-growth polymerisation.

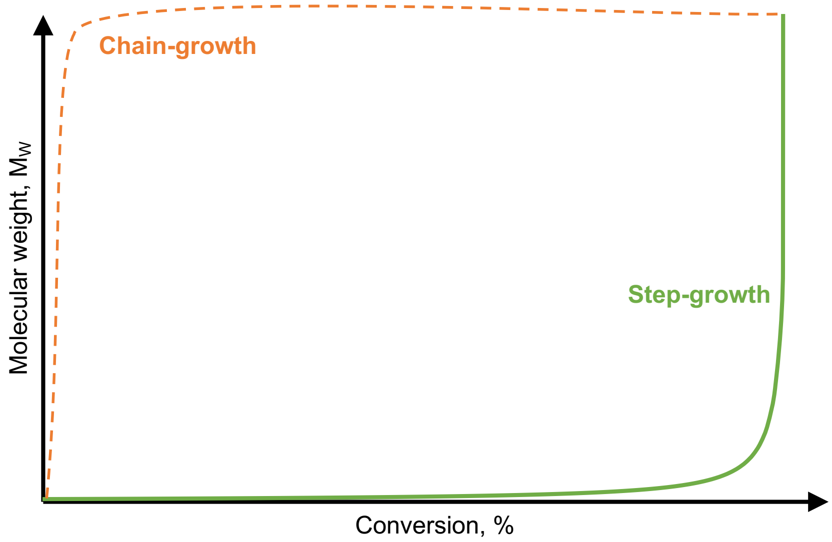

Figure 3.3 – Comparison of the evolution of molecular weight with conversion for chain and step-growth polymerisation.

In the case of equimolar amounts of bifunctional monomers (1:1 ratio), the degree of polymerisation (DP) can be calculated using the Carothers' equation (Equation 3.1),[178] and provides the information about the number of repeat units present in the polymer chain.

$$DP = \frac{1}{1-p}$$

Equation 3.1 – Carothers' equation.[178] DP = degree of polymerisation; p = monomer conversion achieved.

Following Equation 3.1, high values for the degree of polymerisation (>20) are only achieved at high conversions, > 95%. At 50% monomer conversion, only dimers (DP = 2) are expected to form on average (Table 3.1, entry 4). At 90% conversion, the DP increases to 10, which corresponds to a molecular weight of 1,700 Da for poly(glycerol-succinate). At 95% conversion, the DP to the doubles to DP = 20, resulting in poly(glycerol-succinate) with a molecular weight of 3,480 Da. Nonetheless, at the final stages of the polymerisation, when the conversion is between 95-99.9%, it is expected to see a considerable increase in the DP, from 20 to 1,000, corresponding to an increase in M_n to 174,000 Da for poly(glycerol-succinate).

Table 3.1 – Molecular weight prediction of linear poly(glycerol-succinate), following Carothers' equation, for a condensation polymerisation at 10.0-99.9% monomer conversion. [a] calculated through Equation 3.1.

Entry	**Conversion**	**Conversion (p)**	**DP**	$M_n^{theo\ a}$ **(Da)**
1	10.0%	0.1	1.11	193.3
2	20.0%	0.2	1.25	217.5
3	30.0%	0.3	1.43	248.6
4	50.0%	0.5	2.00	348.0
5	60.0%	0.6	2.50	435.0
6	75.0%	0.75	4.00	696.0
7	90.0%	0.9	10.00	1,740.0
8	95.0%	0.95	20.00	3,480.0
9	99.9%	0.99	1000	174,000.0

In the case of an imbalance between the bifunctional groups (ratio 1≠1), the relationship between the DP and the conversion can be calculated by a modification of the Carothers' equation (Equation 3.2).

$$DP=\frac{1+r}{1+r-2\cdot r\cdot p}$$

Equation 3.2 – Modification of Carothers' equation for stoichiometric imbalance factor, r, at a specification monomers conversion p.

$$r=\frac{N_A^o}{N_B^o}$$

Equation 3.3 – Stoichiometric imbalance factor r. N_A^o corresponds to the molar equivalent of A monomer, which is different from N_B^o, the molar equivalent of B monomer. By convention, r is always less than unity, except for an equimolar ratio $N_A^o= N_B^o$.

However, the Carothers' equation does take into consideration polymerisation reactions of multifunctional monomers, where chain branching and crosslinking might occur. Thus, the degree of polymerisation in these cases can be predicted using Equation 3.4.[179]

$$DP=\frac{2}{2-p\cdot f_{av}}$$

Equation 3.4 – Degree of polymerisation for multifunctional monomers[179], where p corresponds to monomer conversion and f_{av} to the average number of functional groups.

Following this equation, the prediction of the degree of polymerisation is valid only up to conversions lower than 80% (Table 3.2, entry 9), due to the possible occurrence of gelation, where the polymer is no longer soluble in solvents. At 50% conversion, the formation of tetramers of glycerol and succinic acid (Table

3.2, entry 4) is predominant. Yet, there is a sudden fourfold increase in the DP (16) at 75% conversion, leading to formation of poly(glycerol-succinate) of higher molecular weight (2,700 Da) (Table 3.2, entry 6). A further 4% increase in conversion, results in an increase in the DP to 80, resulting in a polyester with a molecular weight of 13,900 Da. Nonetheless, at the last stage of the polymerisation, before gelation occurs, at a conversion of 79.9%, a considerable increase in the DP, from 80 to 800 is expected, corresponding to an increase in M_n to 139,200 Da for poly(glycerol-succinate).

Table 3.2 – Molecular weight prediction of branched poly(glycerol-succinate), following Equation 3.4, for a condensation polymerisation at 10.0-80.0% monomer conversion. [a] calculated through Equation 3.4. np = not possible to calculate due to possible gelation.

Entry	Conversion	Fraction of conversion (p)	DP	$M_n^{theo\,a}$ (Da)
1	10.0%	0.1	1.14	198.9
2	20.0%	0.2	1.33	232.0
3	30.0%	0.3	1.60	278.4
4	50.0%	0.5	2.67	464.0
5	60.0%	0.6	4.00	696.0
6	75.0%	0.75	16.00	2,784.0
7	79.0%	0.79	80.00	13,920.0
8	79.9%	0.799	800.00	139,200.0
9	80.0%	0.80	np	np

Polycondensation reactions result in linear, branched or crosslinked polymers, depending on the functionality of the monomers. Generally, condensation polymerisations conducted using dicarboxylic acids and polyols, such as glycerol and succinic acid, have been performed widely in solvent-free systems to avoid the use of toxic solvents. Although, as mentioned previously, high temperatures are often required to melt the dicarboxylic acid. In addition, the removal of the small molecule condensate (e.g. water) is important to shift the reaction equilibrium. It is driven towards the polymer formation according to the principle of *Le Chatelier*. This can be accomplished by heat, high energy vacuum or by a flow of argon or nitrogen,[82] all of which aid mass-transfer, making it more favourable for the by-product in the reaction medium to be transferred to the vapour phase, thus driving the reaction forward. Others have shown that when applying high temperatures to multifunctional monomers, such as glycerol, in the absence of solvent, crosslinking cannot be avoided.[172]

Bifunctional and multifunctional monomers in polycondensation will be discussed below.

3.2.2.1. Linear and branched polyesters

Polymer topology (arrangement in space) is one of the key characteristics of polymers, in addition to the configuration, composition, dispersity, molecular weight and their functional groups. There are several types of polymer topologies (Figure 3.4), and each one will result in different properties and therefore, different applications.

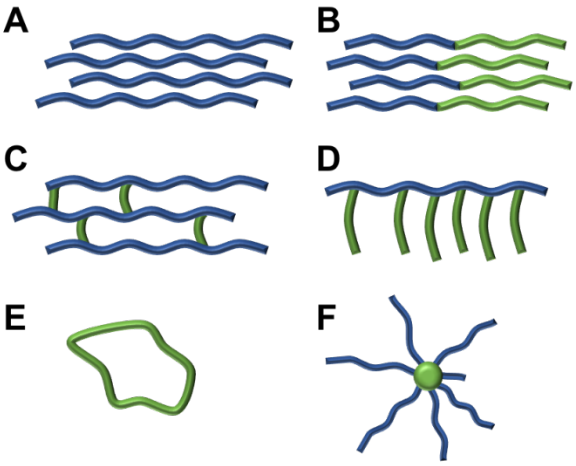

Figure 3.4 – Schematic representation of polymer topology. Depending on monomer composition, sequence and arrangement in space (topology), polymers can be classified as A) linear, B) AB-copolymer, C) cross-linked, D) comb, E) cyclic and F) star polymers.

In general, condensation polymers are formed by A_n + B_m type of monomers, where n and m represents the number of active functional groups. Linear polymers are normally obtained by a combination of A_2 and B_2 or AB monomers and if n and/or m > 2, polymers can be branched or cross-linked.[88] The history of hyperbranched polymers started in 1847 when Berzelius synthesised a polyester resin from tartaric acid (Figure 3.5) and glycerol (B_3 type of monomer) followed by Smith in 1901 who reported the reaction between phthalic acid (A_2 type of monomer) and glycerol.[180]

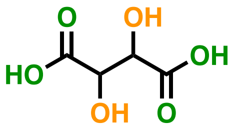

Figure 3.5 – Schematic representation of tartaric acid, a monomer with two different functional groups: two hydroxy groups (in orange) and two carboxy groups (in green).

Only in the 1940s were the terms *branched polymer* and *degree of branching* introduced for the first time by Flory, when he calculated the molecular weight distribution of three-dimensional polymers in the state of gelation.[181-183] Gelation (gel polymer) occurs when the degree of branching reaches a critical point and prior to this point, the polymer is a so-called random hyperbranched polymer.[184] At this stage, the polymer viscosity increases abruptly. Later in 1952, Flory described that branched polymers can be synthesised without the risk of gelation.[185] This was confirmed by a mathematical model, in which highly branched polymers were obtained through polycondensation of a monomer containing one functional group A and two or more functional groups B (AB_n type of monomer, where $n \geq 2$).

Hyperbranched polymers are synthesised by two main techniques:

1) single-monomer methodology (SMS), which is the polymerisation of AB_n monomers – by:

- a) polycondensation of AB_n monomers,
- b) self-condensing ring-opening polymerisation,
- c) self-condensing vinyl polymerisation,
- d) proton-transfer polymerisation;

2) double-monomer methodology (DMM), which is the direct polymerisation of two types of monomer, or a monomer pair which generates hyperbranched polymers – *e.g.* polycondensation of A_2 and B_3 monomers.

Poly(glycerol-succinate) (PGLSA) consists of both A_2 and B_3 type monomers: glycerol is trifunctional (B_3) and succinic acid is bifunctional unit (A_2), and this combination might lead to a branched polymer (Figure 3.6). The step-growth polymerisation of these monomers occurs randomly and not only gelation but also intramolecular cyclisation can occur.[186] MALDI-TOF is the best way to distinguish between cyclic and linear structures.[187]

In branched polymers from A_2 and B_3 type monomers it is possible to distinguish different units (Figure 3.6): A_0, A_1, B_0, B_1 and B_2 units, where A units (A_0 and A_1) and B units (B_0, B_1 and B_2) are from A_2 and B_3 monomers respectively.

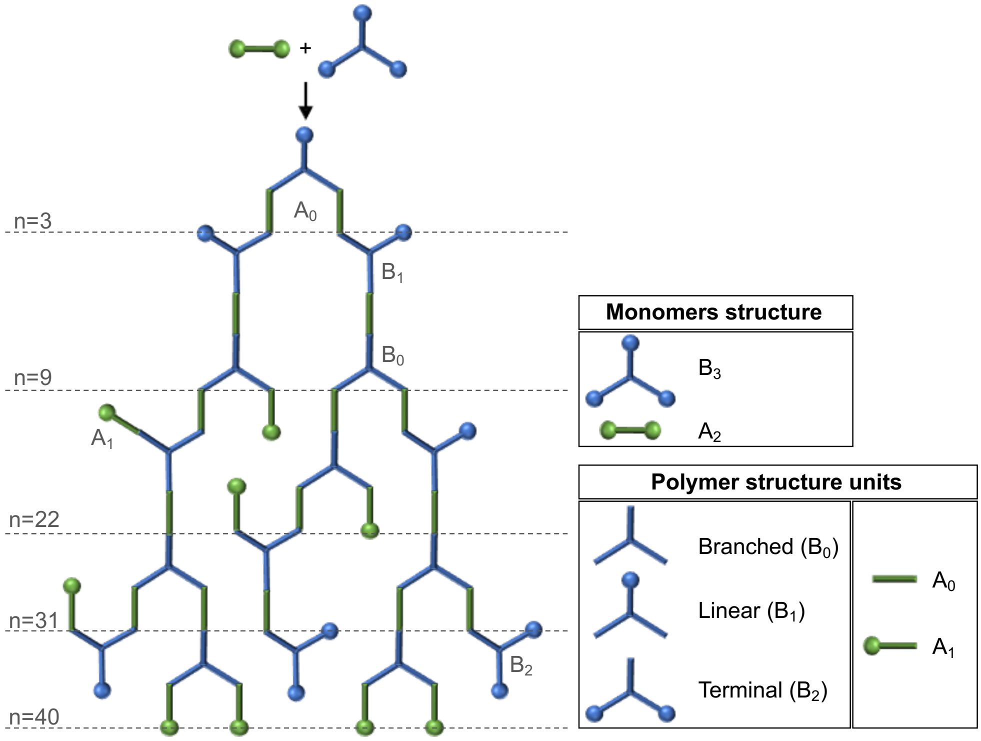

Figure 3.6 – Schematic topology and composition of hyperbranched polymers from A_2 and B_3 monomers. n = number of monomers. (adapted from Chen and Kong [186])

The degree of branching (DB) is an important value to describe quantitatively the branched structure of a polymer. It was first defined by Fréchet[188] and Frey[189-190] (Equation 3.5 and Equation 3.6) for polymers having an AB_n topology using NMR-spectroscopy. The DB defined by Frey is the number of actual dendritic units divided by the maximum possible number of dendritic units and is universally applicable for small and large polymer structures.[191] If a polymer is highly branched, *e.g.* a hyperbranched polymer, the DB value is close to 1 (or 100%). If a polymer is linear, or less branched, the DB value is low (< 5%).

$$DB_{Frey}=\frac{2\times D}{2\times D+L}\times 100$$

Equation 3.5 – Degree of branching as defined by Frey[189-190], for polymers from an AB_n topology. D = dendritic units, L = linear units. Dendritic units correspond to the formation of branched polymers.

$$DB_{Fréchet}=\frac{2\times D+2\times T}{D+T+L}\times 100$$

Equation 3.6 – Degree of branching as defined by Fréchet[188], for polymers from an AB_n topology. D = dendritic units, T = terminal units, L = linear units. Dendritic units correspond to the formation of branched polymers.

When analysing branched polymers from a A_2 + B_3 topology, which is the case in this chapter on PGLSA, these equations result in Equation 3.7 and Equation 3.8.

$$DB_{Frey}=\frac{2\times B_0}{2\times B_0+B_1}\times 100$$

Equation 3.7 – Degree of branching equation defined by Frey[189-190], for polymers from an A_2 + B_3 topology. In a hyperbranched polymer, it is possible to observe different units in the backbone of the polymer: branched units (B) and linear units (L). In PGLSA branching can occur *via* glycerol (B_3 compound). Thus, when a linear unit is obtained (B_1 unit), polymerisation can occur in the positions H_a and H_b, or H_a and H_c of glycerol (Figure 3.10). Thus, B_1 can also be described as $L_{a,b}$ and $L_{a,c}$, respectively.

$$DB_{Fréchet}=\frac{2\times B_0+2\times B_2}{B_0+B_2+B_1}\times 100$$

Equation 3.8 – Degree of branching equation defined by Fréchet[188], for polymers from an A_2 + B_3 topology. In a hyperbranched polymer, it is possible to observed different units in the backbone of the polymer: branched units (B) and linear units (L). In PGLSA branching can occur *via* glycerol (B_3 compound). Thus, when a linear unit is obtained (B_1 unit), polymerisation can occur in the positions H_a and H_b, or H_a and H_c of glycerol (Figure 3.10). Thus, B_1 can also be described as $L_{a,b}$ and $L_{a,c}$, respectively.

The DB is obtained using NMR-spectroscopy by the signal intensities for the respective units in the branched polymer. For the synthesis of PGLSA, it has been predicted theoretically that the lower the ratio of Gly:SA, the earlier the gelation occurs and therefore, the higher the DB (closer to 1 or 100%).[192] Khongphow*, et al.* [46] and Agach*, et al.* [171] (both using a G:SA ratio of 1.5:1) synthesised poly(glycerol-succinate) oligomers, through melt polycondensation (120-190 ºC), and they produced oligoesters with low DB_{Frey} (< 28%).

3.2.3. Catalysts for polyester synthesis

This section will explore the use of chemo- and biocatalysts to synthesise polyesters.

3.2.3.1. Chemocatalysts

The synthesis of polyesters, by polycondensation of diacids with diols, has been extensively studied and it usually requires high temperatures, the use of solvents and high vacuum all of which are not ideal from a sustainable point of view.[193-194] Catalysts are used to increase the rate of a chemical reaction and catalyst driven polycondensation reactions are very important for large scale manufacturing of polyesters.[184] Several catalysts have been studied in the literature for polycondensation reactions, such as titanium butoxide ($Ti(OBu)_4$), titanium isopropoxide (TTIP or $Ti(O\textit{i}Pr_4)$), tin(II) 2-ethylhexanoate ($Sn(Oct)_2$), scandium(III) triflate ($Sc(OTf)_3$), germanium oxide (GeO_2), dibutyltin(IV) oxide (DBTO or Bu_2SnO), and bismuth (III) trifluoromethanesulfonate ($Bi(OTf)_3$), to name a few.

Kolb and Meier [195] analysed three different catalysts, TBD, $Ti(O\textit{i}Pr)_4$ and *p*-TsOH, for the polymerisation of dimethyl 2-decylmalonate with 1,6-hexanediol. At high concentrations of catalyst (10 mol% TBD, $Ti(O\textit{i}Pr)_4$ or *p*-TsOH,) and at 80-100º C, polymers with a molecular weight of 1,600-4,800 Da, with a broad dispersity ($Đ$ = 1.50-2.93), were obtained. However, at lower catalyst concentrations (2 mol%), at 100º C, no polymer was obtained with TBD and *p*-TsOH. By contrast with 2 mol% $Ti(O\textit{i}Pr)_4$ a polymer with a molecular weight of 15,200 Da, with a broad dispersity ($Đ$ = 2.89), was obtained. On decreasing the titanium isopropoxide catalyst concentration even further to 0.5 mol%, a polymer with M_n of 14,500 Da ($Đ$ = 2.02) was obtained. A greener procedure towards novel aliphatic polyesters was developed by Vilela*, et al.* [156] and revealed to be promising. Using $Bi(OTf)_3$ (Bi^{3+} is one of the least toxic heavy metal ions) as the catalyst for the polymerisation of diacids and diols derived from plant oil-based monomers lead to polymers with molecular weights up to 14,000 Da ($2.1 < Đ < 2.7$) with a maximum yield of 79%.

Terzopoulou*, et al.* [196] also studied the effect of selected catalysts in the polycondensation of poly(ethylene furanoate) (PEF): $Ti(OBu)_4$, $Ti(O\textit{i}Pr_4)$, $Sn(Oct)_2$ and DBTO. In this study, at 160º C, and excluding $Sn(Oct)_2$, all the catalysts achieved high conversions (> 90%) after four hours reaction, with molecular weights up to 6,000 Da. By contrast, $Sn(Oct)_2$ showed a considerably lower conversion after four hours, 17%, achieving M_n of only 2,000 Da. Only after twenty hours was conversion raised to a more viable > 90%.

Several authors have investigated the polycondensation of glycerol-based polyesters and the commonly used catalysts are tin or titanium-based. The polycondensation of glycerol and diacids (succinic acid, azelaic acid and glutaric acid) was accomplished with conversions lower than 100%.[50, 172, 197-198] These reactions were done both in the absence, or presence of organic solvents (DMF or DMSO), at high temperatures (135-155 ºC), under reduced pressure (< 1.5 mbar) and with 0.15 wt.% DBTO.[50, 172, 197-198] Wyatt*, et al.* [50,172] synthesised poly(glycerol succinate) in bulk[50] (1.05:1 molar ratio G:SA) and in DMF[172] (1:2 molar ratio G:SA) with a molecular weight of 1,000-2,000 Da with low polydispersities (1.28-1.06). The use of solvents has a significant effect on the molecular weight and the dispersity of the polymer. Using toluene (135 ºC) and a G:SA molar ratio of 2:1, PGLSA with a molecular weight of 112,000 Da (*Đ* = 2.3) was obtained.[197] Stumbé and Bruchmann [198] synthesised poly(glycerol adipate) in bulk (at 150 ºC for 8 h, 1:2 molar ratio to glycerol) with a molecular weight of 23,000 Da with high dispersity, *Đ* = 7.7.

When using polyols, such as glycerol, in polycondensation reactions with diacids, formation of hyperbranched polymers is expected. Metal catalysts such as the ones described in this section, do not show regioselectivity towards primary *versus* secondary hydroxy groups. Gustini*, et al.* [199] studied the effect of different catalysts to obtain a linear sorbitol-based polyester, aiming to get pendant hydroxy groups along the polymer backbone. The authors studied the effect of DBTO, Sc(OTf$_3$), TBD and CaLB (*Candida antarctica* lipase B) as catalysts and concluded that only the enzyme was giving a 100% linear polymer. DBTO and TBD showed low or even no selectivity for primary over secondary hydroxy groups. Nevertheless, Sc(OTf$_3$) showed some selectivity, which had been noted by other authors.[200-202]

3.2.3.2. Biocatalysts

The first enzymatic polycondensation between dicarboxylic acids (C6 – C14) and a diol (ethylene glycol) was reported in 1984, resulting in polymers with molecular weights up to 2,000 Da at 30 ºC after 16 hours, using water as solvent.[203] Decades later, Iglesias*, et al.* [204] investigated the enzymatic polycondensation of glycerol with adipic acid, also at 30 ºC but in the presence of dioxane. After 72 h reaction, they obtained a linear polymer with a molecular weight of 1,300 Da (*Đ* = 1.1) in good yield (> 80%), demonstrating the regioselectivity of the enzyme. Likewise, Pessagno and Baldessari [205] showed the polycondensation of glycerol with dicarboxylic acids (C4, C8 and C6) at 30 ºC in two different solvents (dioxane and tetrahydrofuran), resulted in linear polymers with molecular weights between 1,700 and 2,000 Da, with low dispersity (1.01-1.1). Other authors studied the regioselectivity of CaLB towards the synthesis of linear polyol-based polyesters at different conditions.[150, 206] Hu*, et al.* [207] discovered that the reaction time might be an important feature to take into consideration in order to avoid the branching of polymers, even when using CaLB as catalyst. They claimed that in the polycondensation reaction between *D*-glucitol and adipic acid, linear polyesters were obtained (10,900 Da, *Đ* = 1.6) at reaction times <18 h; increasing the reaction time to 42 h, resulted in esterification of the pendant hydroxy groups giving hyperbranched polyol-based polymers.

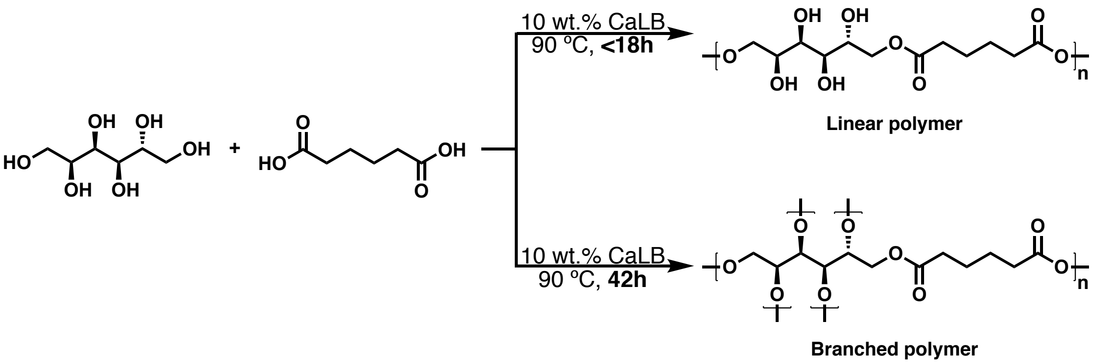

Figure 3.7 – Polycondensation of *D*-glucitol (sorbitol) with adipic acid at different reaction times. Hu*, et al.* [207] studied this reaction and linear polyesters were obtained at reaction times <18h; branched polyesters were obtained increasing the reaction time to 42h.

Similar results were reported by Kulshrestha*, et al.* [208] in the CaLB-catalysed bulk polycondensation of adipic acid, 1,8-octanediol and glycerol, at 70 ºC. After 2 h reaction, a polyester with a M_n of 2,700 Da, with narrow dispersity (*Đ* = 1.6), was obtained. Increasing the reaction time to 18 h resulted in an increase in the polymer molecular weight and dispersity, but linear polyesters were still formed. However, at 42 h reaction time, the obtained soluble product was increasingly branched, with a M_n of 75,600 Da and broad dispersity ($Đ$ = 3.1).

3.3. Aims of the study

The aim of this study is to assess the synthesis of linear poly(glycerol succinate) *via* enzymatic polycondensation.

This work will focus on the enzymatic polycondensation of glycerol and succinic acid using supercritical carbon dioxide. This study will test the hypothesis that enzymes can provide a near ambient temperature, low energy route giving linear polymers. Moreover, our approach will aim to avoid pre-modification of the monomers and hence, less steps are required. Comparison will be made to traditional metal catalysed polycondensation.

This work has the potential to produce biorenewable hydrophilic polyesters using a green and efficient one-pot process.

3.4. Experimental

3.4.1. Materials

All the chemicals and solvents were purchased from Sigma Aldrich (UK) and used as received, unless otherwise indicated. Novozyme® 435 (CaLB immobilised on cross-linked acrylic resin beads) was kindly donated by Novozymes (Denmark), stored at 4 ºC and dried for 24 hours under vacuum (100 mbar) at room temperature (RT) before use. Molecular sieves type 3 and 4 Å, 1.6-2.5 mm beads, were purchased from Fisher Scientific (UK) and used as received. Glycerol (≥ 99.5% purity) was purchased from Sigma Aldrich (UK) and dried for 24 hours under vacuum (10 mbar) at room temperature before use and stored over fresh molecular sieves (4Å) at room temperature. Succinic acid (≥ 99.0% purity) was purchased from Sigma Aldrich (UK) and dried for 24 hours under vacuum (10 mbar) at 50 ºC before use. All the solvents were of analytical grade, and used as received. Carbon dioxide grade 4.0 (minimum purity 99.99%) was purchased from BOC Special Gases (UK) and used as received.

3.4.2. Synthesis methods

3.4.2.1. View cell solubility study of reagents in supercritical carbon dioxide

To visually determine the effect of $scCO_2$ on the physical state of glycerol and succinic acid, a fixed volume view cell (100 mL) was used (Chapter 2, Figure 2.5 and Figure 2.6). In a typical procedure, 0.5 g of reagent (glycerol or succinic acid) was added to a 1 mL glass vial (previously cut to half of its height) and inserted inside the view cell, fixed with Blu-tack®. The windows were sealed and clamped to the body and the pressure was raised to 50 bar. The temperature and CO_2 pressure were raised incrementally to the desired conditions.

3.4.2.2. Synthesis of poly(glycerol succinate) *via* melt polycondensation with and without tin(II) 2-ethylhexanoate as the catalyst

The polymerisations of PGLSA were carried out *via* melt polycondensation with, and without $Sn(Oct)_2$ as the catalyst. Thus, in a typical procedure of 1:1 G:SA molar ratio (Figure 3.8), the succinic acid (54.3 mmol, 6.4 g), glycerol (54.3 mmol, 5.0 g), $Sn(Oct)_2$ (1 wt.% with respect to the total amount of monomers) and molecular sieves (size 4Å, 25 wt.% with respect to the total amount of monomers) were added to a 20 mL three-neck round bottom flask, alongside a magnetic stirrer (300 rpm) applying vacuum to the system. The oil bath temperature was set to 5 ºC higher, in order to ensure the desired temperature in the centre of the round bottom flask (checked with a thermocouple) and the reaction was left to run for the specified reaction time. The reaction was stopped by cooling to room temperature (RT). The molecular sieves were removed by filtration after being solubilised in THF (qualitative Fisherbrand filter paper, supplied by Fisher Scientific) and the filtrate was recovered using a rotary evaporator. To ensure complete removal of the solvent, the samples were placed under reduced pressure, at RT, overnight. Product yield was calculated by dividing the dry product mass by the theoretical mass. The reactions were performed at least twice to check reproducibility. Table 3.3 shows the summary of the reactions conditions conducted *via* melt polymerisation.

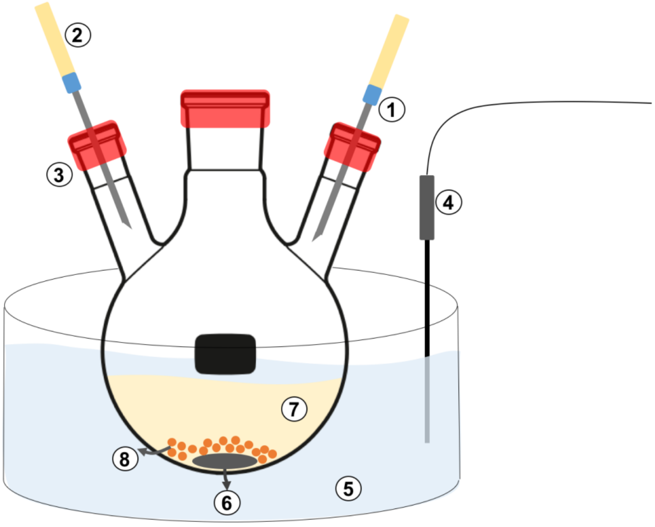

Figure 3.8 – Reaction set up for the synthesis of poly(glycerol succinate) *via* melt polycondensation. Legend: 1 – syringe to collect sample; 2 – vacuum line; 3 – rubber septum; 4 – thermocouple; 5 – oil bath; 6 – magnetic stirrer; 7 – reagents and catalyst/solvent (when present); 8 – molecular sieves, 4 Å.

3.4.2.3. Enzymatic synthesis of poly(glycerol-succinic acid) *via* melt polycondensation

For comparison, the enzymatic polymerisations of poly(glycerol succinate) were carried *via* conventional melt polycondensation with *Candida antarctica* lipase B. Thus, in a typical procedure of 1:1 G:SA molar ratio, the succinic acid (54.3 mmol, 6.4 g), glycerol (54.3 mmol, 5 g), CaLB (desired amount specified in the table below, Table 3.3) and molecular sieves (size 4Å, 25 wt.% to the total amount of monomers) were added to a 50 mL three-neck round bottom flask, along with a magnetic stirrer (300 rpm). If toluene (20 mL) was used as a solvent, it was also added to the reaction mixture. Vacuum was applied only to the neat system. The temperature was set to specific values (Table 3.3) and the reaction was continued for the specified reaction time (Table 3.3). The reaction was stopped by cooling to RT. The crude product was dissolved in THF to separate from the enzyme beads and molecular sieves by filtration. The solvent was removed from the filtrate under reduced pressure, leaving solid polymeric products. To ensure complete removal of the solvent, the samples were placed under vacuum at RT, overnight. The yields are summarised (Table 3.3) and all reactions were performed at least twice to check reproducibility.

Table 3.3 – Summary of the reactions conducted *via* melt polycondensation. *Note:* [a] includes polymer support; ≈ indicates partially solubility of the polymer in water; × indicates no solubility of the polymer in water; ✓ indicates solubility of the polymer in water.

Entry	Ratio (Gly:SA)	Solvent	Reaction time	T ºC	Catalyst	Appearance	Soluble in water
1	1:1	neat	24 h	120 ºC	none	Viscous, white	≈
2	1:1.5	neat	24 h	120 ºC	none	Rigid, white	×
3	1:2	neat	24 h	120 ºC	none	Rigid, white	×
4	1:1	neat	17 h	140 ºC	2 wt.% $Sn(Oct)_2$	Rigid, transparent	×
5	1:1	neat	3 h	140 ºC	2 wt.% $Sn(Oct)_2$	Rigid, transparent	×
6	1:3	neat	2 h	140 ºC	2 wt.% $Sn(Oct)_2$	Rigid, white	×
7	1:3	neat	24 h	110 ºC	25 wt.% CaLB[a]	Waxy, white	✓
8	1:1	neat	24 h	60 ºC	17 wt.% CaLB[a]	Viscous, yellow-transparent	✓
9	1:1	toluene	72 h	100 ºC	5 wt.% CaLB[a]	Waxy, white	✓
10	1:3	toluene	72 h	100 ºC	5 wt.% CaLB[a]	Waxy, yellow	✓
11	1:3	toluene	72 h	55 ºC (1h) 100 ºC (71h)	5 wt.% CaLB[a]	Waxy, white	✓

3.4.2.4. Enzymatic synthesis of poly(glycerol-succinic acid) using supercritical carbon dioxide

In a typical procedure (Figure 3.9) of 1:1 G:SA molar ratio, the succinic acid (16.3 mmol, 1.92 g), glycerol (16.3 mmol, 1.50 g), CaLB (25 wt.%[*] of the total amount of monomers, 0.86 g) and molecular sieves (size 3Å, 25 wt.% with respect to the total amount of monomers, 0.86 g) were added to the stainless steel reaction autoclave described previously (60 mL, Chapter 2, Figure 2.2). The vessel was sealed and pressurised to 50 bar. Subsequently, the temperature was set to 40, 50 or 60 ºC (Table 3.4), and finally the pressure was increased to 275 bar. The reaction was left to run for 24 h, while stirring at 150 rpm. To avoid polymer foaming and blockages in the pipework, the reactions were terminated by cooling the vessel in a water/ice bath (~ 0 ºC) before venting. The CO_2 was vented when the pressure was below 20 bar. Finally, the product was collected and dissolved in 10 mL of THF, gently heating at 40 ºC, for complete dissolution, and filtered to remove the enzyme beads and molecular sieves. The solvent was then removed under reduced pressure, leaving solid polymeric products. To ensure complete removal of the solvent, the samples were dried overnight under vacuum at RT. The product yields are summarized below (Table 3.11). The reactions were performed at least twice to check reproducibility. Table 3.4 shows the summary of the reactions conditions for polymerizations conducted in supercritical conditions.

---

[*] includes polymer support

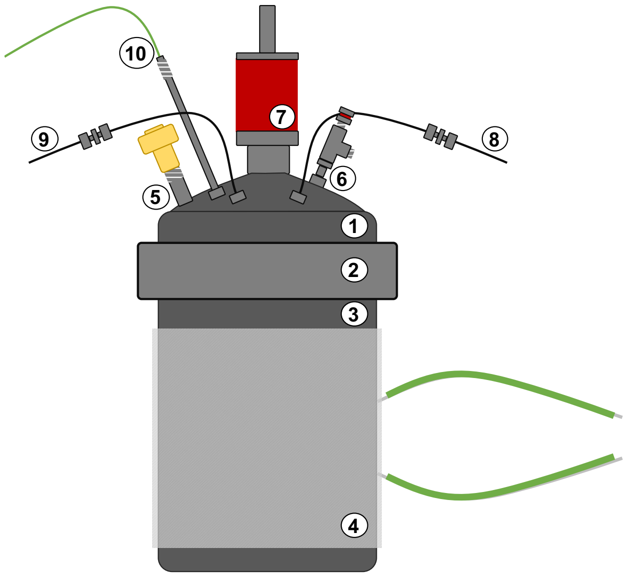

Figure 3.9 – Reaction set up for the synthesis of poly(glycerol succinate) under supercritical conditions. Legend: 1 – head; 2 – clamp; 3 – body; 4 – heating jacket; 5 – safety key; 6 – spring loaded pressure relief valve; 7 – magnetically coupled overhead stirrer; 8 – outlet line; 9 – inlet line; 10 – thermocouple.

Table 3.4 – Summary of reactions conducted using supercritical carbon dioxide at 275 bar. *Note:* [a] includes polymer support ✓ indicates solubility of the polymer in water.

Entry	Ratio (Gly:SA)	T ºC	Reaction time	Catalyst	Appearance	Soluble in water
12	1:1	40 ºC	24h	25 wt.% CaLB[a]	Waxy, yellow	✓
13	1:2	40 ºC	24h	25 wt.% CaLB[a]	Waxy, yellow	✓
14	2:1	40 ºC	24h	25 wt.% CaLB[a]	Waxy, yellow	✓
15	1:1	50 ºC	24h	25 wt.% CaLB[a]	Waxy, yellow	✓
16	1:2	50 ºC	24h	25 wt.% CaLB[a]	Waxy, yellow	✓
17	2:1	50 ºC	24h	25 wt.% CaLB[a]	Viscous, yellow-transparent	✓
18	1:1	60 ºC	24h	25 wt.% CaLB[a]	Waxy, white	✓
19	1:2	60 ºC	24h	25 wt.% CaLB[a]	Waxy, white	✓
20	2:1	60 ºC	24h	25 wt.% CaLB[a]	Waxy, white	✓

3.4.3. Polyester characterisation

The polymer structures were characterised using ^{1}H-NMR, ^{13}C-NMR, GPC, MALDI, FTIR and DSC. All these techniques are discussed in further detail in Chapter 2.

3.5. Results and discussion

This section focuses on the synthesis of PGLSA using a conventional metal-based catalyst ($Sn(Oct)_2$) or a biocatalyst (CaLB), in a solvent-free system (bulk), in the presence of solvent (toluene), and using supercritical carbon dioxide. Control experiments were also performed, in the absence of catalyst in bulk. The principal aim of this work is to develop a 'greener' method for the formation of poly(glycerol succinate). Therefore, $scCO_2$ and enzymes were chosen for the synthesis of glycerol-based polyesters. The syntheses *via* melt polycondensation were conducted for comparison with $scCO_2$ reactions.

The impact of the catalyst, the solvent and the polymerisation conditions were compared, assessing the selectivity to produce linear polyesters.

3.5.1. Melt polycondensation of poly(glycerol succinate) with and without catalyst

PGLSA was first synthesised without any catalyst, *via* melt condensation (Table 3.5). These reactions were conducted at 120 ºC for 24 hours, under vacuum, to drive the reaction towards the formation of product and to study the effect of the glycerol:succinic acid molar ratio. The molar ratio of monomers affects the size and topology of the polymers and as mentioned previously, the lower the ratio of Gly:SA, the earlier gelation occurs and the higher the chances of branched polymer (Figure 3.13). Therefore, the synthesis of glycerol-based polyesters can produce linear or branched products. Succinic acid may react with glycerol at any of its three different alcohol positions, *i.e.* the two primary and the secondary hydroxy groups (Figure 3.10). A branched structure may consist of tri-substituted (B_0), di-substituted (B_1) or mono-substituted (B_2) glycerol units and these different substitution patterns can be distinguished and quantified using NMR spectroscopy techniques. ^{1}H-NMR and ^{13}C-NMR resonance assignments for glycerol and succinic acid units of the poly(glycerol succinate) polymer, will show the possible linear and branched patterns.

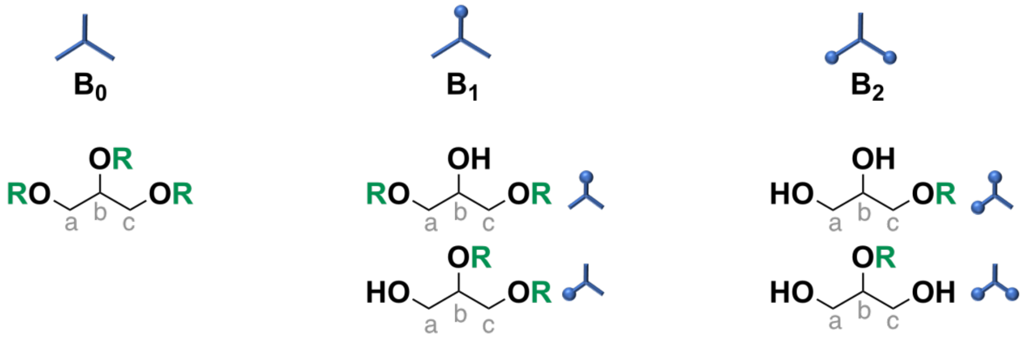

Figure 3.10 – Substitution patterns for the glycerol unit after polymerisation with succinic acid. The schematics next to the structures of glycerol represent the number of hydroxy groups that reacted with succinic acid (*e.g.*  corresponds to the linear structure of glycerol where succinic acid reacted on proton H_a and H_c of glycerol, compare Figure 3.3). *Note:* the blue dot represents an unreacted hydroxy group.

^{1}H-NMR, 2D-HSQC and COSY NMR are powerful techniques to confirm the hypotheses of this work. In other words, the combination of these techniques will make possible the determination of the H_b chemical shifts when it is present in di ( or ) or tri-substituted glycerol unit (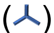), *i.e.* linear and branched structures, respectively. Sample from entry 2, Table 3.5, was analysed using these techniques. Table 3.6 is shown all the chemical shifts assignments for this polymer and Figure 3.11 and Figure 3.12 show the ^{1}H-NMR, 2D-HSQC and COSY-NMR spectra of this poly(glycerol succinate) sample.

Table 3.5 – Synthesis of poly(glycerol succinate) *via* melt polymerisation without catalyst. [a] these M_n values corresponds to the peaks with higher molecular weights, other peaks were detected in the GPC trace, due to the presence of oligomers; [b] determined by Frey's equation (Equation 3.7);

	Entry	Time	G:SA molar ratio	Yield	M_n^{GPC} (Da)	$Đ$	DB[b]	T_g
No catalyst	**1**	24 h	1:1	60%	3,900	> 2	18%	-61 ºC
	2	24 h	1:1.5	60%	8,200	> 2	67%	-18 ºC
	3	24 h	1:2	96%	6,200	> 2	65%	-20 ºC

Table 3.6 – Experimentally determined ^{1}H and ^{13}C-NMR chemical shifts for glycerol and succinate units on the PGLSA polymer (entry 2 from Table 3.5), showing the branching patterns. The schematic representations of branched, linear and terminal polymer units are as follow:  = linear glycerol unit; in this case, the polymerisation occurred in positions a and c,  = linear glycerol unit; in this case, the polymerisation occurred in positions b and c,  = terminal glycerol in the polymer backbone, leaving the hydroxy groups a and c free,  = terminal glycerol in the polymer backbone, leaving the hydroxy groups a and b free, 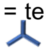 = trisubstituted glycerol unit in the branched polymer backbone,  = terminal unit of succinic acid in the polymer backbone and  = succinic acid unit in the linear/branched polymer backbone. *na* = not assigned; $^{a)}$ chemical shifts in ppm; the solvent used for NMR analysis in this work was acetone-d_6.

	^{1}H-NMR$^{a)}$			^{13}C-NMR$^{a)}$		
Structure & schematic representation	**Ref 46**	**Ref 47**	**This work**	**Ref 46**	**Ref 47**	**This work**
1 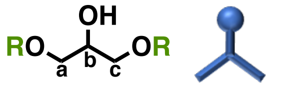	H_a = *na* H_b = 4.06 H_c = *na*	H_a = 4.07 H_b = 3.88 H_c = 4.07	H_a = 3.72-3.50 H_b = 3.83 H_c = 3.72-3.50	C_a = 65.23 C_b = *na* C_c = 65.81	C_a = 65.35 C_b = 66.26 C_c = 65.33	C_a = 66.54 C_b = 70.69 C_c = 65.60
2 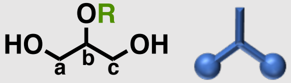	H_a = *na* H_b = 4.89 H_c = *na*	H_a = 3.47 H_b = 4.73 H_c = 3.47	H_a = 3.72-3.50 H_b = 4.88 H_c = 3.72-3.50	C_a = 60.75 C_b = 75.39 C_c = *na*	C_a = 59.85 C_b = 66.26 C_c = 59.85	C_a = *na* C_b = 76.04 C_c = *na*
3 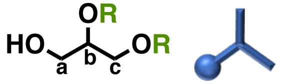	H_a = *na* H_b = 5.08 H_c = *na*	H_a = 4.21 H_b = 4.94 H_c = 3.51	H_a = 4.40-4.05 H_b = 5.07 H_c = 4.40-4.05	C_a = 60.03 C_b = 72.59 C_c = 63.05	C_a = 62.68 C_b = 72.51 C_c = 59.56	C_a = *na* C_b = 73.37 C_c = *na*
4 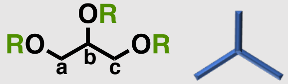	H_a = *na* H_b = 5.29 H_c = *na*	H_a = 4.24 H_b = 5.19 H_c = 4.24	H_a = 4.40-4.05 H_b = 5.28 H_c = 4.40-4.05	C_a = 62.51 C_b = 69.43 C_c = *na*	C_a = 62.17 C_b = 69.09 C_c = 62.17	C_a = 61.13 C_b = 72.61 C_c = 61.13
5 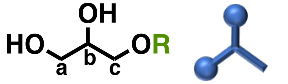	H_a = *na* H_b = *na* H_c = *na*	H_a = 4.04 H_b = 3.65 H_c = 3.39	H_a = 3.72-3.50 H_b = 4.40-4.05 H_c = 3.72-3.50	C_a = 62.04 C_b = 69.82 C_c = 63.51	C_a = 66.00 C_b = 69.04 C_c = 63.23	C_a = 67.94 C_b = *na* C_c = 63.94

Table 3.7 – (continued) *na* = not assigned; [a)] chemical shifts in ppm; the solvent used for NMR analysis in this work was acetone-d_6.

	^{1}H-NMR[a)]			^{13}C-NMR[a)]		
Structure & schematic representation	**Ref 46**	**Ref 47**	**This work**	**Ref 46**	**Ref 47**	**This work**
6 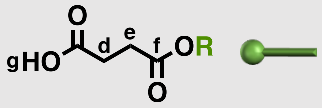	H_e = *na* H_d = 2.66 H_g = 12.20	H_e = *na* H_d = *na* H_g = *na*	H_e = 2.58 H_d = 2.58 H_g = *na*	C_f = 171.86 C_e = *na* C_d = 28.71	C_f = *na* C_e = *na* C_d = *na*	C_f = 172.83 C_e = *na* C_d = 21.27
7 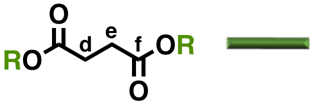	H_e = *na* H_d = *na*	H_e = *na* H_d = *na*	H_e = 2.69-2.61 H_d = 2.69-2.61	C_f = *na* C_e = *na* C_d = 171.86	C_f = *na* C_e = *na* C_d = *na*	C_f = 172.83 C_e = *na* C_d = *na*

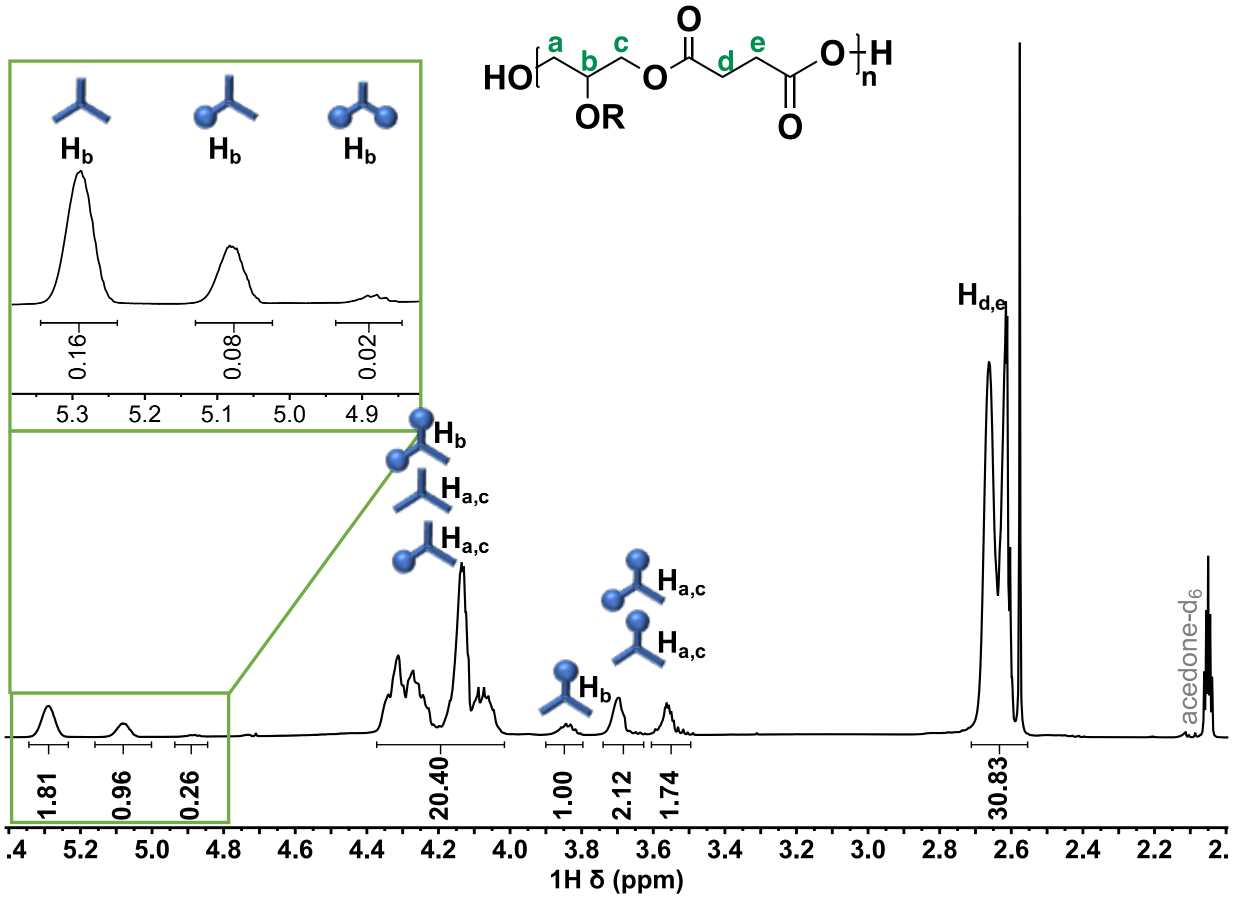

Figure 3.11 – ^{1}H-NMR spectrum of a branched poly(glycerol succinate) polymer (entries 2 from Table 3.3 and Table 3.5). The solvent used was acetone-d$_6$.

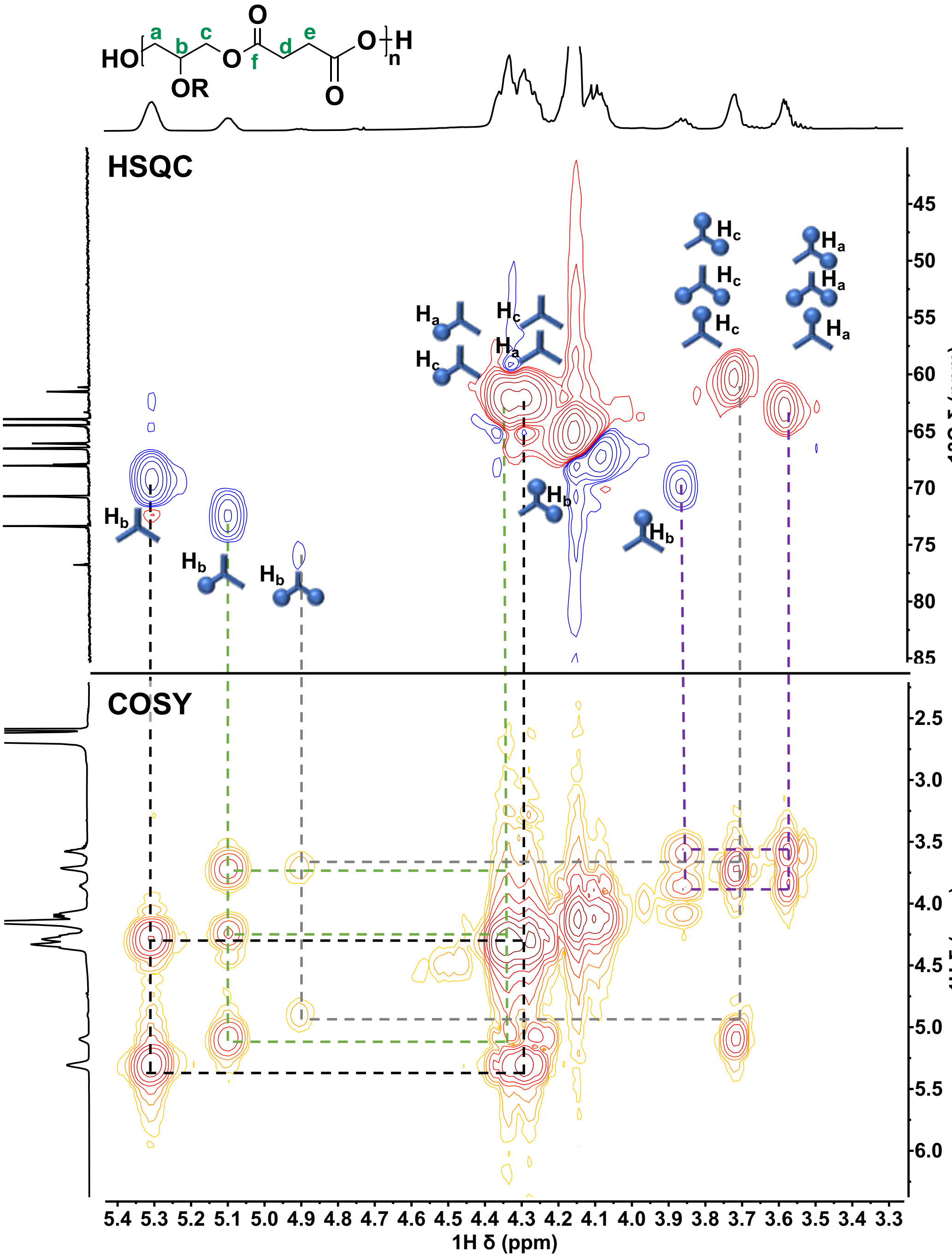

Figure 3.12 – Sections of the HSQC and COSY NMR spectrum showing the assignments of glycerol units in a branched poly(glycerol succinate) polymer (entries 2 of Table 3.3 and Table 3.5). The solvent used was acetone-d_6. In the HSQC spectrum, methylene proton ($–CH_2$) signals are plotted in red. Methine proton ($–CH$) signals are plotted in blue. *Note*: ⅄ this symbol denotes that proton H_b is present in a branched structure. ⅄ this symbol denotes that proton H_b is present in a linear structure and the polymerisation occurred in positions b and c. ⅄ this symbol denotes a terminal glycerol unit proton H_b showing that the polymerisation occurred from position b. The dotted lines reveal some of the proton couplings.

NMR spectroscopy is a well-established technique to characterise complex structures.[47, 172, 209-211] When analysing the ^{1}H-NMR spectrum of this PGLSA sample (Figure 3.11), peak broadening was expected, because of the high molecular weight (8,200 Da) and also as a consequence of possible branching. The spectrum can be divided into two sections:

a) the region at 2.4–2.7 ppm, which corresponds to the protons H_d and H_e (succinic acid unit) in the polymeric backbone;
b) the regions at 3.5–3.7 ppm, 3.80-3.87 ppm, 4.0–4.2 ppm and 4.8–5.4 ppm, which correspond to protons H_a, H_b and H_c in the linear, terminal and branched glycerol units.

However, it is not possible to clearly assign all the signals to the differently substituted glycerol units, and ^{1}H-NMR analysis is revealed to be insufficient for complete structural characterization of the polymer.

Thus, 2D-HSQC and COSY NMR methods were employed, providing information on the H-C couplings. In the HSQC spectrum, one axis corresponds to ^{1}H chemical shift, and the other axis to ^{13}C chemical shifts; the crosspeaks indicate one bond ^{1}H-^{13}C connectivity. The identification of the methylene (–CH_2, red plot line in Figure 3.12) and methine (–CH, blue plot line in Figure 3.12) protons of the esterified primary and secondary hydroxy groups from the polymer backbone is important in order to identify if the polymer is linear or branched. Thus, it follows that the methylene peaks correspond to H_c and H_a protons; methine peaks correspond to H_b protons.

COSY NMR identifies mutually coupled protons within a small number of chemical bonds, *e.g.* < 3. Hence, combining both methods, HSQC and COSY, helps to identify the resonances.

For the 2D-NMR (Figure 3.12) of this PGLSA sample (entry 2, Table 3.5) it is possible to see that for tri-substituted glycerol unit (⅄) the proton H_b (5.28 ppm) couples with proton (⅄)H_c and (⅄)H_a at *ca.* 4.30-4.20 ppm. These couplings are clearly shown using the black dotted lines in Figure 3.12. These assignments, are in good agreement with the assignments found in the literature (Table 3.6).[46-47] In a linear structure, the same H_b proton (⅄) (5.07 ppm), where the polymerisation took place on positions H_b and H_c, couples with the corresponding H_a and H_c protons (⅄, green dotted line in Figure 3.12), at *ca*. 4.40-4.05 ppm. The proton H_b (⅄, *ca*. 3.83 ppm) shows clear coupling with H_a, H_c (⅄) (*ca*. 3.83 and 3.72-3.50 ppm, respectively, and represented by the purple dotted line). Another proton coupling that is observed, although with less intensity than the previous proton coupling described, is between protons ⅄H_b and ⅄H_a, H_c (grey dotted line in Figure 3.12), at *ca*. 4.88 and 3.72-3.50 ppm. The coupling between ⅄H_b and ⅄H_a, H_c is not clear which was expected since the polymer sample corresponds to a branched PGLS. All the assignments represented in Table 3.6 are in good accordance with previous values described by Khongphow*, et al.* [46] and Wyatt and Strahan [47].

The degree of branching was calculated following Equation 3.7, by integrating the resonances corresponding to the H_b protons from B_0 and B_1 structures, using ^{1}H-NMR. The chemical shifts used were: ⅄H_b (B_0) = 5.28 ppm, ⅄H_b (B_1) = 5.07 ppm, ⅄H_b (B_1) = 3.83 ppm.

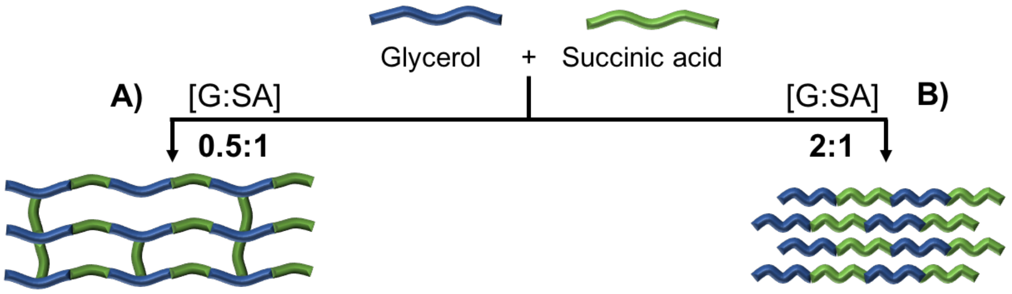

Figure 3.13 – Schematic representation of the effect of changing the molar ratio of the monomers in the synthesis of poly(glycerol succinate), showing the effect on the topology of the polymer. Thus, when there is an excess of succinic acid (A) a branched polymer is expected. On the other hand, when the glycerol is in excess (B) a lower degree of branching is expected.

With a 1:1 molar ratio, a polymer with a molecular weight up to 3,900 Da ($Đ$ > 2) was obtained with 18% of DB, which was partially soluble in water (Table 3.5, entry 1); when increasing the SA content to a G:SA molar ratio of 1:1.5 and 1:2, the DB increased to 58 and 56%, as did the molecular weight of the polymer, resulting in a polymer that was insoluble in water with molecular weights of 11,100 and 6,200 Da ($Đ$ > 2) (Table 3.5, entry 2 and 3). Previous studies have shown the same trend.[171]

To elucidate the PGLSA topology further, MALDI-TOF spectrometry was performed. It is well known that MALDI-TOF can provide valuable information regarding the topology of a polymer.[212] If branched polymers are formed, resulting from the esterification of both primary and secondary hydroxy groups of glycerol, oligomers containing tri-substituted units will show characteristic masses different from those of an oligomer containing only linear di-substituted structures.

Figure 3.14 shows the MALDI-TOF spectrum of the polymer from entries 2, Table 3.5. Below 500 Da, mass spectral data are not valid due to the matrix interference and no ions were detected above 3,000 Da (super DHB matrix: mixture of 2,5-dihydroxybenzoic acid and 2-hydroxy-5-methoxybenzoic acid matrix).

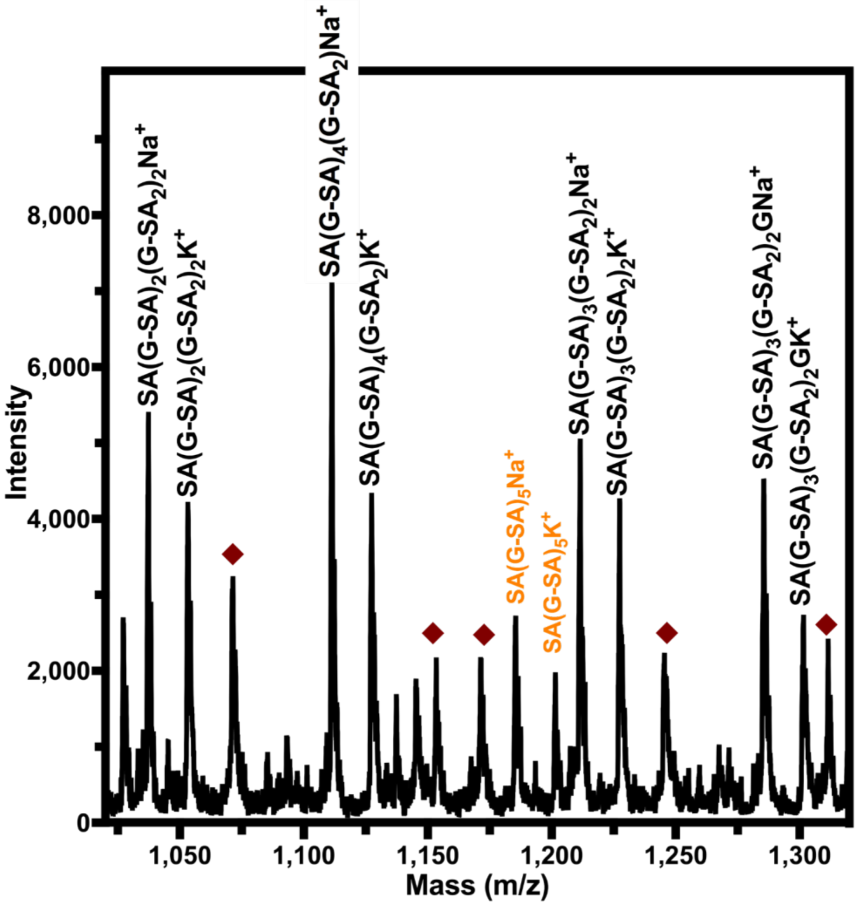

Figure 3.14 – Representative section of a MALDI-TOF mass spectrum of K$^+$ and Na$^+$ adducts of a branched poly(glycerol succinate) (samples from entries 2 from Table 3.3 and Table 3.5). *Note*: ◆ it is an unknown peak; the peaks not assigned are assumed to be noise from the baseline spectrum; G = glycerol; SA = succinic acid; orange annotation denotes the linear structure, black annotation denotes the branched structure.

Table 3.7 shows suggested structures and predicted masses of the sodium and potassium adducts for a branched PGLSA. Since the peaks obtained through the MALDI spectrum match with the predicted masses, the author can confirm that a branched structure was obtained.

Table 3.7 – Suggested structures and predicted masses of the sodium and potassium adducts for the branched poly(glycerol succinate). *Note*: G = glycerol; SA = succinic acid.

Entry	Polymer structure	$(M + Na)^+$	$(M + K)^+$
1	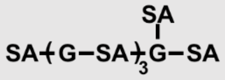 $\mathrm{SA{-}(G{-}SA)_{3}{-}\overset{SA}{G}{-}SA}$	937	953
2	 $\mathrm{SA{-}\overset{SA}{G}{-}SA{-}\overset{SA}{G}{-}SA{-}\overset{SA}{G}{-}SA}$	963	979
3	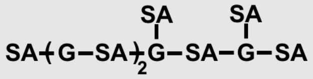 $\mathrm{SA{-}(G{-}SA)_{2}{-}\overset{SA}{G}{-}SA{-}\overset{SA}{G}{-}SA}$	1,037	1,053
4	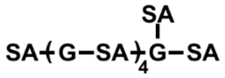 $\mathrm{SA{-}(G{-}SA)_{4}{-}\overset{SA}{G}{-}SA}$	1,111	1,127
5	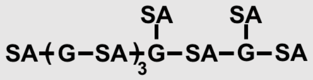 $\mathrm{SA{-}(G{-}SA)_{3}{-}\overset{SA}{G}{-}SA{-}\overset{SA}{G}{-}SA}$	1,211	1,228
6	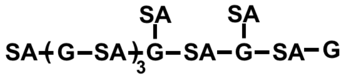 $\mathrm{SA{-}(G{-}SA)_{3}{-}\overset{SA}{G}{-}SA{-}\overset{SA}{G}{-}SA{-}G}$	1,285	1,302

DSC analyses were performed to evaluate the thermal properties of PGLSA, giving valuable information about the interactions between the chains present in the polymer. It is well known that the glass transition (T_g) increases with an increase in molecular weight.[213] However, with hyperbranched polymers, other effects influence the chain interactions as well. Sunder*, et al.* [214] demonstrated that the T_g of a highly polar hyperbranched polymer (with a large number of hydroxy terminal groups) is governed by two factors: a) on one hand the hydrogen bonding of the end groups will lead to an increase in intermolecular forces, and thus a decrease of chain mobility; b) and on the other hand the tendency to generate higher ordered phases (meso- and crystallisation phases). Conversely, Zhu*, et al.* [215] and Khalyavina*, et al.* [216] confirmed that there is a non-negligible influence of branching on the glass transition temperature, especially for polar hyperbranched polymers. They reported that for DB < 27%, the T_g increases with DB; while at DB > 27%, the opposite effect is observed: T_g decreases with increasing DB. In this work, for PGLSA synthesised by melt polycondensation, without metal catalyst (Table 3.5 entries 1-3), the first heating scan showed endothermic melting peaks (T_m). However, on the second heating scans, these endothermic peaks were absent. This might be caused by the evaporation of water. Nonetheless, there is a clear effect of molecular weight on the T_g: the higher the molecular weight (8,200 Da, Table 3.5 entry 2), the higher the T_g (-18 ºC). In addition, there is also a clear effect of branching on the T_g: the lower the branching (DB = 18%, Table 3.5 entry 1), the lower the T_g (-61 ºC); on the other hand, the higher the branching (DB = 67%, Table 3.5 entry 2), the higher the T_g (-18 ºC). This tendency is not in agreement with Zhu*, et al.* [215] where it was stated that there is an increase of the T_g with DB until a maximum of DB = 27%, and then T_g decreases sharply. This effect might occur because of the competition between the junction density and the free volume of terminal units. (T_g = 50 ºC at a DB = 27% and T_g = 32 ºC at a DB = 40%).

Stannous catalysts such as $Sn(Oct)_2$ have been used extensively to catalyse polycondensation reactions, although its utility towards the formation of polyesters is under debate. Terzopoulou*, et al.* [196] studied the effect of the catalyst type on the molecular weight increase of poly(ethylene furanoate) and reported that among the tested catalysts ($Sn(Oct)_2$, tetrabutyl titanate(IV), TTIP and DBTO), $Sn(Oct)_2$ was the catalyst with the lowest activity towards the transesterification of dimethyl 2,5-furandicarboxylate with ethylene glycol.

On the other hand, Winkler*, et al.* [217] and Gubbels*, et al.* [218] confirmed that $Sn(Oct)_2$ is an active catalyst in the synthesis of polyesters. Linear solid polyesters with molecular weights of 9,900 to 11,500 Da, with low dispersities ($Đ$ < 1.6), were obtained after 12 h at 130 ºC, using 1 mol% $Sn(Oct)_2$.[217] By increasing the temperature up to 180 ºC for 24 hours and further 4 hours at 220 ºC, a polymer of lower molecular weight was obtained, with a molecular weight of 3,700 Da and with a higher dispersity ($Đ$ = 2.1).[218] Taking these findings into consideration, the polycondensation of glycerol with succinic acid was performed using 2 wt.% $Sn(Oct)_2$ at 140 ºC, studying the effect of the molar ratio of the monomers (Table 3.8).

From the NMR analysis, the spectra obtained have shown similar results to the polymers synthesised in melt, in the absence of catalyst. The presence of proton H_b in tri-substituted glycerol unit (⅄), *ca*. 5.28 ppm, confirms that the polymers obtained were branched.

Table 3.8 – Synthesis of poly(glycerol succinate) *via* melt polymerisation with $Sn(Oct)_2$. [a] these M_n values corresponds to the peaks with higher molecular weights, other peaks were detected in the GPC trace, due to the presence of oligomers; [b] determined by Frey's equation (Equation 3.7); [c] characterisation not possible because of insolubility. *Note:* nd. = not defined

	Entry	**Time**	**G:SA molar ratio**	**Yield**	**M_n^{GPC} (Da)[a]**	***Đ***	**DB[b]**	**T_g**
$Sn(Oct)_2$	**4**	17 h	1:1	***x-linked*** [c]				-3 ºC
	5a	1 h	1:1	*nd.*	4,500	> 2	17%	–
	5b	2 h	1:1	*nd.*	6,000	> 2	31%	–
	5c	3h	1:1	***x-linked*** [c]				-9 ºC
	6a	1 h	1:3	nd.	7,400	> 3	72%	–
	6b	2 h	1:3	97%	11,400	> 3	87%	-5 ºC

After 17 h, with a ratio of G:SA 1:1, a crosslinked colourless polymer was obtained, showing clearly the synthesis of a crosslinked poly(glycerol succinate) (Table 3.8, entry 4). Thus, the reaction was repeated for 3 h at 140 ºC using 2 wt. % $Sn(Oct)_2$ (Table 3.8, entry 5). After 1 h a polymer with a molecular weight of 4,500 Da with low dispersity and 17% DB was obtained (Table 3.8, entry 5a). After 2 hours, the molecular weight increased to 6,000 Da, maintaining a low dispersity and the degree of branching doubled to 31% (Table 3.8, entry 5b). After 3 hours, an insoluble solid colourless polymer was obtained, showing clear signs of crosslinking.

Increasing the amount of diacid, is expected to result in a higher DB and thus, a polymerisation with a ratio of G:SA 1:3 was performed. After 1 hour, a very viscous polymer with a molecular weight of 7,400 Da (with high dispersity, $Đ$ = 2.4) and a high degree of branching (72%) was obtained (Table 3.8, entry 6a). The reaction was stopped after 2 hours, resulting in a polymer with a molecular weight of 11,400 Da ($Đ$ = 2) with a degree of branching of 87%, confirming that upon increasing the molar ratio G:SA, the branching occurs faster, (Table 3.8, entry 6b).

MALDI-TOF spectrometry was also performed for the polymers synthesised in melt conditions in the presence of $Sn(Oct)_2$ and the spectra obtained were similar to the ones describe in the absence of catalyst (Figure 3.14). The presence of oligomers containing tri-substituted units, resulted from the esterification of both primary and secondary hydroxy groups of glycerol, and show a clear pattern of a branched polymer.

To evaluate the thermal properties of PGLSA synthesised in melt conditions in the presence of $Sn(Oct)_2$, DSC analyses were performed. The same conclusions obtained for the synthesis of PGLSA in the absence of catalyst can be made for the synthesis of PGLSA in the presence of $Sn(Oct)_2$. In the first heating scan, endothermic melting peaks (T_m) are clear. However, this might be caused by the evaporation of water since on the second heating scans, these endothermic peaks were absent. In these polymers, it is also possible to observe a clear effect of molecular weight on the T_g: the higher the molecular weight (11,400 Da, Table 3.8 entry 6b), the higher the T_g (-5 ºC). For entries 4 and 5c from Table 3.8, a crosslinked polymer was obtained so it is expected to have high T_g (-3 and -9 ºC, , Table 3.8 entries 4 and 5c, respectively as compared to -61 ºC from entry 1 - Table 3.5).

Polyesters are used in several applications and glycerol-based polymers have a high potential to be used in cosmetic and medical materials.[146-147] As mentioned and shown previously, using metal-based catalysts, a lack of selectivity to the primary hydroxy groups of glycerol is observed. For some polyol-based polymer applications (e.g. surfactant industry), it is important to retain the hydrophilicity and avoid crosslinking, which means that the secondary hydroxy group of glycerol should not react. In organic chemistry, it is possible to use elaborate protection-deprotection steps to avoid undesirable reactions of hydroxy functional groups.[219-220] Although this procedure is chemically efficient, it uses flammable, corrosive and toxic chemicals, is time consuming, requires excessive purification steps, which are not viable for a polymerisation/industrial application. Thus, finding a convenient, efficient and environmentally friendly procedure towards the synthesis of linear hydrophilic glycerol-based polyesters is of high interest.

3.5.2. Enzymatic polycondensation of poly(glycerol succinate) with and without toluene

Lipases are well known for their regioselectivity during esterification reactions at mild conditions.[221-222] Thus, these features (metal-free reactions using mild conditions and regioselectivity) have been inspiring research on the synthesis of polyol-based polyesters. Almost 20 years ago, Iglesias*, et al.* [204] and Pessagno and Baldessari [205] synthesised glycerol-based polyesters under similar mild conditions, 30 ºC (72 h reaction) using dioxane or tetrahydrofuran as solvents, and molecular sieves to remove the by-product water. They obtained polymers with molecular weights up to 2,000 Da with narrow dispersity showing no branching. Nonetheless, by increasing the temperature to 70 ºC for 42 h (in bulk and under vacuum conditions), Kumar*, et al.* [150] synthesised poly(glycerol succinate) with a molecular weight of 2,500 Da (*Đ* =

1.4), and CaLB showed a regioselectivity of 85% which means that some polymer branching occurred. Increasing the temperature even further to 90 ºC, Yang, *et al.* [223] synthesised a polymer with a molecular weight of 9,000 Da within 24 h, but this time, the dispersity was higher (*Đ* = 3.3) and some branching (16%) was observed. In this study, they compared the effect of CaLB and DBTO in the synthesis of poly(oleic diacid-co-glycerol). After 6h of reaction, with the latter catalyst, a gel was obtained, thus evidencing cross-linking. They concluded that the enzyme must show steric hindrance at the lipase active site, which slows branching and impedes cross-linking reactions.

Taking these results into consideration, in this work poly(glycerol succinate) was synthesised enzymatically. Reactions in a solvent-free system (bulk) and in the presence of toluene were performed in a range in temperatures from 60 to 110 ºC. To shift the reaction equilibrium towards the formation of polyester, the reactions were performed under vacuum, or under an argon stream, in the presence of molecular sieves, (Table 3.9).

In order to evaluate the branching pattern, NMR analyses were performed for PGLSA synthesised enzymatically through melt conditions. Our hypothesis was that the enzyme should show more linear structures. Hence, we would expect an absence of protons H_a, H_b and H_c chemical shifts when at a tri-substituted glycerol unit (⅄), *e.g.* branched structure. As explained previously, ^{1}H-NMR analysis is revealed to be insufficient for complete structural characterization of the polymers. Therefore, 2D-HSQC and COSY NMR methods were also employed. The sample from entry 11, Table 3.9, was analysed using these techniques and Figure 3.15 and Figure 3.16 show the ^{1}H-NMR, 2D-HSQC and COSY-NMR spectra of this poly(glycerol succinate) sample.

Table 3.9 – Synthesis of poly(glycerol succinate) *via* melt polymerisation with CaLB, with and without toluene. [a] these M_n values corresponds to the peaks with higher molecular weights, other peaks were detected in the GPC trace, due to the presence of oligomers. [b] determined by Frey's equation (Equation 3.7).

	Entry	**Time**	**G:SA molar ratio**	**Yield**	**M_n^{GPC} (Da)[a]**	**$Đ$**	**DB[b]**	**T_g**
CaLB no solv	**7**	24 h	1:3	54%	14,900	> 2	11%	-50 ºC
	8	24 h	1:1	61%	3,700	> 2	13%	-55 ºC
CaLB in toluene	**9**	72 h	1:1	96%	5,800	1.27	9%	-50 ºC
	10	72 h	1:3	73%	1,800	> 2	11%	-66 ºC
	11	72 h	1:3	60%	7,300	1.36	9%	-60 ºC

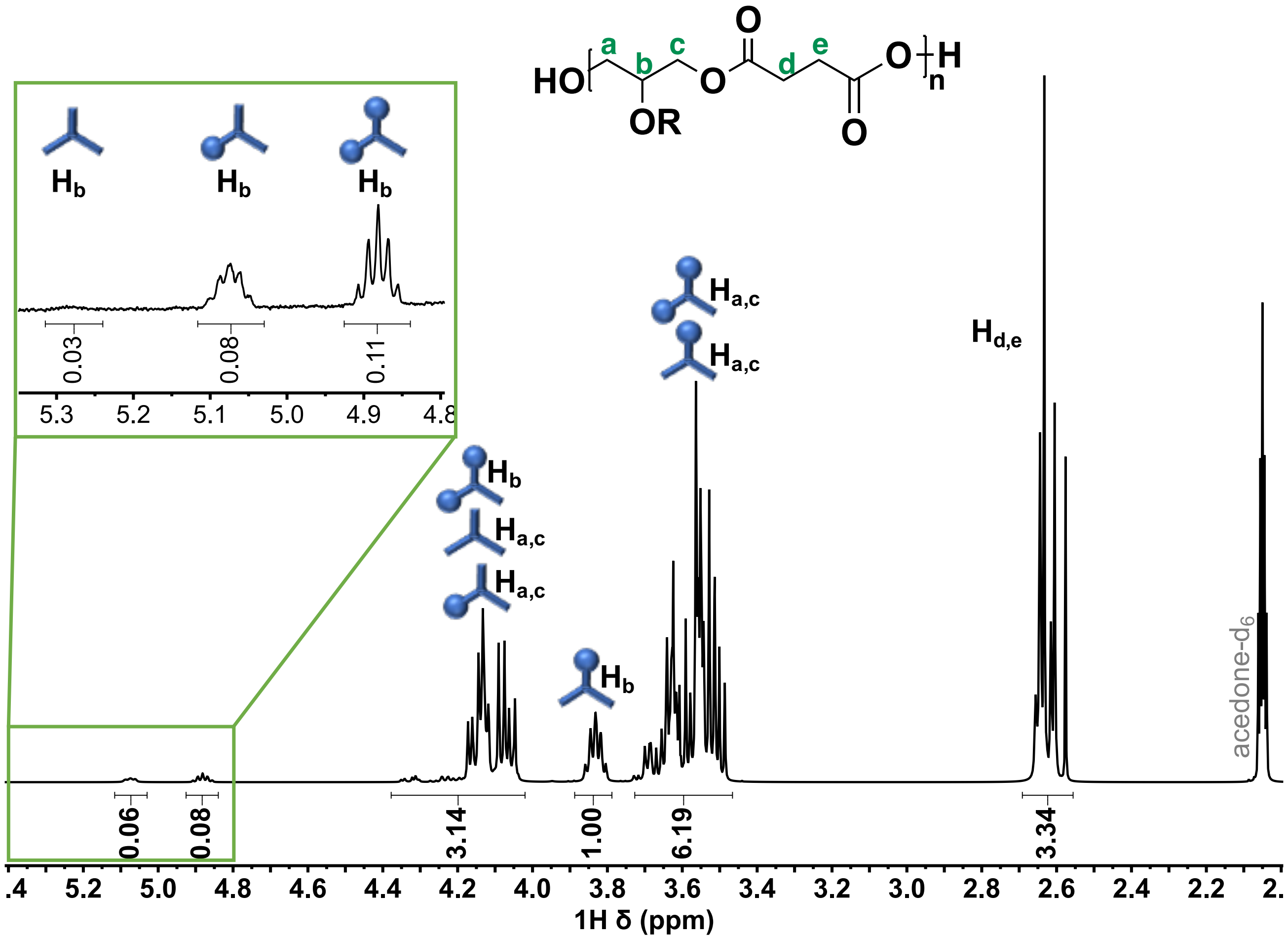

Figure 3.15 – ^{1}H-NMR spectrum of a linear poly(glycerol succinate) polymer (entries 11 of Table 3.9). The solvent used was acetone-d$_6$.

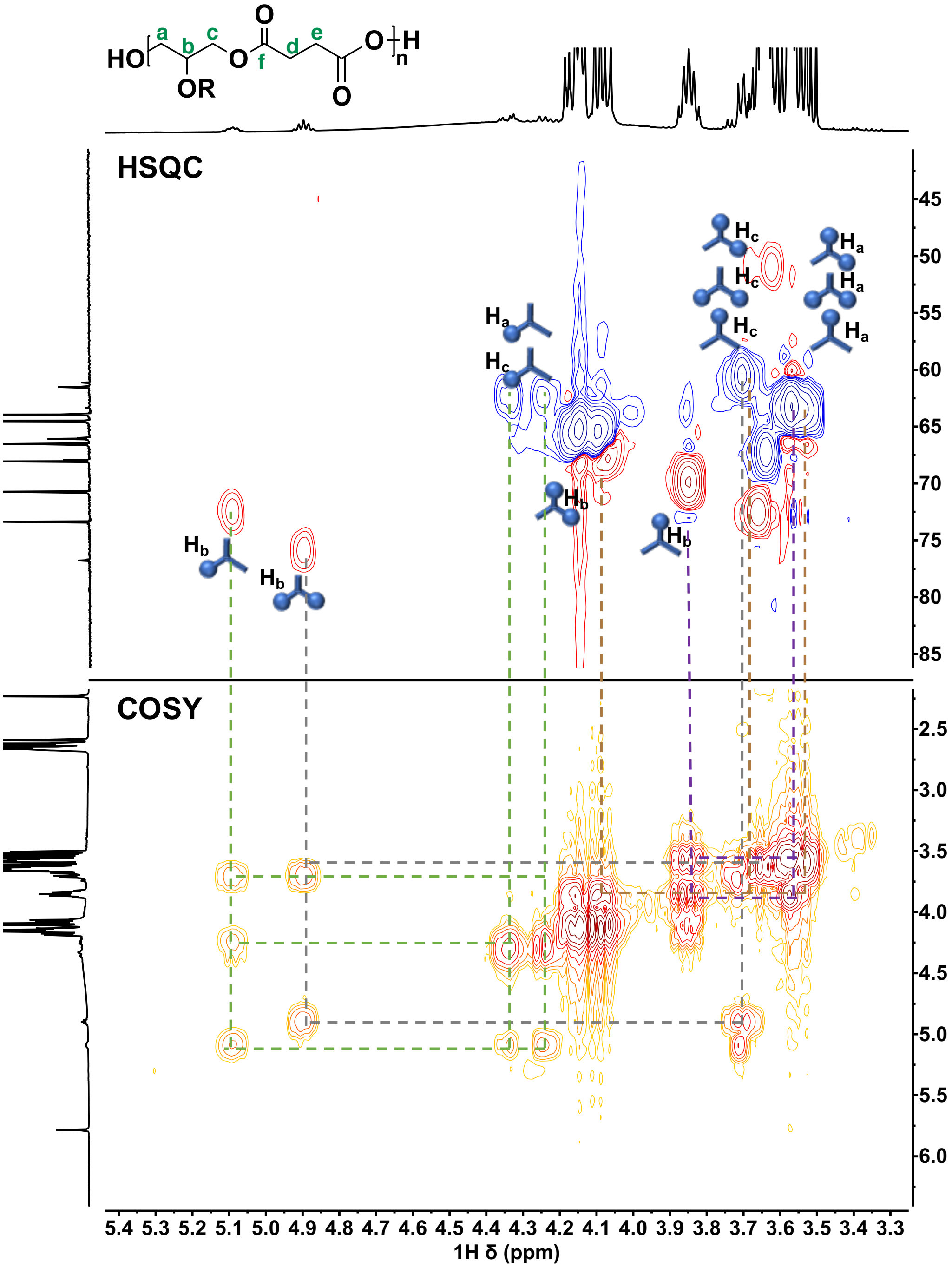

Figure 3.16 –Sections of the HSQC and COSY NMR spectrum showing the assignments of glycerol units in a linear poly(glycerol succinate) polymer (entries 11 of Table 3.9). The solvent used was acetone-d_6. In the HSQC spectrum, methylene proton (–CH$_2$) signals are plotted in blue. Methine proton (–CH) signals are plotted in red. *Note*: ⅄ this symbol denotes that proton H$_b$ is present in a linear structure and the polymerisation occurred in positions b and c. ⅄ this symbol denotes a terminal glycerol unit proton H$_b$ showing that the polymerisation occurred in position b. The dotted lines reveal some of the proton coupling.

The ^{1}H-NMR spectra of PGLSA synthesised *via* enzymatic melt polycondensation (entry 11 from Table 3.9, Figure 3.15), shows the presence of proton H_b in the tri-substituted glycerol units. However, they are significantly less prominent than for the branched PGLSA synthesised with $Sn(Oct)_2$ (Figure 3.11). This confirms the presence of a more linear polymer structure.

In the HSQC spectrum, the identification of the methylene ($–CH_2$, blue plot line in Figure 3.16) and methine ($–CH$, red plot line in Figure 3.16) protons is important in order to identify if the polymer is linear or branched. Thus, it follows that the methylene peaks correspond to H_c and H_a protons; and methine peaks correspond to H_b protons. Therefore, considering the correlation of HSQC and COSY spectra, (Figure 3.16), it was possible to observe that the proton couplings of di-substituted and terminal glycerol units. The green dotted line connects the proton ⅄H_b (5.07 ppm) with the protons ⅄H_a and ⅄H_c, at *ca.* 4.40-4.05 ppm. The grey dotted line connects proton ⅄H_b (4.88 ppm) with the protons ⅄H_c and ⅄H_a (3.72-3.50 ppm). The coupling between the proton ⅄H_b (4.40-4.05 ppm) and the protons ⅄H_a and ⅄H_c (3.72-3.50 ppm) is represented by the brown dotted line. The purple dotted line represents the coupling between ⅄H_b (3.83 ppm) and protons ⅄H_a and ⅄H_c (3.72-3.50 ppm). Most notably, protons H_a, H_b and H_c in a tri-substituted glycerol unit (⅄) could not be observed in the 2D-NMR spectra, demonstrating a predominant linear structure and supporting our hypothesis that branching is lower. The chemical shifts are in good agreement with previous values described by Khongphow*, et al.* [46] and Wyatt and Strahan [47].

The degree of branching was calculated following Equation 3.7, by integrating the resonances corresponding to the H_b protons from B_0 and B_1 structures, using ^{1}H-NMR. The chemical shifts used were: ⅄H_b (B_0) = 5.28 ppm, ⅄H_b (B_1) = 5.07 ppm, ⅄H_b (B_1) = 3.83 ppm.

At a 1:1 G:SA molar ratio with 17 wt.% CaLB at 60 ºC (in bulk), after 24 h a viscous yellow clear polymer with a molecular weight of 3,700 Da was obtained showing some branching (DB = 13%, Table 3.9 entry 8). When increasing the temperature (110 ºC), the loading of enzyme (25 wt.%† CaLB) and the diacid content, it would be expected to observe an increase in branching. However, after a reaction time of 24 h in bulk, a waxy white polymer with a molecular weight of 14,900 Da was obtained showing only 11% branching (Table 3.9, entry 7). This is not in agreement with what was observed previously (polycondensations in the absence of catalyst, or in the presence of Sn(Oct)$_2$) in which the lower the ratio of G:SA, the earlier the gelation occurs and the higher the chances to synthesise a branched polymer. For comparison, the enzymatic synthesis of poly(glycerol succinate) (5 wt.%† CaLB) was also performed in the presence of toluene, at 100 ºC, with an argon stream and with molecular sieves (Table 3.9, entry 9 and 10). After 72 h, using a 1:1 molar ratio of G:SA, a polyester with a molecular weight of 5,800 Da (waxy white polymer) was obtained with only 9% of branching (Table 3.9, entry 9). Upon increasing the succinic acid content (1:3), the molecular weight determined by GPC decreased to 1,800 Da, and the polymer exhibited 11% branching (Table 3.9, entry 10).

Some researchers have performed polycondensation in two steps: firstly, the diacid and alcohol are reacted at a desired temperature in the solvent for 1 hour under argon; only then is catalyst added to the system and the temperature raised to the chosen reaction conditions.[224] Normally, this two-step procedure allows the synthesis of higher molecular weight polymer. Thus, this was also investigated using the same G:SA molar ratio as in the latter reaction (1:3), the diacid, triol and toluene were added to the round bottom flask, under argon, and the reaction temperature was set to 55 ºC for one hour. Afterwards, the enzyme (5 wt.%† CaLB) was added to the system and the temperature was raised to 100 ºC for 71 h (reaction conditions shown in Table 3.3, entry 11). This procedure gave a waxy white polymer with a higher molecular weight, 7,300 Da (*Đ* = 1.3; DB = 9%, Table 3.9 entry 11), than the one synthesised *via* the one step procedure (Table 3.9 entry 10), which is in accordance with the literature.

---

† includes polymer support

MALDI was performed to investigate the topology of these polymers (Figure 3.17 reveals the spectrum obtained from sample 11 from Table 3.9 – reaction conditions shown in entry 11, Table 3.3). The suggested structures and predicted masses of the sodium and potassium adducts for a linear PGLSA are shown below (Table 3.10). The peaks obtained through the MALDI spectrum match with the predicted masses, confirming a more linear structure of PGLSA. Nevertheless, it is still possible to observe some branched structures, which were expected as a consequence of the degree of branching determined by ^{1}H-NMR (DB = 9%). The same conclusions can be made for the other samples of PGLSA synthesised *via* enzymatic melt polycondensation.

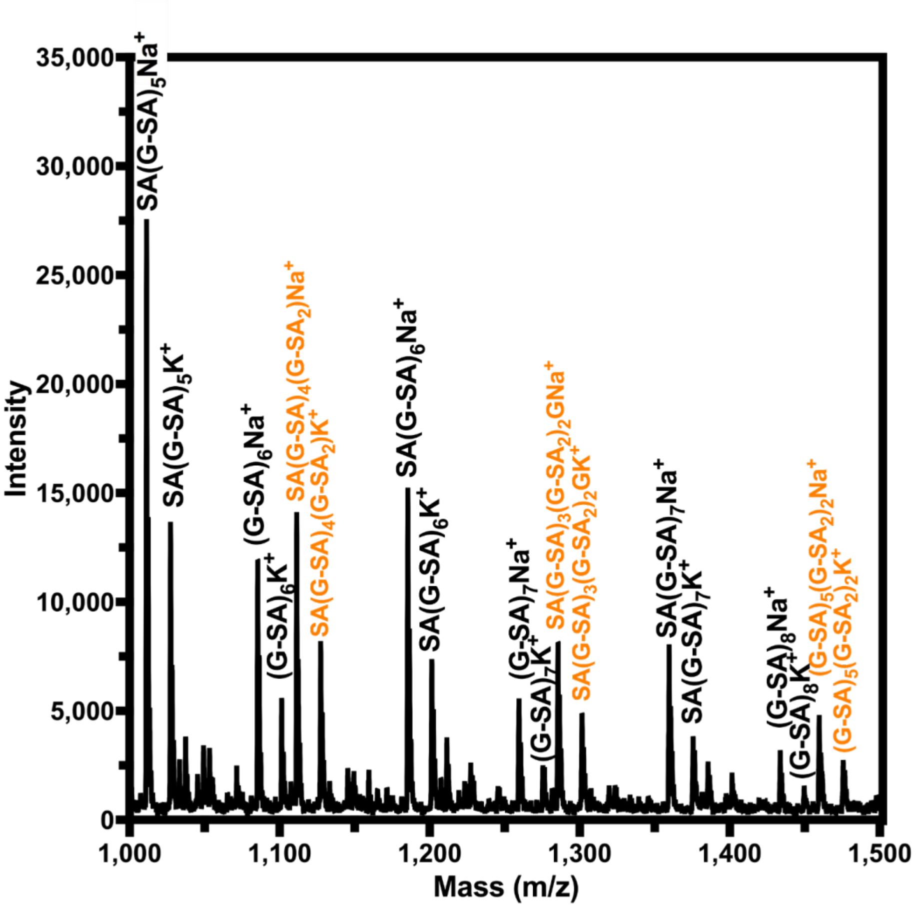

Figure 3.17 – Representative section of a MALDI-TOF mass spectrum showing K^+ and Na^+ adducts of a linear poly(glycerol succinate) (samples from entries 11 from Table 3.3 and Table 3.9). *Note*: the peaks which are not assigned are assumed to be noise from the baseline spectrum; G = glycerol; SA = succinic acid; in orange labels correspond to the branched structures; black annotation denotes the branched structure.

Table 3.10 – Suggested structures and predicted masses of the sodium and potassium adducts for the linear poly(glycerol succinate). *Note*: G = glycerol; SA = succinic acid.

Entry	**Polymer structure**	**$(M + Na)^+$**	**$(M + K)^+$**
1	$\mathrm{SA}(\mathrm{G{-}SA})_5$	1,022	1,038
2	$(\mathrm{G{-}SA})_6$	1,085	1,101
3	$\mathrm{SA}(\mathrm{G{-}SA})_6$	1,185	1,201
4	$(\mathrm{G{-}SA})_7$	1,259	1,275
5	$\mathrm{SA}(\mathrm{G{-}SA})_7$	1,359	1,375
6	$(\mathrm{G{-}SA})_8$	1,433	1,449

Comparing this spectrum with the one obtained previously (PGLSA synthesised in the absence of catalyst or in the presence of the metal catalyst), it was possible to observe different repeated unit patterns. In the later one, more linear oligomers were existent, in contrast with the previous one, where more branched patterns were obtained. This confirms our hypothesis that using CaLB shows more linear structures. Hence, less branched polymer structures.

The T_g's of PGLSA synthesised *via* enzymatic melt polycondensation show a negligible effect of the increase in molecular (Table 3.9). These values in the range of -50 ºC are similar. to the T_g of linear polyesters (such as poly(butylene itaconate and poly(1,5-pentylene adipate)) which were reported previously by several authors, in the range of -60 – -40 ºC.[225-226]

Poly(glycerol succinate) polymers, synthesised *via* enzymatic melt condensation, were also analysed by infrared spectroscopy (ATR FT-IR) and compared with a branched PGLSA (synthesised in the absence of catalyst) (Figure 3.18: linear polymer, sample from entry 11, Table 3.9; branched polymer, sample from entry 2, Table 3.5).

A broad peak appears at *ca*. 3,420 cm^{-1}, which corresponds to –OH functional groups in the backbone (orange trace in Figure 3.18). The more linear the polymer, the more the peak *ca*. 3,420 cm^{-1} increases in intensity, suggesting that the hydroxy functional groups are free, and have not been esterified. This observation was also reported by other authors (for poly(glycerol succinate) polymers).[211] The peak *ca.* 1,700 cm^{-1} corresponds to the –C=O functional groups while the signal at 1,405 and 1,297 cm^{-1} corresponds to the –CH bending. The peak at 1,143 cm^{-1} belongs to the C–O–C stretching. As would be expected, no detectable differences in the IR spectra were apparent at the different synthesis temperatures.

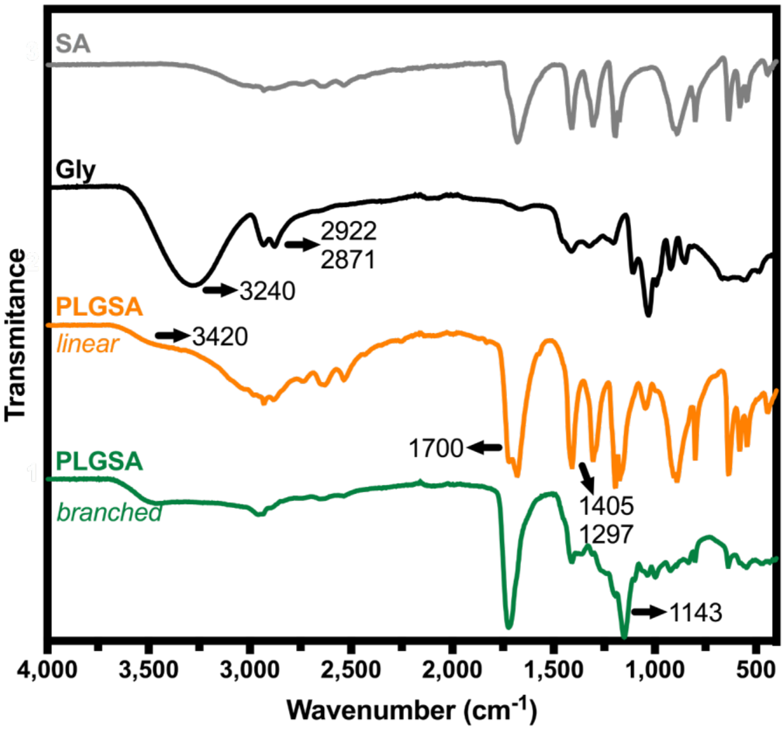

Figure 3.18 – ATR-IR spectra of poly(glycerol succinate), PLGSA, in the spectral range between 4,000 and 400 cm^{-1}. The plot in orange corresponds to a linear polymer (entry 11 of Table 3.9) and in green to a branched polymer (entry 2 of Table 3.5).

The use of CaLB for the synthesis of a polyol-based polyester was found to be a good method to synthesise more linear polyesters with pendant hydroxy groups that could be valuable for further functionalisation, or to create a more hydrophilic polyester. However, the melt condensation process is not ideal due to the use of temperatures higher than 60 ºC. Therefore, in the next section, the use of $scCO_2$ for the synthesis of poly(glycerol succinate) will be discussed at lower temperatures.

3.5.3. Behaviour of glycerol and succinic acid in supercritical carbon dioxide

Two commercially available bio-based monomers, glycerol and succinic acid, have been exploited as building blocks for poly(glycerol succinate) polymers in $scCO_2$.

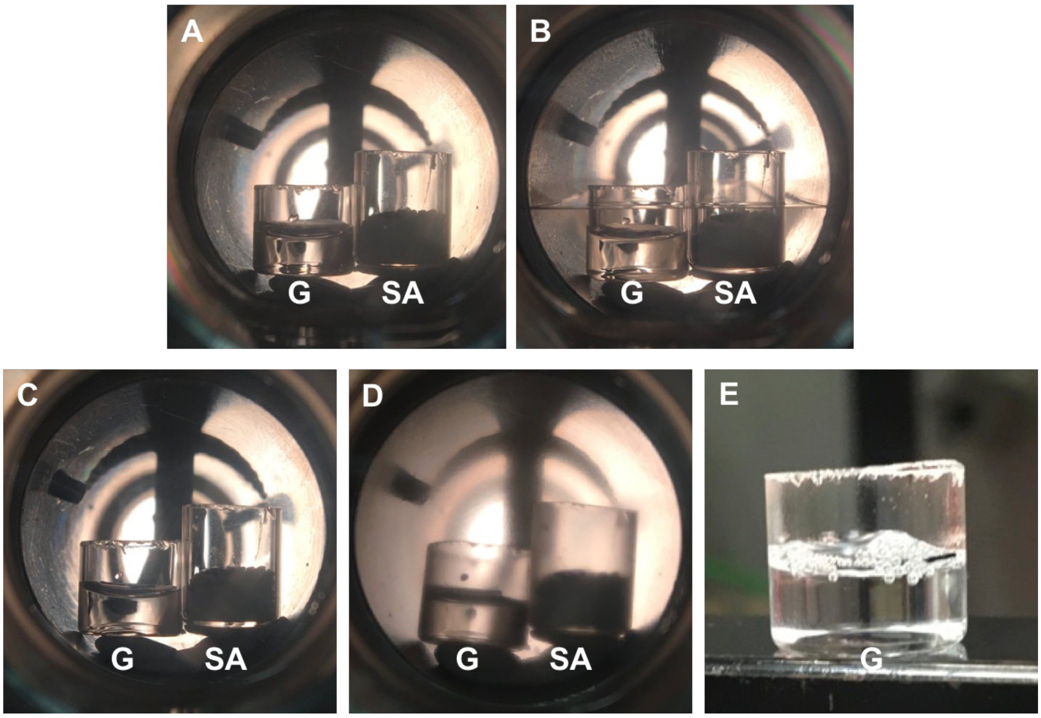

Figure 3.19 – Visual observation of glycerol (G) and succinic acid (SA) at **A)** at ambient pressure (1 bar) and temperature (25 ºC), **B)** at 65 bar and 27 ºC, **C)** at 275 bar and 40 ºC and **D)** at ambient pressure and temperature upon removal of the CO_2 (after 7 hours under pressure). Picture **E)** shows glycerol, at ambient conditions after 7 hours under supercritical conditions, exposing the evidence of CO_2 being released. It is possible to see that succinic acid and glycerol are not soluble in $scCO_2$; nonetheless, it is possible to observe that CO_2 is soluble in glycerol due to the presence of "bubbles" after exposure of CO_2.

The visual observation of the limited solubility of glycerol and succinic acid in $scCO_2$ is shown above (Figure 3.19). The low solubility of succinic acid in $scCO_2$ was already reported previously.[227] However, there is a clear difference before, during and after exposure of glycerol to $scCO_2$ (Figure 3.19, A-E), suggesting that $scCO_2$ might be soluble in glycerol; *e.g.* $scCO_2$ might have the ability to penetrate in between glycerol molecules which is indicated by the appearance of bubbles in the liquid glycerol upon removal of CO_2 (Figure 3.19, E). This was also confirmed by Medina-Gonzalez*, et al.* [228] who studied the phase equilibrium of the CO_2/glycerol system.

This view cell investigation is not a quantitative solubility test. Nevertheless, it does show a clear interaction of $scCO_2$ and monomer. A preliminary polymerisation was carried out at 35 ºC and 275 bar with 25 wt.% CaLB (polymerisation data not reported in this Thesis) for 3, 6 and 24 h. Initially, only oligomers were obtained whilst after 24 h hours, poly(glycerol succinate) was obtained with M_n of 3,000 Da. The same reaction was performed in the absence of $scCO_2$ and, as expected, no polymer was obtained. Consequently, $scCO_2$ plays a crucial role in the polymerisation of poly(glycerol succinate).

3.5.4. Enzymatic polycondensation of poly(glycerol succinate) under supercritical conditions

To the best of the author's knowledge, the enzymatic polycondensation of poly(glycerol succinate) under supercritical conditions has never been investigated. $scCO_2$ is used as a reaction medium to synthesise glycerol-based polyesters at low temperatures, using a bio-catalyst in a solvent-free system.

The polymerisations were carried out for 24 hours at 275 bar with 25 wt.% (includes polymer support) CaLB. The effect of the temperature (40-60 ºC) and the molar ratio of the monomers was investigated (Table 3.11).

Table 3.11 – Synthesis of poly(glycerol succinate) *via* enzymatic supercritical conditions. [a] it was determined by the Frey's equation (Equation 3.7).

	Entry	**Ratio (Gly:SA)**	**Yield**	**M_n^{GPC} (Da)**	**Đ**	**DB**[a]	**T_g**
40 ºC	**12**	1:1	87%	3,400	3.00	5%	-74 ºC
	13	1:2	67%	1,900	1.48	10%	-44 ºC
	14	2:1	59%	1,100	2.85	11%	-74 ºC
50 ºC	**15**	1:1	32%	2,600	2.73	13%	-48 ºC
	16	1:2	49%	1,200	1.27	8%	-40 ºC
	17	2:1	85%	2,700	1.84	3%	-56 ºC
60 ºC	**18**	1:1	84%	1,700	3.41	11%	-55 ºC
	19	1:2	88%	3,500	1.19	8%	-50 ºC
	20	2:1	78%	1,300	3.84	9%	-77 ºC

^{1}H-NMR of PGLSA synthesised under supercritical conditions is shown below (Figure 3.20). All the spectra from the synthesised PGLSA (at different temperatures and G:SA molar ratios) revealed the presence of the same peaks as the polymers synthesised with CaLB in melt conditions. The low intensity of the proton H_b (around 5.28 ppm) in the tri-substituted glycerol unit shows a noticeable low degree of branching.

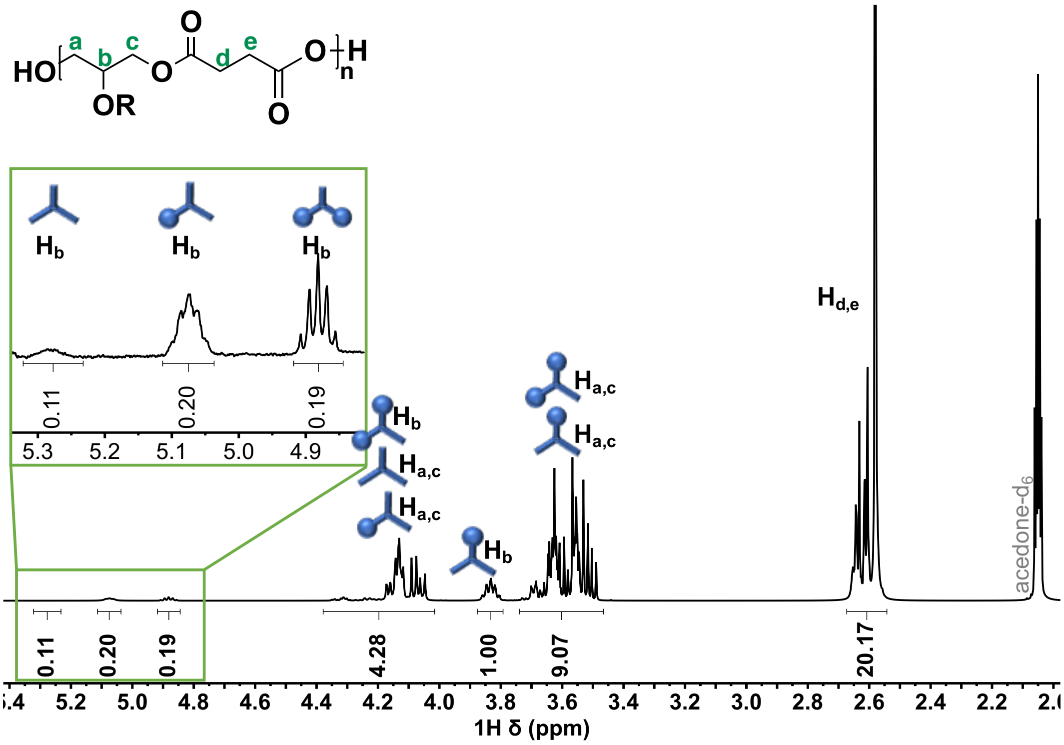

Figure 3.20 – ^{1}H-NMR spectrum of PGLSA enzymatic catalysed under $scCO_2$, at 60 ºC (275 bar) with a G:SA molar ratio of 1:2 (entries 19 from Table 3.4 and Table 3.11).

As discussed previously for the melt polycondensation of PGLSA, with or without a metal catalyst, the lower the ratio of Gly:SA, the earlier the gelation occurs and the higher the DB. However, when using CaLB, the DB in melt polycondensations was not affected by the molar ratio of alcohol:diacid. Under supercritical conditions, the same behaviour can be observed. At 40 ºC and with a molar ratio of G:SA 1:1 (Table 3.11, entry 12), a waxy yellow polymer with a molecular weight of 3,400 Da, with a low DB and a broad dispersity, *Đ* = 3, was obtained. When increasing the diacid content (Table 3.11, entry 13), the branching increased by 5%, while the molecular weight decreased to 1,900 Da (*Đ* = 1.5). Upon increasing the glycerol content to a molar ratio of 2:1 (Table 3.11, entry 13), the molecular weight decreased even more to 1,100 Da

(*Đ* = 2.8), while maintaining a DB of 11%. At 40 ºC, there is no clear effect on the DB (confirmed by NMR and MALDI) when changing the molar ratio of the monomers, but it was possible to observe an effect on the molecular weight.

At a temperature of 50 ºC and an equimolar ratio G:SA 1:1 (Table 3.11, entry 15), a polymer with a molecular weight of 2,600 Da (*Đ* = 2.7) with a low DB of 13% was obtained. Changing the diacid to glycerol ratio, 1:2 and 2:1 (Table 3.11, entries 16 and 17), resulted in polymers with molecular weights of 1,200 Da (*Đ* = 1.2) and 2,700 Da (*Đ* = 1.8), respectively, both with a low DB.

Upon increasing the temperature further to 60 ºC, at a 1:1 molar ratio (Table 3.11, entry 18), a polymer with M_n of 1,700 Da (*Đ* = 3.4) was obtained, again with a low DB of 11%. By varying the diacid and glycerol ratio, 1:2 and 2:1 (Table 3.11, entries 19 and 20), linear polymers with molecular weights of 3,500 Da (*Đ* = 1.2) and 1,300 Da (*Đ* = 3.8) were obtained, respectively. Under supercritical conditions, using a biocatalyst, the effect of molar ratio does not have an impact on branching, at the range in temperatures studied here. This finding proves the regioselectivity of the enzyme under these reaction conditions.

However, the molecular weight fluctuates when changing the reaction conditions. At an equimolar ratio of G:SA 1:1, at 40 ºC, the polymer with the highest molecular weight (3,400 Da) with a broad dispersity (*Đ* = 3) was obtained. Using an excess of diacid, 1:2, at 60 ºC, resulted in the polymer with the highest M_n with 3,500 Da (*Đ* = 1.2). Yet an excess of glycerol resulted in the polymer with the highest molecular weight at 50 ºC, with a M_n of 2,700 Da (*Đ* = 1.8). From the results obtained, there is no clear trend in the synthesis of poly(glycerol succinate).

Regarding the thermal properties of PGLSA synthesised under enzymatic supercritical conditions, no obvious trend was observed. As reported for the linear PGLSA obtained *via* enzymatic melt polycondensation (3.5.1 Melt polycondensation of poly(glycerol succinate) with and without catalyst), PGLSA shows a T_g around -74 – -40 ºC which is in the expected range in glass transition temperatures for linear polyesters.

To show the topology of the synthesised PGLSA enzymatic catalysed under $scCO_2$, MALDI-TOF was performed. The spectrum for the polymer synthesised at 60 ºC, 275 bar for 24 h with a G:SA molar ratio of 1:2 is shown below (Figure 3.21, sample from entry 19 of Table 3.11) and it is similar to the other polymers synthesised. Using this technique confirms the presence of a linear PGLSA. However, since the DB of this polymer is 8%, we would have expected some branching, but much less than was observed for $Sn(Oct)_2$ catalysed reaction, where a DB of 87% was obtained.

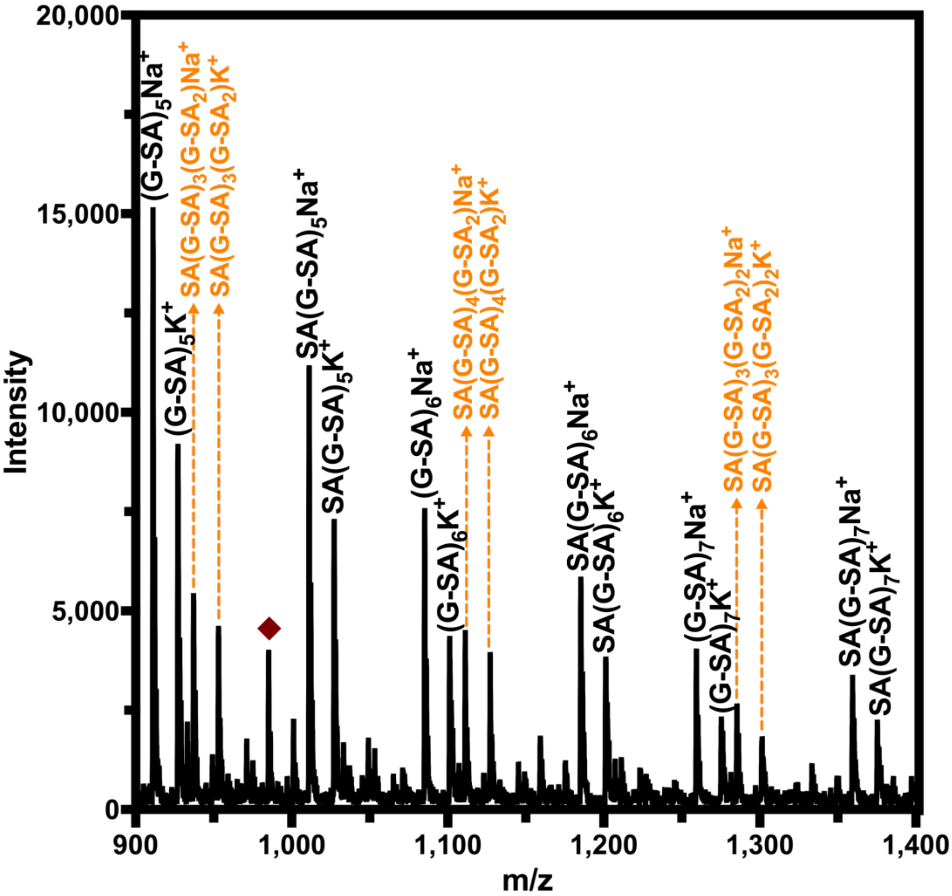

Figure 3.21 – MALDI-TOF mass spectrum section of K^+ and Na^+ adducts of PGLSA synthesised under enzymatic supercritical conditions (entries 19 from Table 3.11). *Note*: ◆ an unknown peak; the peaks not assigned are assumed to be noise from the baseline spectrum; G = glycerol; SA = succinic acid; orange annotation denotes the branched structure of PGLSA; black denotes the linear structure of PGLSA.

Using $scCO_2$ as a reaction medium offers great opportunities. In addition to the fact $scCO_2$ is a more environmentally friendly medium and a solvent-free system, low temperatures and enzymes can be used and it is possible to obtain linear PGLSA.

3.6. Technical note

It took nearly 2 years to understand the enzymatic polycondensation of glycerol and succinic acid under $scCO_2$. Initially, the author faced some challenges to solubilise PGLSA, making it hard to perform a suitable characterisation (GPC and NMR analysis). In addition to this, as a consequence of solubility issues, MALDI results were obtained from samples that contained enzyme beads. The MALDI spectra showed unusual repeating patterns of 44 m/z (Figure 3.22). After several studies and reactions (including kinetic studies, changing of the diacid and polyol – results not shown) the author managed to solve the solubilisation problem. Upon reaction completion, the polymeric samples were dissolved in THF, gently heating at 40 ºC, and filtered to remove the enzyme beads and molecular sieves. MALDI analysis performed after this "purification" step, showed a repeating pattern of 174 m/z (which corresponds to the PGLSA repeated unit). This has confirmed that the presence of the enzyme beads in solution was the problem. Therefore, to prove that the reason of having 44 m/z repeated units was because of the enzyme, CaLB beads were analysed through MALDI. Unexpectedly, a spectrum with a repeating pattern of 44 m/z was obtained (Figure 3.23). The author suspects that this might be related to the ionisation of the acrylic resin, used to immobilise the enzyme.

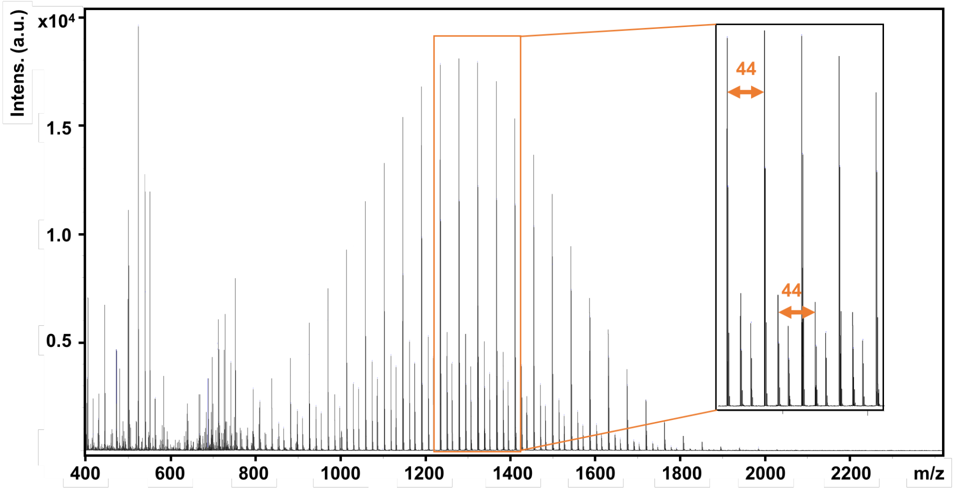

Figure 3.22 – MALDI-TOF spectrum obtained of PGLSA before removing CaLB beads, showing the repeating unit of 44 m/z.

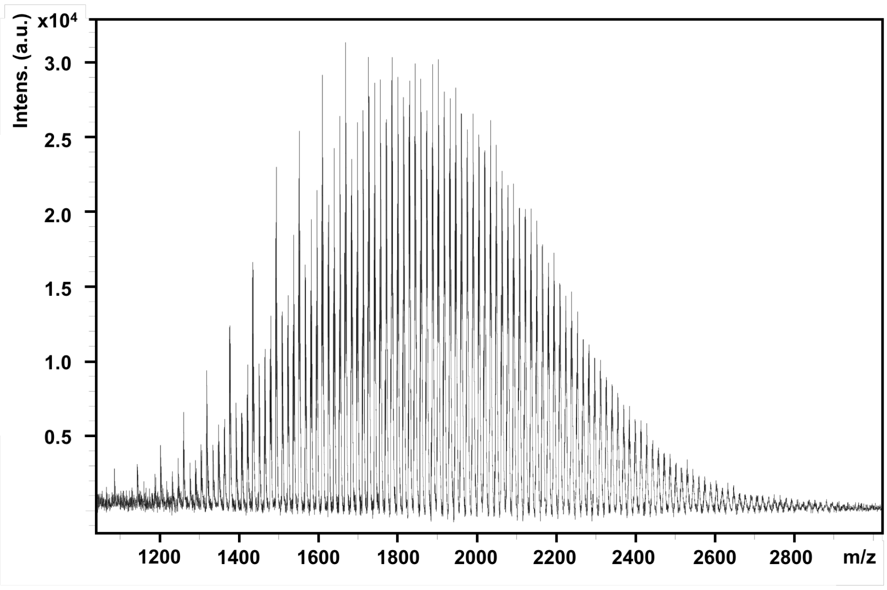

Figure 3.23 – MALDI-TOF spectrum obtained of CaLB beads in solution, showing the repeating unit of 44 m/z.

3.7. Conclusions

This chapter demonstrates a greener approach to synthesise linear poly(glycerol succinate) (PGLSA) using Novozyme 435 under mild conditions. The methodology establishes the synthesis of polymers from renewable sources – glycerol and succinic acid, using $scCO_2$ as the reaction medium.

Initially, the synthesis of PGLSA under conventional conditions through melt polycondensation, in the absence and in the presence of a metal catalyst, was accomplished. Branched and crosslinked polymers were obtained. This procedure is used industrially and requires high temperatures which are not ideal from an environmental point of view. The branched polymer structure obtained was confirmed by ^{1}H-NMR, ^{13}C-NMR, COSY and 2D-HSQC NMR spectroscopy and MALDI-TOF spectrometry.

To avoid branching/crosslinking, Novozyme 435 was used instead of the metal catalyst, in melt polycondensations. Even at high temperatures, CaLB demonstrated to be regioselective. Linear poly(glycerol succinate) structures, with low degrees of branching, were obtained.

However, melt polycondensation reactions still required high temperatures. By exploiting the unique properties of $scCO_2$, it was possible to synthesise linear renewable polyesters with pendent hydroxy groups. This has been possible without the need of high temperatures, large amounts of toxic solvents or pre-modification of monomers. The linear chemical structures were confirmed by ^{1}H-NMR, ^{13}C-NMR, COSY and 2D-HSQC NMR spectroscopy and MALDI spectrometry, showing that there was minimal esterification on the secondary hydroxy group of the glycerol monomer.

This process shows that it is possible to synthesise PGLSA using a green, solvent-free, low-temperature route. Dropping the polymerisation temperature from 140 ºC to 40 ºC has a dramatic effect. Such high-pressure process would be more energetically sustainable than a conventional melt synthesis. Nonetheless, the major drawback of this process, is the need of using a toxic solvent (THF), although in a small amount, to separate the polymer from the enzyme beads. However, this could be overcome by using $scCO_2$ as a plasticiser, with the aim to liquefy the polymer and allow clear separation of the enzyme beads.[105] This was demonstrated by our group previously by placing the enzyme beads in a small wire mesh filter basket and by placing in the bottom of the autoclave. This step not only enables separation of the polymeric products and enzyme beads, but also allows recycling of the enzyme.

In the next chapter (Chapter 4), the possibility of functionalising the hydrophilic groups present in the polymer backbone of linear polyesters synthesised from glycerol will be investigated.

CHAPTER 4. APPLICATION OF GLYCEROL-BASED POLYMERS

4.1. Overview

Surfactants (surface-active agents) are amphiphilic compounds, containing both hydrophilic and hydrophobic moieties in the same molecule. They are widely used as emulsifiers, detergents and foaming agents in several industries: home care, personal care, health care, cleaning, industrial uses and crop care. Since their introduction in the market, around the early 20th century, the production of surfactants from petrochemical sources has continually increased.[229] The global production of surfactants has now reached 18.5 million tons per year and is forecast to grow at a compound growth rate (CAGR) of 5% during the forecast period 2018-2023.[230] Recently, global social-environmental awareness has become a major driving force for both industry and research to exploit new strategies to synthesise more environmentally-friendly and economically viable surfactants.[231] The synthesis of greener surfactants has been recently studied.[45, 112, 231-232]

In this chapter we will explore poly(glycerol succinate) polymer (PLGSA), synthesised using $scCO_2$ and enzymes in Chapter 3. Could these provide a novel methodology for the production of greener surfactants? Thus, this chapter focuses on developing the enzymatic assisted synthesis of glycerol and succinic acid, with specific molar ratio, and investigating end-capping with lauric acid or methoxy poly(ethylene glycerol) (with a molecular weight of 350 Da).

To assess the properties and the efficiency of the surfactants, several analytical methods will be used to characterise the surfactants: ^{1}H-NMR, GPC and DSC. The ability of these compounds to reduce the surface tension of water will be evaluated pre- and post-end capping. Both dynamic and equilibrium (static) surface tension measurements will be performed. The critical micelle concentrations, size of the micelles and the determination of contact angle formed between interfaces will also be determined. Comparisons will be made with commercially available surfactants.

4.2. Introduction

4.2.1. Surfactants

Surfactants (contraction of the term **surf**ace-**act**ive age**nts**) are well known molecules able to modify the surface properties of liquids, typically water. They have at least one lyophilic ('solvent-loving') group and one lyophobic ('solvent-hating') group in the molecule. If the solvent is water or an aqueous solution, then the terms would be 'hydrophilic' and 'hydrophobic', respectively (Figure 4.1).

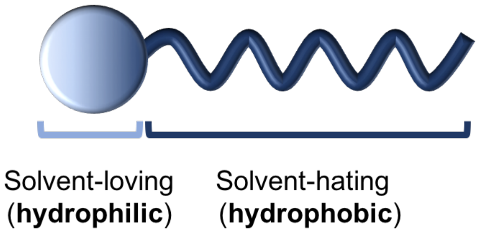

Figure 4.1 – Schematic representation of a surfactant. Light blue part represents the hydrophilic head; dark blue part represents the hydrophobic tail.

Before World War I, the great majority of surfactants present in cleaning and laundering products were from a fatty acid soap derived from natural fats and oil. The first synthetic surfactants for general application were developed in Germany during World War I (1914-1918), as an attempt to overcome shortages of available animal and vegetal fats.[233] These surfactants, resulting from the reaction of propyl, or butyl alcohol, with naphthalene followed by sulfonation, were useful as detergents and they are still in use today. In the early 1960s, alkylbenzene sulfonate (ABS) was the major ingredient used in washing products. The mass production of this surfactant was responsible for sewage effluents producing large amounts of foam in rivers, streams and lakes throughout the world. In addition to the nasty appearance of foam in waterways, the water tended to foam even when coming out of the tap.[234] To combat these problems, chemical industries developed new and efficient processes for the production of petroleum-based surfactants. Moreover, economic and cultural changes, increasing population and the spread of automatic washing machines, etc., led to an increase in surfactant consumption worldwide. In 1945, synthetic surfactants represented only 4% of the total market; by 1970, synthetic surfactants had risen to over 80% of total soap and detergent production.[233]

The properties and applications of surfactants vary with the chemical structure of the "hydrophilic head" and "hydrophobic tail". Two different phenomena can occur with surfactants: adsorption and aggregation. Surfactant molecules in an aqueous environment will migrate to air/water and solid/water interfaces, positioning in such a way to minimise the contact between their hydrophobic groups and water. This process is referred to as adsorption and it results in a change in the properties at the interface. Aggregation, or micellisation, is a process whereby the surfactant molecules aggregate limiting the contact between the hydrophobic groups and the water by forming so called micelles. Micelles are ordered structures (Figure 4.2) that begin to form above a certain concentration value – the critical micelle concentration (CMC), above which the surfactant is no longer homogeneously dispersed at a molecular level into the water phase.[235]

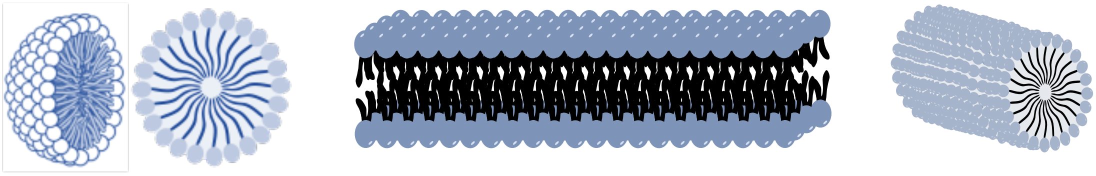

spherical lamellar cylindrical

Figure 4.2 – Typical micelle configurations.

Surfactants exhibit different properties: wetting, foaming/defoaming, emulsification/demulsification, dispersion/aggregation of solids, solubility and solubilisation, adsorption, micellisation, detergency and synergistic interactions with other surfactants.[236] Table 4.1 shows some application areas and corresponding criteria according to several governmental agencies/protocols, such as the European Inventory of existing chemical substances (EINECS), Food and Drug Administration (FDA) and REACH (Registration, Evaluation and Restriction of Chemicals).

Table 4.1 – Criteria to be met in some applications. (adapted from Farn [236])

Application	Criteria
Domestic and industrial cleaning	Surfactants must be biodegradable;
Personal care products	Surfactants must be biodegradable; Low skin and eye irritation; Low oral toxicity
Crop care products	In accordance with EPA regulations; Low toxicity;
Oil field chemicals	Low toxicity;
Food grade emulsifiers	Must meet vigorous food additive standards for toxicity;
Emulsion polymers for coatings, inks and adhesives applications	Must comply with FDA or BGA[‡] regulations for some applications (direct/indirect food contact);

Surfactants are generally classified by ionic types: anionic, cationic, non-ionic and amphoteric (or zwitterionic). Anionic surfactants have a negatively charged (anion) hydrophilic head and dissociate in water into a negatively and positively charged ions (Figure 4.3 B)). They are used in detergent formulations and personal care products[237] and are considered the largest class of surfactants.[238] Cationic surfactants have a positively charged (cation) hydrophilic head and dissociate in water into negatively and positively charged ions (Figure 4.3 C)). These surfactants are used as fabric softeners, hair conditioners and antibacterial agents.[239-240] Non-ionic surfactants do not dissociate in water and have a neutral hydrophilic head (Figure 4.3 A)). These are commonly used in the formulation of emulsifiers, dispersants and low-temperature detergents.[241] Depending on the pH, amphoteric surfactants have the hydrophilic head positively or negatively (or both) charged (Figure 4.3 D)). They are cations in acidic medium, anions in alkaline medium and amphoteric in intermediate pH range. Zwitterionic surfactants are generally used in baby shampoos (less irritating to skin and eye), toiletries and cleaners/detergents.[242]

[‡] BGA (from Bundesgesundheitsamt) is the German Federal Health Department.

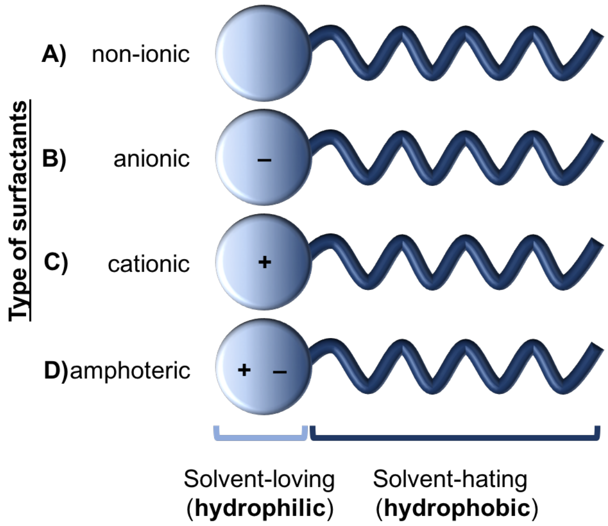

Figure 4.3 – Schematic representation of the different types of surfactants.

4.2.1.1. Surface activity – surface tension

A surfactant is a molecule which, at low concentrations, has the ability to adsorb onto surfaces (or interfaces) of a system and to markedly change the surface (or interfacial) free energies of those surfaces (or interfaces).[243] The term surface corresponds to an interface where one phase is a gas, *e.g.* air. It denotes a boundary between two immiscible phases. The interfacial free energy is the minimum work needed to create that interface, and this free energy can be measured to determine the interfacial tension (same as interfacial free energy) between two phases. Table 4.2 shows the surface tension (SFT) of some compounds; from these values, it can be interpreted that the attractive forces between water molecules are stronger than the ones between chloroform molecules, but weaker than mercury atoms; *e.g.* to a larger SFT value, corresponds to greater intermolecular attractive forces.

Table 4.2 – Surface tension of some compounds. (adapted from Gecol [244])

Compound	Surface tension (γ, mN/m), at 20 ºC
Chloroform	27
Water	72
Mercury	476

The driving force for a surfactant to adsorb at an interface is to lower the free energy of that phase boundary.[238] For example, the surface tension of water at room temperature is equal to the interfacial free energy per unit area of the boundary between water and the air above it (≈ 72 mN/m). When a surfactant is added to this boundary, the surface tension (or the amount of work needed to expand the interface) is reduced (typically ≤ 60 mN/m).[112] This occurs because when the surfactant is present in a system, the molecular interaction at the interface happens between the hydrophilic head of the surfactant and the polar phase molecules, and between the hydrophobic tail of the surfactants and the non-polar phase molecules. This will lower the tension across the interface due to the newly developed interactions being stronger than the interaction between the non-polar and polar surfaces.[244]

4.2.1.2. Surface activity – surfactant aggregation

The tendency of the surfactant molecules to self-assemble in an aqueous medium will depend on their concentration. The lowest surface tension is obtained once the CMC has been reached. Below the CMC, the surfactant molecules are positioned at the liquid-air interface. Increasing the surfactant concentration when the surface is saturated but still below the CMC causes the additional surfactant molecules to disperse in the liquid phase. Further increasing the surfactant concentration to the CMC will cause the surfactant molecules to aggregate into micelles, above which point further addition will simply increase the number of micelles present. (Figure 4.4).

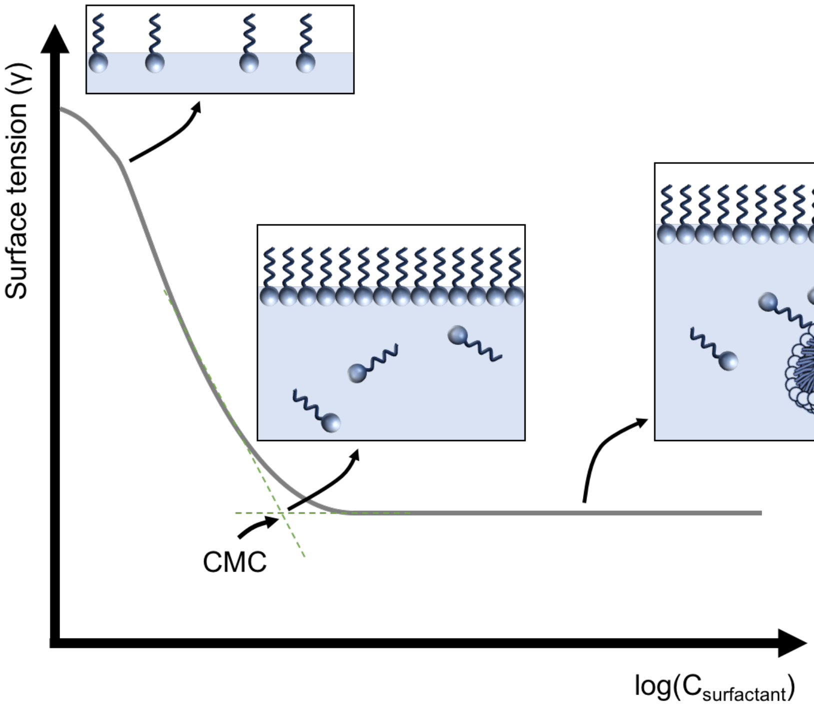

Figure 4.4 – Schematic plot of surface tension versus log of the concentration for an aqueous solution of a surfactant. It is also represented with a schematic illustration of micelle formation with an increase of surfactant concentration.

There are several methods to determine the surface and interfacial tension and they will be described later in this chapter (static and dynamic surface tension methods).

4.2.2. Petrochemical derived surfactants

Of the petrochemically derived surfactants synthesised to date, those derived from the non-ionic and hydrophilic polymeric surfactant, poly(ethylene glycol) (PEG, also known as poly(ethylene oxide), PEO) are by far the most studied class of surfactants. PEG offers several advantages such as high hydrophilicity, flexibility and biocompatibility.[235] Nevertheless, the industrial production of PEG is essentially from petrochemical feedstocks which is not ideal from a sustainable perspective. Fortunately, alternative feedstocks are available. For example, the Acme-Hardesty Company produces biobased PEG with several molecular weights, (200[245], 300[246], 400[247] and 600[248] Da) from bagasse (derived from sugar cane pulp) up to a total biobased content of 60% as certified by the USDA (United States Department of Agriculture).

With regards to hydrophobic surfactants, poly(propylene glycol) (PPG, also known as poly(propylene oxide), PPO) is by far the most studied and used industrially. The A-B-A block copolymer of PEG and PPG (PEG-PPG-PEG; commercially known as Pluronic® by BASF[249] and Synperonic by CRODA[250]) has been used commercially and due to its natural and rapid organisation into micelles, has been explored for pharmaceutical applications. These include cancer targeting, bio-adhesive properties and drug delivery, to name a few.[251] However, PPG does not bio-degrade, and uses petrochemical-based starting materials, which is not ideal from a sustainability point of view.

As mentioned previously, surfactants are widely used in several sectors and have been produced at an enormous scale. Therefore, synthesising biodegradable and biorenewable surfactants, could be an important step forward for a sustainable world.

4.2.3. Surfactants from renewable resources

Surfactants have been historically produced using either petrochemical or oleochemical feedstocks.[252] However, petrochemicals are the most used, and account for around two thirds of the organic carbon in the final products.[229] The perception that global reserves of fossil fuels are finite and the accumulation of waste in landfills and natural habitats are some of the driving forces explore new renewable feedstocks for surfactant production.[253] Dornburg*, et al.* [254] estimated that if surfactants were fully synthesised from renewable resources, in the European Union (EU), the total CO_2 emissions associated with surfactant production and use would reduce by as much as 37%.

Biodegradable and biorenewable polyesters such as poly(lactic acid) (PLA), poly(glycerol-succinate) (PGLSA) and poly(lactic-*co*-glycolic acid) (PLGA) have been combined with PEG, lauric acid (LA) and palmitic methyl ester for the preparation of surfactants, useful for drug delivery, household and industrial purposes (Figure 4.5).[46, 147, 154, 255-260]

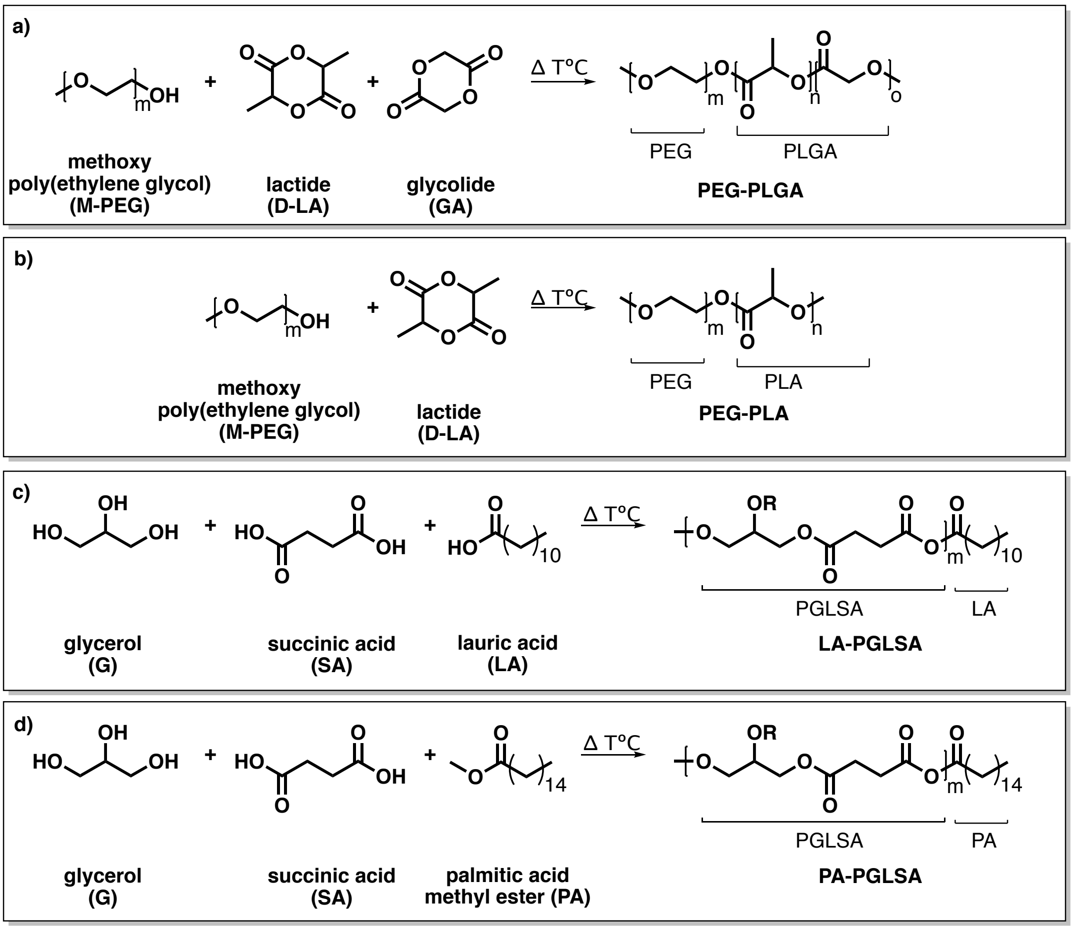

Figure 4.5 – Synthetic scheme for biodegradable and biorenewable amphiphilic polymers: a) synthesis of poly(ethylene glycol)-*block*-poly(lactide-*co*-glycolide) (PEG-PLGA); b) poly(ethylene glycol)-*block*-poly(lactide) (PEG-PLA); c) lauroyl poly(glycerol succinate); d) palmitoyl poly(glycerol succinate).

Jeong*, et al.* [256] synthesised PEG-PLA-PEG triblock copolymers with low dispersity values ($Đ$ = 1.0 – 1.3) and a molecular weight of 3,400 – 3,900 Da that exhibited good surfactant properties, CMC < 0.138 mg/g. However, this synthesis requires a metal catalyst, toluene and high temperature.

Agach*, et al.* [147] synthesised lauroyl PGLSA oligoesters, obtaining oligomers with a molecular weight of 600 Da with a maximum CMC of 0.108 mol/L. Nevertheless, this synthesis required high temperatures. Furthermore, Khongphow*, et al.* [46] synthesised a PGLSA-based surfactant using palmitic acid methyl ester as the hydrophobic component. Again, high temperatures were essential to obtain polymers; surfactants with a molecular weight of 1,800 Da were produced that exhibited relatively low CMC values (up to 0.447 mmol/L). All these syntheses use either toxic solvents (methylene chloride)[255] or high temperatures (150 ºC).[261]

The synthesis of an ideal, sustainable and '*green'* surfactant should avoid high temperatures, toxic solvents and metal catalyst that could lead to residues. Thus, this chapter will focus on the development of a new approach towards the synthesis of greener surfactants.

4.3. Aims of the study

The previous chapter focussed on the use of $scCO_2$ to synthesise linear poly(glycerol succinate) polymers through enzymatic, near-room-temperature polycondensations, without the need to modify monomers (see Chapter 3).

In this Chapter, the aim of study is to use this approach to synthesise '*greener*' surfactants based on glycerol and succinic acid, end-capped with lauric acid or poly(ethylene glycol) in $scCO_2$ (Figure 4.6). Glycerol is a by-product from biodiesel production and, due to the increase of its production, it is imperative to find alternative uses for glycerol. Succinic acid and PEG can be obtained by biomass fermentation. Lauric acid is a naturally occurring fatty acid that can be found in several plants. Therefore, Chapter 4 will firstly focus on the synthesis of '*greener*' poly(glycerol succinate)-based surfactants through low temperatures and enzymatic polycondensations.

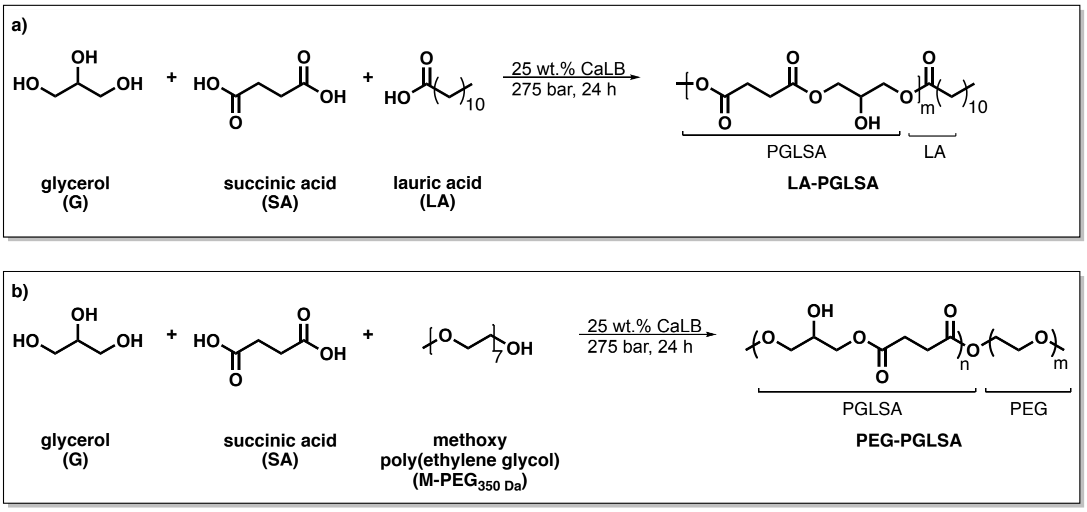

Figure 4.6 – Synthetic scheme proposed for the synthesis of PGLSA end-capped with a) lauric acid and b) methoxy poly(ethylene glycol) (350 Da) under supercritical conditions using CaLB.

Afterwards, this Chapter will focus on the performance of the synthesised surfactants. Focussing on the measurement of the surface tension (in equilibrium and dynamically), the critical micelle concentration, the size of the micelles formed and the contact angle of the surfactant aqueous solution. These results will be compared with commercially available surfactants (which are petrochemical derived).

4.4. Experimental

4.4.1. Materials

Glycerol (≥ 99.5% purity) was purchased from Sigma Aldrich (UK) and dried for 24 hours under vacuum (10 mmbar) at room temperature before use and stored over fresh molecular sieves (4Å, particle sixe 1.6-2.5 mm) at room temperature. Molecular sieves type 3 and 4 Å, 1.6-2.5 mm beads, were purchased from Fisher Scientific (UK) and used as received. Succinic acid (≥ 99.0% purity) was purchased from Sigma Aldrich (UK) and dried for 24 hours under vacuum (10 mmbar) at 50 ºC before use. Lauric acid (≥ 98.0% purity) was purchased from Sigma Aldrich (UK) and used as received. Poly(ethylene glycol) methyl ether with a molecular weight of 350 Da (M-PEG$_{350}$) was purchased from Sigma Aldrich (UK) and stored over fresh molecular sieves (4Å, particle sixe 1.6-2.5 mm) at room temperature. Novozyme® 435 (CaLB immobilised on cross-linked acrylic resin beads) was kindly donated by Novozymes™ (Denmark), stored at 4 ºC and dried for 24 hours under vacuum (100 mbar) at room temperature (RT) before use. The commercial surfactants Tween™ 20 (PEG$_{20}$-sorbitan laurate, ~ 1,200 Da) and NatraGem™ E145 (polyglycerol succinate laurate, ~ 1,300 Da) were supplied by Croda Europe Ltd. (UK). All the solvents were of analytical grade, and used as received. Carbon dioxide grade 4.0 (minimum purity 99.99%) was purchased from BOC Special Gases (UK) and used as received.

4.4.2. Synthesis methods

4.4.2.1. Enzymatic synthesis of lauroyl poly(glycerol-succinate) using supercritical carbon dioxide

In a typical procedure (Figure 3.8 from Chapter 3), succinic acid (5.4 mmol), glycerol (10.9 mmol), lauric acid (1.5 mmol, 28 mol% to the amount of SA), CaLB (25 wt.%[§] to the total amount of monomers) and molecular sieves (size

---

[§] Includes polymer support

3Å, 25 wt.% to the total amount of monomers) were added to the stainless steel reaction autoclave described previously (60 mL, Chapter 2, Figure 2.2). An excess of glycerol was used to ensure the synthesis of glycerol terminated PGLSA, since lauric acid can only react with the hydroxy moieties. The vessel was sealed and pressurised up to 50 bar. Afterwards, the temperature was increased to the desired value (40, 50 or 60 ºC, Table 4.3) before the pressure was increased to 275 bar. The reaction was left to run for 24 h while stirring at 150 rpm. To avoid polymer foaming and consequently blockages in the pipework, the reactions were stopped by cooling the vessel in a water/ice bath (~ 0 ºC) before venting. The CO_2 was vented when the pressure was below 20 bar. Finally, the product was collected and dissolved in 10 mL of tetrahydrofuran (heated at 40 ºC to ensure complete dissolution) and filtered to remove the enzyme beads and molecular sieves. The solvent was then removed under reduced pressure, leaving solid polymeric products. To ensure complete removal of the solvent, the samples were dried under vacuum, at room temperature, overnight. Product yields are summarised below (Table 4.4). The reactions were performed at least twice to check reproducibility.

4.4.2.2. Enzymatic synthesis of PEG-poly(glycerol-succinate) using supercritical carbon dioxide

In a typical procedure (Figure 3.8 from Chapter 3), succinic acid (10.9 mmol), glycerol (5.4 mmol), M-PEG (2.4 mmol, 15 mol% to the total amount of SA and G), CaLB (25 wt.%[**] to the total amount of monomers) and molecular sieves (size 3Å, 25 wt.% to the total amount of monomers) were added to the stainless steel reaction autoclave as described previously (60 mL, Chapter 2, Figure 2.2). An excess of succinic acid was used to ensure the synthesis of SA terminated PGLSA, since M-PEG can only react with the carboxylic acid moieties. The vessel was sealed and pressurised up to 50 bar. Afterwards, the temperature was increased to the desired value (40, 50 or 60 ºC, Table 4.3) before the pressure was increased to 275 bar. The reaction was left to run for 24 h while stirring at 150 rpm. To avoid polymer foaming and consequently blockages in the pipework, the reactions were stopped by cooling the vessel in a water/ice bath (~ 0 ºC) before venting. The CO_2 was vented when the pressure was below 20 bar. Finally, the product was collected and dissolved in 10 mL of tetrahydrofuran (gently heated at 40 ºC, to ensure complete dissolution) and filtered to remove the enzyme beads and molecular sieves. The solvent was then removed under reduced pressure, leaving solid polymeric products. To ensure complete removal of the solvent the samples were dried under vacuum overnight at room temperature. Product yields are summarised below (Table 4.5). The reactions were performed at least twice to check reproducibility.

Table 4.3 – Summary of reactions conducted using supercritical carbon dioxide at 275 bar for 24 hours. *Note:* [a] includes polymer support; X = co-monomer, poly(ethylene glycol) with molecular weight of 350 Da (PEG_{350}) or lauric acid (LA); ✓ indicates solubility in water.

Entry	**Ratio (Gly:SA:X)**	**X**	**T ºC**	**Catalyst[a]**	**Appearance**	**Soluble in water**
1	2:1:0.15	LA	40 ºC	25 wt.% CaLB	Waxy white	✓
2	2:1:0.15	LA	50 ºC	25 wt.% CaLB	Waxy white	✓
3	2:1:0.15	LA	60 ºC	25 wt.% CaLB	Waxy white	✓
4	1:2:0.15	PEG_{350}	40 ºC	25 wt.% CaLB	Waxy yellow	✓
5	1:2:0.15	PEG_{350}	50 ºC	25 wt.% CaLB	Waxy yellow	✓
6	1:2:0.15	PEG_{350}	60 ºC	25 wt.% CaLB	Waxy yellow	✓

4.4.3. Surfactant characterisation

Polymeric surfactant structures were analysed using ^{1}H-NMR spectroscopy, GPC and DSC. All these techniques are discussed in further detail in Chapter 2.

4.4.3.1. Tensiometry

Surface tension measurements were made using the Wilhelmy plate method and a bubble tensiometer, measuring equilibrium (static) and dynamic surface tensions, respectively (described in detail in Chapter 2). Measurements were made in duplicate and the commercial surfactants Tween^{TM} 20 and NatraGem^{TM} E145 were assessed for comparison.

For the dynamic surface tension measurements all the synthesised poly(glycerol succinate) polyesters along with the corresponding end-capped polymers with lauric acid and PEG_{350} were assessed, typically at 1 wt.%, 0.5 wt.% and 0.1 wt.% in water.

For the equilibrium (static) surface tensions, all the synthesised poly(glycerol succinate) polyesters along with the corresponding end-capped polymers with lauric acid and PEG_{350} were assessed, typically at 1 wt.% in water.

4.4.3.2. Critical Micelle Concentration

The CMC was determined using the Wilhelmy plate method. The system contains an automated dispensing unit which enables a high number of measuring points across a broad concentration range (10,000 – 0.1 mg/L). Starting at a concentration of 1 wt.% (10,000 mg/L) in water, the polymer solution was diluted stepwise and surface tension measurements taken at each concentration. Surface tension *versus* concentration (logarithmic scale) was plotted and the CMC value was determined by the intersection between lines (descending and *quasi*-horizontal lines).

4.4.3.3. Dynamic Light Scattering

DLS analyses were performed in order to determine the hydrodynamic volume of the surfactant aggregates/micelles, in an aqueous solution (described in detail in Chapter 2). Analyses were performed at room temperature (25 ºC) on a 100 µL sample at concentrations between 1 – 0.001 wt.%.

4.4.3.4. Contact angle measurement

To evaluate the contact angle of the surfactants, the static sessile drop method was used on the surface of parafilm plate (OCA 15EC model). The aqueous droplet of surfactant was gently dropped on the parafilm surface using a microliter syringe. SCA20 (version 1.60) software was used to analyse the shape and to measure the contact angle of the surfactants.

4.5. Results and discussion

This section will focus on the enzymatic synthesis of poly(glycerol succinate)-based surfactants under $scCO_2$ conditions. The principal aim of this study is to develop a '*greener*' approach towards the formation of useful surfactants. The addition of lauric acid or poly(ethylene glycol) to PGLSA is here discussed (Figure 4.6). Correspondingly, their properties, as surfactants, are also compared with each other, and with commercially available surfactants.

4.5.1. Enzymatic synthesis of lauroyl poly(glycerol succinate) under supercritical conditions

The "green" synthesis of PGLSA based surfactants has not yet been extensively studied. To the best of the author's knowledge, the enzymatic polycondensation of PGLSA based surfactants under supercritical conditions has never been investigated. Consequently, the enzymatic synthesis of lauroyl PGLSA (LA-PGLSA) *via* $scCO_2$, at different temperatures: 40, 50 and 60 ºC is discussed first. The novel methodology developed and described in Chapter 3 was used for the synthesis of biorenewable and biodegradable surfactants. The reactions (Table 4.4) were conducted at 275 bar for 24 h, with 25 wt.%[**] CaLB and with an excess of glycerol, to ensure the synthesis of glycerol terminated PGLSA, since lauric acid can only react with the hydroxy moieties (Figure 4.7).

[**] Includes polymer support

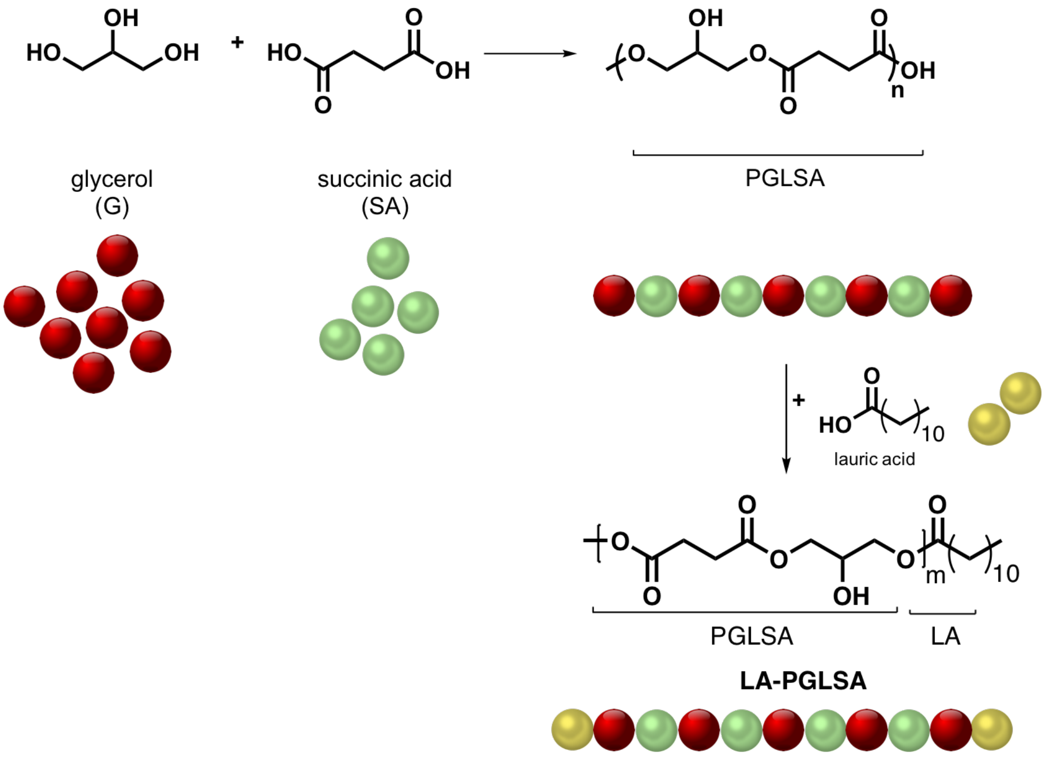

Figure 4.7 – Schematic representation of the synthesised of LA-PGLSA, demonstrating the excess of glycerol, to ensure the synthesis of glycerol terminated PGLSA.

Table 4.4 – Synthesis of lauroyl-poly(glycerol succinate) under enzymatic supercritical conditions, at 275 bar. [a] calculated through ^{1}H-NMR from the ratio between the integrals of the peaks of the polymer backbone and the end-group peak, using Equation 4.1; [b] determined by the Frey's equation (Equation 3.3 on Chapter 3).

Entry	**T ºC**	**Ratio (Gly:SA:LA)**	**Yield**	**M_n^{GPC} (Da)**	**Đ**	**M_n^{NMR}(Da)[a]**	**DB[b]**	**T_g**	**T_m**
1	40 ºC	2:1:0.15	85%	1,700	1.5	2,200	12%	–	48 ºC
2	50 ºC	2:1:0.15	96%	1,400	> 3	2,600	10%	-72 ºC	50 ºC
3	60 ºC	2:1:0.15	92%	2,000	1.8	2,800	5%	-78 ºC	50 ºC

Through ^{1}H-NMR, it was possible to calculate the M_n^{NMR} of the synthesised polymers. The integrals assigned to the PGLSA backbone, normalised to the methyl group of the LA end-capper, were used to estimate the molar mass (Equation 4.1 and Figure 4.9).

$$M_n^{NMR} = \frac{\frac{I_e-4}{4}+\frac{I_f-1}{1}+\frac{I_c}{4}}{3} \times 174 + 56 + 2 \times 200$$

Equation 4.1 – Average molecular weight of LA-PGLSA calculated through ^{1}H-NMR, using the integration of the peaks H_a (0.88 ppm, terminal methyl group from LA), H_e (I_e, 3.50-3.72 ppm), H_f (I_f, 3.83 and 5.07 ppm) and H_c (I_c, 2.58-2.69 ppm). The values 174, 56 and 200 are for the molar mass of: repeat unit of PGLSA, glycerol unit used as linker (to react with LA) and LA unit, respectively.

For the LA-PGLSA synthesis, an excess of glycerol was used to ensure the attachment of LA to the terminal units of glycerol. Therefore, the calculation of M_n^{NMR} focussed on the specific NMR signals of the terminal glycerol units linker, not those of the repeating unit of the PGLSA backbone. Hence, in Equation 4.1, for the integration peaks of H_e (I_e, 3.50-3.72 ppm) and H_f (I_f, 3.83 ppm) it was subtracted the 5 protons that correspond to the glycerol unit as linker (Figure 4.9). By adding the contribution of SA (I_c), the resulted value was multiplied by 174, which is the molar mass of the repeat unit of PGLSA. Afterwards, it was added 56 (which is the molar mass of glycerol as linker) and 2 x 200, which is the molar mass of lauric acid. Nevertheless, it is important to mention that if the calculation of the M_n^{NMR} had been done considering all the glycerol units, the value would not have been significantly different.

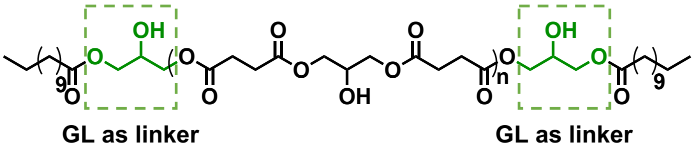

Figure 4.8 – Schematic representation of LA-PGLSA, highlighting in green the GL unit used as linker, and which is not part of the repeating unit of the PGLSA backbone. *Note:* GL = glycerol.

To evaluate the successful attachment of LA to the PGLSA backbone, Equation 4.2 was used.

$$\text{LA-PGLSA}(\%)^{NMR} = \frac{I_d/4}{I_a/6} \times 100$$

Equation 4.2 – Percentage of LA attached to the PGSLA backbone.

The calculated M_n^{NMR} (Table 4.4, Figure 4.9, Figure A 1 and Figure A 2 from Appendix) show good agreement with the values obtained through GPC. In addition to the molecular weight, all the polymerisations of LA-PGLSA polymers show a low degree of branching (DB) (Table 4.4), which was expected because of the extensive study of branching described in Chapter 3.

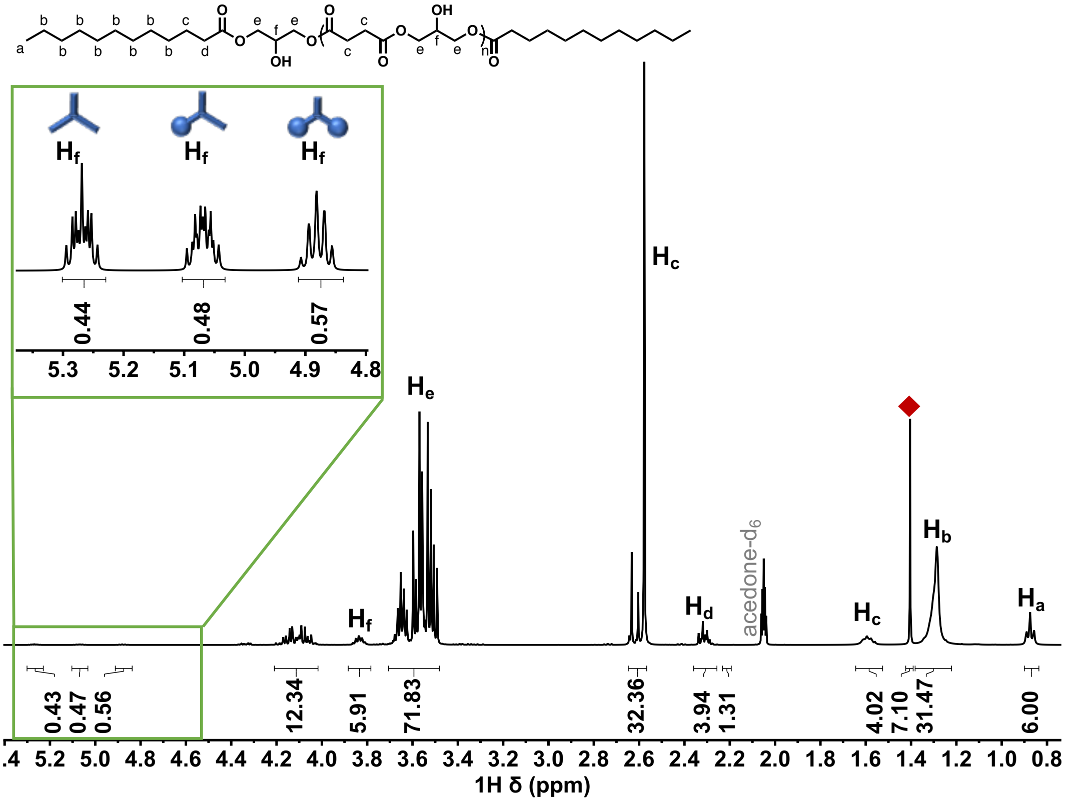

Figure 4.9 – ^{1}H-NMR spectrum of LA-PGLSA from entry 1, Table 4.4. The solvent used was acetone-*d*$_6$. Integrals of the peaks of H_a (0.88 ppm, terminal methyl group from LA), and H_e (3.50-3.72 ppm), H_f (3.83 ppm) and H_c (2.58-2.69 ppm) (backbone of PGLSA) can be used to estimate the average molecular weight of the polymer. The peak at 1.29ppm, H_b, is assigned to the –CH$_2$– in the LA chain, while peaks at 1.59 and 2.31 ppm, H_c and H_d, are assigned to the –CH$_2$– close to the carboxy group of LA (–C**H$_2$**–C**H$_2$**–COO–). *Note*: ◆ is an unknown peak; the schematic representations shown in the highlighted region (5.4-4.8 ppm) corresponds to the branched, linear and terminal glycerol units as follow: ⅄● = linear glycerol unit; in this case, the polymerisation occurred in positions e, ●⅄ = linear glycerol unit; in this case, the polymerisation occurred in positions e (right) and f, ●⅄● = terminal glycerol in the polymer backbone, leaving the hydroxy groups e free, ⅄ = trisubstituted glycerol unit in the branched polymer backbone; the ^{1}H-NMR spectra for the other LA-PGLSA polymers are available in the Appendix (Figure A 1 and Figure A 2).

The LA-PGLSA synthesised at 40 °C (entry 1, Table 4.4; Figure 4.9) was obtained with 85% yield and a molecular weight of 1,700 Da (M_n^{GPC}) (DB = 12%) and, through Equation 4.2, it has 98.5% of the detected LA attached to the PGLSA backbone. This shows a high yield of end-capping LA units added to the PGLSA *via* enzymatic polycondensation under supercritical conditions.

When increasing the temperature to 50 ºC, (entry 2, Table 4.4), the yield increased to 96% although the M_n^{GPC} decreased to 1,400 Da (DB = 10%). This polymer shows a successful 99% attachment of LA to the PGLSA backbone. Increasing even further to 60 ºC, a polymer was obtained with a molecular weight of 2,000 Da (M_n^{GPC}) (DB = 5%) and 92% yield. In addition, it was confirmed that 96.5% of LA is attached to the PGLSA backbone. Changing the polymerisation temperature did not have a noteworthy effect upon the molecular weight of the polymers. Hence, from a sustainable viewpoint it is clear that at 40 ºC would be a better choice to polymerise LA-PGLSA.

The thermal properties of LA-PGLSA polymers were investigated through differential scanning calorimetry (DSC). As expected, low glass transition temperatures (T_g) were obtained. However, at 40 ºC it was not possible to detect the T_g (Figure 4.10 A and B). It is well known that thermal properties of polymeric structures can be affected not only by the degree of polymerisation, but also by the type of end-groups.[262-263] Since the LA-PGLSA synthesised polymers have similar molecular weights and structure, there is no significant difference in the thermal properties. These results are consistent with what has been shown previously by other authors with similar polyesters.[232] Tween™ 20 (also known as polyoxyethylene (20) sorbitan monolaurate), a commercially available non-ionic surfactant, has T_g of *ca.* -61 ºC and a T_m *ca*. -15 ºC.[264] These values are a consequence of the branched structure of the polar head and the acyl chain which increase the free volume between polymeric chains. LA-PGLSA polymers also exhibit the presence of a polar head and the acyl chain with 12 carbons, which increases the free volume in between polymeric chains and, therefore, leads to a low T_g. Nevertheless, the melting points of LA-PGLSA were *ca.* 48-50 ºC, which are close to values obtained by other authors for similar polyesters (linear polyesters based on pentaerythritol, succinic acid and lauric acid).[265]

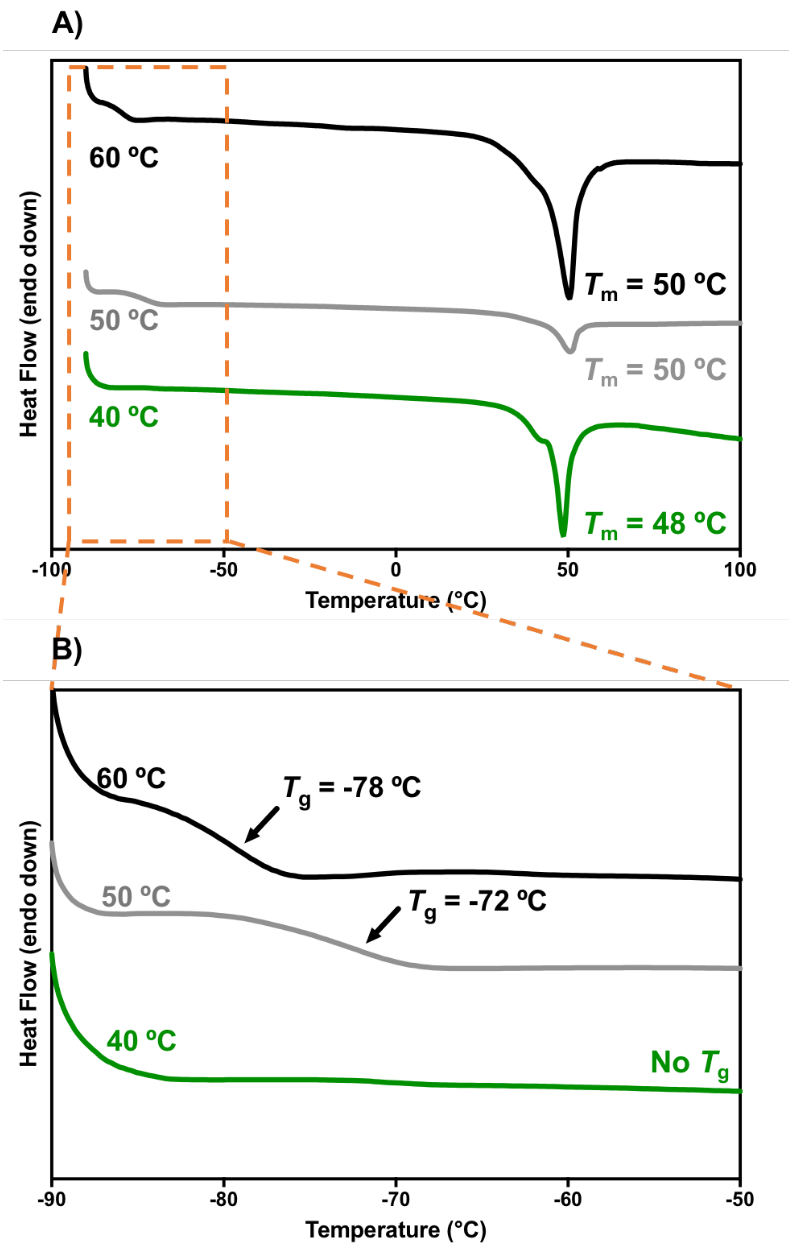

Figure 4.10 – DSC traces (2nd heating scans are shown) of the copolymers LA-PGLSA synthesised under enzymatic supercritical conditions at 40, 50 and 60 °C. A) These traces show the detection of the T_g and T_m of LA-PGLSA; the highlighted region in orange is zoomed in below, in B) to demonstrated the T_g of the LA-PGLSA.

4.5.2. Enzymatic synthesis of PEG-poly(glycerol succinate) under supercritical conditions

The synthesis of poly(ethylene glycol)-based surfactants has been extensively studied because it offers several advantages such as flexibility and biocompatibility. The industrial production of PEG uses mainly petrochemical starting materials, although the Acme-Hardesty company produces biobased PEG, using bagasse as feedstock.[266]

Hence, we will discuss the enzymatic synthesis of PEG-PGLSA *via* $scCO_2$, at different temperatures: 40, 50 and 60 °C. The novel methodology developed and described in Chapter 3 has been used for the synthesis of biorenewable and biodegradable surfactants. The reactions (Table 4.5) were conducted at 275 bar for 24 h, with 25 wt.%[††] CaLB and with an excess of succinic acid, to ensure the synthesis of succinic acid terminated PGLSA, since M-PEG can only react with the carboxy moieties (Figure 4.11).

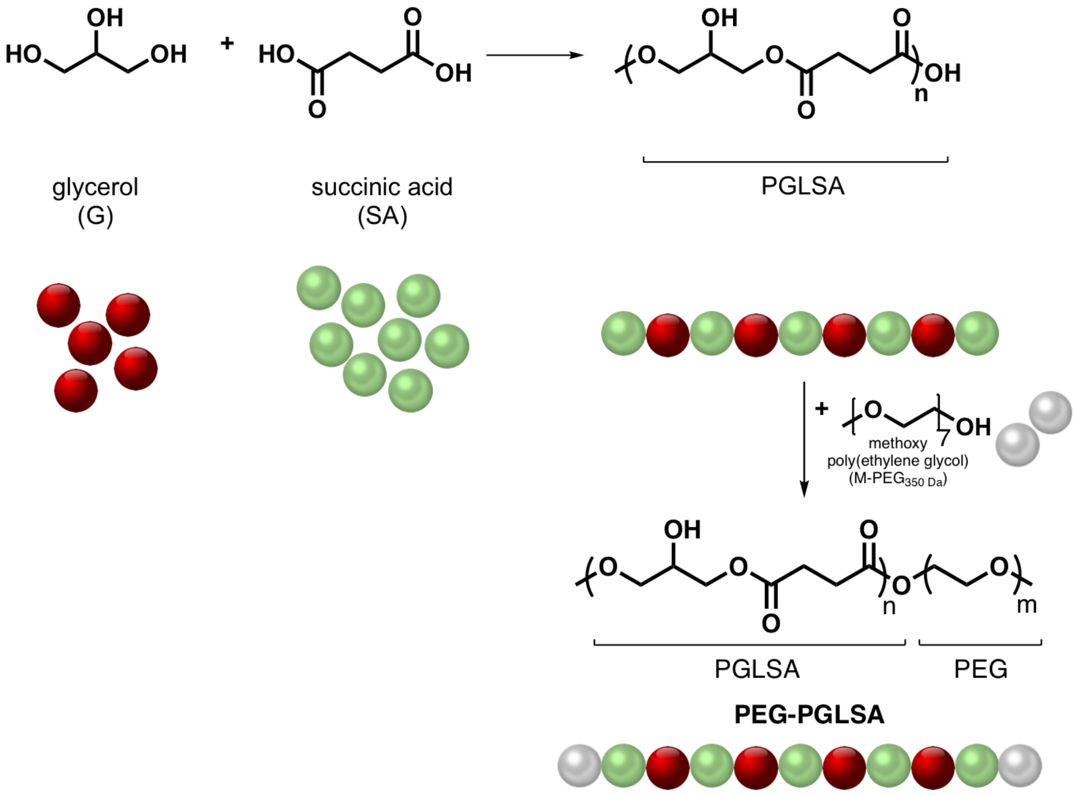

Figure 4.11 – Schematic representation of the synthesised of PEG-PGLSA, demonstrating the excess of succinic acid, to ensure the synthesis of succinic acid terminated PGLSA.

The synthesis of PEG-based surfactant under enzymatic $scCO_2$ has been done by Curia and Howdle [232]. In this study, amphiphilic copolymers based on azelaic acid and 1,6-hexanediol were developed as building blocks of the hydrophobic backbone; these copolymers were end-capped with methoxy poly(ethylene glycol) chains. Also using supercritical carbon dioxide, Goddard,

---

[††] Includes polymer support

et al. [112] synthesised "green" surfactants, based on the polymerisation of sorbitol and lactide. The replacement of conventional solvents by $scCO_2$ has revealed to a good medium for enzymatic polymerisation reactions towards the formation of surfactants.[267]

Table 4.5 – Synthesis of PEG-poly(glycerol succinate) under enzymatic supercritical conditions, at 275 bar. [a] calculated through ^{1}H-NMR from the ratio between the integrals of the peaks of the polymer backbone and the end-group peak, using Equation 4.3; [b] it was determined by the Frey's equation (Equation 3.3 on Chapter 3).

Entry	**T ºC**	**Ratio (Gly:SA:PEG)**	**Yield**	**M_n^{GPC} (Da)**	**Đ**	**M_n^{NMR}(Da)[a]**	**DB[b]**	**T_g**	**T_m**
4	40 ºC	1:2:0.15	93%	1,200	1.8	2,000	13%	-45 ºC	–
5	50 ºC	1:2:0.15	85%	3,800	>2	2,200	0%	-75 ºC	–
6	60 ºC	1:2:0.15	94%	1,500	>2	2,200	0%	-74 ºC	–

Through ^{1}H-NMR, it was possible to calculate the M_n^{NMR} of the synthesised PEG-PGLSA. The integrals assigned to the PGLSA backbone, normalised to the methyl group of the M-PEG end-capper, were used to estimate the molar mass through Equation 4.3.

$$M_n^{NMR} = \frac{\frac{I_e\text{-}31.6}{4}+\frac{I_f}{1}+\frac{I_d\text{-}4}{4}}{3} \times 174 + 82 + 2 \times 350$$

Equation 4.3 – Average molecular weight of PEG-PGLSA calculated through ^{1}H-NMR, using the integration of the peaks H_a (3.29 ppm, terminal methyl group from M-PEG), H_e (I_e, 3.50-3.72 ppm), H_f (I_f, 3.83 and 5.09 ppm) and H_d (I_d, 2.58-2.69 ppm). The value 31.6 corresponds to the integral of the peak assigned to the –C**H₂**– from M-PEG (^{1}H-NMR spectrum in Figure A 3 – Appendix); these protons overlap with the protons $–CH_2–$ from the glycerol unit (H_e). The values 174, 82 and 359 are for the molar mass of: repeat unit of PGLSA, succinic acid unit used as linker (to react with M-PEG) and M-PEG unit, respectively.

For the PEG-PGLSA synthesis, an excess of SA was used to ensure the attachment of M-PEG to the terminal units of SA. Therefore, the calculation of M_n^{NMR}, focussed on the specific NMR signals of the terminal SA unit as linker, not those of the repeating unit of the PGLSA backbone (Figure 4.12). Hence, in Equation 4.3, for the integration peaks of H_d (I_d, 2.58-2.69 ppm), the 4 protons that correspond to the SA unit as linker were subtracted (Figure 4.13). By adding the contribution of glycerol, I_f (3.83 and 5.09 ppm) and I_e-31.6 (3.50-3.72 ppm), the resulted value was multiplied by 174, which is the molar mass of the repeat unit of PGLSA. Afterwards, it was added 82 (which is the molar mass of succinic acid as linker) and 2 x 350, which is the molar mass of M-PEG. To the integration of H_e (I_e) it was subtracted 31.6 which corresponds to the integration of protons –C**H₂**– from M-PEG (^{1}H-NMR spectrum in Figure A 3 – Appendix), which overlap with protons –C**H₂**– from the glycerol unit. Nevertheless, as aforementioned previously (section 4.5.1 in this Thesis), if the calculation of the M_n^{NMR} had been done considering all the succinic acid units, the M_n value would not have been significantly different.

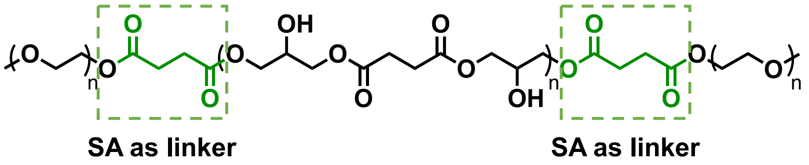

Figure 4.12 – Schematic representation of PEG-PGLSA, highlighting in green the SA unit used as linker, and which is not part of the repeating unit of the PGLSA backbone. *Note:* SA = succinic acid.

The determination of the successful attachment of M-PEG to the PGLSA is not possible due to the overlap of the peaks (Figure A 4 in Appendix). The region of 4.40-4.05 ppm, (previously described in detail in Chapter 3, section 3.5.1.) corresponds to the protons $H_{f,e}$ of glycerol unit (H_f as terminal group (⅄) and/or to the H_e protons in a linear structure (⅄) when the polymerisation took place on positions 2 and 3 of glycerol), and overlaps with the H_c proton, attributed to the –C**H₂**–O– of M-PEG linked to the PGLSA backbone (Figure A 4 in Appendix). Hence, Equation 4.2 cannot be used for the PEG-PGLSA.

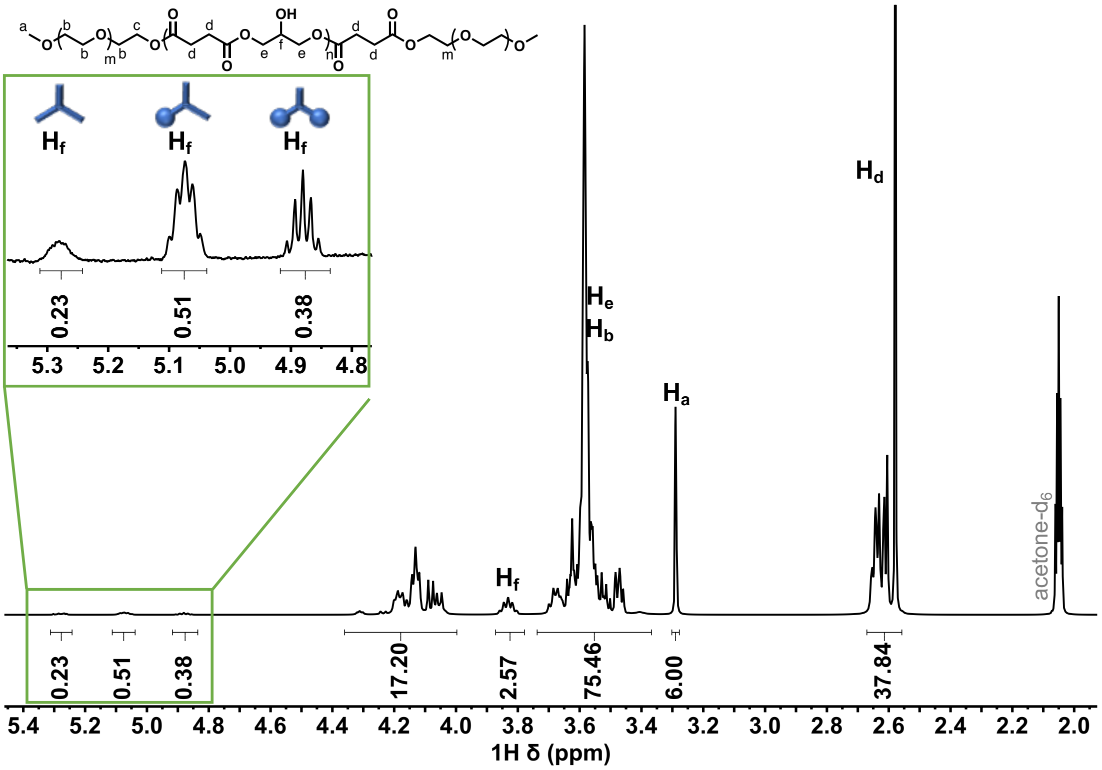

Figure 4.13 – ^{1}H-NMR spectrum of PEG-PGLSA from entry 4, Table 4.5. The solvent used was acetone-*d*₆. Integrals of the peaks of H_a (3.29 ppm, terminal methyl group from M-PEG), and H_e (3.50-3.72 ppm), H_f (3.83 ppm) and H_d (2.58-2.69 ppm) (backbone of PGLSA) can be used to estimate the average molecular weight of the polymer. The protons H_b, from the M-PEG backbone, are overlapped with the –CH_2– protons from the glycerol unit. *Note:* the schematic representations shown in the highlighted region (5.4-4.8 ppm) correspond to the branched, linear and terminal glycerol units as follows: ⅄ = linear glycerol unit; in this case, the polymerisation occurred in positions e, ⅄ = linear glycerol unit; in this case, the polymerisation occurred in positions e (right) and f, ⅄ = terminal glycerol in the polymer backbone, leaving the hydroxy groups e free, ⅄ = trisubstituted glycerol unit in the branched polymer backbone; the ^{1}H-NMR spectra for the other PEG-PGLSA polymers are available in the Appendix; H_d protons corresponds to both succinic acid units as linker and as part of the backbone.

The calculated M_n^{NMR} (Table 4.5 and Figure 4.13) show good agreement with the values obtained through the GPC technique and shows (although indirectly) successful attachment of M-PEG$_{350\ \mathrm{Da}}$ to PGLSA polyester. Even varying the temperature conditions to synthesise PEG-PGLSA, the degree of branching was low, which was expected. As mentioned previously, CaLB has selectivity to the primary hydroxy groups and, therefore, the formation of linear polymer is preferred.

At 40 ºC (entry 4, Table 4.5), a PEG-PGLSA with a molecular weight of 1,200 Da ($M_\mathrm{n}^\mathrm{GPC}$) ($Đ$ = 1.8, DB = 13%) was obtained with a good yield, 93%. When increasing the temperature to 50 ºC (entry 5, Table 4.5), there was a sudden increase in molecular weight, 3,800 Da ($M_\mathrm{n}^\mathrm{GPC}$) ($Đ$ > 2, DB = 0%, 85% yield). By contrast, the polymerisation of LA-PGLSA at the same temperature, 50 ºC (entry 3, Table 4.4), showed a decreased $M_\mathrm{n}^\mathrm{GPC}$ (1,400 Da) when comparing to 40 ºC (1,700 Da). Increasing further to 60 ºC, (entry 6, Table 4.5), PEG-PGLSA with a molecular weight of 1,500 Da ($M_\mathrm{n}^\mathrm{GPC}$) ($Đ$ > 2, DB = 0%) and 94% yield was obtained. It is well known that increasing the reaction temperature should increase polymer molecular weight.[268] But the data show that the lowest molecular weight polymers were obtained at 40 and 60 ºC, and the highest at 50 ºC. This could be a result of a reduction of enzyme activity at higher temperature. Nevertheless, throughout this work, it was already obtained higher molecular weight PGLSA-based polymers at 60 ºC, showing that the enzyme activity is not the reason for this decrease on the polymer M_n at 60 ºC. From these data, it is possible that inaccuracy during reagents measurements (from batch to batch) outweighs the influence of the reaction temperature on the polymer characteristics. As mentioned previously in Chapter 3, polycondensation reactions between polyols and diacids are dependent on the molar ratio of the reagents. If there is a slight change on the ratio (G:SA:LA molar ratio of 2:1:0.15,), the molecular weight of the polymer will be different. Hence, further investigations are required to fully understand the effect on M_n of the polymerisation temperature.

The thermal properties of PEG-PGLSA polymers were measured by DSC. As expected, low T_g values were obtained (Table 4.5 and Figure 4.14) as reported previously for similar polyesters.[232] The T_g for the samples synthesised at 40 ºC (-45 ºC) (entry 4, Table 4.5) were higher than those produced at 50 and 60 ºC (-75 and -74 ºC, respectively) (entries 5 and 6, Table 4.5). From this T_g

value, -45 ºC it seems that there are more intermolecular forces in the polymer chain. This small increase of the T_g could be caused by three reasons. First, might be lower incorporation of M-PEG in the PGLSA backbone. PEG is considered to be a plasticiser, decreasing the glass transition of polymers.[269] However, although this glass temperature is higher than the other synthesised PEG-PGLSA polymers, it is still in the range in glass transition temperatures for linear polyesters.[268, 270] Secondly, the influence of polymer branching might be also responsible for this discrepancy in values. At 40 ºC, PEG-PGLSA showed a DB of 13%, while at 50 and 60 ºC, no branching was detected. The increase of the degree of branching could increase the entanglements between the polymer chains resulting in a higher T_g. Thirdly, the existence of more oligomers in the polymers synthesised at 50 and 60 ºC (reflected by the high dispersities obtained) might influence the T_g. Generally, small molecules (oligomers) are effective as plasticisers, having the capacity in lowering the T_g of the host polymer.[271-274]

By contrast to the LA-PGLSA polymers, no T_m values were detected for the PEG-PGLSA polymers. Curia [232] synthesised a polyester (based on azelaic acid, hexanediol and PEG_{350}), and observed a T_m *ca.* 20-40 ºC, but this work is based on the polycondensation of monomers (diacid and diol) with higher numbers of carbon atoms hence giving opportunity for molecular packing and the onset of crystallinity. M-PEG_{350} has a T_m *ca*. -8 ºC.[275] Additionally, it is known that the melting points of polyesters are dependent on the number of carbon atoms in the diacid/diol monomer: a diacid/diol with higher number of C atoms, will result in polyesters with higher T_m.[276] In the present work, glycerol and succinic acid have much shorter carbon chains. Therefore, this might explain the absence of T_m values in PEG-PGLSA polyesters.

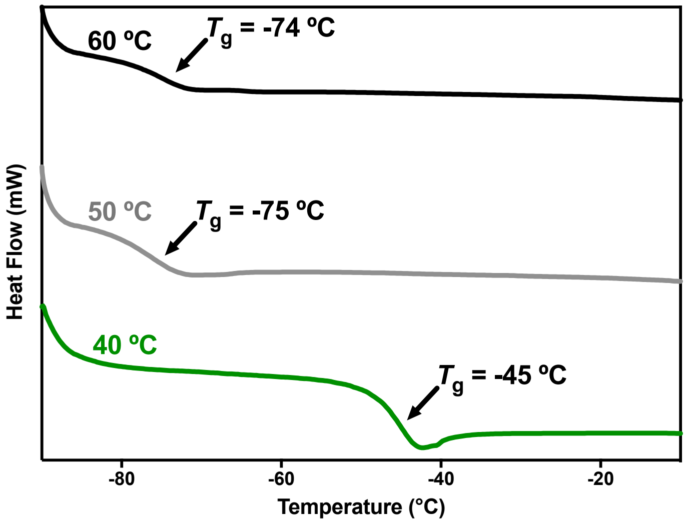

Figure 4.14 – DSC traces (2nd heating scans are shown) of the copolymers PEG-PGLSA synthesised under enzymatic supercritical conditions at 40, 50 and 60 ºC. This trace section shows the detection of the T_g of PEG-PGLSA.

4.5.3. Assessment of surfactant performance of glycerol-based surfactants

This section explores the performance of lauroyl poly(glycerol succinate) and PEG-poly(glycerol succinate) as surfactants. There are clear differences in the structure of LA-PGLSA and PEG-PGLSA. In the latter, since there is an excess of SA content in the PGSLA block, there will be fewer hydroxy pendant groups and thus, it is expected to be slightly hydrophobic. Consequently, the addition of a more hydrophilic end-capper was achieved, M-PEG (Figure 4.15 B)). In the case of LA-PGLSA, there is an excess of glycerol content in the PGSLA block, it will have more hydroxy pendant groups and thus, it is expected to be more hydrophilic. Consequently, the addition of a more hydrophobic end-capper was achieved, LA (Figure 4.15 A)).

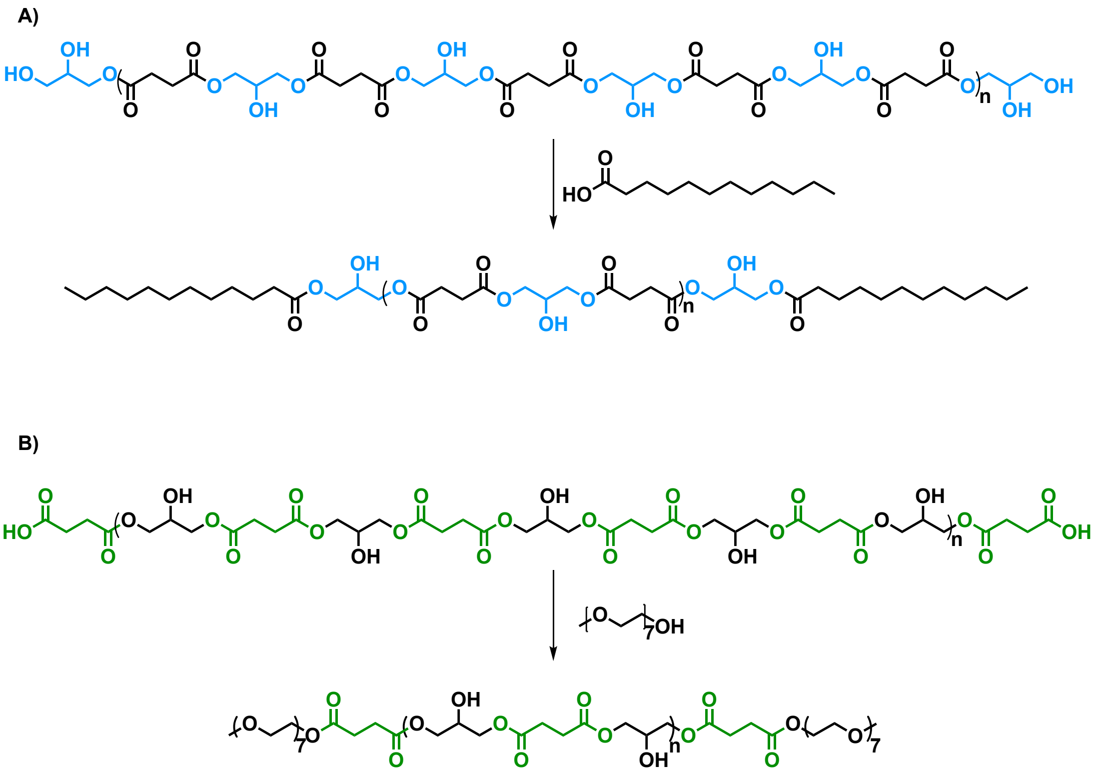

Figure 4.15 – Schematic representation of the synthesis of A) LA-PGLSA and B) PEG-PGLSA.

4.5.3.1. Surface tension measurement

As mentioned previously, water has a surface tension (σ) of ≈ 72 mN/m. A compound which can reduce the surface tension is classified as a surfactant and, in this work, according to industry standards (those used at CRODA), the surface tension should be reduced below 60 mN/m to be classed as a good surfactant. To confirm the surface activity of the synthesised PGLSA-based surfactants, dynamic and static surface tension measurements were performed. The results were compared to the surface tension reductions achieved using commercial surfactants, Tween^{TM} 20 and NatraGem^{TM} E145.

PGLSA (with G:SA of 1:2 and 2:1) reduce the surface tension of water to only *ca*. 63 mN/m, when measured dynamically or statically. Therefore, for the purpose of this work, the PGLSA has no surface active properties (Figure 4.16 and Figure 4.17).

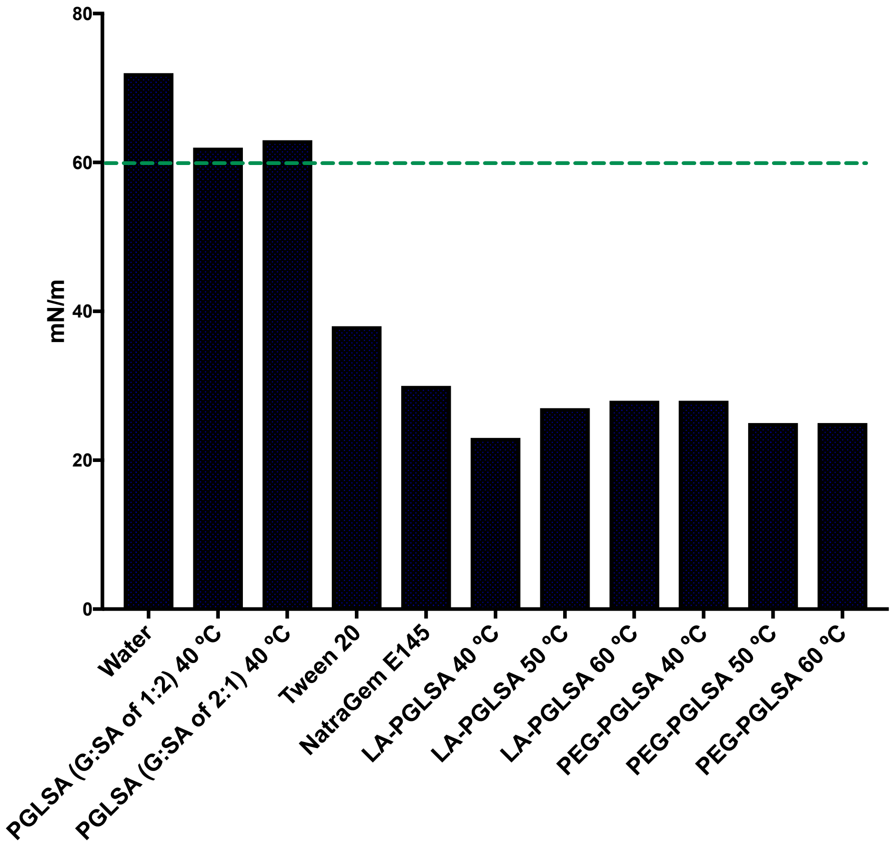

Figure 4.16 – Static surface tension of water, PGSLA not end-capped (with 1:2 and 2:1 G:SA molar ratio, both with 1 wt.%), commercial surfactants (Tween^{TM} 20 – 1,200 Da, NatraGem^{TM} E145 – 1,300 Da, both with 1wt.%) and the synthesised surfactants (1 wt.%) at different temperatures, end-capped with LA and PEG. Compound below the green dashed line are considered to have surface active properties. (LA-PGLSA 40 ºC – 1,700 Da; LA-PGLSA 50 ºC – 1,400 Da; LA-PGLSA 60 ºC – 2,000; PEG-PGLSA 40 ºC – 1,200 Da; PEG-PGLSA 50 ºC – 3,800 Da; PEG-PGLSA 60 ºC – 1,500 Da).

The products from the synthesis of PGLSA end-capped with LA and PEG were observed to become surface active, revealing static surface tensions between $23 < \sigma < 28$ mN/m (Figure 4.16). The commercial surfactants tested, Tween^{TM} 20 and NatraGem^{TM} E145, give a surface tension of 38 and 30 mN/m, respectively. LA-PGLSA and PEG-PGLSA are considered to be biorenewable and biodegradable, revealing good surface active properties. Comparing the results obtained for these polyesters with the commercial surfactants from petrochemical feedstocks showed that PGLSA-based surfactants revealed a more significant reduction of the static surface tension.

The dynamic surface tension indicates how fast compounds migrate to the water-bubble interface at a specific concentration and within a given time frame. The 1 wt.% concentrations of PGLSA-based surfactants are reported here (Figure 4.18) while the 0.5 and 0.1 wt.% concentrations are shown in the appendix (Figure A 6 and Figure A 7, respectively). It is known that the rate of reduction in surface tension, before reaching the CMC induced plateau, is dependent on the surfactant concentration. The higher the surfactant concentration, the faster the surface tension is likely to plateau

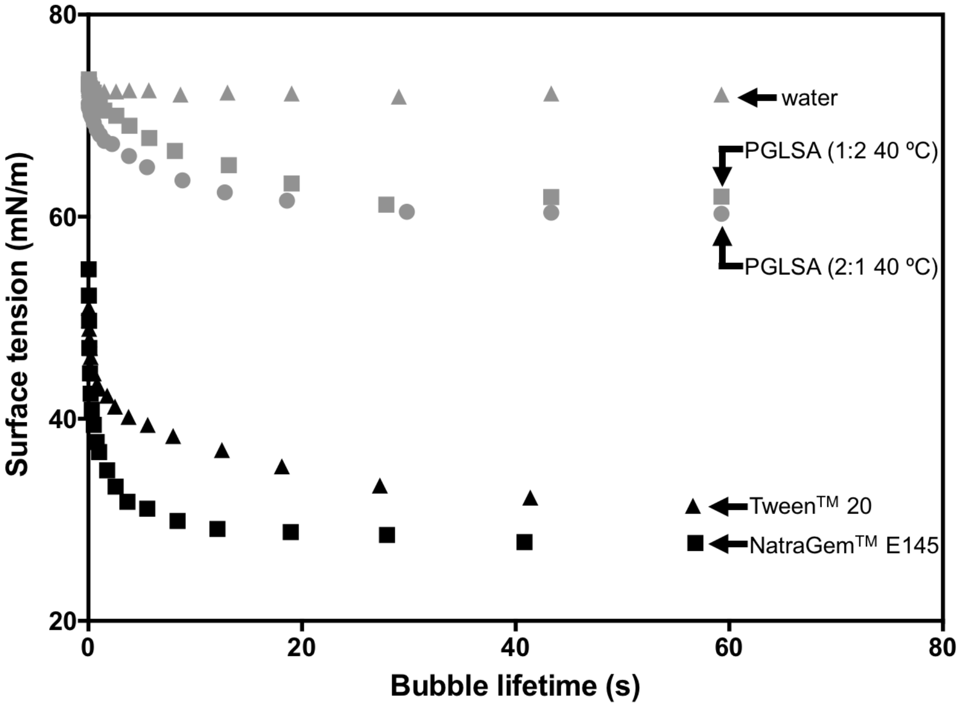

Figure 4.17 – Bubble Tensiometer determination of dynamic surface tension at increasing bubble lifetimes for water, 1 wt.% PGLSA (G:SA 1:2 and 2:1, synthesised at 40 ºC), and commercial surfactants with 1 wt.%, Tween™ 20 and NatraGem™ E145.

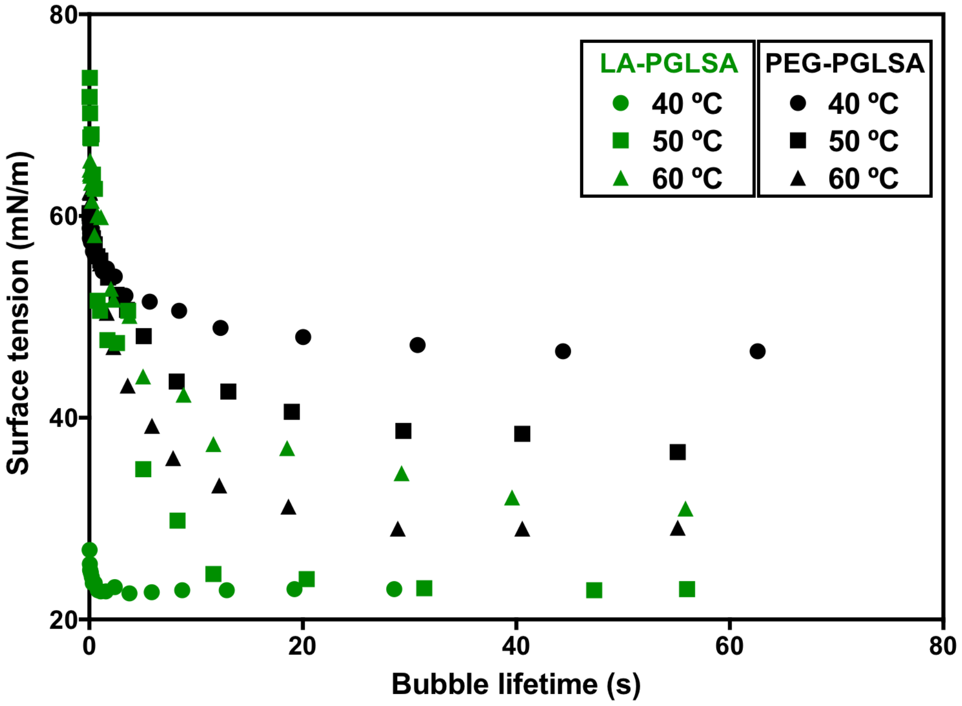

Figure 4.18 – Bubble Tensiometer determination of dynamic surface tension at increasing bubble lifetimes for LA-PGLSA (1 wt.%) synthesised at different temperatures (40, 50 and 60 ºC, green symbols) and PEG-PGLSA (1 wt.%) synthesised at different temperatures (40, 50 and 60 ºC, black symbols).

LA-PGLSA synthesised at 40 and 50 ºC reduced the surface tension of water to 23 mN/m, with the compounds quickly migrating to the surface interface shown by a prompt drop in the surface tension (bubble lifetime of 3 and 11 seconds, respectively, Figure 4.18). LA-PGLSA synthesised at 60 ºC reduce the surface tension of water to 31 mN/m and the compounds migrated to the surface interface at a slower rate (bubble lifetime of 18 seconds, Figure 4.18).

PEG-PGLSA 40 ºC shows a maximum reduction in the surface tension of water to 46 mN/m and the compounds migrate to the surface at a slower rate than LA-PGSLA (bubble lifetime of 20 seconds, Figure 4.18). When increasing the PEG-PGLSA synthesis to 50 and 60 ºC, the surface tension of water was reduced to 36 and 29 mN/m respectively, and all the PEG-PGLSA compounds migrate to the surface at the same rate at bubble lifetimes of 20 seconds (Figure 4.18). These results were comparable with the commercial surfactants tested, in which Tween^{TM} 20 reduced the surface tension to 31 mN/m (bubble lifetime of 35 seconds) and NatraGem^{TM} E145 to 27 mN/m (and the compounds migrate at a faster rate than Tween^{TM} 20, having a bubble lifetime of 29 seconds) (Figure 4.17). Interestingly, the dynamic surface tension of PEG-PGLSA decreases with increasing of the surfactant synthesis temperature.

Comparing the static (equilibrium) and dynamic surface tensions for all the PGLSA-based surfactants, higher values were obtained for the dynamic surface tension.

In summary, PGLSA-based surfactants show similar or, in some cases, superior ability to reduce the surface tension of water compared with the commercial surfactants. These commercial compounds come from petrochemical feedstocks. Therefore, these data make these PGLSA-based surfactants strong candidates as the next generation of surfactants, since they are almost exclusively biorenewable and biodegradable.

4.5.3.2. Surfactant aggregation: critical micelle formation

The micelle formation depends on the surfactant concentration. Increasing concentration decreases the surface tension until the critical micelle concentration (CMC) is reached, where the surfactant will start to aggregate in solution.

Since LA-PGLSA (synthesised at 40 ºC) revealed the greatest solution surface tension reduction of 23 mN/m we determined its CMC (Figure 4.19). The CMC values for the other compounds – commercial available and the others PGLSA-based surfactants, are reported in Appendix, Figure A 8 – Figure A 10. This was accomplished by the automated measurements of the surface tension of the surfactant at a range of concentrations (1-0.007 wt.%), using the static Wilhelmy plate tensiometer. In this way, the CMC of LA-PGLSA 40 ºC was determined to be 462 mg/L (0.05 wt.%, Table 4.6).

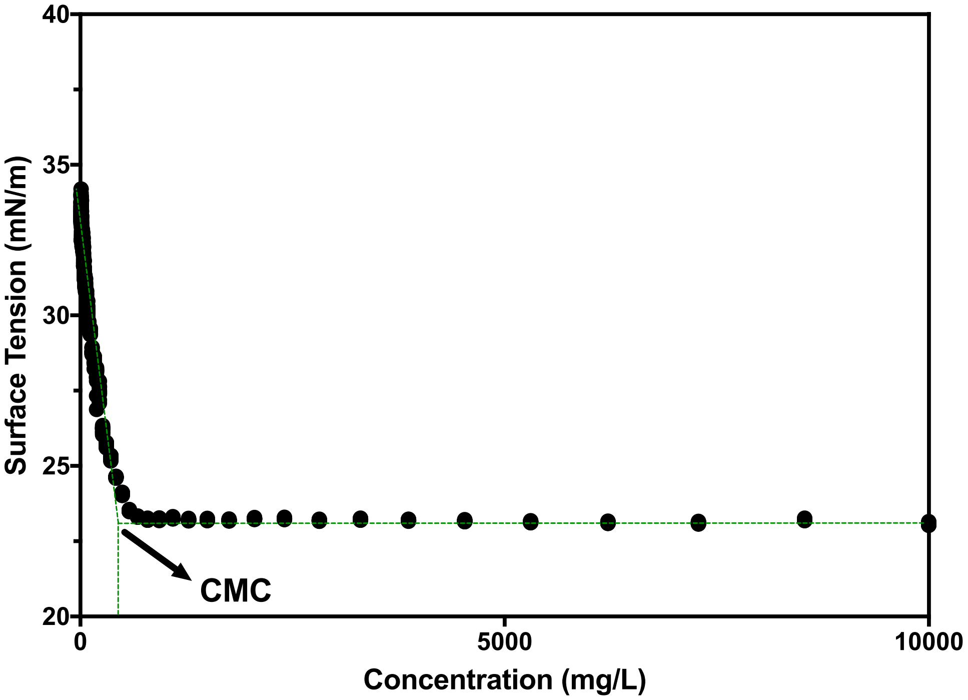

Figure 4.19 – Surface tension measurements of LA-PEG at 40 ºC at several concentrations. The CMC value is determined by the intersection of the two linear dotted green lines.

Table 4.6 – CMC values of synthesised and commercial surfactants. [a)] molecular weight determined by the supplier. The CMC values were determined by the static Wilhelmy plate tensiometer.

Entry	Compound	M_n^{GPC}	CMC (mg/L)	CMC (wt.%)
1	Tween™ 20	1,200 Da[a)]	289	0.02
2	NatraGem™ E145	1,300 Da[a)]	312	0.03
3	LA-PGLSA 40ºC	1,700 Da	462	0.05
4	LA-PGLSA 50ºC	1,400 Da	223	0.02
5	LA-PGLSA 60ºC	2,000 Da	838	0.08
6	PEG-PGLSA 40ºC	1,200 Da	530	0.05
7	PEG-PGLSA 50ºC	3,800 Da	640	0.06
8	PEG-PGLSA 60ºC	1,500 Da	>10,000	>1

The petrochemical-derived non-ionic commercial surfactants typically have a CMC < 0.1 wt.%.[277] Tween™ 20 and NatraGem™ E145 are efficient surfactants at concentrations as low as 290 (0.03 wt.%) and 310 mg/L (0.03 wt.%), respectively (entries 1 and 2, Table 4.6). LA-PGLSA synthesised at 40 ºC was able to decrease the surface tension to 23 mN/m, with a plateau revealing a CMC value of 462 mg/L (0.05 wt.%) (entry 3, Table 4.6). At 50 ºC, LA-PGSA decreased the surface tension to 27 mN/m, revealing a CMC value of 220 mg/L (0.02 wt.%) (entry 4, Table 4.6). Increasing the synthesis temperature to 60 ºC, the surfactant becomes efficient only at a higher concentration, 830 mg/L (0.08 wt.%) (entry 5, Table 4.6), decreasing the surface tension to 28 mN/m. Theoretically, the CMC depends on the chemical structure of the surfactant: the CMC decreases strongly with increasing alkyl chain length of the surfactant; the CMC increases as the polar head becomes larger.[278] The LA-PGLSA 60 ºC reveals a lower degree of branching (DB = 5%), while at 40 and 50 ºC, LA-PGLSA obtained DB of 12 and 10%, respectively. The increase of the CMC at 60 ºC might be due to the presence of more hydroxy pendant groups in the polar head.

PEG-PGLSA surfactants gave higher CMC values compared to LA-PGLSA. These data were expected because M-PEG is a very hydrophilic end-capper polymer (more hydrophilic than the PGLSA block used for the LA-PGLSA surfactants). Therefore, as a consequence of the increase of hydrophilicity, higher CMC values were obtained for PEG-PGLSA surfactants.[278] At 40 ºC, PEG-PGLSA was able to decrease the surface tension to 28 mN/m, where it reaches the CMC value of 530 mg/L (0.05 wt.%), concentration and becomes an efficient surfactant (entry 6, Table 4.6). For the polymer synthesised at 50 ºC, there was a slight increase in the CMC to 640 mg/L (0.06 wt.%) (σ = 25 mN/m) (entry 7, Table 4.6). The PEG-PGLSA 60 ºC obtained, surprisingly, a much higher CMC value, > 10,000 mg/L (> 1 wt.%). This might be a consequence of uncertainty in the amount of M-PEG attached to the PGLSA backbone. The presence of free M-PEG (unattached to the PGLSA) might be the reason for this high value (entry 8, Table 4.6).

A compound that has the ability to reduce the surface tension of water but has a high CMC value, does not mean it is a compound with less surface active properties. For some applications, having high CMC values is of great importance, such as for emulsifiers and solubilisers, useful in laundry detergents and clean-up of oil spills.[279] It is beneficial for a detergent to have high concentrations of surfactant molecules to perform efficiently. However, for cosmetic and personal care products, a lower CMC value is preferable, which indicates that less surfactant is needed to saturate interfaces and form micelles.[280]

When comparing these results with the commercial surfactants, excluding the compound PEG-PGLSA 60 ºC, the synthesised PGLSA-based surfactants are revealed to have promising surface active properties ($\sigma \leq 60$ mN/m) for personal care products. These surfactants become efficient at low concentrations (≤ 0.08 wt.%) showing that they efficiently self-assemble and aggregate causing the surface tension to plateau. These results are consistent with the petrochemical derived non-ionic commercial surfactants ($\sigma \leq 60$ mN/m and CMC ≤ 0.1 wt.%[277]) useful for cosmetic and personal care products.

4.5.3.3. Dynamic light scattering

Dynamic light scattering (DLS) was used to investigate the hydrodynamic diameter of the self-assembled structures in an aqueous environment.

The values obtained for the size of the self-assembled structures of PGLSA-based polymers are in the range of 170-280 nm (entries 3-8 from Table 4.7). Personal care and cosmetics applications require self-assembled aggregates in a size range between 200-500 nm.[281] For drug delivery, self-assembled aggregates must typically be smaller than 200 nm;[282] structures with dimensions below 100 nm usually required in pharmaceutical formulations (characterised by a higher efficiency of penetration through the blood vessel walls)[283-284].

Most of the Z-average values are in good agreement with the mean peak size, suggesting that the aggregates formed are relatively monodisperse. This was not the case for LA-PGLSA 50 ºC and PEG-PGLSA 40ºC (entries 4 and 6, Table 4.7). In these polymeric samples, the Z-average (543nm and 631 nm, respectively) was considerably larger than the peak size (404 nm and 263 nm, respectively). This might be cause by the presence of larger aggregates (with size > 5,000 nm) as a result of the purity of the sample, leading to side-products agglomerating and affecting DLS readings.

Table 4.7 – Size distribution of surfactant micelles measured by DLS. The measurements were done at surfactant concentrations higher than it CMC value. [a] concentration close to CMC value. [b] value reported from peak 2 because a higher peak was also present in DLS trace, > 5,000 nm, explaining the high Z-average reported.

Entry	Compound	CMC (wt. %)	Concentration (wt. %)	Z-average (d, nm)	Peak size (d, nm)	PDI
1	Tween™ 20	0.02	0.1	100.5 (±9.2)	106.6 (±7.2)	0.5 (±0.08)
2	NatraGem™ E145	0.03	0.1	370 (±34.5)	379 (±144)	0.4 (±0.04)
3	LA-PGLSA 40ºC	0.05	0.1	274 (±25.5)	224 (±16.1)	0.3 (±1.24)
4	LA-PGLSA 50ºC	0.02	0.1	543 (±82.2)	404 (±49.3)[b]	0.4 (±0.05)
5	LA-PGLSA 60ºC	0.08	0.2	247 (±9.5)	243 (±7.0)	0.2 (±0.03)
6	PEG-PGLSA 40ºC	0.05	0.1	631 (±119.7)	263 (±96.8)[b]	0.5 (±0.1)
7	PEG-PGLSA 50ºC	0.06	0.1	280 (±18.7)	289 (±51.2)	0.3 (±0.03)
8	PEG-PGLSA 60ºC	>1	1[a]	178 (±3.1)	212 (±8.2)	0.3 (±0.01)

It is well understood that the sizes of the self-assembled structures are influenced by the molecular weight of the building blocks, the length of the end-cappers, and the hydrophobicity of the non-polar block.[232] Two different surfactant molecules were analysed. LA-PGLSA polymer possesses a more hydrophilic block (PGLSA) which was end-capped with LA (FA), the hydrophobic block. Whereas PEG-PGLSA polymer possesses a more hydrophobic block (PGLSA) which was end-capped with PEG, the hydrophilic block.

Focusing on the latter, it has been stated that the higher the molecular weight of the amphiphilic polymer, the larger the micelle size aggregate. For example, the synthesis of PEG-based surfactants resulted in different micelle sizes depending on the M_n obtained: 163 nm for $PEG_{5,000Da}$-poly(pentadecalactone) ($PEG_{5,000Da}$-PPDL, M_n ~ 22,000 Da[285]), 23 nm for PEG_{550Da}-poly(hexanediol azelate) (PEG-PHAz, M_n ~ 2,000 Da[232]) and < 30 nm for poly(ethylene glycol)–distearoyl phosphatidyl ethanolamine (PEG_{750Da}-DSPE surfactants, M_n ~ 2,000 Da[286]).

Therefore, the data from this work has shown the same trend: PEG-PGLSA synthesised at 50 ºC resulted in a polymer with a M_n of 3,800 Da with a micelle size of 280 nm. Whereas the PEG-PGLSA synthesised at 60 ºC resulted in a polymer with M_n of 1,500 with a micelle size of 178 nm.

Focusing on the other type of surfactant (where the polymeric core is more hydrophilic and a hydrophobic block is attached to it, *e.g.* a FA), it has been shown that increasing the M_n of the hydrophobic block will result in a decrease of the aggregate size.[232, 282] This effect might be related to the core crystallinity and, hence, the ability to 'pack' more easily in the crystalline regions, which will influence the core size and, consequently, the micelle size. From the results obtained in this Thesis, the M_n of the polymers LA-PGLSA synthesised at 40 and 60 ºC were 1,700 and 2,000 Da, respectively, leading to the formation of 274 and 246 nm micelles sizes, respectively. Therefore, the PGLSA crystallinity and the presence of LA-block might explain this trend in micelle sizes values.

Nevertheless, the micelles size between the two end-capped PGLSA-based polymers are not significant, revealing a similar micelle size range (with the exception of LA-PGLSA synthesised at 50 ºC and PEG-PGLSA synthesised at 40 ºC, as discussed above). The size distribution of the PGLSA-based compounds gave similar values to the commercial surfactants tested: NatraGem^{TM} E145 and Tween^{TM} 20, (100-300 nm). These preliminary results show that all the synthesised PGLSA-based surfactants formed self-assembled aggregates with suitable size for personal care and cosmetic applications.

It is known that the size of a micelle is dependent on the concentration and that surfactant molecules tend to self-organised into more stable particles with increasing concentration. Generally, an increase of surfactant concentration will result in a decrease in the particle size.[287] This trend was observed in the obtained data apart from the polymer LA-PGLSA synthesised at 50 ºC (entries 3 and 4 from Table 4.8) and PEG-PGLSA synthesised at 40 ºC (entries 7 and 8, Table 4.8) where there is not significant different on the micelle size with surfactant concentration increase.

The increase in concentration of PEG-PGLSA synthesised at 50 and 60 ºC is shown below (entries 9-12, Table 4.8) and it is possible to observe this trend, where there is a decrease in the micelle size with increase of the surfactant concentration. This was also observed for LA-PGLSA synthesised at 40 and 60 ºC (entries 1, 2, 5 and 6, Table 4.8). This behaviour might be due to the increase of the number of self-assembled particles, increasing the repulsion forces between micelles and the diffusion speed of the particles, resulting in a decrease in the hydrodynamic size.[287-288]

Table 4.8 – Z-average measured by DLS of the PGLSA-based surfactants at different concentrations.

Entry	Compound	Concentration (wt. %)	Z-average (d, nm)
1	LA-PGLSA 40 ºC	0.1	274 (± 25)
2		0.01	342 (± 35)
3	LA-PGLSA 50 ºC	0.1	543 (± 82)
4		0.01	562 (±173)
5	LA-PGLSA 60 ºC	0.5	317 (± 26)
6		0.001	579 (± 11)
7	PEG-PGLSA 40 ºC	0.1	631 (± 119)
8		0.01	562 (± 45)
9	PEG-PGLSA 50 ºC	1	404 (± 51)
10		0.01	602 (± 74)
11	PEG-PGLSA 60 ºC	1	178 (± 178)
12		0.5	650 (± 162)

Nevertheless, further investigations are desirable in order to fully understand the self-assembly of the PGLSA-based surfactants (such as TEM analysis to determine the shape to the surfactants and the influence of surfactant concentration in the size/shape of the self-assembled structure).

4.5.3.4. Contact angle measurement

The contact angle or wetting angle (*θ*) measures the wettability of a solid by a liquid and is defined as the angle between a liquid and solid interface. When a contact angle is low (< 90 ºC) it indicates high surface wettability; a higher contact angle (> 90 ºC) shows the opposite (Figure 4.20).[289] This property is of pivotal importance for different applications, including: cleaning, lubrication, coating and printing, to name a few.[290] The addition of surfactants into aqueous solutions will reduce the surface tension of water and solid-water interfacial tension. Therefore, it will enhance the ability of aqueous solutions to wet and spread over solid surfaces.[291]

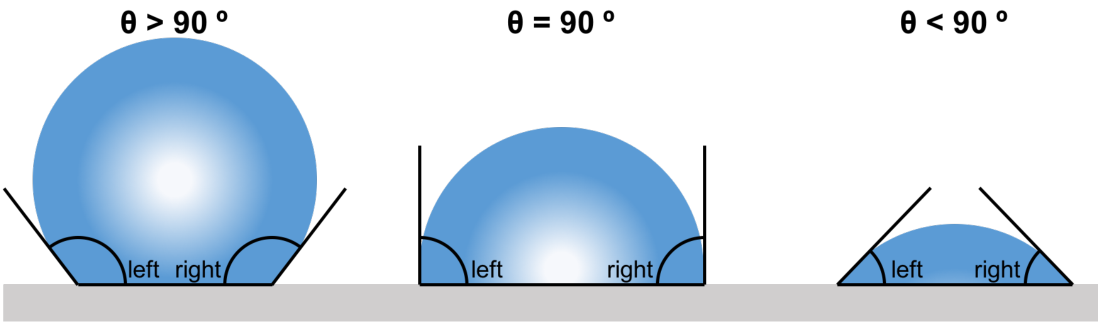

Figure 4.20 – Illustration of contact angles formed by static sessile drop, on a surface of parafilm plate.

For reference, a water droplet on a hydrophobic parafilm surface forms an angle of 110/109 º (left and right, respectively) (entry 1, Table 4.9). These angles were similar to the angles obtained from the droplet of aqueous PGLSA polymers not end-capped with LA or PEG, obtaining angles near 100 º (entries 4 and 5, Table 4.9). This shows that the synthesised polyester that are not end-capped have minimal ability to reduce the interfacial tension between the water solution and the solid surface. The commercial surfactants Tween^{TM} 20 and NatraGem^{TM} E145 presented lower contact angles of 91/90 º and 63/61 º, respectively, corresponding to a clear decrease in the solution interfacial tension (entries 2 and 3, Table 4.9). The synthesised end-capped PGLSA in general revealed a reduction in the interfacial tension, because the values obtained range from 75 º < θ < 90 º (entries 6-11, Table 4.9).

As mentioned previously, Tween^{TM} 20 is comprised of poly(ethylene oxide), sorbitan and lauric acid, which is similar to synthesised PEG-PGLSA. Therefore, it is unsurprising that the PEG-PGLSA gave similar contact angles.

NatraGem^{TM} E145 is comprised of glycerol, succinic acid and lauric acid, structurally similar to LA-PGLSA and, consequently, comparable contact angles were obtained.

The synthesised PGLSA-based surfactants under enzymatic supercritical conditions revealed promising results, demonstrating similar contact angles to comparable commercially available surfactants. PGLSA-based surfactants enhance the ability of aqueous solutions to wet and spread over solid surfaces further corroborating their surfactant potential for applications relating to cleaning products.

Table 4.9 – Contact angles (left and right) of water, commercial surfactants at 0.5 wt.% (Tween^{TM} 20 and NatraGem^{TM} E145), PGLSA at 0.5 wt.% (with G:SA of 1:2 and 2:1, synthesised at 40 ºC), 0.5 wt.% of LA-PGLSA (synthesised at 40, 50 and 60 ºC) and 0.5 wt.% of PEG-PGLSA (synthesised at 40, 50 and 60 ºC).

Entry	**Compound**	**Left angle**	**Right angle**
1	Water	110 ± 0.2	109 ± 0.3
2	Tween^{TM} 20	91 ± 2.3	90 ± 2.6
3	NatraGem^{TM} E145	63 ± 2.3	61 ± 2.5
4	PGLSA 1:2 40 ºC	103 ± 1.1	104 ± 2.0
5	PGLSA 2:1 40 ºC	96 ± 0.5	96 ± 0.6
6	LA-PGLSA 40ºC	75 ± 6.2	73 ± 7.2
7	LA-PGLSA 50ºC	74 ± 5.9	75 ±6.7
8	LA-PGLSA 60ºC	79 ± 5.5	78 ± 6.0
9	PEG-PGLSA 40ºC	88 ± 0.9	88 ± 0.4
10	PEG-PGLSA 50ºC	93 ± 0.6	93 ± 0.6
11	PEG-PGLSA 60ºC	90 ± 0.9	90 ± 3.8

4.6. Conclusions

The novel and green methodology developed in Chapter 3 for synthesising polyesters from a polyol and a diacid in the presence of an enzyme has been exploited in this chapter to develop surfactants based on glycerol and succinic acid end-capped with lauric acid or poly(ethylene glycol). The polymerisations were carried out at a fixed pressure of 275 bar, with 25 wt.%[‡‡] of CaLB at a range of temperatures: 40 – 60 ºC, achieving high yields (> 85%). To synthesise these polymers (with the molecular weight obtained) at these remarkably low temperatures would have never been possible without the use of $scCO_2$ as reaction medium.

Initially, LA-PGLSA and PEG-PGLSA were analysed by ^{1}H-NMR, GPC and DSC to confirming the enzymatic synthesis of linear polyesters.

Afterwards, the evaluation of the performance of lauroyl poly(glycerol succinate) and PEG-poly(glycerol succinate) as surfactants was assessed. Both synthesised surfactants were shown to have the ability to decrease the surface tension of water to as low as 23 mN/m. These compounds have competitive surface active properties when comparing with commercially available surfactants, demonstrating that PGLSA-based surfactants might find applications as body-care formulations. Regarding the CMC values, the synthesised PGLSA-based surfactants become efficient at low concentrations (0.02-0.08 wt.%) showing that they efficiently self-assemble and aggregate causing good surface tension to plateau. These results are comparable with the Tween™ 20 and NatraGem™ E145 revealing that PGLSA-based surfactants show promising results to be used as surfactants in cosmetic applications. Examining the contact angle formed between the aqueous surfactant and a hydrophobic surface, PGLSA-based surfactants revealed an obvious reduction on the interfacial tension, $75^{\circ} < \theta < 90^{\circ}$, which will enhance the ability of aqueous solutions to wet and spread over solid surfaces, which is a very important characteristic of wetting agents.

[‡‡] Includes polymer support

To summarize, the biodegradable and biorenewable PGLSA-based polymers synthesised at mild temperatures, under enzymatic supercritical conditions, have been successfully demonstrated to be interesting candidates as surface-active agents. Further analysis needs to be done to investigate more in-depth the self-assembly of these polymers in water, evaluating the shape of the structures created upon the formation of aggregated structures and to evaluate their potential in cosmetic formulations.

CHAPTER 5. THE IRONWEED OPPORTUNITY

5.1. Overview

Currently, epoxidised oils are produced from petrochemical feedstocks or by chemical epoxidation of fats and vegetable oils. They are commonly used in the plastics industry as an additive in the formulation of polyvinyl chloride (PVC) and in the coating industry for synthesising tough layers resistant to alkalis, acids and solvents.[292] The synthesis process of these materials are expensive and contain volatile organic solvents,[293] which are not ideal from the economic and environmental point of view. The need to find natural epoxidised oils is increasing and these are preferable to synthetic epoxidised oils.

Ironweed plant, which is found in abundance in Ethiopia, is a non-commercial weed and its seeds contain 40 wt.% natural epoxy oil. The synthesis of new building blocks from this oil has not been investigated in great detail.[60, 294-295] Additionally, *Vernonia galamensis* oil contains up to 80 wt.% of vernolic acid, a mono-unsaturated fatty acid with an additional epoxide functionality. The presence of these two functional groups (an alkene and an epoxide) offers great opportunities to synthesise new building blocks for polycondensation reactions. To the best of the author's knowledge, the derivatisation of vernolic acid, to synthesise new monomers for polycondensation has not yet been reported. Consequently, this chapter will focus on the synthesis of vernolic acid-based monomers, from *Vernonia galamensis* oil, for polycondensations, which are discussed later in Chapter 6.

In this Chapter, the extraction of the oil from Ironweed, using $scCO_2$ is described. Subsequently, the saponification process of the oil to obtain vernolic acid will be reported. Finally, the synthesis of vernolic acid-based monomers is discussed.

5.2. Introduction

In recent decades, alternative feedstocks from biomass, are beginning to replace fossil feedstocks (at least in part) and have received a lot of attention.[296] The total amount of biomass production is 170 billion tonnes per year and 3.5% (~6 billion tons) is presently being used for human needs.[297-298] The rest is used in the natural ecosystems (feed for wild animals) or is lost when biomass is obtained for humans (by burning) or because of the natural mineralisation process.[299] The synthesis of new chemicals from biomass has received increasing attention in the last decades.[300-303] Using triglycerides in polymer science is one example of this type of research.[59, 296, 304] Most of these polymers are cross-linked, hard polymers (thermoset and coating materials).[304-306]

The use of renewable raw materials wherever and whenever possible is one crucial step towards a more sustainable development due to the exhaustion of petrochemical resources and their environmental impact.[59, 306] Therefore, there has been a lot of interest in using agricultural raw materials to produce biobased chemicals.[142] Using agricultural resources (more specifically the waste, or resources that do not require much preparation such as weeds) has several advantages such as their availability, low cost and most importantly, their favourable environmental profile.

5.2.1. Vernonia galamensis sp.

Vernonia galamensis is an annual shrub native to east Africa, (including Ethiopia, Kenya and northern Tanzania).[60, 304, 307] It can grow in a variety of ecological habitats ranging from dry areas with a yearly rainfall of 200 mm, to rich forested areas with a rainfall of 1,850 mm.[60] The flower head of *V. galamensis* is 3-4 cm (Figure 5.1) wide and the seeds are dark brown, *ca*. 5 mm long (Figure 5.2). It belongs to the *Vernonia* species, member of the family *Compositae*. *Vernonia galamensis* seeds contain up to 40% of natural epoxy oil (triglycerides), depending on the place where it grows.[57, 59-60]

Figure 5.1 – Ironweed (*Vernonia galamensis* sp) plants which can be found in Ethiopia. (Images from Nydick [308]).

Figure 5.2 – Ironweed (*Vernonia galamensis* sp) seeds. (Image from Richard [309]).

5.2.1.1. Vernonia oil

Vernonia galamensis oil contains vernolic acid (70-80 wt.%, VA, 12,13-epoxy-9-decenoic acid), linoleic acid (12-14 wt.%), oleic acid (4-6 wt.%), stearic acid (2-3 wt.%), palmitic acid (2-3 wt.%) and a trace of arachidic acid.[57, 60] Chemically, vernonia oil (VO) is very similar to the synthetic epoxidised soybean (ESO) and linseed oils (ELO) (Figure 5.3). Soybean oil contains only 50% of linoleic acid as its principal fatty acid (FA) while linseed oil contains 57% of linoleic acid.[60] VO contains 70-80% of its principal natural epoxidised FA – VA (Figure 5.4), which makes it an attractive raw material.

VA, which is present in the VO that can be extracted from *Vernonia galamensis* seeds, shows interesting properties to be used in chemistry. There are only a few examples in the literature using this molecule, mainly focusing on the production of epoxy coatings,[57] thermoplastics[58] and biodegradable polymers (see section 1.3.2.1. of this Thesis).[59] Therefore, VA is a compound that needs further investigation.

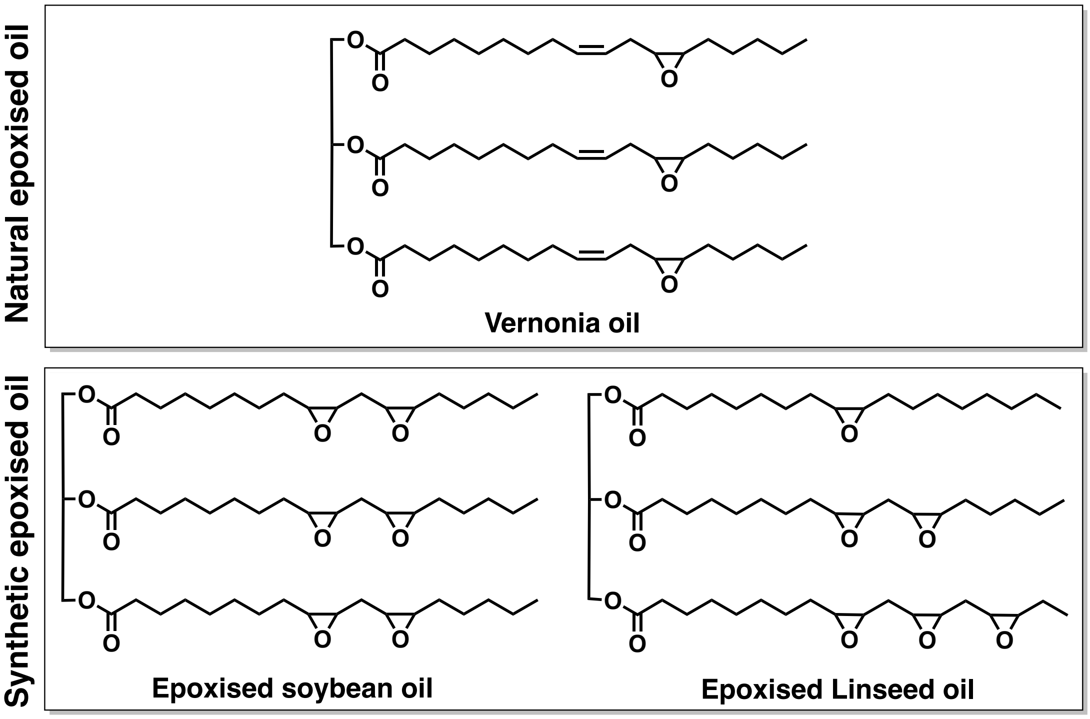

Figure 5.3 – Chemical structures of Vernonia, epoxidised soybean and linseed oil.

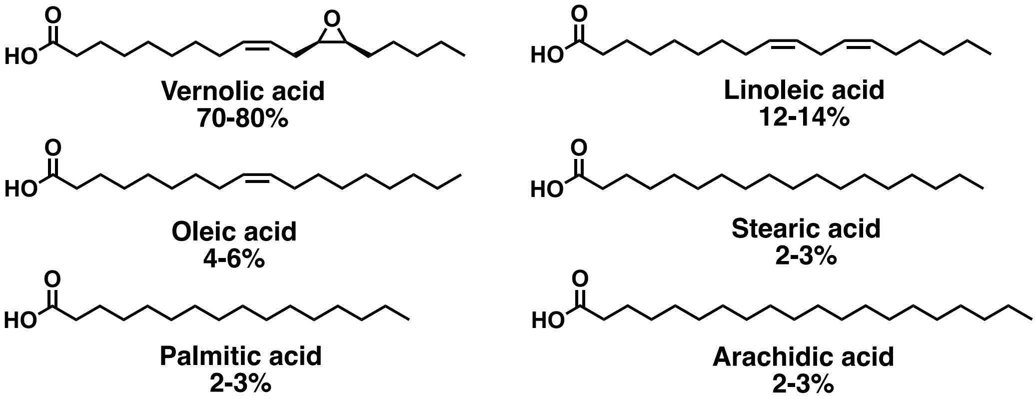

Figure 5.4 – Fatty acid contents present in vernonia oil.

5.2.2. Importance of epoxides

Epoxides are very versatile organic intermediates as a consequence of their reactive oxirane moiety. They can be opened by various nucleophiles or undergo elimination, reduction or rearrangements to other intermediates with the retention or inversion of the configuration. These active oxiranes are key building blocks for the synthesis of fine chemicals for a variety of industrial, pharmaceutical and biological processes.[310-311]

Epoxidised oils (EO) are normally used in the plastics industry as an additive in the formulation of polyvinyl chloride (PVC) and in the coating industry for preparing tough layers resistant to alkalis, acids and solvents.[60, 312-313] Industrially, epoxy oils are produced by modifying petrochemicals. Usually they are expensive and contain volatile organic solvents[293] which are not ideal from the economic and environmental point of view.

5.2.2.1. Current challenges in epoxide synthesis

The formation of epoxides has been studied since the beginning of the last century, where Prileschajew discovered that olefins react with peroxybenzoic acid to form epoxides (Figure 5.5).[314] The epoxidation of long-chain olefins and unsaturated fatty acids (FA) of vegetable oils (canola, soybean and linseed oil, to name a few) is carried out on an industrial scale,[315-318] and the annual production of epoxy-based materials is 259,000 tonnes in Europe.[319]

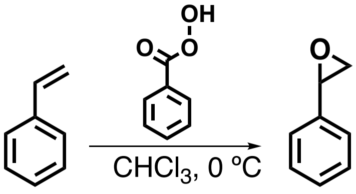

(1) **(2)**

Figure 5.5 – Prilezhaev epoxidation reaction.

As a consequence of the demand for new compounds for pharmaceutical products and new materials, there has been an extensive search for viable epoxidation reactions over the last decades, to develop less expensive and environmentally more benign approached.[311, 320] Nevertheless, these procedures still require several steps and involve energy intense processes, such as washing steps, using solvents (toluene[321], diethyl ether[315] and *tert*-butanol[318], to name a few) and reaction temperatures of 85 ºC.[318, 322] The most common procedure for the epoxidation of oils is based on Daniel Swern's methodology (developed in 1949), wherein use of acetic acid, sulfuric acid and hydrogen peroxide is crucial.[323]

These reaction conditions have several downsides. Strong acids are nonselective, cause equipment corrosion, can initiate undesirable oxirane ring-opening (in the presence of water, leading to the formation of secondary hydroxy groups) and they must eventually be neutralised and removed from the product.[321] To overcome the undesirable ring opening of the epoxide, a chemo-enzymatic epoxidation technique has been developed, using a lipase immobilised on an acrylic resin (*Candida antarctica* lipase B, CaLB).[324-325]

Thus, using naturally occurring epoxide oils, where chemical modifications are not required, is highly desirable.

5.2.2.2. Naturally occurring epoxides

Naturally occurring epoxides are found in more than 60 species of plants (Table 5.1).[326-327] These compounds are usually present as long-chain glycerides such as *cis*- and *trans*-9,10-epoxystearic acid (Figure 5.6 **(3a) (3b)**, also known as epoxyoleic acid), *cis*-15,16-epoxylinoleic acid (Figure 5.6 **(4)**), *cis*-12,13-epoxyoleic acid (also known as vernolic acid, Figure 5.6 **(5)**) and *cis*-

9,10-epoxy-12-octadecenoic acid (also known as coronaric acid, the vernolic acid isomer Figure 5.6 **(6)**). [328]

Table 5.1 – Plant species containing epoxy acids in the seed oil.

Family	Epoxy content in oil	References
Compositae (39 species)	0.2–80%	Morris and Holman [329] Earle and Jones [330] Jones and Earle [331]
Cruciferae (1 species)	1%	Gunstone and Morris [332]
Cucurbitaceae (1 species)	0.7%	Morris and Holman [329]
Dipsacaceae (3 species)	11–32%	Tallent, *et al.* [333]
Euphorbiaceae (3 species)	57–72%	Bharucha and Gunstone [334] Kleiman, *et al.* [335] Gunstone and Sykes [336]
Leguminosae (2 species)	6–7%	Morris, *et al.* [337] Morris and Holman [329]
Malcaceae (13 species)	0.4–7%	Hopkins and Chisholm [338] Hopkins and Chisholm [339]
Olacaceae (1 species)	1%	Morris [340]
Onagraceae (1 species)	10%	Jr., *et al.* [341]
Sterculiaceae (1 species)	0.2%	Morris and Holman [329]
Valerianaceae (1 species)	30%	Tallent, *et al.* [333]
Zygophyllaceae (1 species)	4%	Morris and Holman [329]

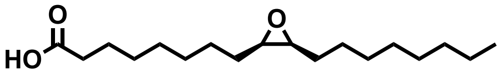

(3a)

***cis*-9,10-epoxystearic acid**
also known as *cis*-epoxyoleic acid

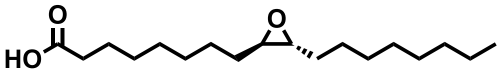

(3b)

***trans*-9,10-epoxystearic acid**
also known as *trans*-epoxyoleic acid

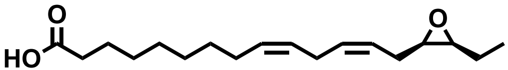

(4)

***cis*-15,16-epoxylinoleic acid**

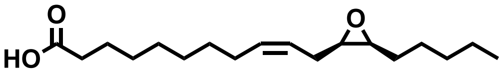

(5)

***cis*-12,13-epoxyoleic acid**
also known as vernolic acid

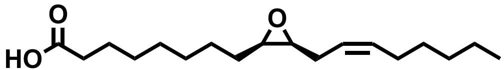

(6)

***cis*-9,10-epoxy-12-octadecenoic acid**
also known as coronaric acid

Figure 5.6 – Naturally occurring epoxides found in Compositae, Dipsaceae, Euphorbiaceae, Malvaceae and Dipterocarpaceae plant families.

The epoxy acid **(3a)** was first isolated in 1959, from *Tragopogon porrifolius* seed oil[342] and the *trans*-isomer **(3b)** in 1961, from orujo oil (olive oil waste).[343] The epoxy acid **(4)** was found in 1959, isolated from *Camelina sativa* seed oil.[332] Vernolic acid, **(5)** was first found in 1954, in *Vernonia anthelmintica* seed oil.[344] The vernolic acid isomer **(6)** was found in *Chrysanthemum coronarium* seed oil in 1959.[345] The *Vernonia galamensis* was reported to have the seeds with the highest content of an epoxy fatty acid, vernolic acid **(5)**.[346]

New chemicals produced from renewable resources, such as *Vernonia galamensis* seeds, are attractive from a sustainable perspective. VO has recently received attention due to its unique properties as a natural epoxide oil. Since VO has naturally valuable different functional groups, the synthesis of new functionalities (such as the epoxide) through organic synthesis is not required. Therefore, the synthesis of these ‘green’ compounds could potentially minimize waste disposal problems (associated with the vast range of synthetic steps require to synthesise new compounds), which is one of the concerns when using petrochemical feedstocks.

Hence, the ironweed plant was chosen for this work since it has high quantity of VA which has two functional groups (an alkene and an epoxide) that offers great opportunities to synthesise new building blocks for polycondensation reactions. In the literature, VO has been reacted with dibasic acids,[307] diamines[347] and (meth)acrylates[348] to form polymers. Nevertheless, the synthesis of new building blocks, from this oil, for applications other than resin and coating applications has scarcely been investigated.[60, 294-295]

5.2.3. Extraction of vegetable oils

As mentioned previously in Chapter 1, the extraction of vegetable oils can be accomplished by

1) pressing techniques,
2) using organic solvents (liquid-solid extraction)
3) or by using a greener approach, using $scCO_2$ extraction.

The extraction of VO has been studied in detail using organic solvents and it is known that depending the region where *Vernonia galamensis* weed grows, the oil content will vary.[57, 60, 349-351] Ncube*, et al.* [349] performed the extraction of VO using cold acetone, -20 ºC, and obtained 30% oil content. Whereas Bhardwaj*, et al.* [351] extracted 32.4-36.9% of VO at room temperature using a mixture of *n*-hexane/isopropanol (3:2 v/v). Soxhlet extraction (using *n*-hexane, at *ca.* 70 ºC) has also been used to obtain VO and Grinberg*, et al.* [60] obtained 38% oil content.

Using $scCO_2$ to extract vegetable oils has been proven to be a better approach from a sustainable point of view.[122-123] This approach is a great alternative to using high temperatures and volatile solvents to obtain faster mass transfer. Other advantageous properties include the gas-like viscosity, liquid-like density and a faster diffusivity than in organic solvents at ambient conditions.[110, 352] In addition, supercritical fluid extraction (SFE) generally operates at relatively low temperatures and the vegetable oil is obtained free of solvent.[110] To the best of the authors knowledge, only King*, et al.* [353] performed the extraction of VO from *Vernonia galamensis* seeds by SFE. The extraction was performed at 138, 345 and 690 bar and at 40º, 60º, 80º and 100 ºC. Higher temperatures and pressures favoured oil solubility, leading to higher content of extracted oil (*ca.* 17%). Adding 5, 10 and 15% of ethanol (relative to CO_2) as co-solvent resulted in an increase of the extraction efficiency: at 690 bar and 100 ºC, the oil content increased to 27, 39 and 47%, respectively. Nevertheless, these extracts may contain other moieties besides VO, such as polar lipids, water and some protein content.[354]

The separation of the oil from $scCO_2$ is carried out by modifying the thermodynamic properties of the CO_2: the solvation power of $scCO_2$ can be modified by manipulating the pressure and temperature (see section 1.6.1.1. of this Thesis). In this work, the separation process of the oil extracted from *Vernonia galamensis* seeds was achieved by decreasing the pressure and a mixture of fatty acids (FAs) is obtained. However, we are interested in just one – vernolic acid. The ideal separation process would be by fractionation, based on the different FA's solubility in $scCO_2$. However, in this work, the FAs fractionation was not accomplished. A more detailed description of SFE is described in Chapter 1.

5.2.4. Vernolic acid

5.2.4.1. The vernolic acid opportunity for new building blocks

Vernonia oil (VO) is mainly composed of triglycerides: an ester derived from glycerol and three fatty acids. To obtain pure vernolic acid, a hydrolysis step is required to hydrolyse these esters bonds.

When using *n*-hexane to do the extraction of VO (soxhlet extraction), in addition to triglycerides (TG), the oil contains some impurities which must be removed to get pure vernolic acid. Some of these impurities are:

a) free fatty acids (FFA), which may be built up due to enzymatic processes (lipase) resulting from damage to the seed
b) moisture and solvent
c) pigment materials
d) primary and secondary oxidation products, waxes and saponifiable and odoriferous materials.

Three main steps are required to remove these impurities – bleaching, degumming and neutralisation.

VA *per se* is not an ideal monomer to use in polycondensation. As mentioned in Chapter 1 and Chapter 3, to do a polycondensation reaction, the monomers need to be bifunctional or multifunctional. The presence of an alkene and epoxy group in VA offers great opportunities to modify this fatty acid into new monomers suitable for polycondensation. To the best of our knowledge, the functionalisation of vernolic acid, to synthesise new building blocks for polycondensation, has not yet been reported. Ideally, the author would like to convert VA into a monomer with two functional groups able to undergo polycondensation, such as: carboxylic acid and a hydroxy group.

5.2.4.1.1. The synthesis of allylic alcohols

The presence of a reactive epoxide in VA offers great opportunities to functionalise this fatty acid, leading to the formation of a wide variety of products. The conversion of epoxides into their corresponding allylic alcohol is an example and it has been studied in the literature due to its properties and applications: resins, waxes, nylons, plastics, corrosion inhibitors, cosmetics and bioactive fatty acids for biomedicals.[355-356]

Kraus and Frazier [357] studied the transformation of epoxides into allylic alcohols by using iodotrimethylsilane (TMSI) and 1,5-diazabicyclo-[5.4.0]undec-5-ene (DBN) (upper reaction in Figure 5.7). In their work, the ring-opening of the epoxide of compound **(7)** proceeded rapidly. Nevertheless, the dehydrohalogenation step (formation of the double bond) was not complete until the reaction temperature was raised to reflux (~ 90 ºC). After 48 h reaction, compounds **(8)** were obtained.

Kato*, et al.* [355] also performed the synthesis of several allylic alcohols from epoxy fatty acids (lower reactions in Figure 5.7). Each epoxide **(9, 11, 13, 15)** was treated with excess of lithium diisopropylamide (LDA) in tetrahydrofuran, at 0 ºC or -78 ºC, providing the respective allyl alcohol. The reactions revealed good yields (60% and 85%) and there was no formation of by-products.

From: *Journal of Organic Chemistry* **1980,** *45* (13), 2579-2581

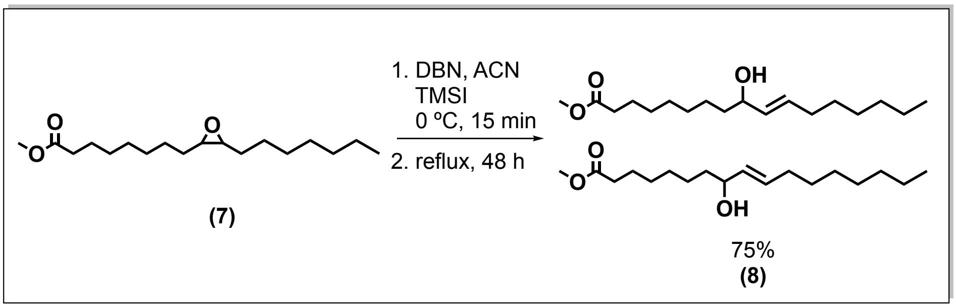

From: *Bioscience, Biotechnology and Biochemistry* **1993,** *57* (2), 283-287

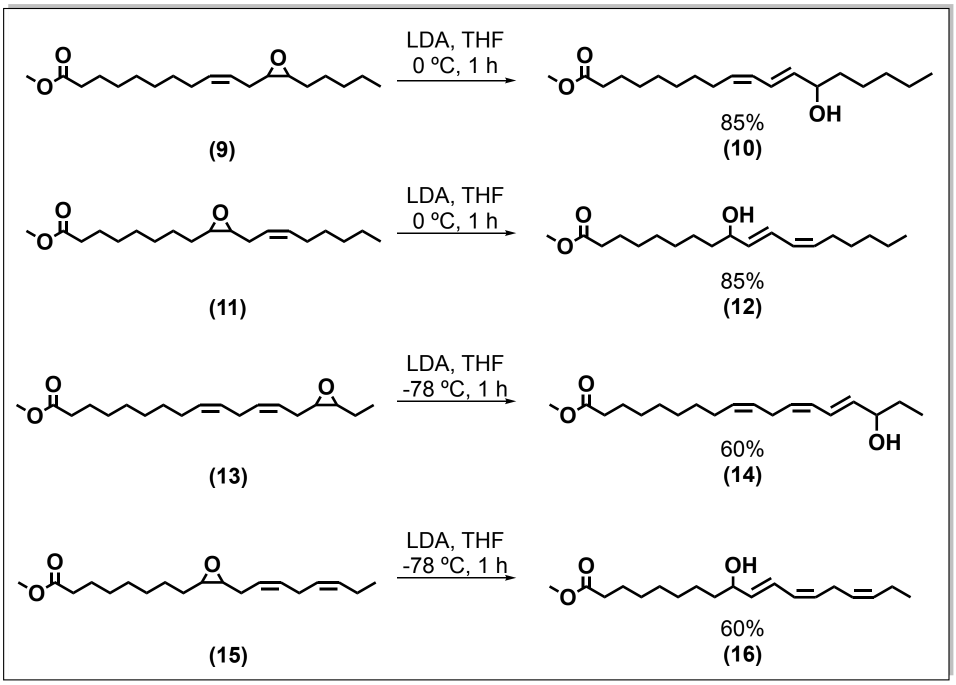

Figure 5.7 – Synthesis of allylic alcohols from different epoxides. Upper reaction from Kraus and Frazier [357] and lower reactions from Kato*, et al.* [355]

Gunstone [295] synthesised a dihydroxy acid from vernolic acid obtained from the oil extracted from *Vernonia anthelmintica* seeds. As a consequence of the high reactivity of the epoxy group in vernolic acid **(5)**, in the presence of a weak acid, such as acetic acid, oxirane ring opening occurs quickly, before the basic hydrolysis, leading to the formation of the dihydroxy-acid **(17)** (70% yield).

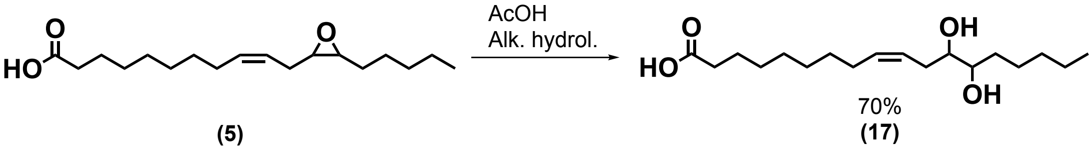

Figure 5.8 – Synthesis of a dihydroxy acid, from vernolic acid, by treatment with a weak acid before the basic hydrolysis reported by Gunstone.[295]

5.2.4.1.2. Oxidation of epoxides into aldehydes

The C–C bond cleavage of epoxides with periodic acid (HIO_4) or metaperiodic acid (H_5IO_6) has been studied in organic synthesis (Figure 5.9).[358-360]

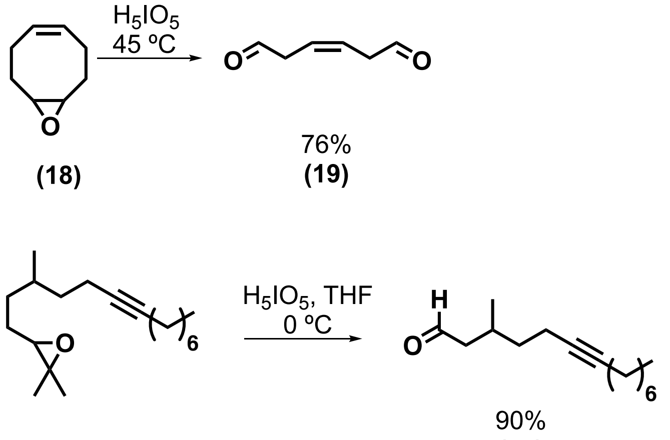

(18) (19) (20) (21)

Figure 5.9 – Synthesis of aldehyde compounds from epoxides.

The proposed mechanism for the oxidation of epoxides with periodic acid is still uncertain. However, some authors proposed a possible mechanism in which there is the formation of a periodate complex of the epoxide and subsequent cleavage as illustrated below (Figure 5.10).

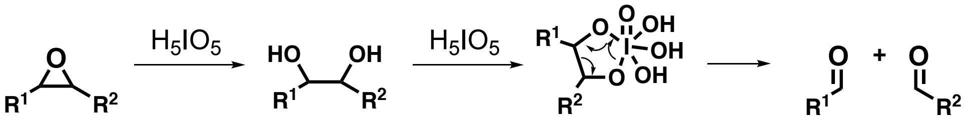

Figure 5.10 – Possible mechanism for the oxidation of an epoxide, with periodic acid, leading to the formation of aldehydes.

Binder*, et al.* [361] studied the one-pot cleavage of C–C bonds of several epoxides, in the absence of catalyst, leading to the formation of aldehydes. The authors conclude that the epoxide opening is the rate-limiting step of the reaction and that tri-substituted epoxides generally gave aldehydes in higher yields compared to mono-substituted epoxides (Figure 5.11). This effect might be due to the ease of epoxide hydrolysis. Less reactive compounds **(22)**, **(24)** and **(26)** required at least 4-5 equivalents of periodate to facilitate full consumption of starting materials. The oxidation of the tri-substituted epoxide **(30)** in the presence of THF/H_2O gave the highest yield (91%).

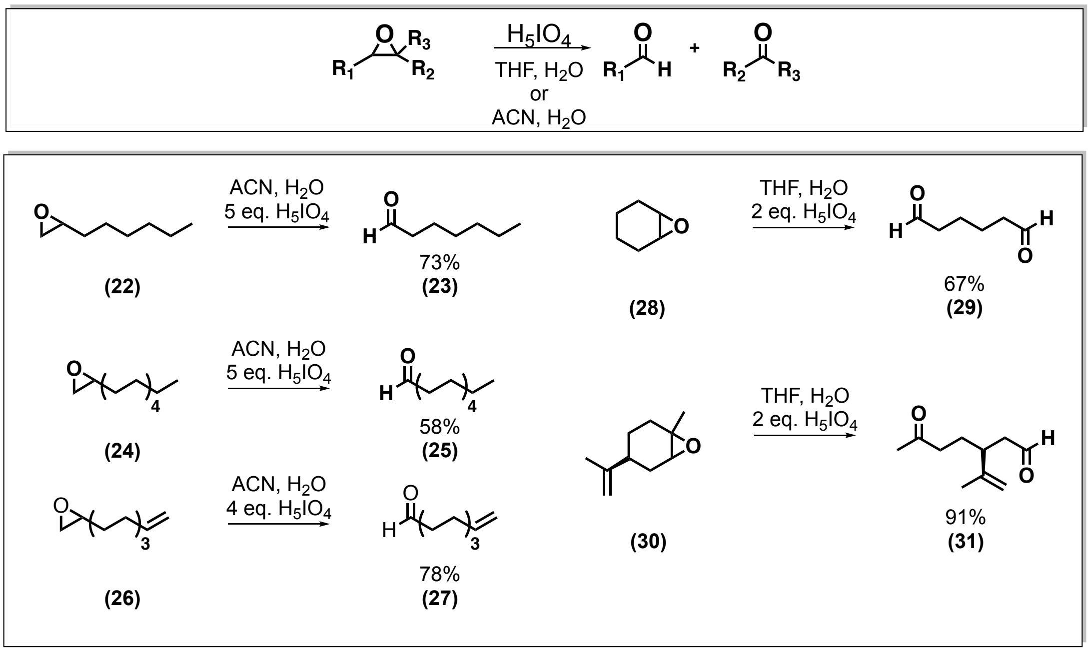

Figure 5.11 – Oxidative cleavage of aliphatic epoxides with periodic acid in tetrahydrofuran/water or acetonitrile/water.[361]

Also Gunstone [295] synthesised aldehydes by the use of periodate compounds. Nevertheless, he treated compound **(17)** with periodate leading to the formation of compound **(32)** (volatile aldehyde) and **(33)** (solid aldehyde-acid).

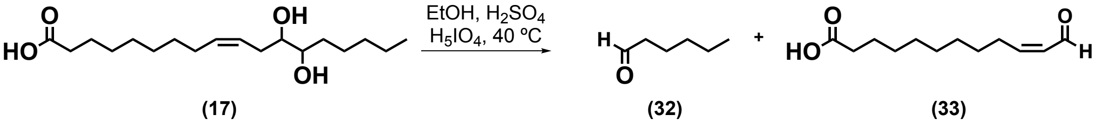

Figure 5.12 – Synthesis of aldehydes from the treatment of dihydroxy-acid **(4a)** with periodic acid.[295]

5.2.4.1.3. The synthesis of dicarboxylic acids from aldehydes

Oxidising aldehydes into carboxylic acids (Figure 5.13) is a well-studied reaction because carboxylic acids are known to be some of the most valuable intermediates and precursors for chemical productions and pharmaceuticals (such as to prepare antibacterial compounds).[362-363] In addition to these applications, the synthesis of new dicarboxylic acids would give great opportunities for new polycondensation reactions with diols, leading to the formation of new materials.

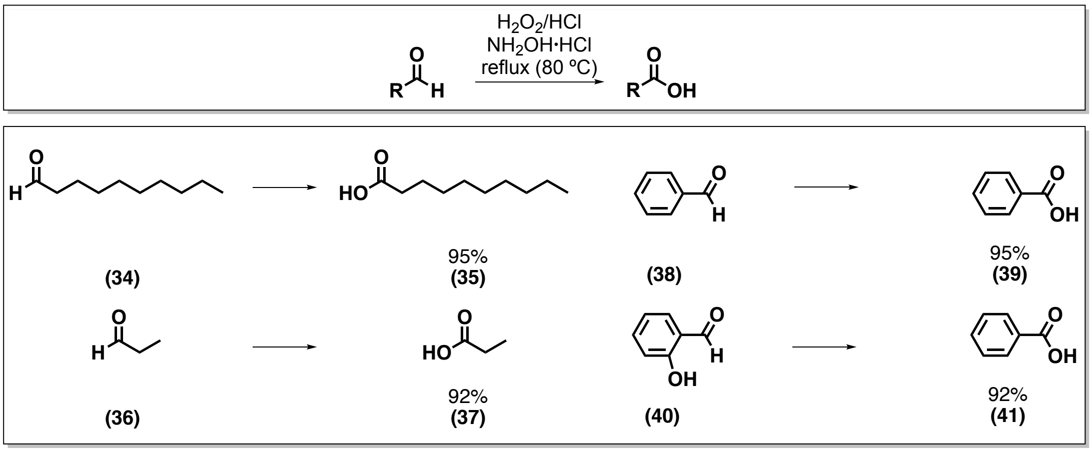

Figure 5.13 – Synthesis of carboxylic acid from aldehyde upon treatment with H_2O_2/HCl in the presence of hydroxylamine hydrochloride ($NH_2OH{\cdot}HCl$) as a method to oxidise the aromatic or aliphatic aldehyde, in acetonitrile (ACN).[364]

Bahrami*, et al.* [364] studied the synthesis of a variety of carboxylic acids from different aldehydes in high yields. In this work, H_2O_2/HCl was used in the presence of hydroxylamine hydrochloride ($NH_2OH{\cdot}HCl$) as a method to oxidise aromatic and aliphatic aldehydes.

Kon*, et al.* [365] studied the palladium(II)-catalysed oxidation of ***α***,***β***-unsaturated aldehydes, in the presence of hydrogen peroxide, to give ***α***,***β***-unsaturated carboxylic acids (Figure 5.14). Using hydrogen peroxide is the key to this work, since the only by-product of these reactions is water. In addition, the authors proved that this method is scalable, performing the oxidation of aldehyde **(44)** at a 10 g scale, maintaining the yield high (74%).

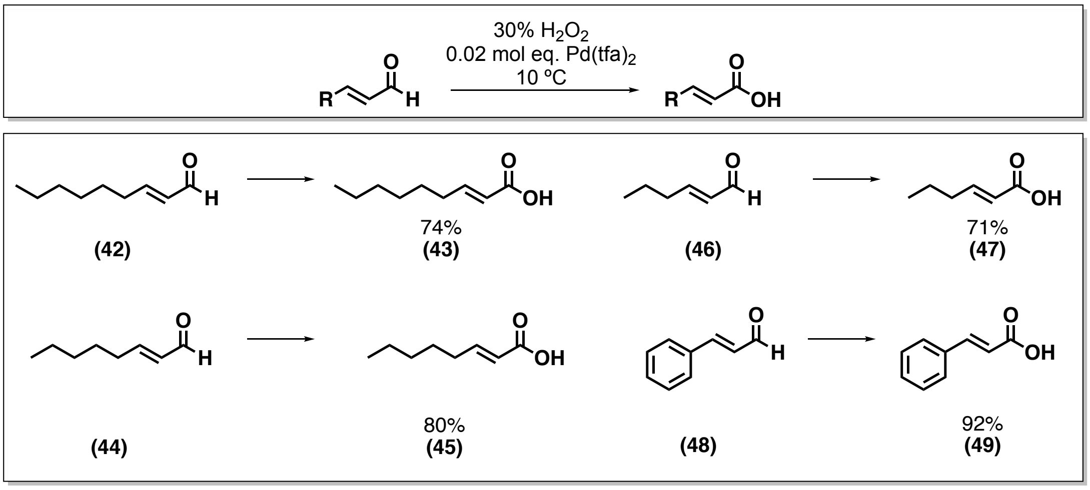

Figure 5.14 – Oxidation of various ***α***,***β***-unsaturated aldehydes with hydrogen peroxide, catalysed by $Pd(tfa)_2$.[365]

Tanaka, *et al.* [366] also studied the iron-catalysed oxidation of ***α***,***β***-unsaturated aldehydes to ***α***,***β***-unsaturated carboxylic acid using O_2 as the oxidant agent (Figure 5.15). Molecular oxygen is a readily available and inexpensive oxidant and would keep the oxidation with 100% atom efficiency, generating no waste. The key for a successful conversion to ***α***,***β***-unsaturated carboxylic acid lies in the alkali metal carboxylate additive used, since it enhances the selectivity of the Fe catalyst used. Higher yields and selectivity were obtained when salts containing larger monocations were added (CH_3COONa and CF_3COOK) whilst the addition of Zn salt ($(CF_3COO)_2Zn$) was less effective. In addition, there was no formation of products in the absence of the catalyst.

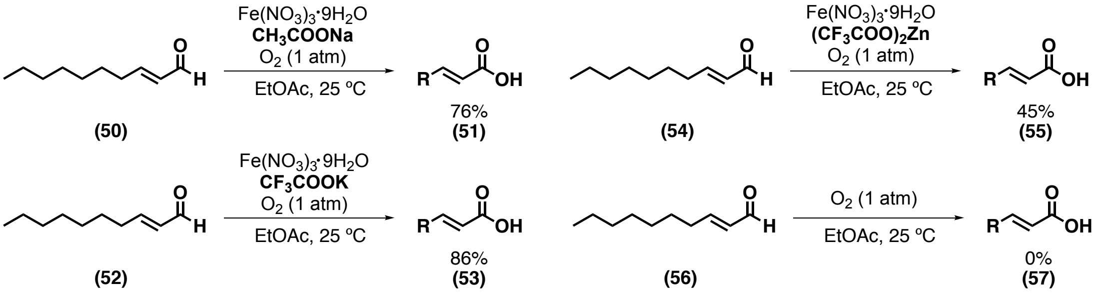

Figure 5.15 – Oxidation of *trans*-2-decenal **(25)** in the presence of a combination of O_2 and a Fe catalyst, whose catalytic activity is induced by the simple addition of alkali metal carboxylate (CH_3COONa, CF_3COOK and $(CF_3COO)_2Zn$).[366]

5.2.4.1.4. The synthesis of primary alcohols from carbonyl compounds

The reduction of carbonyl compounds into alcohols has been widely studied in the literature and it is well known that aldehydes are readily reduced by hydride agents, such as lithium aluminium hydride ($LiAlH_4$) and sodium borohydride ($NaBH_4$). Nystrom and Brown [367] studied the transformation of heptaldehyde **(58)** to heptyl alcohol **(59)** using $LiAlH_4$ obtaining high yield (86%, Figure 5.16).

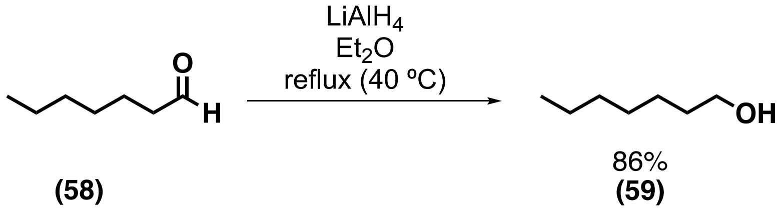

Figure 5.16 – Synthesis of a primary alcohol from an aldehyde, using $LiAlH_4$ and ether as solvent.[367]

Chapuis [368] performed the reduction of a more complex aldehydes (**(60)** and **(62)**) into primary alcohols, also using $LiAlH_4$. Both reactions occurred readily achieving high yields.

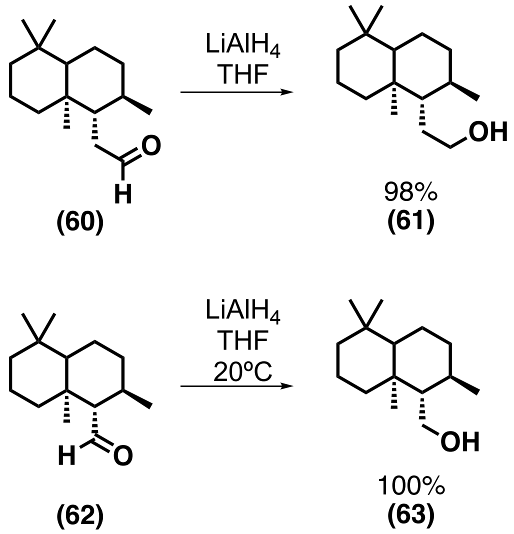

Figure 5.17 – Synthesis of more complex alcohols from aldehydes, using $LiAlH_4$.

5.3. Aims of the study

The aim of this study is to synthesise new monomers from vernolic acid present in *Vernonia galamensis* oil, to be further polymerised through polycondensation (which will be discussed in Chapter 6).

Initially, this work will focus on the extraction of the oil from *V. galamensis* seeds using $scCO_2$. $scCO_2$ was previously shown to be a better solvent for oil extraction than organic solvents because of its 'greenness'. In this study, the focus is to determine whether the extraction of VO from *Vernonia galamensis* seeds can benefit from the use of $scCO_2$ in terms of reducing downstream purification steps to obtain pure VA. Finally, the functionalisation of vernolic acid towards the synthesis of new monomers will be investigated.

5.4. Experimental

5.4.1. Materials

Clean and dried *Vernonia galamensis* seeds were supplied from Addis Ababa University, Ethiopia. Sodium hydroxide, *tert*-butyl alcohol and potassium hydroxide were obtained from Fisher and used as received. All the solvents used in this session (methanol, glacial acetic acid, *n*-hexane, tetrahydrofuran, dichloromethane and ethyl acetate) were obtain from Sigma-Aldrich and used as received. Periodic acid (99%) and hydrogen chloride were obtained from Alfa Aesar and used as received. Palladium(II) trifluoroacetate was obtained from Sigma-Aldrich and used as received. Glacial acetic acid, obtained from VWR, was used as received. *n*-butyllithium (*n*-BuLi) was obtained by Acros Organics and used as received. Lithium diisopropylamide (LDA) was prepared from *n*-BuLi and diisopropylamine (99.9%, Acros Organics) following literature procedures.[369] Carbon dioxide grade 4 (minimum purity 99.99%) was purchased from BOC special Gases (UK) and used as received. Carbon dioxide, food grade (99.90%), was purchase from Beer gas Cymru. Air- and moisture-sensitive materials were manipulated under argon or nitrogen using syringe and Schlenk techniques.

5.4.2. Synthesis methods

5.4.2.1. Conventional extraction of vernonia oil and its treatment

5.4.2.1.1. Soxhlet extraction

Soxhlet extraction uses organic solvents. This apparatus has 3 compartments (Figure 5.18). To extract the oil from 5 g of *Vernonia galamensis* ground seeds (griding process with a coffee grinder, Krüpss^{TM}), *n*-hexane (250 mL) was used at *ca.* 80 ºC. The vapour (from the heated solvent) is condensed and channelled into the Soxhlet extractor. Once the organic solvent in the extractor reaches the overflow level, a siphon unloads the organic solvent-lipids mixture back into the round-bottom flask. This cycle is repeated for 9 h, to guarantee no more lipids can be extracted from the residue. To obtain the oil (1.9 g, 95% of extraction efficiency) the solvent is removed under reduced pressure.

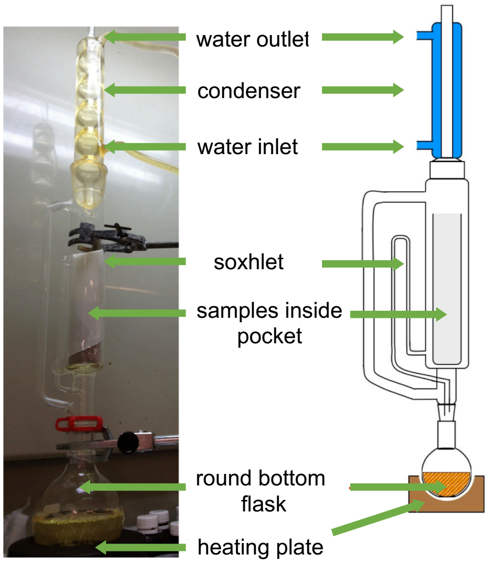

Figure 5.18 – Soxhlet extraction apparatus.

5.4.2.1.2. Oil treatment

5.4.2.1.2.1. Bleaching

To remove pigments, the oil (5 g of VO extracted by soxhlet) was mixed with 5 to 8 wt.% of activated charcoal at 60 ºC with continuous stirring for one hour. The bleached oil (85%, 4.25 g) was then isolated by hot filtration.

5.4.2.1.2.2. Degumming

This process removes impurities in the colloidal state. The bleached oil (4.25 g) was mixed with 2.5 to 5 wt.% of distilled water at 60-70 ºC for one hour, followed by centrifugation at 5,000 rpm. The phases were separated and the oil (80%, 3.4 g) was dried at 60 ºC on a rotary evaporator.

5.4.2.1.2.3. Neutralisation

The degummed oil was neutralised by the addition of an alkali solution. Thus, degummed vernonia (3.4 g) oil was mixed with sodium hydroxide solution (5 wt.% of 0.1 M NaOH) and then heated to 40 ºC followed by stirring for 30 min. Afterwards, the suspension was passed through the centrifugal separator, separating the soap from the neutral oil. The oil fraction (85%, 2.89 g) was dried for one hour on a rotary evaporator at 60 ºC.

5.4.2.2. Supercritical carbon dioxide extraction of vernonia oil

To process the extraction of the oil by $scCO_2$ (Figure 5.20), different milling processes of *Vernonia galamensis* seeds were evaluated, to understand if the grindding would affect the oil extraction. Thus, it was studied three different equipments (Figure 5.19): common coffee grinder (Krupps^{TM}), cross beater mill (Glen Creston Ltd.), in which the seeds passed through a 0.5 mm screen and a BDC Ltd. roller mill, in which the seeds passed through a 2.5 mm screen.

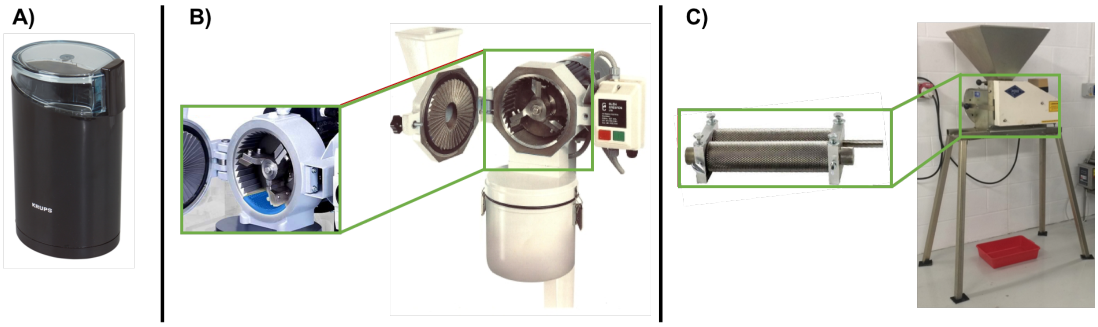

Figure 5.19 – Apparatus to mill *Vernonia galamensis* seeds: A) coffee grinder (Krupps^{TM}), B) cross beater mill (Glen Creston Ltd.) and C) roller mill (BDC Ltd.).

Approximately 600 g of milled seeds were extracted using a Thar SFE 500 system (Thar technologies). The seeds were loaded into the extractor and the CO_2 (Beer gas Cymru food grade) was previously liquefied through a cooling unit (Fisher Scientific Isotemp). The liquid CO_2 was delivered to the pre-heater and converted into a supercritical fluid prior to entering the extractor. The temperature, pressure and flow-rate were selected according to the experiment (Table 5.2). The maximum extraction time was 5h30m. Samples were collected every 30 min throughout the course of the extraction. The extracts were all collected at 40 ºC and at atmospheric pressure in the separator.

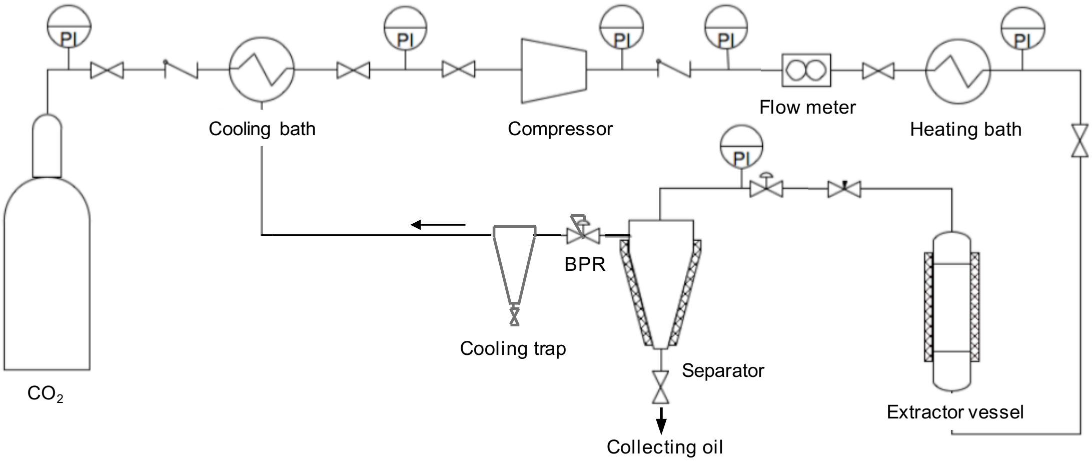

Figure 5.20 – Schematic representation of the high-pressure apparatus for oil extraction. *Note*: PI = pressure indicator, BPR = back pressure regulator.

5.4.2.3. Hydrolysis of oil

50 mL MeOH and 5 g (0.12 mol) NaOH were transferred to a 250 mL distilling flask, equipped with a magnetic stirrer bar. The flask was then fitted with a condenser, and the mixture heated to reflux until complete dissolution of the sodium hydroxide. To the hot alkaline solution 5.12 g (5.5 mmol), of vernonia oil was added. The resulting brown solution was refluxed with continuous stirring for 10 min, after which it was immediately transferred into a beaker. 100 g ice was added, mixed thoroughly, followed by the addition of 100 mL water while mixing. The cold mixture was filtered under vacuum to afford an off-white solid soap in the filter bed. The soap was transferred into a beaker and mixed with another 100 g ice and 100 mL water and then acidified with 4 mL glacial acetic acid. The acidified mixture was filtered under vacuum immediately to produce a white solid. The cold white solid was transferred into a beaker, containing 100 mL hexane, and after dissolution the resulting mixture was transferred in to a funnel and the phases were separated. The organic layer was dried with $MgSO_4$ and, afterwards, the hexane was removed under reduced pressure to afford crude vernolic acid. Purification of the vernolic acid was accomplished by low-temperature recrystallization. Hexane (50 mL) was added to a 150 mL beaker containing the crude VOAC and the beaker was placed on dry ice. The resulting solid was filtered under vacuum and rinsed with an additional 50 mL of cold hexane to give pure vernolic acid (90%, 4.6 g).

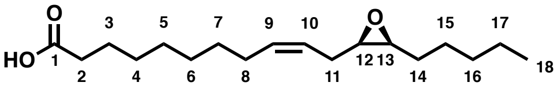

^{1}H-NMR (400 MHz, $CDCl_3$) δ 5.58 – 5.46 (1H, m, H-9), 5.47 – 5.35 (1H, m, H-10), 2.93 (2H, m, *J* 7.4, 4.1 Hz, H-12,13), 2.34 (2H, t, *J* 7.5 Hz, H-2), 2.18 (1H, m, *J* 14.3, 6.6 Hz, H-11), 2.03 (2H, q, *J* 7.0 Hz, H-8), 1.63 (2H, q, *J* 7.4 Hz, H-14), 1.58 – 1.23 (16H, m, H-3, 4, 5, 6, 7, 15,16,17), 0.97 – 0.85 (3H, t, *J* 7.4 Hz, H-18); ^{13}C-NMR (100 MHz, $CDCl_3$) δ 179.5 (C-1), 132.7 (C-9), 124.1 (C-10), 57.4 (C-12 or 13), 56.8 (C-12 or 13), 34.1 (C-2), 31.9, 29.6, 29.3, 29.2, 29.1, 27.9, 27.5, 26.4, 26.4, 24.8 (C-3), 22.7, 14.2 (C-18). HRMS (ESI+) m/z $[M+Na]^+$ calcd. for $C_{18}H_{32}NaO_3^+$ 319.2244; found 319.2249.

5.4.2.4. Synthesis of vernolic acid-based monomers

5.4.2.4.1. Synthesis of (S,9Z,11E)-13-hydroxyoctadeca-9,11-dienoic acid

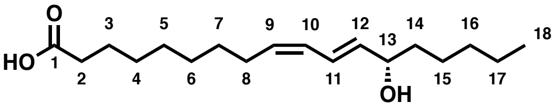

To a solution of diisopropyl amine (40.5 mmol) in dry THF (20 mL) cooled to - 78 ºC, *n*-BuLi in hexane (2.2 M, 37.1 mmol, 17 mL) was added dropwise *via* a dropping funnel, followed by rinsing with THF (5 mL). The reaction mixture was warmed to 0 ºC for 30 min while stirring. Vernolic acid (16.8 mmol, 4.98 g) in THF (150 mL) was added dropwise over 1 h, rinsing the dropping funnel with THF (10 mL). The reaction mixture was stirred for 1 h. Upon completion (TLC), the reaction mixture was quenched with NH_4Cl (sat. aq.), added dropwise at 0 ºC. The organic layer was separated and the aqueous layer was washed with dichloromethane (3 x 50 mL). The combined organic fractions were washed with HCl (2 M, 50 mL) and dried with $MgSO_4$ and the solvent was removed under reduced pressure, yielding (S,9Z,11E)-13-hydroxyoctadeca-9,11-dienoic acid as a yellow low melting solid (4.94 g, 16.7 mmol, 99% yield); ^{1}H-NMR (400 MHz, $CDCl_3$) δ 6.48 (1H, m, *J* 15.2, 11.1, 1.2 Hz, H-11), 5.97 (1H, t, *J* 11.0, 1.1 Hz, H-10), 5.66 (1H, dd, *J* 15.2, 6.8 Hz, H-12), 5.43 (1H, dt, *J* 10.8, 7.6 Hz, H-9), 4.17 (1H, q, *J* 6.1 Hz, H-13), 2.33 (2H, t, *J* 7.4 Hz, H-2), 2.17 (2H, q, *J* 9.8, 7.4, 4.1, 2.4 Hz, H-8), 1.62 (2H, m, *J* 7.4 Hz, H-3), 1.53 (2H, m, H-14), 1.42 – 1.34 (2H, m, H-7), 1.34 – 1.24 (12H, m, H-4,5,6,15,16,17), 0.92 – 0.84 (3H, t, *J* 7.4 Hz, H-18); ^{13}C-NMR (100 MHz, $CDCl_3$) δ 179.5 (C-1), 135.8 (C-12), 132.9 (C-9), 128.0 (C-10), 126.0 (C-11), 73.1 (C-13), 37.4 (C-14), 34.1 (C-2), 31.9, 29.5, 29.0, 29.0, 29.0, 27.7 (C-8), 25.2 (C-7), 24.8 (C-3), 22.7, 14.2 (C-18); HRMS (ESI+) m/z $[M+Na]^+$ calcd. for $C_{18}H_{32}NaO_3^+$ 319.2249; found 319.2244.

5.4.2.4.2. Synthesis of (12S,13S,Z)-12,13-dihydroxyoctadec-9-enoic acid

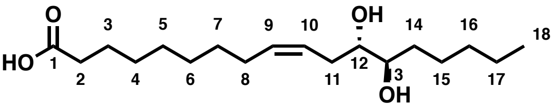

Vernolic acid (7.4 mmol, 2.19 g) was dissolved in glacial acetic acid (50 mL) and heated to 95 ºC for 24 h. The glacial acetic acid was removed under vacuum and the residue was taken up in MeOH (80 mL) and 3.7 M KOH (74.2 mmol, 4 g) and the resulting mixture was stirred for 1 h. Hydrochloric acid (2 M) was added until a pH of 4 was achieved, the product was extracted with diethyl ether (4 x 25 mL), dried with $MgSO_4$, filtered and the solvent removed under reduced pressure to yield the crude product as an orange oil (2.52 g). The product was dissolved in a 20% ethyl acetate in petroleum ether and precipitated by cooling to -78 ºC. The product was filtered at -78 ºC and rinsed with petroleum ether (3 x 25 mL) at -78 ºC, to give the (12S,13S,Z)-12,13-dihydroxyoctadec-9-enoic acid as a white solid (1.54 g, 4.90 mmol, 66%); ^{1}H NMR (400 MHz, $CDCl_3$) δ 5.62 – 5.53 (1H, m, H-9), 5.42 (1H, t, J 10.9, 8.2, 1.5 Hz, H-10), 3.48 (2H, ddt, J 5.8, 4.1, 2.9 Hz, H-12,13)), 2.34 (2H, t, J 7.3 Hz, H-2), 2.32 – 2.24 (2H, m, H-11), 2.10 – 2.00 (2H, m, H-8), 1.64 (2H, q, J 7.2 Hz, H-3), 1.53 – 1.45 (2H, m, H-14), 1.41 – 1.24 (14H, m, H-4,5,6,7,15,16,17), 0.92 – 0.85 (3H, m, H-18); ^{13}C NMR (100 MHz, $CDCl_3$) δ 179.0 (C-1), 133.8 (C-9), 124.9 (C-10), 74.1 (C-12 or 13), 74.0 (C-12 or 13), 33.9, 32.0, 31.9, 29.4, 29.0, 28.9, 27.4 (C-8), 25.5 (C-14), 24.8 (C-3), 22.8, 14.2 (C-18); HRMS (ESI+) m/z [M+Na]+ calcd. for $C_{18}H_{34}NaO_4^+$ 337.2355; found 337.2345.

5.4.2.4.3. Synthesis of (E)-12-oxododec-10-enoic acid

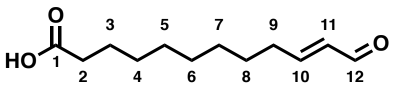

To a solution of Vernolic acid (6.75 mmol, 2 g) dissolved in THF (20 ml) and H_2O (20 ml), H_5IO_6 (13.49 mmol, 3 g) was added in one portion and stirred for 72 hours. Upon completion, the product was extracted into diethyl ether (3 x 20 ml) and the combined organic extracts were rinsed with brine (20 ml), dried over $MgSO_4$, filtered and the solvent removed under reduced pressure to yield the crude product as a yellow oil. The product was isolated by column chromatography using silica (PE 60%/EtOAc 40%) (4.34 mmol, 920 mg, 64%, yellow oil); ^{1}H NMR (400 MHz, $CDCl_3$) δ 9.45 (1H, d, *J* 7.92 Hz, H-12), 6.83 (1H, dt, *J* 15.6, 6.8 Hz, H-10), 6.09 (1H, ddt, *J* 15.6, 7.9, 1.5, H-11), 2.25-2.33 (2H, tdt, *J* 5.88, 3.59, 1.99 Hz, H-9), 1.65-1.20 (12H,m, H-3, 4, 5, 6, 7, 8); ^{13}C NMR (100 MHz, $CDCl_3$) δ 194.53 (12), 179.71 (1), 159.35 (10), 132.95 (11), 34.11, 34.07, 32.74, 28.98, 28.93, 28.90, 27.76, 26.94, 24.63.

5.4.2.4.4. Synthesis of (E)-dodec-2-enedioic acid

Procedure A

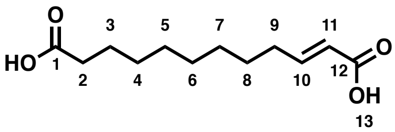

To a suspension of $Fe(NO_3)_3 \cdot 9H_2O$ (0.2 g, 0.01 mmol) and CF_3COONa (27.2 mg, 0.20 mmol) in ethyl acetate (0.6 mL), (*E*)-12-oxododec-10-enoic acid (0.2 g, 0.94 mmol), was added, under an atmosphere of oxygen. After stirring for 40 h at 25 ºC, ethyl acetate (3.66 mL) and 1 M HCl (1.22 mL) were added. $Na_2S_2O_4$ (sat. aq.) was added to the organic phase to quench residual peroxide. The product was extracted with Na_2CO_3 (sat. aq.; 3 x 1.22 mL). The aqueous phase was acidified with concentrated HCl. The dicarboxylic acid product was extracted with CH_2Cl_2 (3 x 1.22 mL) and the solvent was removed under reduced pressure, to give the crude title product as pale-yellow liquid. HRMS (ESI+) m/z [M+Na]$^+$ calcd. for $C_{12}H_{20}NaO_4^+$ 251.1259; found 251.1259.

Procedure B

A mixture of (*E*)-12-oxododec-10-enoic acid (200 mg, 0.94 mmol) and Pd(tfa)$_2$ (6.26 mg, 0.02 mmol) was vigorously stirred at 10 ºC for 10 min. 1.8 mmol of aqueous 30% H_2O_2 (% v/v) was added dropwise over 1 h. The mixture was stirred at 10 °C for 2 h and the reaction was monitored until completion (TLC). The organic phase was separated and washed with $Na_2S_2O_3$ (sat. aq.). The crude material was purified by silica gel column chromatography (PE 60%/EtOAc 40%) to give the title compound as pale yellow product (yield = 33%). HRMS (ESI+) m/z [M+Na]$^+$ calcd. for $C_{12}H_{20}NaO_4^+$ 251.1259; found 251.1259.

5.4.2.4.5. Synthesis of dodec-2-ene-1,12-diol

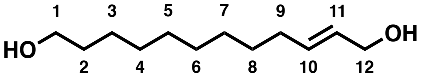

To a solution of the (E)-12-oxododec-10-enoic acid (100 mg, 0.471 mmol) in Et_2O (5 mL) at 0 ºC, a suspension of $LiAlH_4$ (53.7 mg, 1.4 mmol, 3 eq.) in Et_2O (5 mL) was added over 15 minutes. The reaction was quenched with a saturated aqueous solution of Rochelle's salts, stirred for one hour and extracted into dichloromethane (3 x 5 mL). The organic extracts were combined and dried over $NaSO_4$ and the solvent was removed under reduced pressure to give the product as a colourless oil (84 mg, 89%); ^{1}H NMR (400 MHz, $CDCl_3$) δ 5.70 – 5.50 (2H, m, H-10,11), 4.06 – 3.99 (2H, m, H-12), 3.57 (2H, t, J = 6.7 Hz, H-1), 1.94 – 2.03 (2H, m, H-9), 1.58 – 1.45 (2H, m, H-2), 1.38 – 1.17 (12H, m, H-3,4,5,6,7,8); ^{13}C NMR (100 MHz, $CDCl_3$) δ 133.26 (C-10), 128.99 (C-11), 63.65 (C-12), 62.88 (C-1), 32.74 (C-9), 32.21, 29.42, 29.38, 29.12, 29.06, 25.75.

5.4.3. Vernonia oil characterisation

Vernonia oil was characterised using GC and NMR, previously described in detail in Chapter 2.

5.4.4. Characterisation of vernonia-based monomers

Vernonia-based monomers were characterised using GC and NMR, previously described in detail in Chapter 2.

5.5. Results and discussion

5.5.1. Extraction of vernonia oil

Prior to the extraction, the seeds needed to be milled to make the oil accessible to the solvent (organic solvent or $scCO_2$). Thus, three different milling processes were used (Figure 5.21): a) using a common coffee grinder (Krupps^{TM}), in which the seeds are pulverised, b) cross beater mill (Glen Creston Ltd.), in which the seeds passed through a 0.5 mm screen and c) a roller mill (BDC Ltd.), in which the seeds passed through a 2.5 mm screen. From the milling process using the coffee grinder, in which it is not possible to control the size of the milled particles, the ground seeds resulted in a powder-like material. Therefore, most of the oil may adhere into the internal walls of the coffee grinder, leading to a loss of oil. Using the other two milling processes, it was possible to choose the thickness of the screen. The ideal milling process is the one in which the seeds are cut in half (roller mill) and not smashed (coffee grinder).

	Coffee grinder	**Cross beater mill**	**Roller mill**
Thickness screen	< 0.5 mm	0.5 mm	2.5 mm
Soxhlet extraction	✓	✗	✗
$scCO_2$ extraction	✓	✓	✓

Figure 5.21 – Appearance of *Vernonia galamensis* seeds after the milling processes.

The oil content of *Vernonia galamensis* seeds was determined by Soxhlet extraction, using *n*-hexane as a solvent, and the seeds were milled with a coffee grinder. An oil content of 40% was obtained which corresponds to a higher oil content than Grinberg*, et al.* [60] under similar conditions (38% oil). This further extraction of 2% of oil might be due to the origin where *Vernonia* *galamensis* sp. grown or the grinding process of the seeds. It is known that depending the local the plant grows, will result in different oil content.[292] The ironweed used in this work was grown in Ethiopia and the one used by Grinberg*, et al.* [60] was grown in Israel.

When performing the SFE, the extraction efficiency (EE, Equation 5.1) was determined using as the maximum accessible oil content the one determined by soxhlet, 40% $w/w_{\text{fresh seeds}}$:

$$\text{Extraction efficiency (EE, w/w)} = \frac{m_{\text{extracted oil}}}{0.40 \times m_{\text{fresh milled seeds}}} \times 100$$

Equation 5.1 – Determination of extraction efficiency.

The conditions for the SFE of VO are summarised below (Table 5.2). The oil extraction was carried out with a 1 L Thar SFE 500 extractor filled with ~ 650 g of milled seeds and samples were collected every 30 minutes, until complete extraction, *e.g*. until no oil was possible to collect.

Table 5.2 – Extraction conditions for VO from *Vernonia galamensis* seeds with $scCO_2$. *Note*: [a] The extraction efficiency is lower than expected due to a leak at the beginning of the extraction resulting in a loss of ~15% of oil.

Entry	**Milling process**	**$m_{\text{milled seeds}}$ (g)**	**$m_{\text{max oil}}$ (g)**	**Q_{CO2} (g/min)**	**$P_{bar}/T_{°C}$**	**EE (%)**
1	Coffee grinder	55.0	22.0	40	450/60	70.7
2	Cross beater mill	681.4	272.6	40	450/60	70.5
3	Roller mill	646.8	258.7	40	450/60	80.2
4	Roller mill	660.7	264.3	60	450/60	68.3[a]

The extraction time and efficiency were very similar irrespective of the milling process (Figure 5.22). Using the coffee grinder and cross beater mill processes, with a CO_2 flow rate of 40 g/min, the EE was very similar, 70.7 and 70.5%, respectively. Whereas using the roller mill, at the same CO_2 flow rate, the EE% increased to 80.2%. This indicates that the milling process of the seeds is very important and confirms what we were expecting. Cutting the seed in half is a better option to make to oil accessible for extraction and, consequently, no oil is lost during the milling process.

To determine the extraction rate (Equation 5.2), it was considered the amount of oil extracted at the beginning of the extraction, at a certain time (90 minutes):

$$\text{Extraction rate } (g_{oil}/\text{min}) = \frac{\%\text{oil}_{\text{extracted at 90 min}}}{\text{extraction time, 90 min}}$$

Equation 5.2 – Determination of the extraction rate.

The CO_2 flow rate was increased to 60 g/min (entry 4, Table 5.2) to investigate whether a higher extraction rate could be obtained. When increasing the flow rate of CO_2, a larger amount of CO_2 is in contact with the seeds at any given time. Therefore, a larger amount of oil is extracted in less time.[370] The effect of the flow rate is shown below (Figure 5.23 and Figure 5.24). When using the same milling system to grind the seeds (roller mill process – using 40 and 60 g/min_{CO2}, entries 3 and 4 from Table 5.2, respectively), an increase of the extraction rate is observed, 0.42 and 0.65 g_{oil}/min respectively, which confirms that the higher the flow rate, the larger the amount of oil is extracted at a specific time.

Regarding the mass transfer model, it is possible to observe two different models: constant extraction rate (controlled by external mass transfer) and diffusion-controlled rate (governed by internal mass transfer). At the first instants of extraction (up to 120 min, Figure 5.22 A)), the extraction is governed by external mass transfer between the solvent ($scCO_2$) and the solid material (milled seeds). $scCO_2$ carries the easily accessible solute from the broken seeds during this phase. Therefore, at this period, it is possible to observe a constant extraction rate. After ≥ 150 min extraction time (Figure 5.22 B)), the extraction is controlled by the internal diffusion, which means the extraction occurs in the less accessible oil present in the seed. Hence, at this period, it is observed a diffusion-controlled rate extraction.

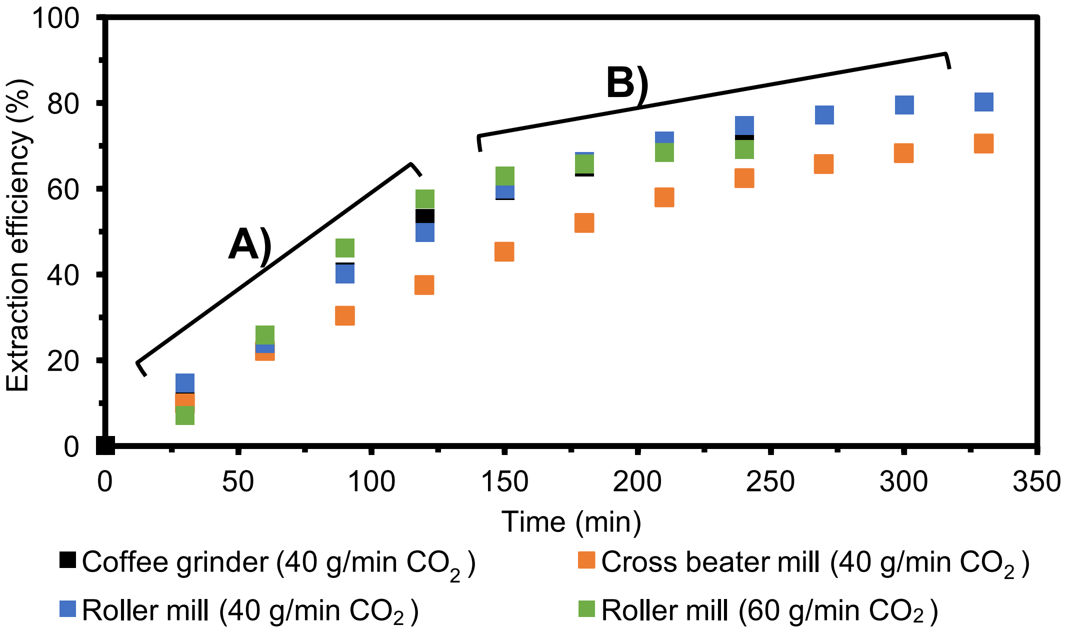

Figure 5.22 – Efficiency of oil extraction from *V. galamensis* seeds using $scCO_2$ for different milling processes and at a flow rate of CO_2 of 40 and 60 g/min_{CO2}. *Note:* A) corresponds to an extraction controlled by external mass transfer and B) internal mass transfer.

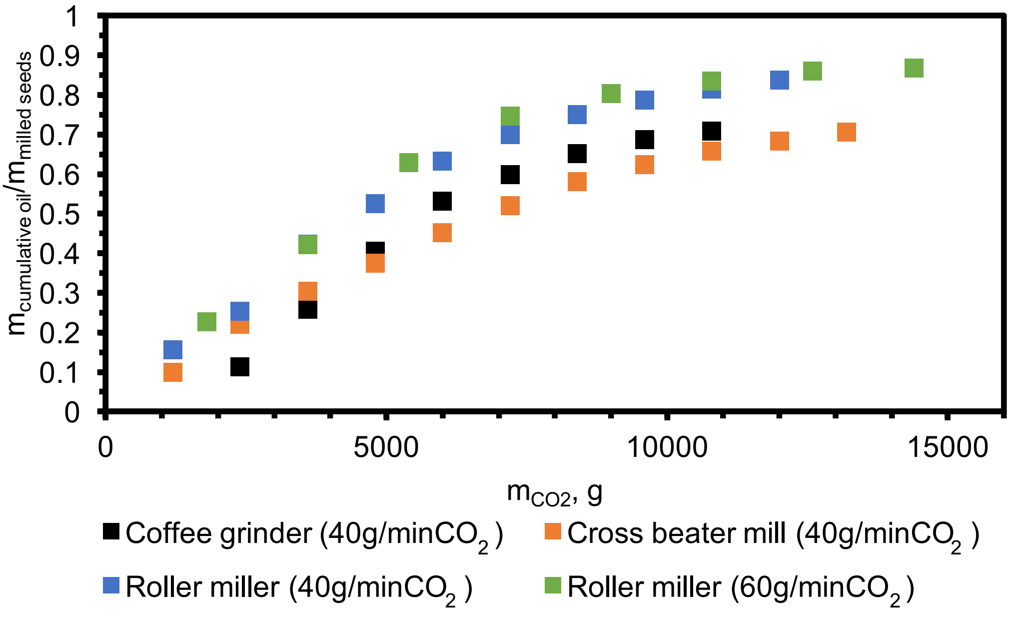

Figure 5.23 –Oil extracted using different milling processes and a flow rate of 40 or 60 g/min_{CO2} as a function of the total amount of CO_2 used (oil loading – amount of oil extracted at a giving amount of CO_2).

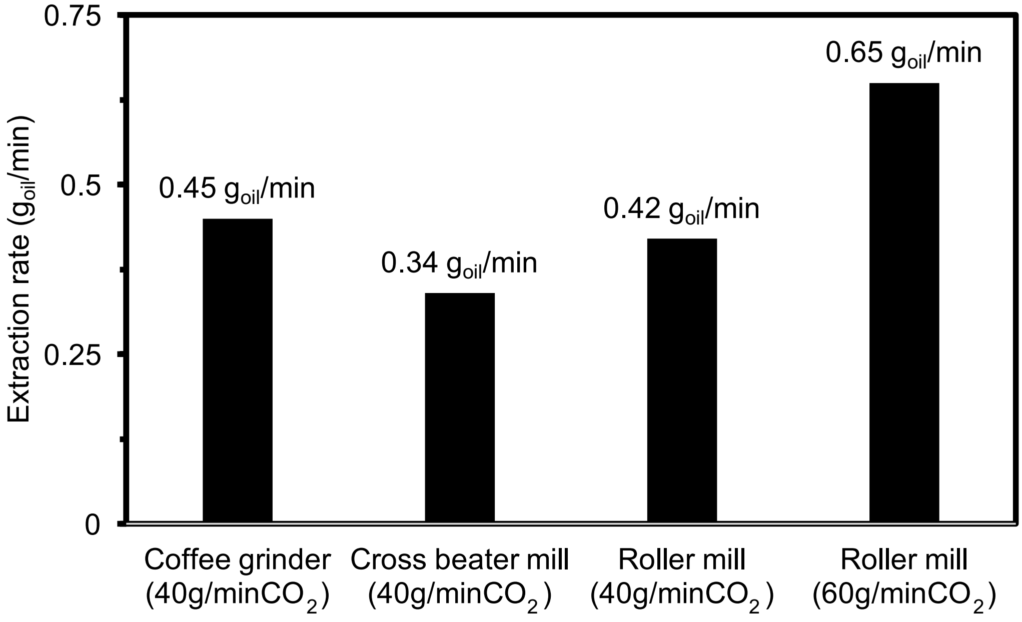

Figure 5.24 – Extraction rates obtained, and determined using Equation 5.2.

King*, et al.* [353] used higher temperatures, pressures and flow rate of CO_2 and confirmed that at a higher T ºC, P (bar) and amount of CO_2 extracted more quantity of oil. As it is possible to observe below (Table 5.3), using higher pressure and temperature, it is possible to extract a higher oil content at a specific amount of CO_2 due to the higher solubility of VO in $scCO_2$.

Table 5.3 – Oil content (%) obtained in this work, at 450 bar and 60 ºC, and in King*, et al.* [353] work, at 690 bar and 100 ºC, at a specific amount of CO_2. *Note:* the amount of extracted oil is lower than expected due to a leak at the beginning of the extraction resulting in a loss of ~15% of oil.

Amount of CO_2	**This work[a)]**	**King*, et al.* [353]**
60 g	–	17%
121 g	–	17.5%
182 g	–	16.5%
303 g	–	17%
363 g	–	**36%**
1,800 g	2%	–
5,400 g	18%	–
12,600 g	**31%**	–

The oil (FAME) was analysed by GC and the content of vernolic acid was *ca.* 79-80% for all SFEs. The composition of the oil is shown below (Table 5.4).

Table 5.4 – Fatty acid content in *Vernonia galamensis* oil extracted with *n*-hexane (soxhlet) and $scCO_2$ (w/w %).

	$scCO_2$	**soxhlet**
Palmitic acid	2.80 ± 0.3	2.9 ± 0.3
Linoleic acid	8.71 ± 0.6	10.0 ± 0.5
Oleic acid	3.95 ± 0.3	4.6 ± 0.2
Stearic acid	3.64 ± 0.2	0.7 ± 0.1
Vernolic acid	**79.26 ± 1.2**	**66.0 ± 0.5**
11-Eicosenoic acid	0.43 ± 0.1	0.4 ± 0.2
Arachidic acid	0.43 ± 0.1	0.5 ± 0.3
Others	< 0.01	10.1 ± 0.2

The fatty acid content in the oil is slightly different when extracted by *n*-hexane compared to $scCO_2$. This implied that at supercritical conditions, the solubility of triglycerides (with higher VA content) increased due to an increase in the solvent density, resulting in a higher yield of these fatty acids than with soxhlet extraction. This has been observed previously.[371-373] In addition, GC-MS analysis revealed that a larger fraction of other compounds is co-extracted when using Soxhlet extraction with *n*-hexane.

A slight decrease in VA content (~4%) with extraction time is observed (Figure 5.25), which could be due to the presence of wax towards to the end of the extraction.

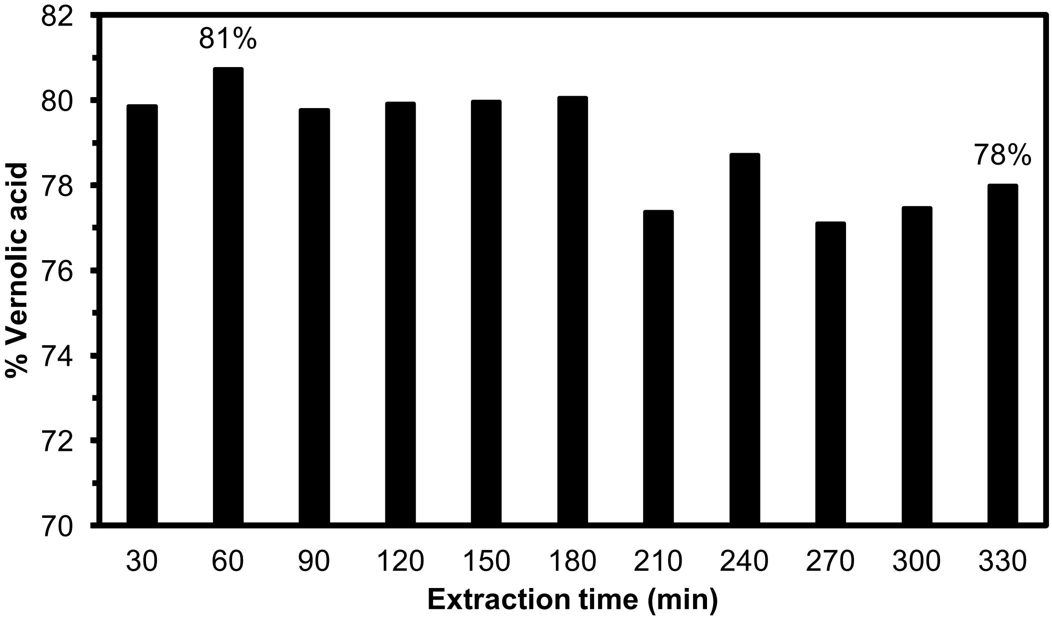

Figure 5.25 – Content of vernolic acid (according to GC analysis) in the oil from extraction no 2 (Table 5.2).

In the high-pressure apparatus for oil extraction, the separator, where the oil sample is collected, is followed by a cold trap (after back pressure regulator, BPR, Figure 5.20) to collect volatile compounds. When collecting samples every 30 minutes, some product was occasionally collected in the cold trap. The extraction at 60 g/min$_{CO2}$ (entry 4, Table 5.2), both the products collected in the separator and in the cold trap were analysed. However, both corresponded to vernonia oil of the same composition (Figure 5.26).

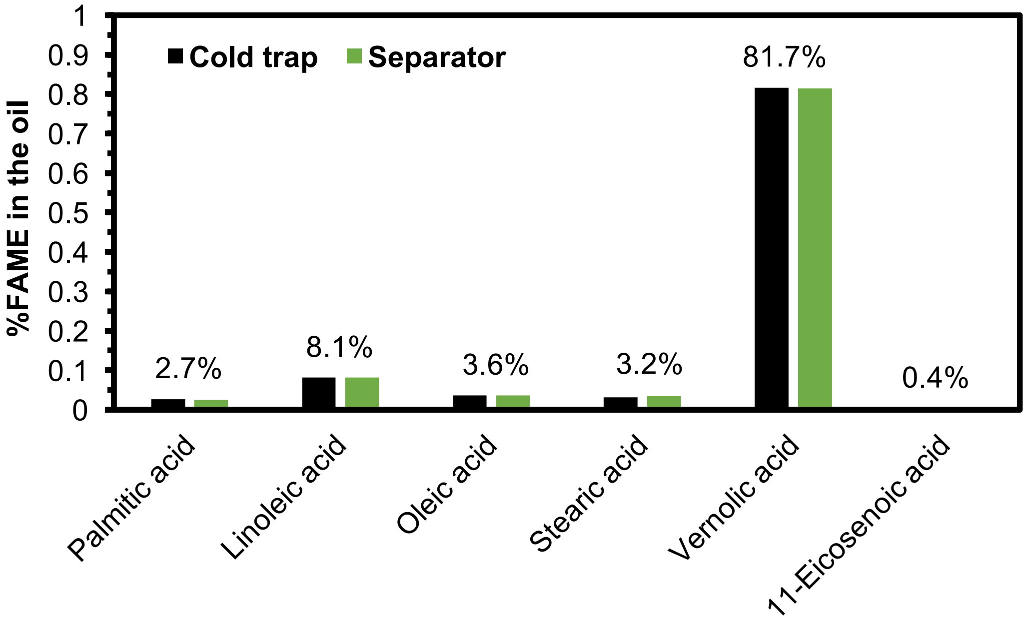

Figure 5.26 – Fatty acid content from the oil collected in the cold trap and the separator (entry 4, Table 5.2) after 75 minutes of extraction.

The SFE extracted oil is lime-green at the first minutes of extraction and dark-green at the end of the extraction (Figure 5.27). The dark-green colour might be due to the presence of wax and water.

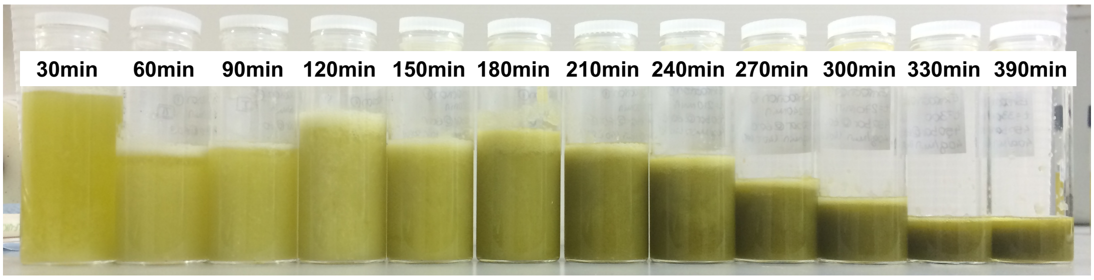

Figure 5.27 – Appearance of the collected oil during the course of the extraction.

After SFE, the residual milled seed particles have a different appearance. The residue from extraction of entry 4 (Table 5.2 and Figure 5.28 C) seemed to be drier than the other ones obtained from the extractions of entries 2 and 3 from Table 5.2 (Figure 5.28 A and B, respectively). A soxhlet extraction was performed using these seeds after CO_2 extraction and the oil content was less than 1% confirming that SFE was quantitative.

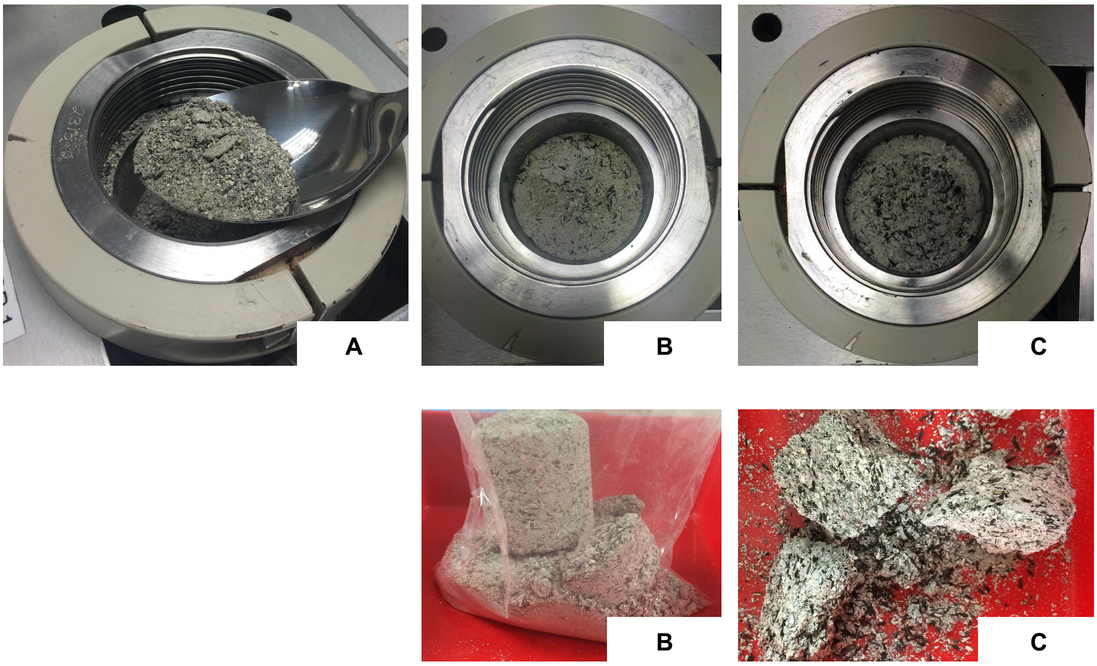

Figure 5.28 – *Vernonia galamensis* seeds after $scCO_2$ oil extraction. *Note:* A) entry 2 from Table 5.2; B) entry 3 from Table 5.2; C) entry 4 from Table 5.2.

Hence, considering the EE% obtained by $scCO_2$, *ca*. 80%, and that milder conditions are used, using an organic solvent has several disadvantages:

a) Organic solvents are hazardous
b) Costly and high-purity solvents are needed
c) Potential release of toxic emissions during extraction
d) Time-consuming procedure
e) Non-selective extraction
f) Extraction of other compounds than FA (*ca.* 10.1 w/w %)

Performing the extraction of oil from ~ 650 g seeds with supercritical carbon dioxide offers numerous advantages:

a) using milder conditions, 60 ºC and 450 bar; therefore, less energetic intensive
b) faster oil extraction (5h30m compared to 9 h with soxhlet)
c) extraction of only the lipid portion of the seeds, having only few other compounds then FA (< 0.01 w/w %)
d) extracted oil free of solvent

5.5.2. Isolation of vernolic acid

As mentioned previously (page 197), oil extraction with $scCO_2$ results in fewer or no impurities (< 0.01 w/w %) as compared to soxhlet extraction (~10.1 w/w%). This was quantified by GC-MS (Table 5.4) and NMR (Figure 5.29) analysis. Thus, no further purification prior to saponification was necessary for the oil extracted with $scCO_2$ and bleaching, degumming and neutralisation steps could be omitted.

The ^{1}H-NMR spectra of the oil obtained using soxhlet extraction and SFE using CO_2 is shown below (Figure 5.29). Resonances in the expanded region (in the orange box) shows for the presence of possible some impurities (such as pigments, colloids, fibres and proteins). Several studies have shown that using supercritical carbon dioxide to extract oil is a better choice due to the presence of few or no impurities since in $scCO_2$ proteins, polysaccharides, sugars and mineral salts are insoluble.[104]

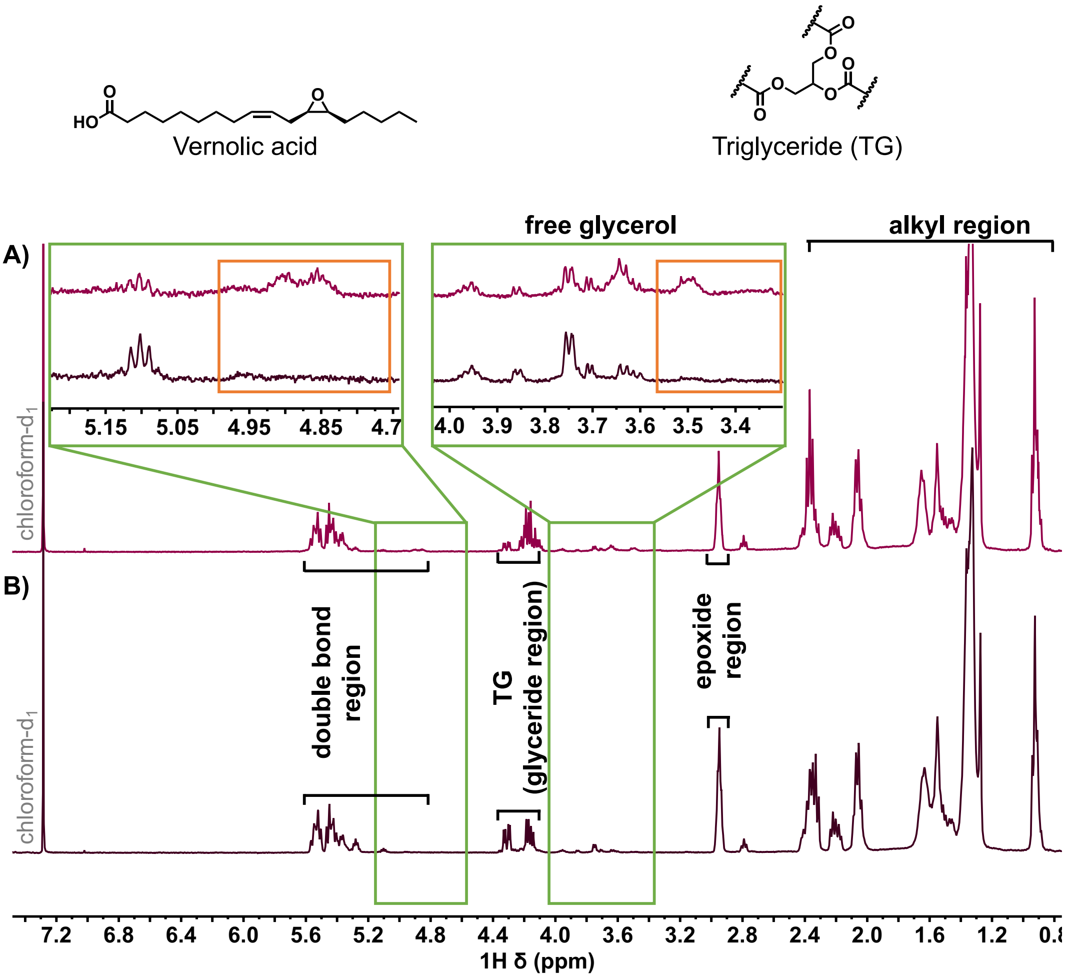

Figure 5.29 – ^{1}H-NMR spectra of the oil extracted using A) organic solvents (*n*-hexane, soxhlet; represented by the purple plot) and B) scCO$_2$ (represented by the black plot). The enlarged ^{1}H-NMR spectra show the region corresponding to resonances from free glycerol (*ca.* 4.0-3.6 ppm) and double bonds region (*ca.* 5.2-4.7 ppm). *Note:* in the orange box is highlighted the presence of some impurities in the soxhlet oil extraction.

The saponification procedure starts with an alkaline solution (sodium hydroxide in methanol) to hydrolyse the oil (triglycerides, TG), breaking the ester bond between glycerol and FA. The FAs and glycerol mixture were washed with water, to remove glycerol. Afterwards, a neutralisation step (addition of a weak acid, glacial acetic acid) is required in order to remove salts and have only FAs. Thus, the mixture was washed with *n*-hexane. Through low-temperature recrystallisation, pure vernolic acid was obtained. As shown below, low-temperature recrystallisation was essential to obtain pure vernolic acid (Figure 5.30). ^{1}H-NMR analysis showed that before low-temperature recrystallisation (Figure 5.30 A), impurities (presence of other FA) are present (highlighted in grey).

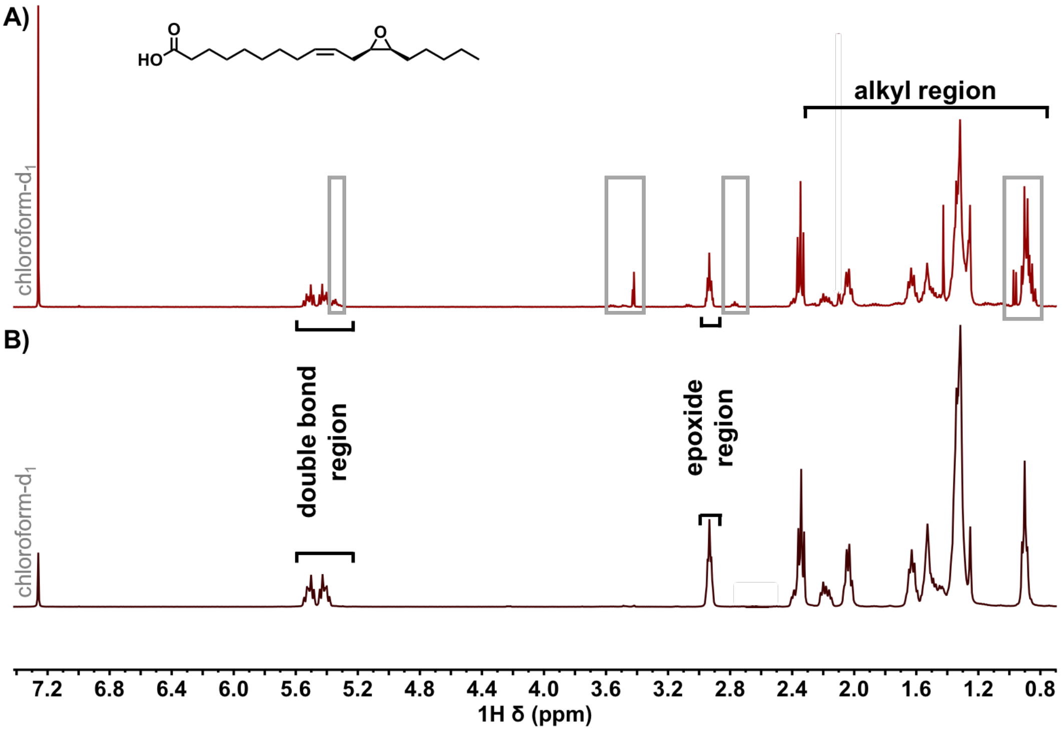

Figure 5.30 – ^{1}H-NMR spectra of the hydrolysis product of the oil extracted by scCO$_2$. A) crude product before low-temperature recrystallisation and B) pure vernolic acid after low-temperature recrystallisation. *Note*: in the grey rectangles highlight some impurities (other FA) present in the crude product, evidencing that the low-recrystallisation step is crucial to get pure VA.

^{1}H-NMR and COSY spectra of pure VA are shown below (Figure 5.31 and Figure 5.32, respectively), providing valuable information about H-H coupling. The coupling of protons H_f (*ca.* 5.54 ppm) and H_g (*ca.* 2.06 ppm) is evident from the COSY spectrum (grey dotted lines, Figure 5.32). The coupling between protons H_e (*ca.* 5.45 ppm) and H_d (*ca.* 2.22 ppm) is shown through the orange dotted lines. The purple dotted line labels the coupling between protons H_c (*ca.* 2.96 ppm) and H_d (*ca.* 2.22 ppm). The blue dotted line reveals the coupling between protons H_c (*ca.* 2.96 ppm) and H_b (*ca.* 1.66 ppm). In addition, it was possible to observe the coupling between protons H_f (*ca.* 5.54 ppm) and H_e (*ca.* 5.45 ppm). The coupling between protons from the alkyl region is not highlighted. However, proton H_a reveals a chemical shift at 0.93 ppm. The integration of the ^{1}H-NMR spectrum (Figure 5.31) confirms the purity of the VA. In MS, a peak at +319.22 m/z is observed which corresponds to vernolic acid ionised with Na^{+} (VA = 296.24 g/mol; Na^{+} = 22.98 g/mol).

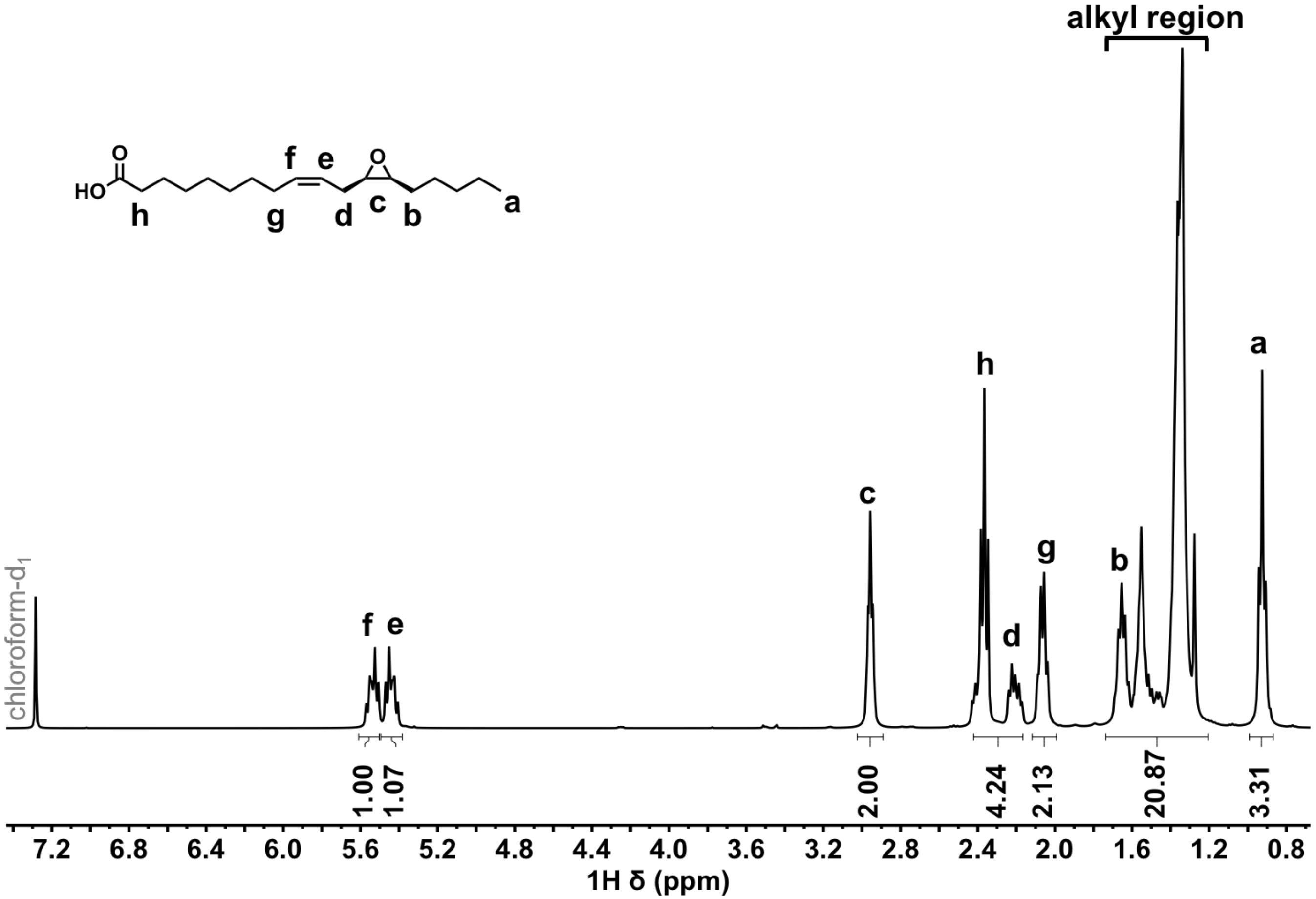

Figure 5.31 – ^{1}H-NMR spectrum of Vernolic acid after low-temperature recrystallisation. The solvent used was chloroform-d.

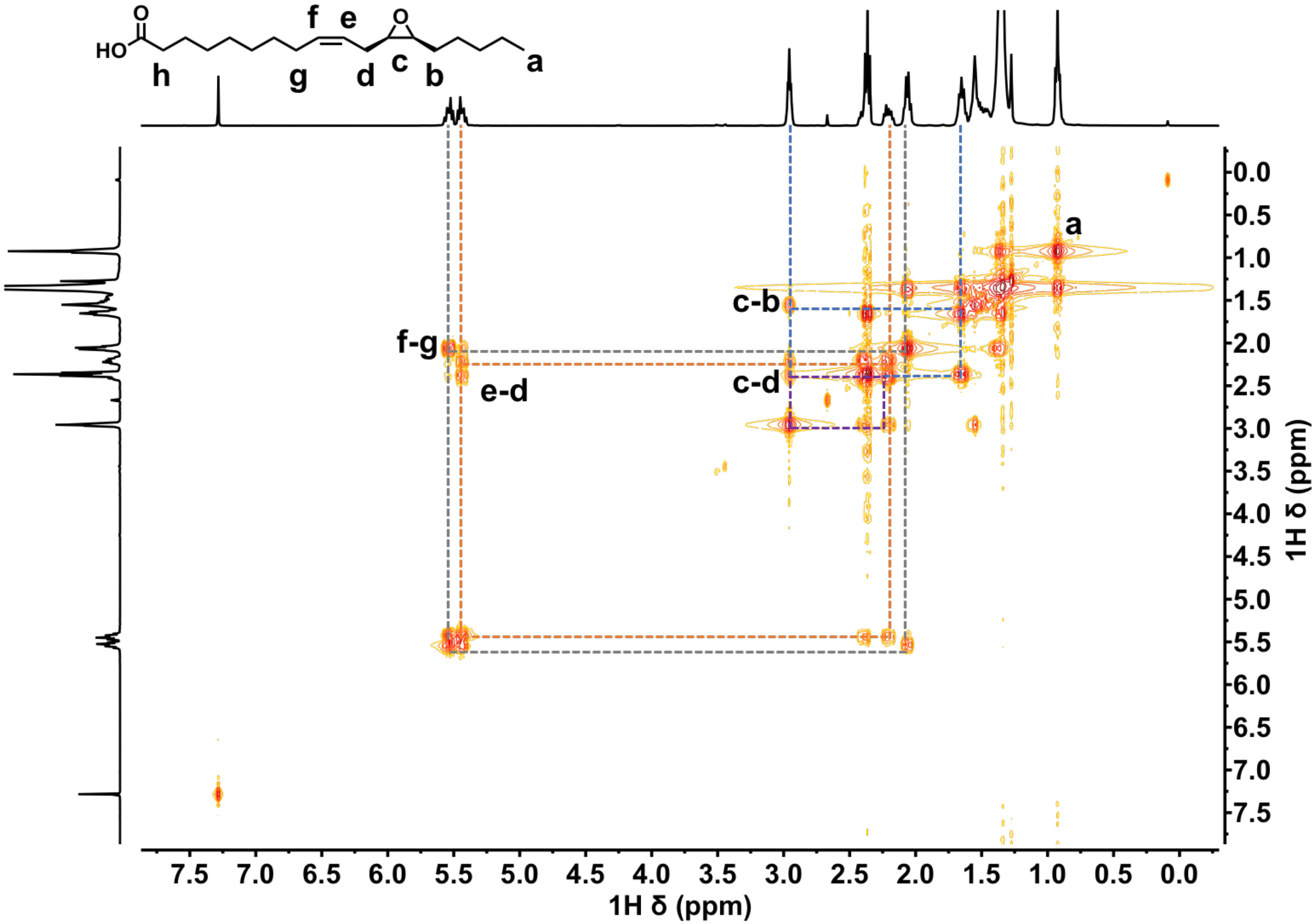

Figure 5.32 – COSY spectrum of Vernolic acid after low-temperature recrystallisation. The solvent used was chloroform-d_2. The dotted lines highlight some of the proton couplings.

5.5.3. Synthesis of vernolic acid-based monomers

Once the vernolic acid was isolated, we aimed to derivatise it to produce a series of new monomers which could undergo polycondensation reactions (Chapter 6). For polycondensation reactions, AB, AB_2 and A_2 + B_2 types of monomers are interesting to synthesise different polymer structures. Specifically, an allylic alcohol ((S,9Z,11E)-13-hydroxyoctadeca-9,11-dienoic acid) (a AB-type monomer), a dihydroxy acid (12,13-dihydroxyoctadec-9-enoic acid) (an AB_2-type monomer), a dicarboxylic acid ((E)-dodec-2-enedioic acid) (a A_2-type monomer) and a diol ((E)-dodec-2-ene-1,12-diol) (a B_2-type monomer) were synthesised by making use of the epoxide functionality of VA.

5.5.3.1. Synthesis of (S,9Z,11E)-13-hydroxyoctadeca-9,11-dienoic acid

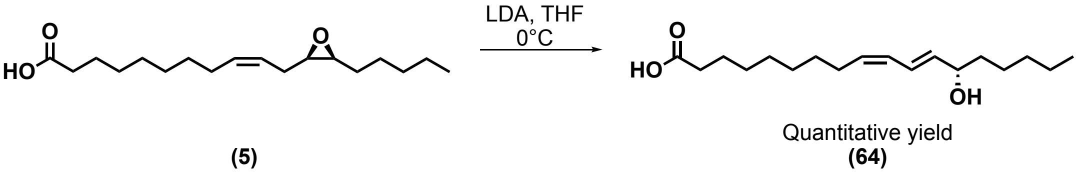

Figure 5.33 – Synthesis of coriolic acid, (S,9Z,11E)-13-hydroxyoctadeca-9,11-dienoic acid **(64)**.

Vernolic acid **(5)** was treated with excess lithium diisopropylamide (6 eq. LDA) in THF following a procedure by T. Kato *et al.*[355] . This lead to the opening of the epoxide functional group yielding the corresponding allyl alcohol **(64)**. The reaction was monitored by thin-layer chromatography (TLC plate) to confirm completion of the reaction. The crude product was isolated using column chromatography (silica gel, PE 60%/EtOAc 40%). The final product was obtained in quantitative yield and characterised by ^{1}H-NMR, ^{13}C-NMR and MS, confirming the successful synthesis of the allyl alcohol. After further optimisation, it was found that the vast excess of LDA was not required to achieve complete conversion. A modest excess of LDA (2.5 eq.) was sufficient to obtain the allylic alcohol monomer in quantitative yield, which greatly improves the atom economy of the synthesis and purification *via* chromatography was unnecessary. The reaction mechanism of the conversion of oxiranes to allyl alcohols is well known[374] and it is shown below (Figure 5.34). The strong base LDA abstracts the most acidic proton, leading to the opening of the epoxide, to form the allylic alkoxide. Subsequent protonation then yields the allylic alcohol **(64)**. This building block could self-condensate leading to the formation of a linear polyester with a pendant alkyl chain with 5 carbons.

Figure 5.34 – Reaction mechanism for the conversion of oxiranes to allylic alcohols.

5.5.3.2. Synthesis of (12S,13S,Z)-12,13-dihydroxyoctadec-9-enoic acid

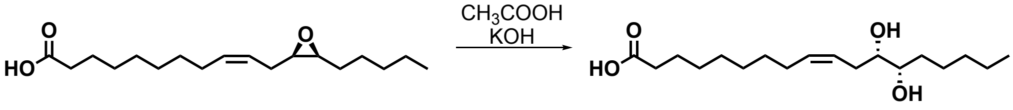

(5)

(65)

Figure 5.35 – Synthesis of 12,13-dihydroxyoctadec-9-enoic acid **(65)**.

To obtain a dihydroxy carboxylic acid monomer **(65)**, Vernolic acid **(5)** was treated with a weak acid (glacial acetic acid) to activate the epoxide functional group to then proceed with the ring opening with a basic nucleophilic attack with KOH following a procedure by Gunstone.[295] The reaction was monitored by thin-layer chromatography (TLC plate) to confirm completion of the reaction.

After the dissolution of the product in (20%) ethyl acetate in petroleum ether (-78 ºC), the pure dihydroxy acid **(65)** was obtained by low-temperature filtration at -78 ºC, with 90% yield. This acid a highly viscous liquid. The mechanism associated with this reaction is depicted below (Figure 5.36). There is a proton transfer from the acetic acid, leading to the formation of the conjugate acid of the epoxide. Subsequently, the acidic epoxide is attacked by the nucleophile KOH, leading to the ring opening of the oxirane resulting in anti-hydroxylation.

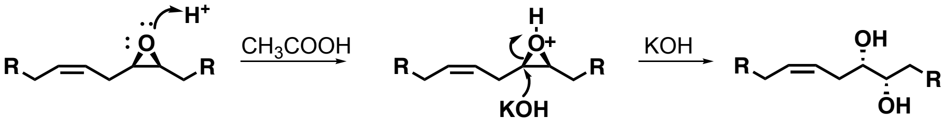

Figure 5.36 – Reaction mechanism for the conversion of oxiranes to dihydroxy acid.

5.5.3.3. Synthesis of (E)-12-oxododec-10-enoic acid

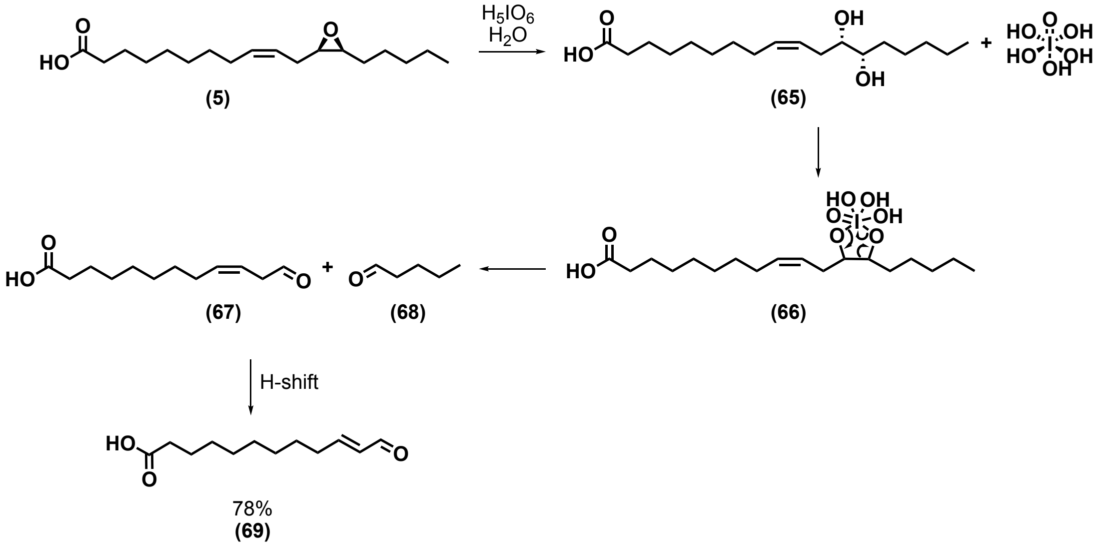

Figure 5.37 – Synthesis of 12-oxododec-10-enoic acid **(69)**.

The synthesis of the traumatin aldehyde **(69)** was accomplish by the oxidative cleavage of the C-C bond of the epoxide present in VA with periodic acid (H_5IO_6) in water and *tert*-butyl alcohol (TBA). Following the conditions reported by Binder *et al.*,[361] there was the formation of a cyclic intermediate which rearranges to form the aldehyde followed by a selective double bond migration (Figure 5.10). The reaction was monitored by thin-layer chromatography (TLC plate) to confirm completion of the reaction. The pure product was obtained as a yellow oil in 78% yield. Figure 5.36

5.5.3.4. Synthesis of (E)-dodec-2-enedioic acid

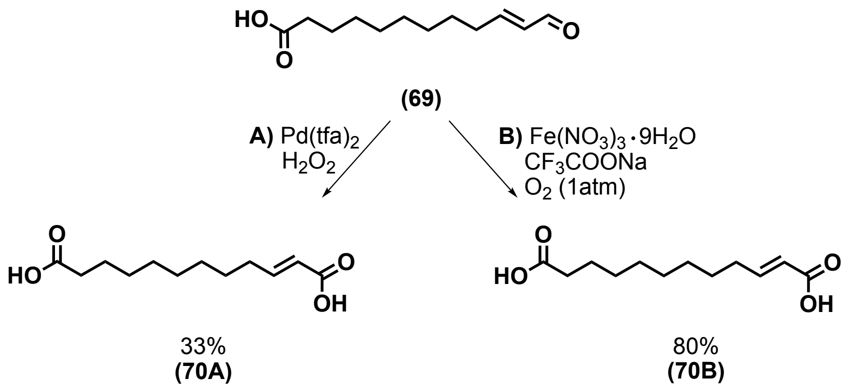

Figure 5.38 – Synthesis of dodec-2-enedioic acid **(70)**.

To obtain traumatic acid **(70)** the oxidation of traumatin aldehyde **(69)**, was attempted by two procedures (Figure 5.38).

Y. Kon *et al.*[365] reported a Palladium(II)-catalysed oxidation of $\boldsymbol{\alpha},\boldsymbol{\beta}$-unsaturated aldehydes with hydrogen peroxide (as an oxidant) to give $\boldsymbol{\alpha},\boldsymbol{\beta}$-unsaturated carboxylic acids in high yields (> 67%). However, when using these reaction conditions for the oxidation of traumatin aldehyde a modest yield of 33% was obtained.

Recently, S. Tanaka *et al.*[366] reported the selective oxidation of $\boldsymbol{\alpha},\boldsymbol{\beta}$-unsaturated aldehydes to $\boldsymbol{\alpha}$, $\boldsymbol{\beta}$-unsaturated carboxylic acids by O_2, using an iron catalyst with high conversions (>76%). Although the underlying mechanism of this reaction not yet fully understood, the same conditions were used to oxidise traumatin aldehyde **(69)** to traumatic acid **(70)**. A considerable increase in the yield to 80% was observed as compared to the previous procedure and a pale-yellow liquid was obtained as the product.

5.5.3.5. Synthesis of dodec-2-ene-1,12-diol

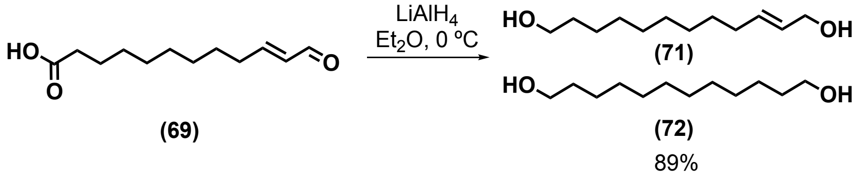

Figure 5.39 – Synthesis of dodec-e-ene-1,12-diol **(71)**.

The synthesis of the diol compound **(71)**, from the previously synthesised traumatin aldehyde **(69)**, was accomplished by a reduction reaction using Lithium aluminium hydride ($LiAlH_4$) as the reducing agent. It is known that $LiAlH_4$ is a powerful and nonselective reducing agent that readily reduces carboxylic acids, aldehydes and lactones to the corresponding alcohols.[375] Therefore, adapting the conditions published elsewhere,[367-368] the reducing agent $LiAlH_4$ was added to a solution of **(69)** in diethyl ether, resulting in the corresponding primary alcohol **(71)** (colourless oil, 89% yield). However, the presence of an additional compound **(72)** became evident from NMR analysis. This side product is the result of a double reduction by $LiAlH_4$ which affects the double bond and was already reported in the literature.[376-377] The mechanism for this reaction is well understood and it is shown below (Figure 5.40). Initially, a hydride from $LiAlH_4$ is transferred to the carbon atom of the aldehyde group and a salt is formed containing an anionic aluminium complex. The protonation of the alkoxide creates the primary alcohol from the intermediate complex.

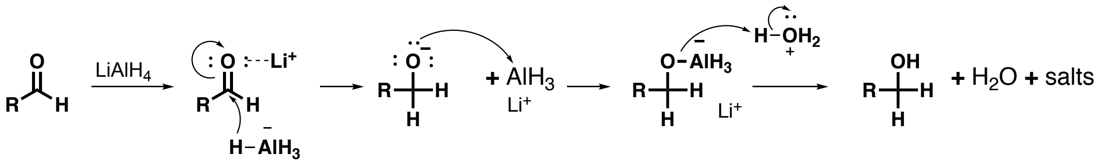

Figure 5.40 – Reaction mechanism for the conversion of aldehydes to alcohols using $LiAlH_4$.

5.6. Conclusions

The synthesis of new compounds from renewable raw materials has received a lot of attention in the past years. Therefore, this chapter describes the synthesis of monomers from vernolic acid, a fatty acid present in the oil extracted from *Vernonia galamensis* seeds.

Initially, the extraction of the oil under supercritical conditions was investigated. Using mild conditions (450 bar and 60 ºC), the effect of the milling process of the *Vernonia galamensis* seeds and the influence of the CO_2 flow rate was analysed, obtaining a maximum extraction efficiency of 80%. The milling process showed an effect on the oil extraction efficiency. When using a coffee grinder and a cross beater mill, the seeds were crushed which resulted in the loss of oil in the milling machine. However, using the roller mill, the seeds were cut in half, making the oil more accessible, and resulting in a higher extraction efficiency. In addition, an effect of the flow rate was also noticeable. As expected, the higher the Q_{CO2}, the higher the extraction efficiency. The extraction of the oil using $scCO_2$ was compared to the extraction using *n*-hexane. Using $scCO_2$ proved to be a better and greener approach for the extraction of the oil from *Vernonia galamensis* seeds not only from the sustainable point of view (using milder conditions), but also because of the purity of the oil: the oil extracted with $scCO_2$ contained fewer impurities compared to the oil extracted with *n*-hexane. Therefore, the oil obtained from the supercritical fluid extraction was used to isolate vernolic acid, by the hydrolysis of the triglycerides, yielding 90% of vernolic acid.

Finally, five building blocks were synthesised from vernolic acid, adapting procedures from the literature. Firstly, VA was converted into the allylic alcohol **(64)** in quantitative yield and high purity under mild conditions. The formation of an unsaturated dihydroxy acid **(65)**, was accomplished by reacting VA with acetic acid. This allyl alcohol was isolated by a simple low-temperature filtration in 90% yield. Afterwards, the synthesis of a dicarboxylic acid was accomplished by two step procedure. In the first step, VA was treated with periodic acid to give the aldehyde **(69)** (78% yield); secondly, this aldehyde

(69) was oxidised (in the presence of O_2 and using an iron catalyst) to the dicarboxylic acid **(70B)** (80% yield). Finally, the synthesis of the diol **(71)** was accomplished by the reduction of the aldehyde **(69)**, using $LiAlH_4$.

The different VA-based building blocks might be valuable for different applications, such as the synthesis of VA-based polymers, which is going to be investigated in the next chapter (Chapter 6).

CHAPTER 6. POLYMERS FROM THE *V. GALAMENSIS* SP. PLATFORM

6.1. Overview

In the last decades, the ongoing development of the bio-refinery concept has led to the introduction of new building blocks for novel materials.[157, 378] The investigation of new monomer structures is of high interest. In Chapter 5, it was demonstrated that new monomers for polycondensation reaction can be synthesised from the oil of the *Vernonia galamensis* sp. plant. Here the synthesis of new polymers from the monomers synthesised and described previously is presented. Three different polymers are synthesised through polycondensation:

1. Self-condensation of the allylic alcohol in the melt and in $scCO_2$, using stannous octanoate as the catalyst.
2. Self-condensation of the dihydroxy acid in the melt and in $scCO_2$, using stannous octanoate as the catalyst.
3. Polycondensation of dodece-2-ene-1,12-diol and azelaic acid, a monomer commercially, in the presence of toluene and in $scCO_2$ using enzyme catalysis.

The polymers are characterised by ^{1}H-NMR, GPC and DMA in order to carefully assess their structural and thermal properties.

6.2. Introduction

The availability of a growing number of inexpensive sources (petroleum based compounds) suitable to produce macromolecular materials during the 1900s, gave birth to ‘the plastic age’, in which we still live today.[379] Due to the expected depletion of petrochemical sources, there is now high interest for biobased resources. Depending on the source, monomers and polymers can be divided into two groups:[379]

1. Vegetal biomass, including terpenes,[380] cellulose,[381] plant oils[304] or sugars[220] to name a few.
2. Animal biomass, including chitin/chitosan[382] or casein.[383]

Among those, vegetable biomass constitutes the main source for renewable polymers (80% worldwide yearly production, the remaining 20% being animal biomass).[384] Vegetable triglycerides were the first renewable resources exploited by man as raw materials for synthetic polymers primarily for coating applications (drying oils). Because of these functionalities, plants oils have received a lot of scientific and technological attention in the last decades. As described in the previous chapter, vegetable oils can be extracted from different plant species such as soybean, corn, linseed and the castor oil plant.[385] These renewable resources have been used as sources for the synthesis of vegetable oil-based polymers.

6.2.1. Polycondensation of fatty acid-based monomers

Fatty acids (FAs) have been used in the development of polymers for biomedical applications and personal care products.[386] They have been considered for these purposes since they are generally inert, inexpensive, biocompatible and potentially biodegradable. In addition, these FA-based polymers are preferred over petrochemical-based due to environmental issues. Polyesters, polyanhydrides and polyamides are some examples of polymers obtained using FAs as building blocks.[387]

FA-based polyesters can be obtained by three main routes:

1. polycondensation of hydroxycarboxylic acids
2. polycondensation of dicarboxylic acid and a diol
3. ring-opening polymerisation of lactones

This work will focus on the polycondensation reactions. Ricinoleic acid (RA) is a difunctional fatty acid which can be polymerised without any further modification and it is obtained by the hydrolysis of castor oil. Slivniak and Domb [388] studied the thermal self-polycondensation of RA (Figure 6.1 A)) at 150 ºC and a polyester with a molecular weight of 4,300 Da was obtained after 12 hours reaction. The same authors also performed the synthesis of RA and LA co-polyesters (Figure 6.1 B)), at the same temperature to give polymers with a molecular weight 2,000-5,800 Da after 12 hours reaction.

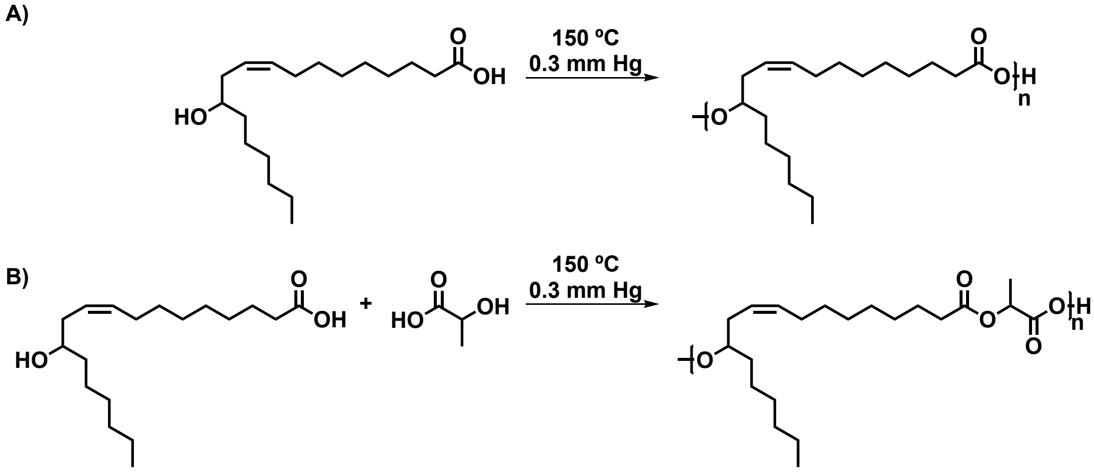

Figure 6.1 – Schematic representation of the synthesis of A) poly-RA through self-condensation of RA and B) poly(RA-LA) through polycondensation of RA and LA.[388]

Most of the FAs are mono-functional and hence, cannot be used as monomers for polymerisations. They need to be converted into a good monomer to be polymerised. The synthesis of malonate derivatives, from saturated fatty acid methyl esters, for polycondensation reactions with 1,6-hexanediol was studied by Kolb and Meier [195]. Using 1 mol% $Ti(OiPr)_4$ as the catalyst at 120 ºC, resulted in a polymer with a high molecular weight of 22,100 Da, with a high dispersity ($Đ$ = 2.02). In this work, it was found that the longer the aliphatic side-chains of the polyesters, the higher the T_m of the resulting polymers, ranging from -3 to 27 ºC. This suggests that the length of the side-chain influences the thermal properties, in which non-polar interactions are the main driving force of crystallinity of the polyesters.

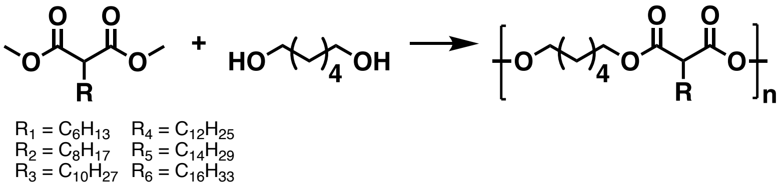

Figure 6.2 – Synthesis of malonate-derived polyesters, through the polycondensation with 1,6-hexanediol, using 1 mol% Ti(OiPr)$_4$ as the catalyst at 120 ºC.[195]

The polycondensation of FA derived compounds can be also accomplished by the self-condensation of hydroxycarboxylic acids. Testud*, et al.* [389] studied the polycondensation of FA-based AB$_n$-type monomers. In contrast to what was described by Kolb and Meier [195] and Winkler*, et al.* [217], Ti(OiPr)$_4$ revealed to be a poor catalyst for the polycondensation of methyl-9,10-dihydroxystearate (M2HS) (Figure 6.3). Zinc acetate (Zn(OAc)$_2$), TBD and sodium methoxide (NaOMe) showed better results at 160 ºC, reaching a monomer conversion of 95% after 15 h reaction. Branched polymers with molecular weights in the range of 3,500-6,100 Da (2.46 < *Đ* < 3.08) were obtained. The dispersity values were characteristic of a branched materials obtained through polycondensation.[390] Increasing the temperature to > 200 ºC and the reaction time to more than 40 h, favoured the formation of insoluble gel-like polymers, which is in agreement with previous studies.[186, 191]

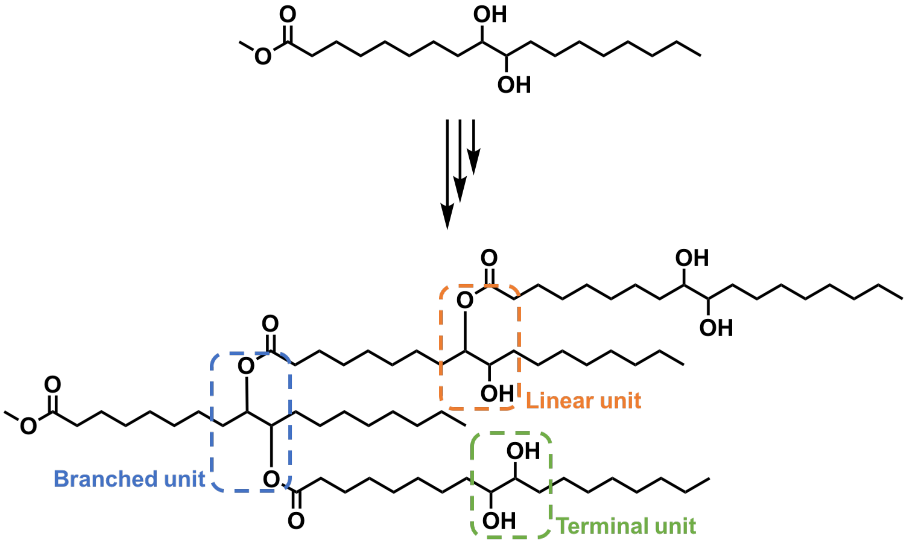

Figure 6.3 –Polycondensation of methyl-9,10-dihydroxystearate (M2HS) through a two-step reaction: 2 hours at 120 ºC under argon flow followed by 13 hours at 160 ºC under reduced pressure. Different catalysts were tested: zinc acetate (Zn(OAc)$_2$), TBD and sodium methoxide (NaOMe).[389]

Winkler*, et al.* [217] studied the polycondensation of dimethyl itaconate (DMI) with different diols using different catalysts (Figure 6.4).

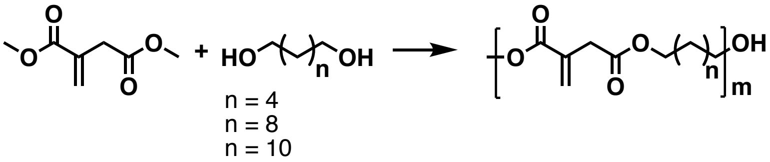

Figure 6.4 – Polycondensation of dimethyl itaconate (DMI) with different diols.[217]

Using 1,5,7-Triazabicyclo[4.4.0]dec-5-ene (TBD), titanium isopropoxide ($Ti(OiPr)_4$) or *p*-toluenesulfonic acid (PTSA) as catalysts was found to be not ideal since low molecular weight polymers or completely insoluble materials were obtained. The presence of the vinylic double bonds led to cross-linking of the polymer chains. To overcome this issue, the authors introduced a radical inhibitor, 4-methoxyphenol, to the system and, in the presence of $Sn(Oct)_2$, linear polymers with a molecular weight of 9,900–11,500 Da ($1.64 < Đ < 1.85$) were obtained (Table 6.1).

Table 6.1 – Polycondensation of dimethyl itaconate with different diols and in the presence of 1 mol% $Sn(Oct)_2$, 4-methoxyphenol (to avoid radical-mediated side reactions), at 130 ºC, under argon atmosphere (10^{-2} mbar).[217]

Entry	Diol	M_n (Da)	Đ
1	1,6-hexanediol	11,500	1.64
2	decane-1,10-diol	10,200	1.85
3	dodecane-1,12-diol	9,950	1.75

6.2.2. Vernonia-based polymers

As mentioned in the previous chapter, vernolic acid (VA) can be extracted from *Vernonia galamensis* sp. plant seeds. Vernolic acid is an interesting structure because it contains both a double bond and an oxirane ring. These functional groups could be valuable for the synthesis of new materials. In the literature, there are few examples using VA, or the vernonia oil (VO), for the synthesis of new materials. Using the Elsevier's database Scopus (www.scopus.com) and searching for scientific documents with the key words:

vernolic acid + *polymers*, *vernonia oil* + *polymers* or *vernonia galamensis* + *polymers*, only 22 documents were found (Table 6.2 and Figure 6.5).

Table 6.2 – Articles found by searching for the key words *vernolic acid* + *polymers*, *vernonia galamensis* + *polymers* or *vernonia oil* + *polymers*. Search performed through Elsevier's database Scopus (www.scopus.com).

Year	Paper title	Ref
2014	Direct polymerization of vernonia oil through cationic means	304
2014	Enzymatic synthesis of epoxy fatty acid starch ester in ionic liquid-organic solvent mixture from vernonia oil	59
2014	Substrates for PHA biosynthesis	391
2009	The biosynthesis of cutin and suberin as an alternative source of enzymes for the production of bio-based chemicals and materials	392
2007	Fatty acids in vernonia produced in the mid-Atlantic region of the United States	351
2004	Vernonia oil-based acrylate and methacrylate polymers and interpenetrating polymer networks with epoxy resins	393
2004	Synthesis and polymerization of a radiation curable hyperbranched resin based on epoxy functional fatty acids	394
2003	Fat-derived aziridines and their N-substituted derivatives: Biologically active compounds based on renewable raw materials	395
2003	Synthesis of 13(14)-hydroxy-cis-10-nonadecenyl amine hydrochloride	396
2001	Soluble polymers from a multifunctional natural oil	397
2000	Vernonia oil seed production in the mid-Atlantic region of the United States	398
2000	Natural oil-based polymers: opportunities and challenges	399
1997	Syntheses of 12-aminododecanoic and 11-aminoundecanoic acids from vernolic acid	400
1994	New chemical derivatives based on Vernonia galamensis oil	60
1993	Naturally functionalized triglyceride oils in interpenetrating polymer networks	401
1993	Semi-interpenetrating polymer networks composed of poly(ethylene terephthalate) and vernonia oil	402
1993	Vernonia oil based semi-IPN's with poly(ethylene terephthalate)	403
1990	Interpenetrating polymer networks based on functional triglyceride oils and other not yet commercial renewable resources	404
1989	Synthesis of toughened elastomer from vernonia galamensis seed oil	307
1985	Simultaneous interpenetrating networks based on vernonia oil polyesters and polystyrene. Part 2: A comparison of the reactivities of vernonia oil and castor oil toward the formation of polyesters	405

1983	Interpenetrating polymer networks from triglyceride oils containing special functional groups: a brief review	406
1983	Vernonia oil characterization and polymerization, and simultaneous interpenetrating polymer networks based on vernonia oil-sebacic acid/polystyrene-DVB compositions	407

To the date, epoxy resins and elastomers are the materials synthesised from vernolic acid (see section 1.3.2.1. of this Thesis). Therefore, materials from vernolic acid (extracted from *Vernonia galamensis* sp. seed oil) still needs further investigation.

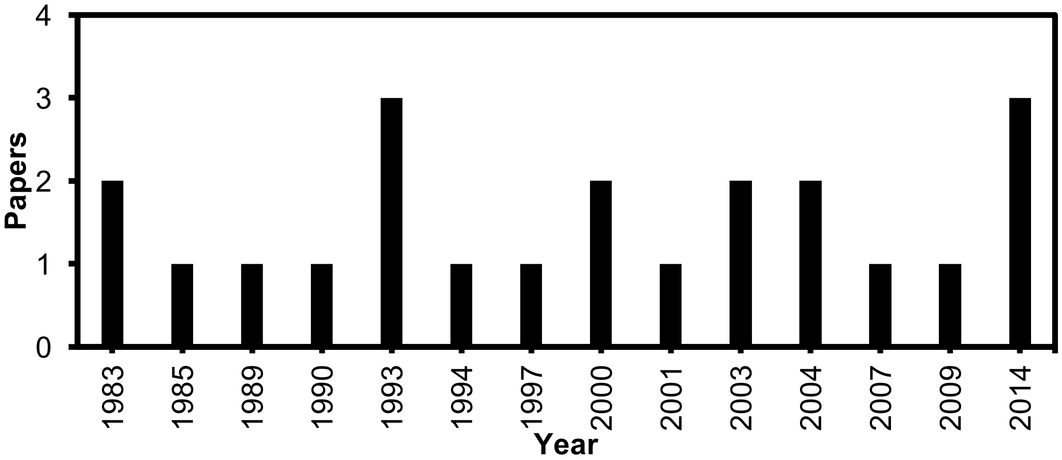

Figure 6.5 – Scientific publications as a function of publication year searching for vernolic *acid + polymers*, *vernonia galamensis + polymers* or *vernonia oil + polymers* as the topic with Scopus (Elsevier's database).

6.3. Aims of study

The aim of this study is to synthesise new polymers from vernolic acid-based monomers, which were synthesised in the previous chapter (Chapter 5) (Table 6.3).

Initially, this chapter focuses on the melt self-polycondensation of (S,9Z,11E)-13-hydroxyoctadeca-9,11-dienoic acid (HA) and (12S,13S,Z)-12,13-dihydroxyoctadec-9-enoic acid (DHA), using $Sn(Oct)_2$ as the catalyst. The condensation of dodec-2-ene-1,12-diol (DED) with azelaic acid (AZ) will also investigate in the presence of a lipase (*Candida antarctica* lipase B, CaLB) in toluene.

Additionally, the same polycondensations were conducted using supercritical carbon dioxide ($scCO_2$). This study tests the hypothesis that using $scCO_2$ gives polymers with similar properties to the ones synthesised in melt condensation, whilst using milder conditions.

Table 6.3 – Monomer structures and respective name and abbreviation used in this Thesis.

Monomer structure	Compound name & abbreviation
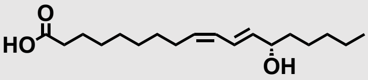	(S,9Z,11E)-13-hydroxyoctadeca-9,11-dienoic acid **HA**
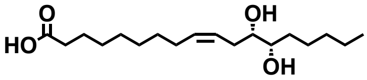	(12S,13S,Z)-12,13-dihydroxyoctadec-9-enoic acid **DHA**
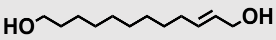	dodec-2-ene-1,12-diol **DED**
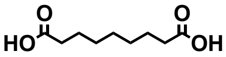	azelaic acid **AZ**

6.4. Experimental

6.4.1. Materials

Stannous(II) 2-ethylhexanoate (tin octanoate, $Sn(Oct)_2$) was purchase from Sigma Aldrich and used as received. Scandium(III) triflate ($Sc(OTf)_3$) was purchase from Sigma Aldrich and used as received. Novozyme® 435 (CaLB immobilised on cross-linked acrylic resin beads) was kindly donated by Novozymes (Denmark), stored at 4 ºC and dried for 24 hours under vacuum (100 mbar) at room temperature (RT) before use. Molecular sieves type 3 and 4 Å, 1.6-2.5 mm beads, were purchased from Fisher Scientific (UK) and used as received. Carbon dioxide grade 4.0 (minimum purity 99.99%) was purchased from BOC Special Gases (UK) and used as received. All solvents were analytical grade and used as received.

6.4.2. Synthesis methods

6.4.2.1. Melt polycondensation of vernonia-based monomers

6.4.2.1.1. Polycondensation of (S,9Z,11E)-13-hydroxyoctadeca-9,11-dienoic acid

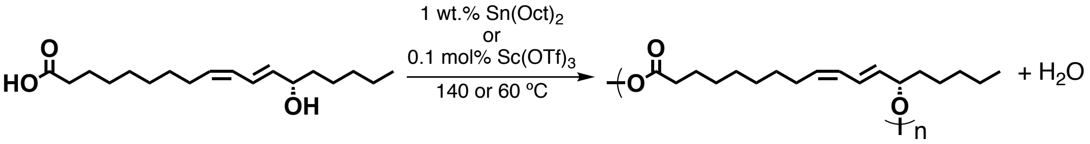

The polymerisation of (S,9Z,11E)-13-hydroxyoctadeca-9,11-dienoic acid (HA) was carried out *via* melt polycondensation with $Sn(Oct)_2$ or $Sc(OTf)_3$ as the catalyst. Thus, in a typical procedure, the monomer (3.55 mmol) and $Sn(Oct)_2$ (1 wt.% with respect to the total amount of monomer) or $Sc(OTf)_3$ (0.1 mol% with respect to the total amount of monomer) were added to a 20 mL three-neck round bottom flask, alongside a magnetic stirrer (300 rpm) while applying vacuum to the system. The mixture was heated to the reaction temperature in an oil bath and the reaction was left to run for the specified time (Table 6.4). The reaction was stopped by cooling to room temperature (RT). Monomer conversion was determined by NMR, using the ratio between the integrations of proton H_b* (as monomer) and proton H_a (Table 6.10) (see Figure 6.7). The reactions were performed at least twice to check reproducibility. The summary of the reactions conditions conducted *via* melt polymerisation are shown below (Table 6.4).

Table 6.4 – Summary of the polycondensation of (S,9Z,11E)-13-hydroxyoctadeca-9,11-dienoic acid conducted *via* melt polycondensation.

Entry	Reaction time	T ºC	Catalyst	Appearance
1	1h30m	140 ºC	1 wt.% $Sn(Oct)_2$	Viscous, beige
2	4h30m	140 ºC	1 wt.% $Sn(Oct)_2$	Viscous, brown
3	19h30	140 ºC	1 wt.% $Sn(Oct)_2$	Viscous, brown
4	1 h	60 ºC	0.1 mol % $Sc(OTf)_3$	Liquid, beige
5	2 h	60 ºC	0.1 mol % $Sc(OTf)_3$	Liquid, beige
6	3 h	60 ºC	0.1 mol % $Sc(OTf)_3$	Viscous, light brown
7	4 h	60 ºC	0.1 mol % $Sc(OTf)_3$	Viscous, brown

6.4.2.1.2. Polycondensation of (12S,13S,Z)-12,13-dihydroxyoctadec-9-enoic acid

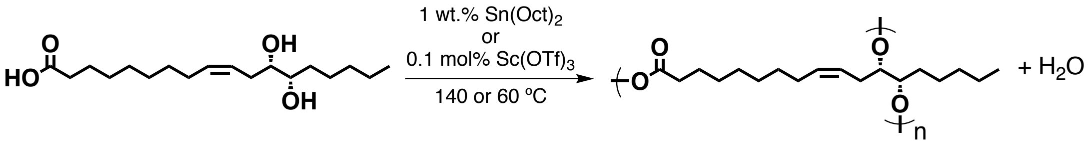

The polymerisation of (12S,13S,Z)-12,13-dihydroxyoctadec-9-enoic acid (DHA) was carried out *via* melt polycondensation with $Sn(Oct)_2$ or $Sc(OTf)_3$ as the catalyst. Thus, in a typical procedure, the monomer (3.55 mmol) and $Sn(Oct)_2$ (1 wt.% with respect to the total amount of monomer) or $Sc(OTf)_3$ (0.1 mol% with respect to the total amount of monomer) were added to a 20 mL three-neck round bottom flask, alongside a magnetic stirrer (300 rpm) applying vacuum to the system. The mixture was heated to the reaction temperature in an oil bath and was left to run for the specified reaction time (Table 6.5). The reaction was stopped by cooling to room temperature (RT). The reactions were performed at least twice to check reproducibility. A summary of the conditions for melt polymerisation are shown below (Table 6.5).

Table 6.5 – Summary of the polycondensation of (12S,13S,Z)-12,13-dihydroxyoctadec-9-enoic acid conducted *via* melt polycondensation.

Entry	Reaction time	T ºC	Catalyst	Appearance
8	1 h	140 ºC	1 wt.% $Sn(Oct)_2$	Viscous, transparent
9	3 h	140 ºC	1 wt.% $Sn(Oct)_2$	Viscous, transparent
10	4h30	140 ºC	1 wt.% $Sn(Oct)_2$	Sticky, transparent
11	7 h	140 ºC	1 wt.% $Sn(Oct)_2$	Sticky, transparent
12	19h30	140 ºC	1 wt.% $Sn(Oct)_2$	Gel, transparent
13	1 h	60 ºC	0.1 mol % $Sc(OTf)_3$	Liquid, transparent
14	2 h	60 ºC	0.1 mol % $Sc(OTf)_3$	Liquid, transparent
15	3 h	60 ºC	0.1 mol % $Sc(OTf)_3$	Liquid, transparent
16	5 h	60 ºC	0.1 mol % $Sc(OTf)_3$	Viscous, yellow

6.4.2.1.3. Polycondensation of dodec-2-ene-1,12-diol and azelaic acid

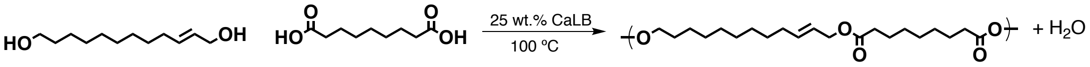

The polymerisation of dodec-2-ene-1,12-diol (DED) with azelaic acid (AZ) was carried out *via* polycondensation with CaLB as the catalyst. Thus, in a typical procedure using a 1:1 molar ratio of DED:AZ, the DED (3.55 mmol, 0.71 g), AZ (3.55 mmol, 0.67 g), molecular sieves (size 4Å, 25 wt.% with respect to the total amount of monomers) and toluene (1 mL) were added to a 20 mL three-neck round bottom flask, alongside a magnetic stirrer (300 rpm) and the reaction was left to run under an argon atmosphere. The reaction mixture was heated for one hour at 55-60 ºC in an oil bath (Table 6.6). Thereafter, CaLB (25 wt.%[§§] with respect to the total amount of monomers) was added and the temperature was increased to 100 ºC and left to run for 46 hours. The reaction

---

[§§] Includes polymer support

was stopped by cooling to room temperature (RT). The molecular sieves and CaLB were removed by filtration after dissolving the reaction mixture in THF (qualitative Fisherbrand filter paper, supplied by Fisher Scientific) and the solvent was removed under reduced pressure. The samples were dried under vacuum pressure, at RT, overnight. The monomer conversion was calculated through NMR, using the integration of proton H_f (of the monomer) against the integration of protons H_b and H_c (Table 6.13) (see Figure 6.17). The summary of the reactions conditions conducted *via* polymerisation are shown below (Table 6.6).

Table 6.6 – Summary of the polycondensation of dodec-2-ene-1,12-diol (diol) with azelaic acid (diacid) conducted polycondensation in of toluene, under a stream of argon. *Note*: the ration diol:diacid was 1:1; [a] Includes polymer support.

Entry	Reaction time	T ºC	Catalyst[a]	Appearance
17	2 h	100 ºC	25 wt.% CaLB	Liquid, transparent
18	4 h	100 ºC	25 wt.% CaLB	Viscous, yellow
19	20 h	100 ºC	25 wt.% CaLB	Viscous, orange
20	26 h	100 ºC	25 wt.% CaLB	Viscous, orange
21	48 h	100 ºC	25 wt.% CaLB	Viscous, orange

6.4.2.2. Polycondensation of vernonia-based monomers in supercritical carbon dioxide

6.4.2.2.1. Polycondensation of (S,9Z,11E)-13-hydroxyoctadeca-9,11-dienoic acid

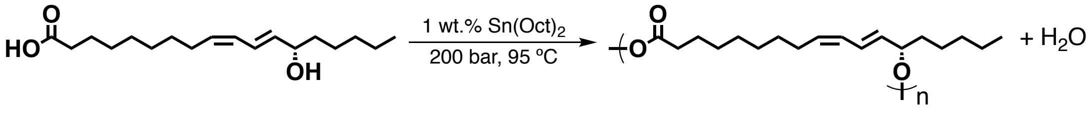

In a typical procedure, HA (3.55 mmol), $Sn(Oct)_2$ (1 wt.% with respect to the total amount of monomer) and molecular sieves (size 3Å, 25 wt.% with respect to the total amount of monomer) were added to the stainless steel reaction autoclave described previously (20 mL, Chapter 2, Figure 2.3). The vessel was sealed and pressurised to 50 bar. Subsequently, the temperature was set to 95 ºC and finally the pressure was increased to 200 bar. The reaction was left to run for 3, 6 and 24 h, while stirring at 150 rpm. To avoid polymer foaming and blockages in the pipework, the reactions were terminated by cooling the vessel in a water/ice bath (~ 0 ºC) before venting. The CO_2 was vented when the pressure was below 20 bar. Finally, the product was collected and dissolved in 10 mL of THF, and filtered to remove molecular sieves. The solvent was then removed under reduced pressure, leaving the polymeric products. The samples were dried overnight under vacuum, at RT. Monomer conversion was determined by NMR, by the ratio between the integrations of proton H_b* (as monomer) and proton H_a (Table 6.14) (see Figure 6.20). The summary of the reactions conditions for polymerizations conducted in supercritical conditions are showed below (Table 6.7).

Table 6.7 – Summary of the polycondensation of HA conducted in $scCO_2$ at 275 bar.

Entry	Reaction time	T ºC	Catalyst	Appearance
22	3 h	95 ºC	1 wt.% $Sn(Oct)_2$	Viscous, dark brown
23	6 h	95 ºC	1 wt.% $Sn(Oct)_2$	Viscous, dark brown
24	24 h	95 ºC	1 wt.% $Sn(Oct)_2$	Viscous, dark brown

6.4.2.2.2. Polycondensation of (12S,13S,Z)-12,13-dihydroxyoctadec-9-enoic acid

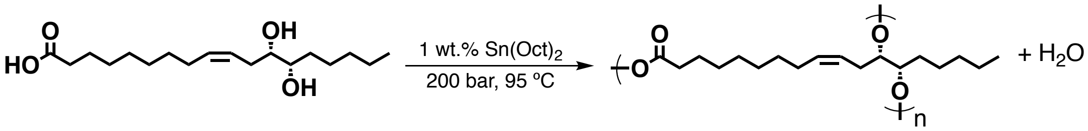

In a typical procedure, DHA (3.55 mmol), $Sn(Oct)_2$ (1 wt.% with respect to the total amount of monomer) and molecular sieves (size 3Å, 25 wt.% with respect to the total amount of monomer) were added to the stainless steel reaction autoclave described previously (20 mL, Chapter 2, Figure 2.3). The vessel was sealed and pressurised to 50 bar. Subsequently, the temperature was set to 95 ºC and finally the pressure was increased to 200 bar. The reaction was left to run for 3, 6 and 24 h, while stirring at 150 rpm. To avoid polymer foaming and blockages in the pipework, the reactions were terminated by cooling the vessel in a water/ice bath (~ 0 ºC) before venting. The CO_2 was vented when the pressure was below 20 bar. Finally, the product was collected and dissolved in 10 mL of THF, and filtered to remove the molecular sieves. The solvent was then removed under reduced pressure, leaving the polymeric products. The samples were dried overnight under vacuum, at RT. The summary of the reactions conditions for polymerisations conducted in supercritical conditions are showed below (Table 6.8).

Table 6.8 – Summary of the polycondensation of (12S,13S,Z)-12,13-dihydroxyoctadec-9-enoic acid conducted in $scCO_2$ at 275 bar.

Entry	Reaction time	T ºC	Catalyst	Appearance
25	3 h	95 ºC	1 wt.% $Sn(Oct)_2$	Waxy, beige
26	6 h	95 ºC	1 wt.% $Sn(Oct)_2$	Waxy, beige
27	24 h	95 ºC	1 wt.% $Sn(Oct)_2$	Waxy, dark orange

6.4.2.2.3. Polycondensation of dodec-2-ene-1,12-diol and azelaic acid

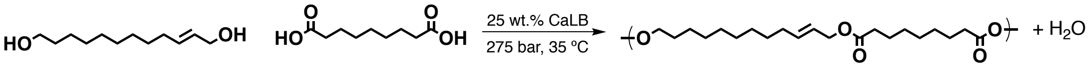

For a reaction with 1:1 molar ratio of DED:AZ, the DED (3.55 mmol, 0.71 g), AZ (3.55 mmol, 0.67 g), CaLB (25 wt.%[***] with respect to the total amount of monomers) and molecular sieves (size 3Å, 25 wt.% with respect to the total amount of monomer) were added to the stainless steel reaction autoclave described previously (20 mL, Chapter 2, Figure 2.3). The vessel was sealed and pressurised to 50 bar. Subsequently, the temperature was set to 35 ºC and finally the pressure was increased to 275 bar. The reaction was left to run for 24 h, while stirring at 150 rpm. To avoid polymer foaming and blockages in the pipework, the reactions were terminated by cooling the vessel in a water/ice bath (~ 0 ºC) before venting. The CO_2 was vented when the pressure was below 20 bar. Finally, the product was collected and dissolved in 10 mL

[***] Includes polymer support

of THF, and filtered to remove the enzyme beads and molecular sieves. The solvent was then removed under reduced pressure, leaving the polymeric product. The samples were dried overnight under vacuum at RT. The monomer conversion was calculated through NMR, using the integration of proton H_f (of the monomer) against the integration of protons H_b and H_c (Table 6.15) (see Figure 6.26). The reaction conditions for this polymerization conducted in $scCO_2$ is shown below (Table 6.9).

Table 6.9 – Summary of the polycondensation of dodec-2-ene-1,12-diol (DED) with azelaic acid (AZ) conducted in $scCO_2$ at 275 bar. *Note*: the molar ratio of diol:diacid was 1:1; [a] Includes polymer support.

Entry	**Reaction time**	**T ºC**	**Catalyst**[a]	**Appearance**
28	24 h	35 ºC	25 wt.% CaLB	Viscous, orange

6.4.3. Polymer characterisation

The polymer structures were characterised using ^{1}H-NMR, GPC and DMA. All these techniques are described in Chapter 2.

6.5. Results and discussion

6.5.1. Melt polycondensation of vernonia-based monomers

To the best of the author's knowledge, the melt polycondensation of the synthesised vernonia-based monomers (in which vernolic acid was obtained from the extracted vernonia oil) has never been investigated.

6.5.1.1. Polycondensation of (S,9Z,11E)-13-hydroxyoctadeca-9,11-dienoic acid (HA)

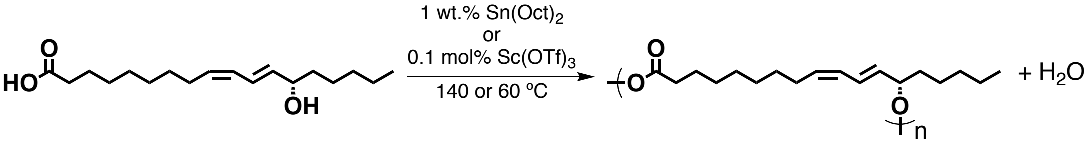

Figure 6.6 – Polycondensation reaction of HA monomer using 1 wt.% $Sn(Oct)_2$, or 0.1 mol% $Sc(OTf)_3$, at 140 or 60 ºC.

(S,9Z,11E)-13-hydroxyoctadeca-9,11-dienoic acid (HA) was first polymerised, *via* melt condensation, using 1 wt.% $Sn(Oct)_2$ (entries 1-3, Table 6.10) and 0.1 mol % $Sc(OTf)_3$ (entries 4-7, Table 6.10). When using $Sn(Oct)_2$ the polymerisations were conducted at 140 ºC, whilst the polymerisation was conducted at 60 ºC when using $Sc(OTf)_3$ as the catalyst. In addition, vacuum was applied into the system, to drive the reaction towards the formation of the product.

Ideally, the conversion should be accessed using the ratio of the integrals of proton H_b (adjacent to the hydroxyl group, which reacts in the polycondensation) as monomer and polymer. However, proton H_b, upon polymerisation and formation of the ester bond, shifts close to the C=C double bond region and this causes difficulties with integration. Therefore, although not 100% accurate, the ratio between the integrations of proton H_b* (as monomer) and proton H_a are used to determine the conversion of the reaction (Figure 6.7).

Table 6.10 – Polymerisation of HA polymer *via* melt polycondensation. [a] Monomer conversion was determined by NMR (Figure 6.7), by the ratio between the integrations of proton H_b (as monomer) and proton H_a; [b] these M_n values corresponds to the peaks with higher molecular weights, other peaks were detected in the GPC trace, due to the presence of oligomers.

	Entry	**Time**	**Conversion**[a]	M_n^{GPC} **(Da)**[b]	***Đ***	T_g
$Sn(Oct)_2$	**1**	1h30m	99%	2,100	> 2	–
	2	4h30m	99%	11,600	> 2	–
	3	19h30	99%	34,400	> 2	-23 ºC
$Sc(OTf)_3$	**4**	1 h	70%	1,300	> 2	–
	5	2 h	80%	1,300	> 2	–
	6	3 h	86%	5,500	> 2	–
	7	4 h	90%	7,800	> 2	-27 ºC

After 4.5 h of polymerisation catalysed with $Sn(Oct)_2$ (Figure 6.7 B)), from the integration of proton H_b*, the conversion was 99%. Upon formation of the ester bond, the chemical shift of H_b shifts to higher frequencies. However, the chemical shift of this proton, overlaps with the resonances of the double bonds protons (H_c, H_d, H_e and H_f), *ca.* 6.50–5-20 ppm. Considering the integration of protons H_c, H_d, H_e and H_f, before polymerisation (Figure 6.7 A)), it gives a value of 3.98, which corresponds to these 4 protons. Upon polymerisation, (Figure 6.7 B)), the integration in the same region gave 4.75, which confirms the presence of proton H_b upon formation of the ester bond.

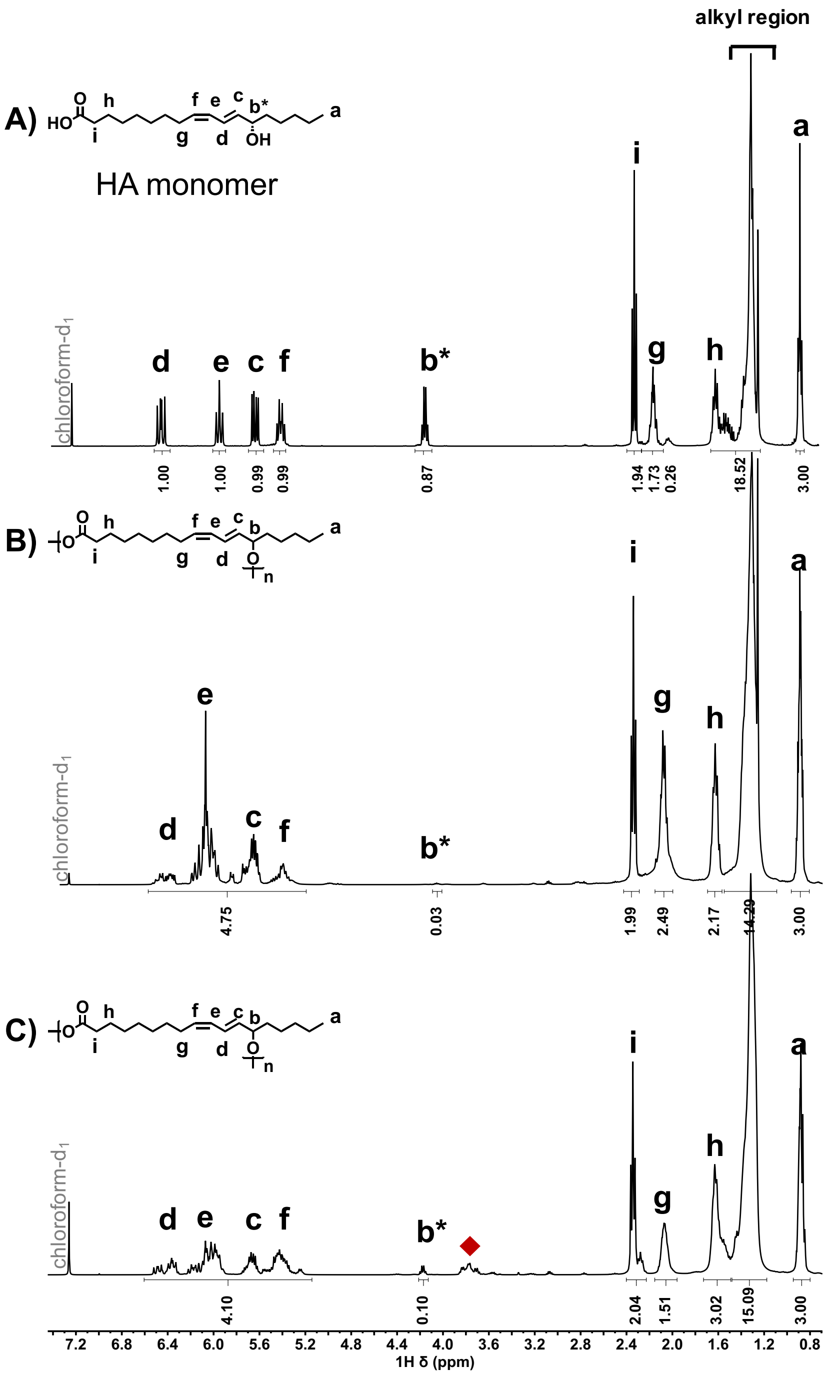

Figure 6.7 – ^{1}H-NMR spectra of A) (S,9Z,11E)-13-hydroxyoctadeca-9,11-dienoic acid monomer (HA), and the polymerisation product of HA *via* melt condensation catalysed with B) $Sn(Oct)_2$ (4h30 reaction, entry 2 of Table 6.10) and C) $Sc(OTf)_3$ (4 h reaction, entry 7 of Table 6.10). The solvent used was chloroform-d. *Note*: H_b proton as part of the monomer structure is represented as b*; due to overlap of the resonance of proton H_b (upon polymerisation) with the C=C double bonds protons (H_c, H_d, H_e and H_f), this assignment is not represented in the spectra, but it is present in this region 6.50–5-20 ppm; ◆ = corresponds to the presence of an unknown impurity.

After 19h30 polymerisation time (Figure 6.8), the broadening of the resonances is noticeable, due to the increase of the polymer molecular weight, which is characteristic for a NMR spectrum of a polymer. Through GPC analysis, there is an increase of the molecular weight with time and, after

19h30, a polymer with a molecular weight up to 34,400 Da, with high dispersity (*Đ* > 2), was obtained (entry 3, Table 6.10). The high dispersity is due to the presence of oligomeric chains.

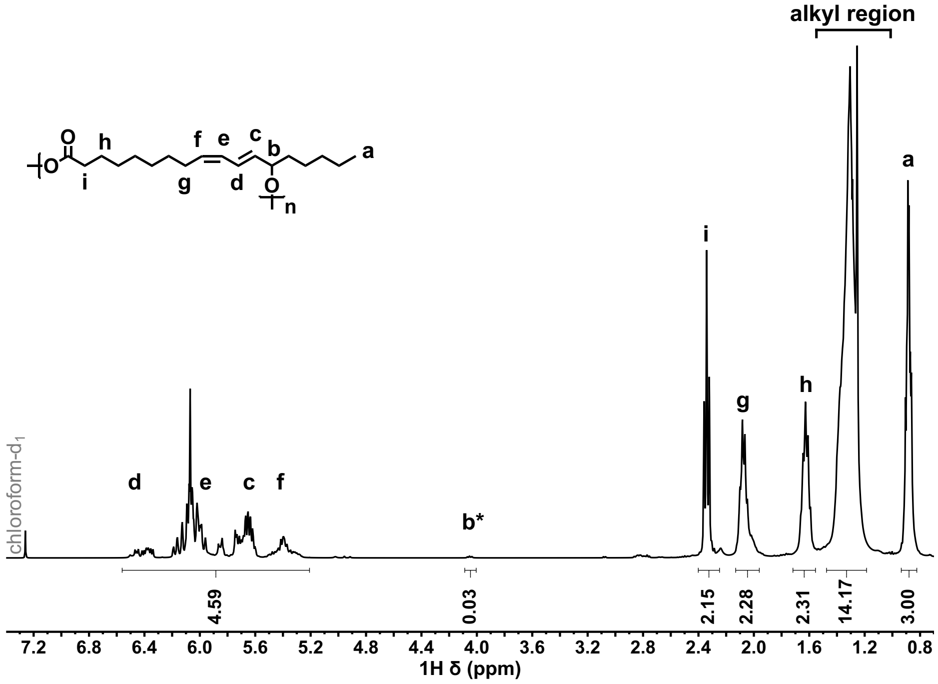

Figure 6.8 – ^{1}H-NMR spectrum of the polymerisation of HA after 19h30m (entry 3 of Table 6.10). The solvent used was chloroform-d$_1$. *Note*: H_b proton as part of the monomer structure is represented as b*; due to overlap of the resonance of proton H_b (upon polymerisation) with the C=C double bonds protons (H_c, H_d, H_e and H_f), his assignment is not represented in the spectra, but it is present in this region 6.50–5-20 ppm;

According to Carothers equation, DP= $^1/_{1\text{-}p}$ (p = conversion), 99% conversion should give a polymer with a molecular weight of 26,000 Da. After 1h and 19h30 reaction, from GPC analysis, polymers with molecular weights of 2,100 and 34,400 Da (respectively) were obtained, both with high dispersities. It is important to note that in step-growth polymerisation, a high molecular weight polymer is only obtained at high conversions (Table 6.11). Monomer conversion is measured by NMR and its limit of detection (LOD) is accurate to 1%. From the Carother's equation it was expected that a 99% conversion, as reported in this work, would produce a theoretical M_n of 26,000 Da. However, from GPC a M_n of 34,000 Da was achieved. This can be explained by examining the influence of conversion on theoretical M_n using the Carothers equation (Table 6.11). Here it is shown that small variances in the conversion

95-99.3% result in a large variation in M_n^{theo}, while the reported conversion would still be 99%.

Table 6.11 – Molecular weight prediction of HA polymer, following Carothers' equation (DP= $^1/_{1-p}$ (p = conversion)), for a condensation polymerisation at 95.0-99.3% monomer conversion.

Entry	Conversion	Conversion (p)	DP	M_n^{theo} (Da)
1	95.0%	0.95	20.00	5,200
2	99.0%	0.99	100.00	26,000
3	99.1%	0.991	111.11	28,900
4	99.2%	0.992	125.00	32,500
5	99.3%	0.993	142.80	37,100

Nevertheless, there are other possible factors that might explain these discrepancies. First, the polymers analysed are crude where no purification steps were performed to remove the presence of low molecular weight fraction of the product mixture. Second, the possible formation of cyclic chains can occur by direct esterification of the end-groups present in this AB-type of monomer or by the transesterification of an OH-end group with a –COO-group present in the (same) polymer chain (back-biting). In order to detect the presence of these possible cyclic structures, the author tried to analyse the polymeric samples through MALDI. Unfortunately, the ionisation of the polymeric samples was not enough to detect a signal. Several matrices were analysed to optimise the ionisation process however, further optimisation of MALDI procedures is required to improve the ion formation pathway. Consequently, the discrepancies found in the M_n calculated through the Carothers equation and through GPC might be related to NMR LOD, the presence of low-molecular weight molecules (oligomers) and the possible formation of cyclic structures.

The Lewis acid catalyst ($Sc(OTf)_3$) has been used for the synthesis of polyesters *via* melt polycondensations of dicarboxylic acid and diols[200, 408] (and polyols[199]), at low temperatures. Using 0.05 mol% $Sc(OTf)_3$ at 60 ºC (under reduced pressure) to condensate adipic acid and 3-methyl-1,5-pentanediol, after 6 hours reaction, a polymer with 1,600 Da ($Đ > 2$) with >99% yield was obtained.[408] Therefore, since $Sc(OTf)_3$ can synthesise polyesters at such low temperatures (from a sustainable point of view this is desirable) the polymerisation of HA catalysed by this scandium catalyst was evaluated.

When using the scandium catalyst, it was found that the lower temperature (60 ºC), the reaction was slower than the polymerisation catalysed with $Sn(Oct)_2$. After two hours' reaction, a polymer with 80% conversion and a molecular weight of 1,200 Da (*Đ* > 2) (entry 5, Table 6.10) was obtained. With a further two hours' polymerisation, a polymer with 90% conversion and a molecular weight of 7,800 Da (*Đ* > 2) was obtained (entry 7, Table 6.10, Figure 6.7). Nevertheless, it is known that, in general, using lower temperatures would not favour the formation of polymers with lower molecular weight.[409-412]

Dynamic mechanical analysis (DMA) was performed to evaluate the thermal properties of these polymers. A low glass transition temperature (T_g) was expected for this polymer structure due to the presence of an alkyl side chain. It is well known that an increase in length of a flexible side chain reduces T_g.[413-414] This effect occurs as a consequence of an increase in the flexibility and volume in between the polymer chains. DMA analysis (Figure 6.9), confirmed the low T_g of these polymers: -23 and -27 ºC (product of the tin and scandium catalysts, respectively, Table 6.10). However, this value might be influenced by the presence of oligomers in the sample. Normally, small molecules are efficient as plasticisers, lowering the T_g of the host polymer.[271-274] Therefore, the T_g measure might be erroneously low because of the presence of the fraction of low molecular-weight chains.

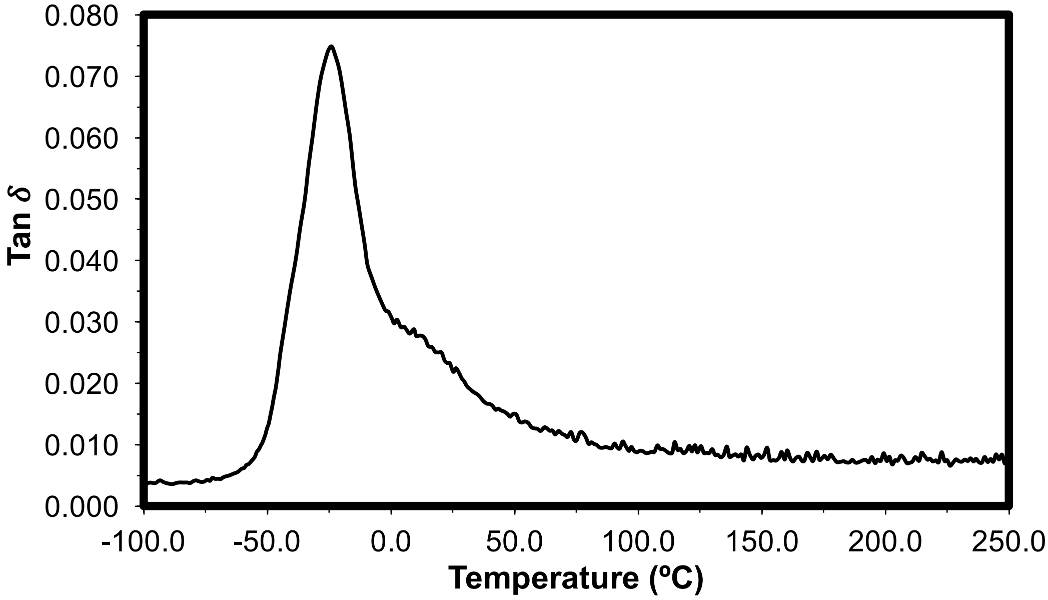

Figure 6.9 – DMA trace showing the T_g of the HA polymer obtained from entry 3, Table 6.10.

6.5.1.2. Polycondensation of (12S,13S,Z)-12,13-dihydroxyoctadec-9-enoic acid (DHA)

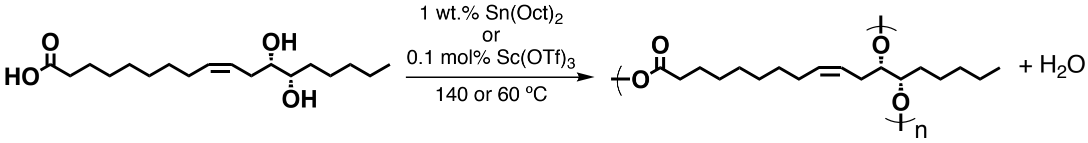

Figure 6.10 – Polycondensation reaction of DHA monomer using 1 wt.% $Sn(Oct)_2$, or 0.1 mol% $Sc(OTf)_3$, at 140 or 60 ºC.

(12S,13S,Z)-12,13-dihydroxyoctadec-9-enoic acid (DHA) was first polymerised, *via* melt condensation, using 1 wt.% $Sn(Oct)_2$ (entries 8-12, Table 6.12) and 0.1 mol % $Sc(OTf)_3$ (entries 13-16, Table 6.12). When using $Sn(Oct)_2$ the polymerisations were conducted at 140 ºC, and at 60 °C when using $Sc(OTf)_3$ as the catalyst. In addition, vacuum was applied to the system, to drive the reaction towards the formation of the product.

DHA is a dihydroxy acid and thus, an AB_2 type monomer which is expected to form a branched polymer. As mentioned in Chapter 3, branched polymers can be synthesised by the polycondensation of AB_n type of monomers, where $n \geq 2$.

The molecular weight of the polymer synthesised using $Sn(Oct)_2$ increases with time, as expected. After a reaction time of seven hours, a soluble polymer with a molecular weight of 8,400 Da ($Đ > 2$) was obtained and, after nearly twenty hours, the polymer was partly insoluble, mostly likely due to cross-linking/branching. Before GPC analysis, the sample needs to pass through a filter and the insoluble polymeric portion might have remained in the filter. Therefore, the GPC results are obtained only from the soluble polymer portion, with a molecular weight of 7,900 ($Đ > 2$). The overlapping of the chemical shifts of protons H_c () and H_d () with the protons H_c and H_d of the monomer, makes it impossible to determine the monomer conversion from ^{1}H-NMR spectroscopy. Nevertheless, the clear broadening of the peaks (Figure 6.12 B)) indicates polymer formation. In addition, since DHA is a AB_2-type monomer, other structures were expected to be obtained (Figure 6.11), and additional chemical shifts were detected in the ^{1}H-NMR spectrum (Figure 6.12

B)). These peaks were identified through COSY-NMR (Figure A 12 in Appendix).

Table 6.12 – Synthesis of DHA polymer *via* melt polycondensation. [a] the overlapping of the chemical shifts of protons H_d and H_c as a monomer and a terminal group of the polymeric chain makes impossible to measure the conversion; [b] these M_n values corresponds to the peaks with higher molecular weights, other peaks were detected in the GPC trace, due to the presence of oligomers; [c] determined by Frey's equation ($DB_{Frey}=\frac{2\times B_0}{2\times B_0+B_1}\times 100$, B_0 = branched structure, B_1 = linear structure). *Note*: nd. = not determined.

	Entry	**Time**	**Conversion**[a]	M_n^{GPC} **(Da)**[b]	**Đ**	**DB**[c]	T_g
Sn(Oct)$_2$	**8**	1 h	nd.[a]	1,100	> 2	27%	–
	9	3 h		1,300	> 2	30%	–
	10	4h30		5,100	> 2	40%	–
	11	7 h		8,400	> 2	41%	–
	12	19h30		7,900	> 2	49%	-23 ºC
Sc(OTf)$_3$	**13**	1 h	nd.[a]	1,100	> 2	–	–
	14	2 h		1,200	> 2	–	–
	15	4 h		1,200	> 2	–	–
	16	5 h		2,900	> 2	–	-38 ºC

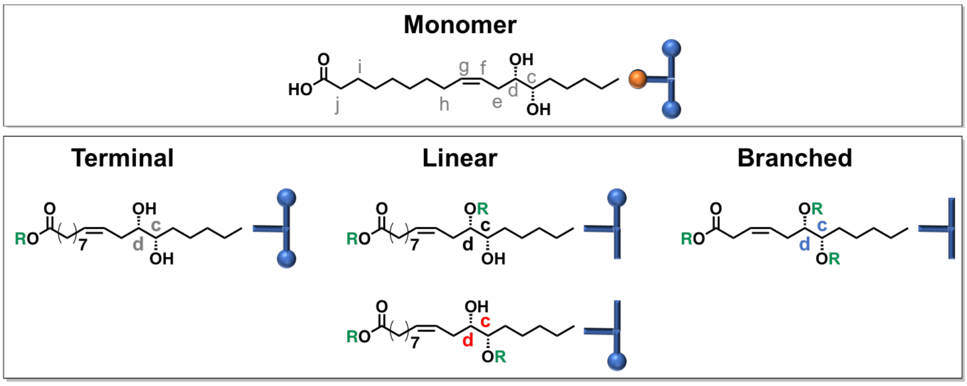

Figure 6.11 – Substitution patterns for the DHA polymer. The schematics next to the structures represent the number of hydroxy groups that reacted (*e.g.* ⊣ corresponds to the linear polymer structure, where a second monomer reacts with proton H_c). *Note:* the blue dot represents an unreacted hydroxyl group, and the orange dot represents an unreacted carboxyl group.

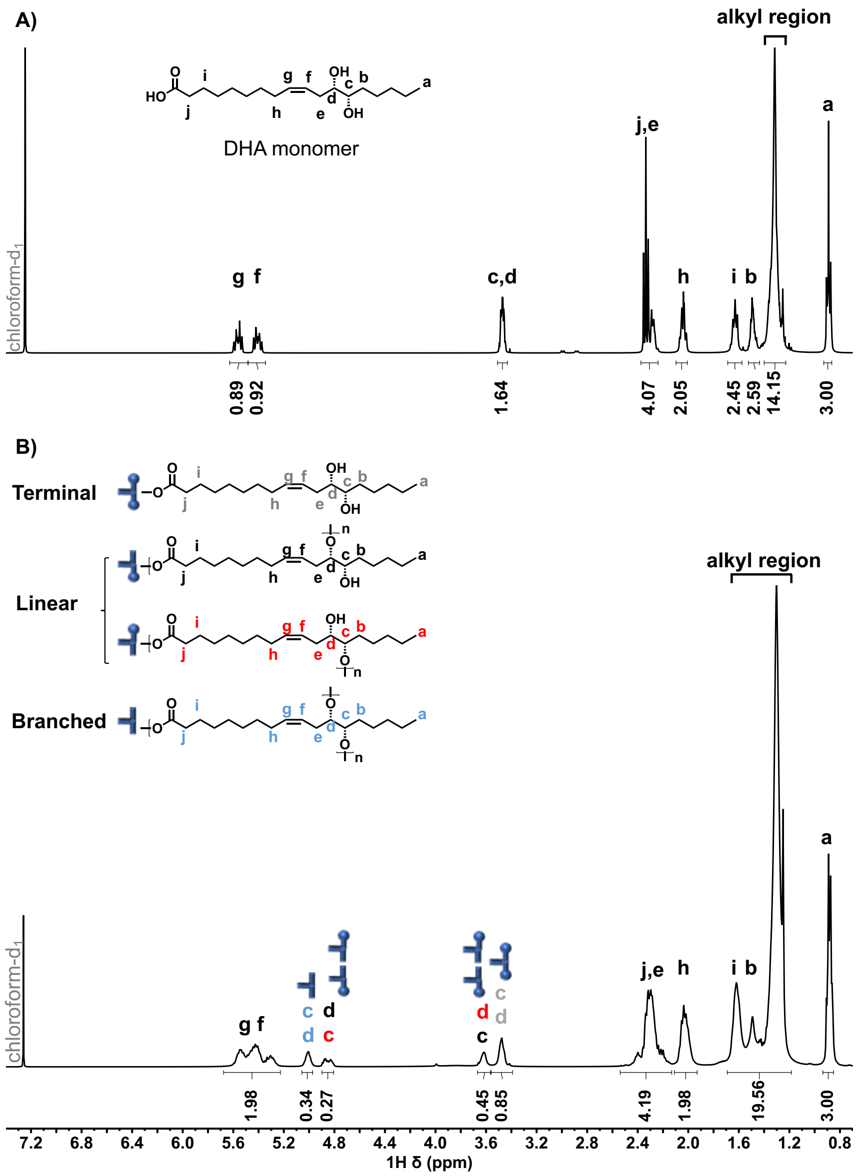

Figure 6.12 – ^{1}H-NMR spectra of the A) DHA monomer and B) branched DHA polymer (entry 12 from Table 6.12), catalysed with Sn(Oct)$_2$ at 140 °C (19h30m reaction time). The solvent used was chloroform-d$_1$.

$$DB_{Frey}=\frac{2\times B_0}{2\times B_0+B_1}\times 100$$

Equation 6.1 – Degree of branching equation defined by Frey.[189-190]

From the NMR spectra obtained (Figure 6.12 and Figure A 12 in Appendix), it was possible to identify that protons H$_c$ and H$_d$ of the terminal unit (┤) are at *ca.* 3.52-3.40 ppm. When the polymerisation occurs, the formation of the ester bond can occur in proton H$_c$ or/and H$_d$, if there is the formation of a linear or branched polymer, respectively. Hence, when the formation of a linear polymer occurs on the hydroxyl group on the vicinity of proton H$_c$ (┤), this proton will shift to *ca.* 4.90-4.80 ppm, and proton H_d (⊣, of the same linear polymer chain), will shift to *ca*. 3.67-3.56 ppm. When the polymerisation of a linear polyester occurs on the hydroxyl group on the vicinity of proton H_d (⊣), this proton will shift to *ca.* 4.90-4.80 ppm, and proton H_c (⊣, of the same linear polymer chain), will shift to *ca*. 3.67-3.56 ppm. When a branched polymer is formed, protons H_c (⊣) and H_d (⊣) shift to at *ca*. 5.05-4.97 ppm. Protons H_g and H_f, corresponding to the C=C double bond, shift to at *ca.* 5.67-5.23 ppm.

To gain a better insight into the polymer structure, the degree of branching (DB) was calculated from ^{1}H-NMR data following Frey's equation (Equation 6.1, introduced in Chapter 3) by integrating the resonances corresponding to the protons H_c and H_d from B_0 (⊣, at *ca.* 5.05-4.97 ppm) and B_1 (⊣ and ⊣, at *ca.* 4.90-4.80 and 3.67-3.56) units. For the DHA polymers synthesised using $Sn(Oct)_2$, DB in the range of 27-49% were obtained (Table 6.12). The formation of branched polymers started early in the polycondensation reaction. From 1 to 3 hours reaction time, the DB increased from 27 to 30% (entries 8 and 9 from Table 6.12). A further reaction increase to 7 and 19.5 h, the branching improved up to 41 and 49%, respectively (entries 10 and 11 from Table 6.12). As expected, using $Sn(Oct)_2$ there was preference for more branched material. Therefore, while the polymer grows, there is the synthesis of linear and branched polymer chains.

When using the $Sc(OTf)_3$ catalyst (0.1 mol%), the polymerisation was performed at a lower temperature of 60 ºC, and the polymerisation rate seems to be slower when compared with the $Sn(Oct)_2$ catalysed reaction. After five hours, a polymer with a molecular weight of 2,900 ($Đ$ > 2) was obtained. Interestingly, the DB was found to dramatically depend on the type of the catalyst used. The polycondensation catalysed with $Sc(OTf)_3$ yielded a linear polymer, with a DB = 0%, at the reaction conditions specified above (Figure 6.13). From the NMR spectrum shown below (Figure 6.13 B)), protons H_c (⊣) and H_d (⊣) at *ca.* 5.05-4.97 ppm are missing, confirming linear polymer.

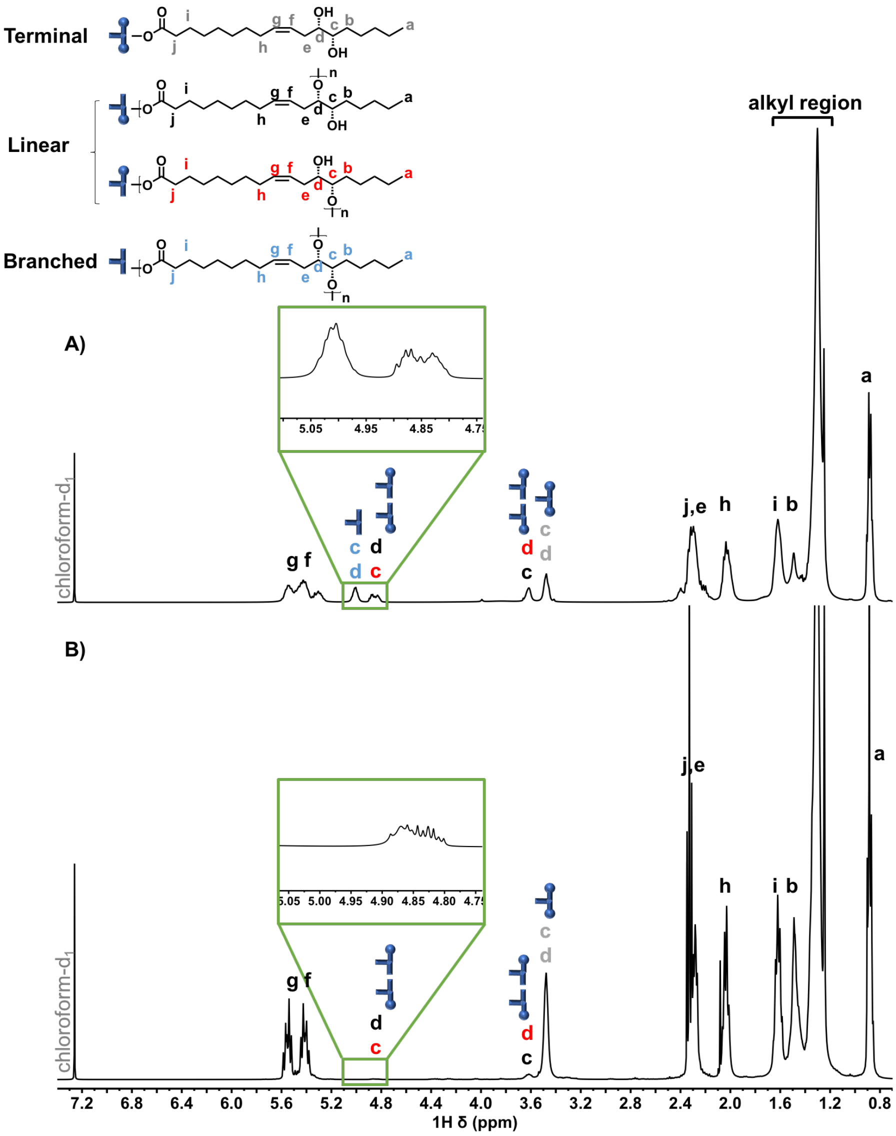

Figure 6.13 – ^{1}H-NMR spectra showing the assignments of the polymeric chains obtained when the polycondensation is catalysed by A) $Sn(Oct)_2$ (polymer from entry 12 Table 6.12) and B) $Sc(OTf)_3$ (polymer from entry 16 Table 6.12). *Note:* the green box is highlighting the region of proton H_c and H_d chemical shifts in a branched (upper spectrum) or linear structure (lower spectrum).

The thermal analysis of DHA polymers was performed using DMA (Figure 6.14). Taking the presence of the pendant alkyl group but also the occurrence of branching into consideration (DB = 49 and 0% when using the $Sn(Oct)_2$ and $Sc(OTf)_3$, respectively), different glass transitions were expected. Sharp peaks at *ca.* -38 and -23 ºC were obtained when using $Sn(Oct)_2$ and $Sc(OTf)_3$, respectively. In addition, a smaller broad 'peak' at 115 ºC was observed, when using the $Sn(Oct)_2$ catalyst. Nevertheless, this latter peak (Figure 6.14), is broad and less intense and could be a result of an artefact present in the sample or could be caused by polymer degradation. However, there is a clear difference in the glass transitions obtained and there are two reasons that might justify this behaviour. Firstly, the difference of the molecular weight of the polymers (7,900 and 2,900 Da) will greatly affect the T_g. The higher the molecular weight, the higher the glass transition. In addition, the degree of branching will increase the entanglements between the polymer chains resulting in a higher T_g. It is also important to note that the polymers are crude, where no purification was made. Therefore, there is still the presence of oligomers, reflected by the high dispersities obtained. Hence, and as mentioned previously, this might affect the measurement of the T_g. Further analysis (such as TGA and further optimisation of DMA parameters) is required to gain a better insight in the thermal properties of the DHA polymer.

Testud, *et al.* [389] investigated the polycondensation of a similar monomer, methyl-9,10-dihydroxystearate (M2HS) using TBD as the catalyst at 170 ºC. In this work, a branched polymer (DB = 41%) with a molecular weight up to 7,600 Da ($Đ$ > 12) was obtained. This polymer had a T_g of -22 ºC, which is in accordance with what was obtained in this Thesis.

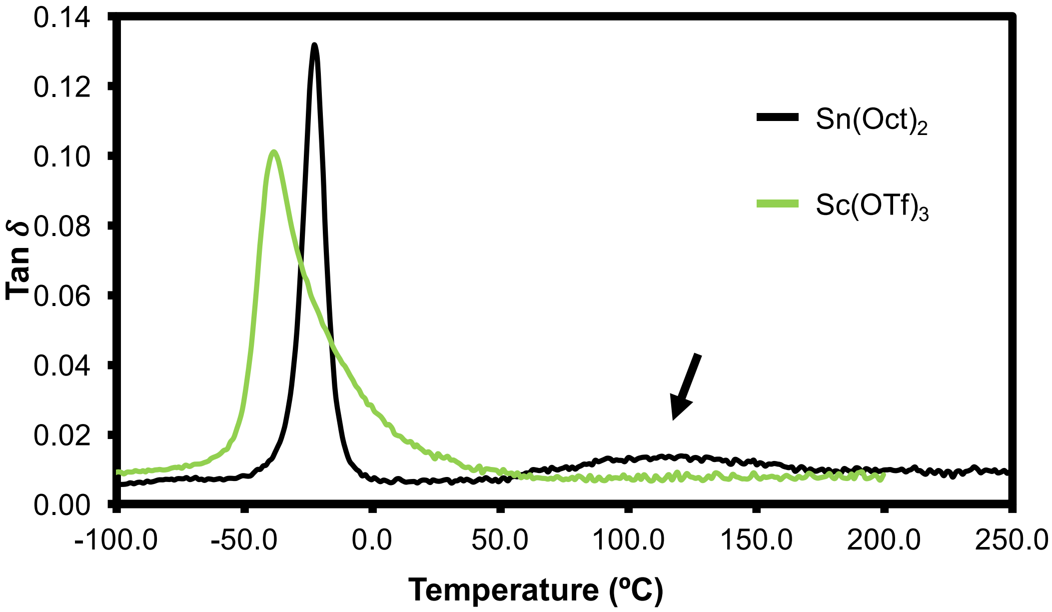

Figure 6.14 – DMA traces showing the T_g of the DHA polymers, catalysed by $Sn(Oct)_2$ and $Sc(OTf)_3$, corresponding to entries 12 and 16 of Table 6.12.

6.5.1.3. Polycondensation of dodec-2-ene-1,12-diol (DED) and azelaic acid (AZ)

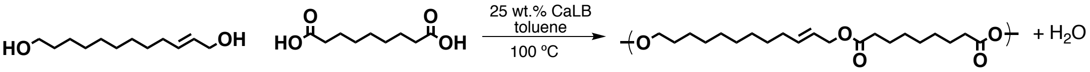

Figure 6.15 – Polycondensation reaction of DED with AZ 25 wt.%[†††] CALB at 100 ºC in toluene.

The polycondensation of dodec-2-ene-1,12-diol (DED) with azelaic acid (AZ) was accomplished *via* condensation using 25 wt.%[‡‡‡] CaLB in the presence of molecular sieves and toluene, under an argon atmosphere (entries 17-21, Table 6.13). AZ (T_m ~ 110 ºC) is a natural occurring dicarboxylic acid, in which can be found in wheat, rye and barley.[415-416] It is important to mentioned that the DED used for the melt polycondensation is not pure. As mentioned previously, from the reduction of (E)-12-oxododec-10-enoic acid (compound **(69)** from the previous chapter) a mixture of two diols (compounds **(70)** and **(71)** from the previous chapter), were produced (see section 5.5.3.5 of this Thesis). Therefore, the monomer used is a mixture of two diols, with and without the double bond. Nevertheless, to simplify the nomenclature, DED refers to the mixture of diols (Figure 6.16).

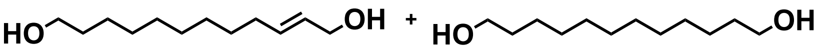

DED monomer

Figure 6.16 – Schematic representation of the structure of the DED monomer use, which is a mixture of two diols.

The DED and AZ were first reacted at 55-60ºC in toluene for one hour, under an argon atmosphere, for mixing. Only then, CaLB was added to the system and the temperature raised to 100 ºC. Normally, this two-step procedure allows the synthesis of high molecular weight polymer.[224] As discussed in more detail in Chapter 3, CaLB is more reactive towards primary alcohols.[150, 204-206] Hence, since DED possesses primary hydroxyl groups, CaLB is expected to efficiently catalyse the polycondensation.

After 4 hours, a polymer with 75% monomer conversion and a molecular weight of 4,600 Da ($Đ > 2$) was obtained (entry 18, Table 6.13). Increasing the reaction time to 46 hours, resulted in a liquid orange polymer with a M_n of

---

[†††] Includes polymer support

5,500 Da (*Đ* > 2, 87% monomer conversion) (entry 21, Table 6.13). This increase of only ~1,000 Da in molecular weight when increasing the reaction time to 46 hours certainly indicates that the polymerisation process is slow. This could be due to catalyst deactivation at the reaction temperature, resulting in a decrease in the activity of the enzyme. For example, Taresco*, et al.* [222] found that at higher reaction temperatures polymers with lower molecular weight are formed in the enzymatic (CaLB) polycondensation of glycerol with adipic acid. In addition, the possible formation of cyclic structures might be another factor. To check the presence of these structures, MALDI analysis were performed. Unfortunately, the ionisation of the polymer was not effective and MALDI could not shed light the process.

Table 6.13 – Polycondensation of dodec-2-ene-1,12-diol (DED) with azelaic acid (AZ) in toluene using CaLB as the catalyst. [a] The conversion was calculated through NMR, using the integration of proton Hf (of the monomer) against the integration of protons H_b and H_c; [b] these M_n values corresponds to the peaks with higher molecular weights, other peaks were detected in the GPC trace, due to the presence of oligomers; [c] it was not possible to determine the conversion due to the presence of solvent in the sample.

	Entry	**Time**	**Conversion[a]**	**M_n^{GPC} (Da)[b]**	**Đ**	**T_g**
CaLB	**17**	2 h	nd.[c]	4,300	> 2	–
	18	4 h	75%	4,600	> 2	–
	19	20 h	82%	4,800	> 2	–
	20	26 h	84%	5,100	> 2	–
	21	48 h	87%	5,500	> 2	-5 ºC

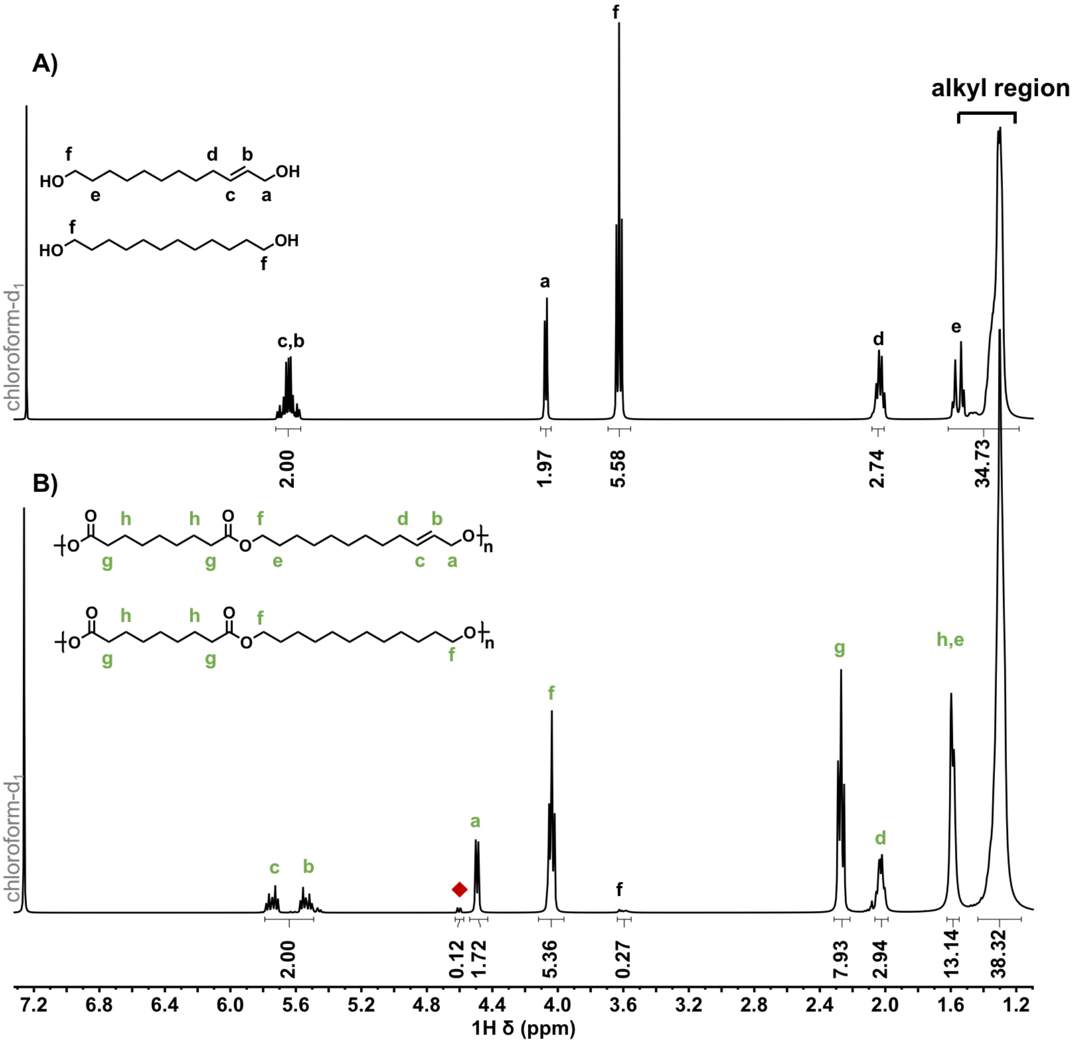

Figure 6.17 – ^{1}H-NMR spectrum of the A) DED monomer (mixture of diols) and the B) linear DED-AZ polymer (entries 21 from Table 6.13), catalysed with CaLB at 100 ºC (48h reaction time). The solvent used was chloroform-d_1. *Note*: ◆ it is an unknown doublet peak. *Note*: the black protons letters are assigned to the monomer structures, and the green to the polymers.

From ^{1}H-NMR analysis it was possible to see the formation of polymer (Figure 6.17). A clear shift of the resonances of protons H_a and H_f was observed upon polymerisation, *i.e.* upon formation of the ester bond. The triplet corresponding to proton H_f, shifted from 3.57 ppm to 4.04 ppm. Likewise, the doublet corresponding to proton H_a, shifted from 4.06-3.99 ppm to 4.53-4.47 ppm. The assignment of protons H_c and H_b was possible after COSY analysis (Figure A 11 shown in Appendix). Also through ^{1}H-NMR analysis it was confirmed that both diols (from DED monomer) contributed to polymer formation (Figure 6.17). The integration of the peak at *ca.* 2.31-2.21 ppm (which corresponds to protons H_g, upon polymerisation) corresponds to 7.93. If there was only one mixture of the diol, this integration should be 4.

The thermal analysis of the DED-AZ polymer was performed by DMA. A higher T_g was expected to obtain than for the DHA and HA polymers as a consequence of the linearity of the DED-AZ polymer. A T_g of -5 ºC was observed, which confirms our hypothesis (Figure 6.18). Nevertheless, the presence of oligomers (since no purification was performed after polymerisation and it is confirmed by the high dispersity obtained by GPC analysis) might decrease the actual T_g value of the polymeric chain.

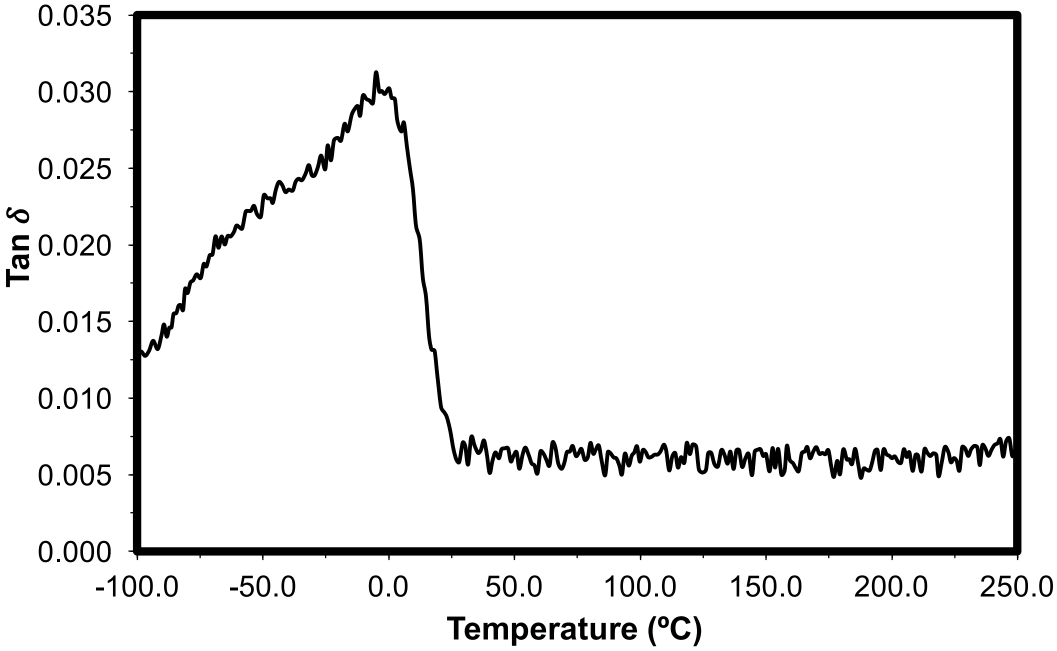

Figure 6.18 – DMA trace of the DED-AZ polymer (entry 21, Table 6.13) showing a T_g of -5 °C.

6.5.2. Polycondensation of vernonia-based monomers in supercritical carbon dioxide

To the best of the author's knowledge, this is the first time that the synthesis of polyesters from vernonia-based monomers has been attempted under $scCO_2$ conditions, using milder conditions than the ones applied in melt polycondensation (described above).

6.5.2.1. Behaviour of the vernolic acid derived monomers in supercritical carbon dioxide

(S,9Z,11E)-13-hydroxyoctadeca-9,11-dienoic acid (HA) and (12S,13S,Z)-12,13-dihydroxyoctadec-9-enoic acid (DHA) were exploited as building blocks for the formation of HA and DHA polymers in $scCO_2$. Therefore, the interaction of these monomers with $scCO_2$ was investigated.

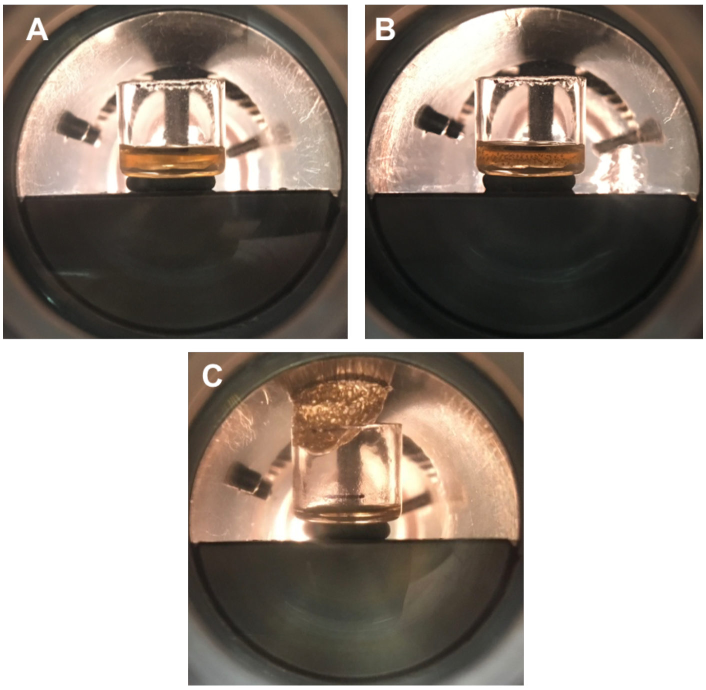

Figure 6.19 – Visual observation of HA monomer at **A)** ambient pressure (1 bar) and temperature (25 ºC), **B)** at 200 bar and 95 ºC and **C)** at ambient pressure (1 bar) and temperature (25 ºC) upon removal of the CO_2 (after 7 hours under pressure). The same observations were made for the DHA monomer.

There is a clear difference before, during and after exposure of HA monomer to $scCO_2$ (Figure 6.19). The presence of bubbles in the monomer HA (Figure 6.19 B)) is an indication that $scCO_2$ is soluble in HA. In addition, upon removal of CO_2 (Figure 6.19 C)), the HA monomer was pulled out of the vial to the view cell's internal walls. This occurred as a consequence of the release of CO_2 from the HA molecules. The same behaviour was observed for the (12S,13S,Z)-12,13-dihydroxyoctadec-9-enoic acid (DHA) monomer.

This view cell investigation demonstrates a clear interaction of $scCO_2$ with the monomers, where $scCO_2$ is soluble in HA.

6.5.2.2. Polycondensation of (S,9Z,11E)-13-hydroxyoctadeca-9,11-dienoic acid

The polymerisations of HA were conducted for 3, 6 and 24 hours at 200 bar and 95 ºC with 1 wt.% $Sn(Oct)_2$ as the catalyst (Table 6.14). Because of the low amount of HA monomer available and since polymerisations using $Sc(OTf)_3$ as the catalyst yielded a polymer with low monomer conversion contributing to polymers with lower M_n in the melt, $Sn(Oct)_2$ was chosen as the catalyst for the polycondensation of HA under $scCO_2$ conditions. ^{1}H-NMR spectra of the HA polymers are shown below (Figure 6.20).

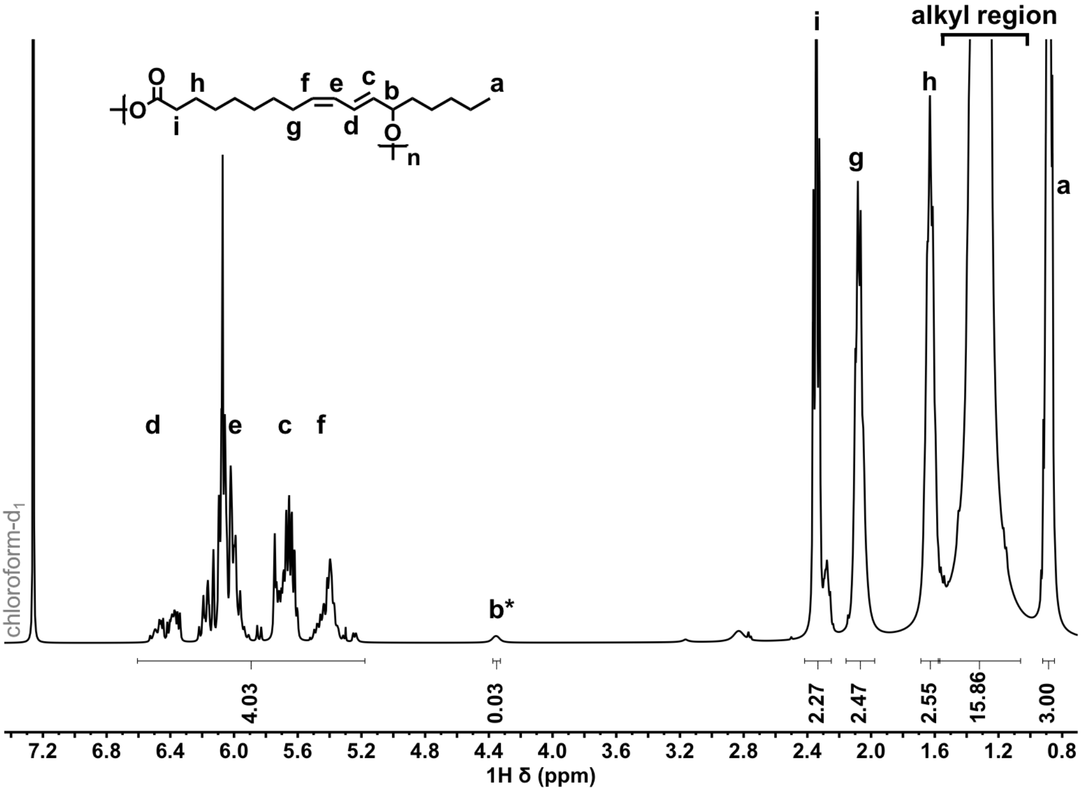

Figure 6.20 – ^{1}H-NMR spectrum of HA polymer synthesised using $Sn(Oct)_2$ at 95 ºC and 200 bar for 24 hours (entry 24 from Table 6.14). The solvent used was chloroform-d_1. *Note*: H_b proton as part of the monomer structure is represented as b*; due to overlap of the resonance of proton H_b (upon polymerisation) with the protons in the vicinity of the C=C double bonds (H_c, H_d, H_e and H_f), this assignment is not represented in the spectra, but it is present in this region: 6.50–5-20 ppm.

Table 6.14 – Synthesis of (S,9Z,11E)-13-hydroxyoctadeca-9,11-dienoic acid (HA) conducted *via* $scCO_2$ at 275 bar and 95 ºC. [a] Monomer conversion was determined by NMR, by the ratio between the integrations of proton H_b (as monomer) and proton H_a; [b] these M_n values corresponds to the peaks with higher molecular weights, other peaks were detected in the GPC trace, due to the presence of oligomers.

Entry	**Time**	**Conversion**[a]	**M_n^{GPC} (Da)**[b]	**$Đ$**	**T_g**
22	3 h	97%	7,700	> 2	-26 ºC
23	6 h	97%	9,800	> 3	-20 ºC
24	24 h	99%	63,000	> 3	-31 ºC

After 3, 6 and 24 hours reaction, polymers with a molecular weight up to 7,700 ($Đ$ > 2), 9,800 ($Đ$ > 2) and 63,000 ($Đ$ > 3) were obtained (Table 6.14). The broad dispersity obtained in all these polymerisations was the result of the presence of a large portion oligomers (Figure 6.21). When comparing the polycondensations conducted in $scCO_2$ and in the melt, the same trends are observed and the evolution of the M_n with increasing reaction time is very similar.

As mentioned previously, in the melt condensation, at the last stage of the polycondensation reaction, a small change in the conversion will result in a large increase in the molecular weight of the polymer. According to Table 6.11, where it shows the prediction of HA polymer following Carothers' equation, a 99% conversion should result in a polymer with M_n^{theo} of 26,000 Da. However, a polymer with 99% conversion (as reported here and measured by NMR) and a molecular weight of 63,000 Da was obtained. Since monomer conversion is determined by NMR and its LOD is accurate to 1%, the conversion may not be entirely representative for this reaction.

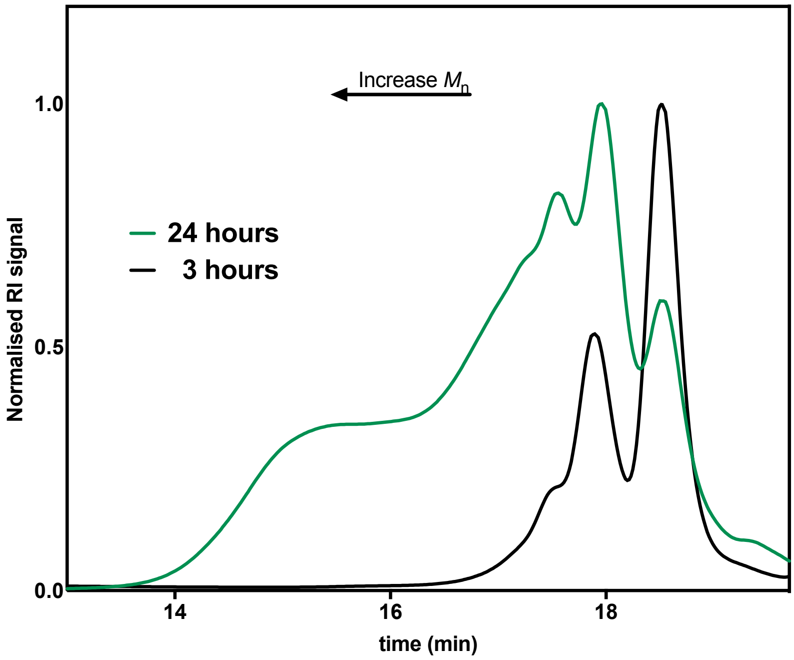

Figure 6.21 – GPC traces of the HA polymers synthesised using $Sn(Oct)_2$ at 95 ºC and 200 bar for 3 and 24 hours (entries 22 and 24 from Table 6.14, respectively).

With respect to the thermal properties, a lower T_g (-31 ºC) was obtained for the HA polymer when using $scCO_2$ as reaction medium as compared to the melt polymerisation (-23 ºC, after 19h30m) after a reaction time of 24 h. Even though a low T_g was expected due to the polymer structure (presence of a pendant alkyl group), after 24 hours polycondensation with $scCO_2$, a polymer with M_n up to 63,000 Da was obtained. This polymer has higher molecular weight than the polymer obtained in melt conditions (34,400 Da; T_g = -23 ºC). Hence, a higher T_g than -23 ºC was predicted but -31 ºC was obtained (Figure 6.22). Normally, small molecules (*e.g.* oligomers) are efficient as plasticisers, having the ability in lowering the T_g of the host polymer.[271-274] The HA polymer synthesised in $scCO_2$ showed a broader dispersity ($Đ$ > 3) than the HA polymer synthesised in the melt conditions ($Đ$ > 2). The presence of more oligomeric chains might be the cause of this lower T_g. Nevertheless, the observed range of glass transition temperatures is in agreement with what has been published previously for similar polyesters.[417-418]

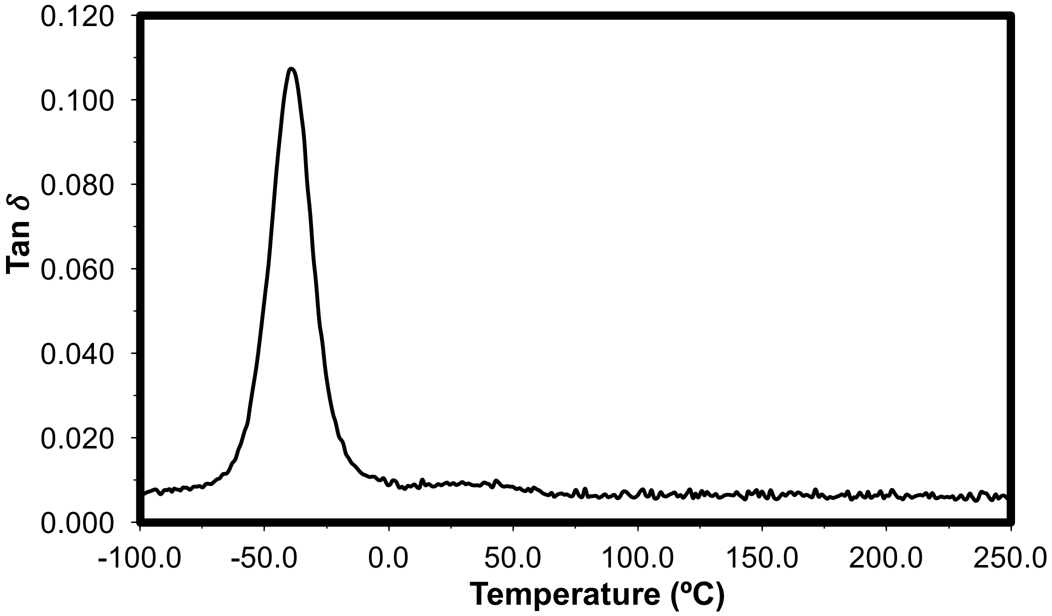

Figure 6.22 – DMA trace showing the T_g of the HA polymer obtained from entry 24, Table 6.14.

6.5.2.1. Polycondensation of (12S,13S,Z)-12,13-dihydroxyoctadec-9-enoic acid (DHA)

The polymerisation of the DHA polymer was accomplished under similar conditions to the HA polymer (200 bar, 95 ºC with 1wt.% $Sn(Oct)_2$) for 3, 6 and 24 hours. The ^{1}H-NMR spectra of the DHA polymers are shown below (Figure 6.23).

As mentioned previously, DHA is an AB_2 type monomer which could lead to the formation of a branched polymer. After a reaction time of 6 hours, only oligomers were observed (M_n = 800 Da, Figure 6.23 A)). Nevertheless, after 24h, a polymer with a molecular weight of up to 5,900 Da ($Đ > 2$) was obtained. From ^{1}H-NMR analysis (Figure 6.23) it was possible to observe polymer formation by the broadening of the signals for the sample obtained after 24 hours of polycondensation (Figure 6.23 B)).

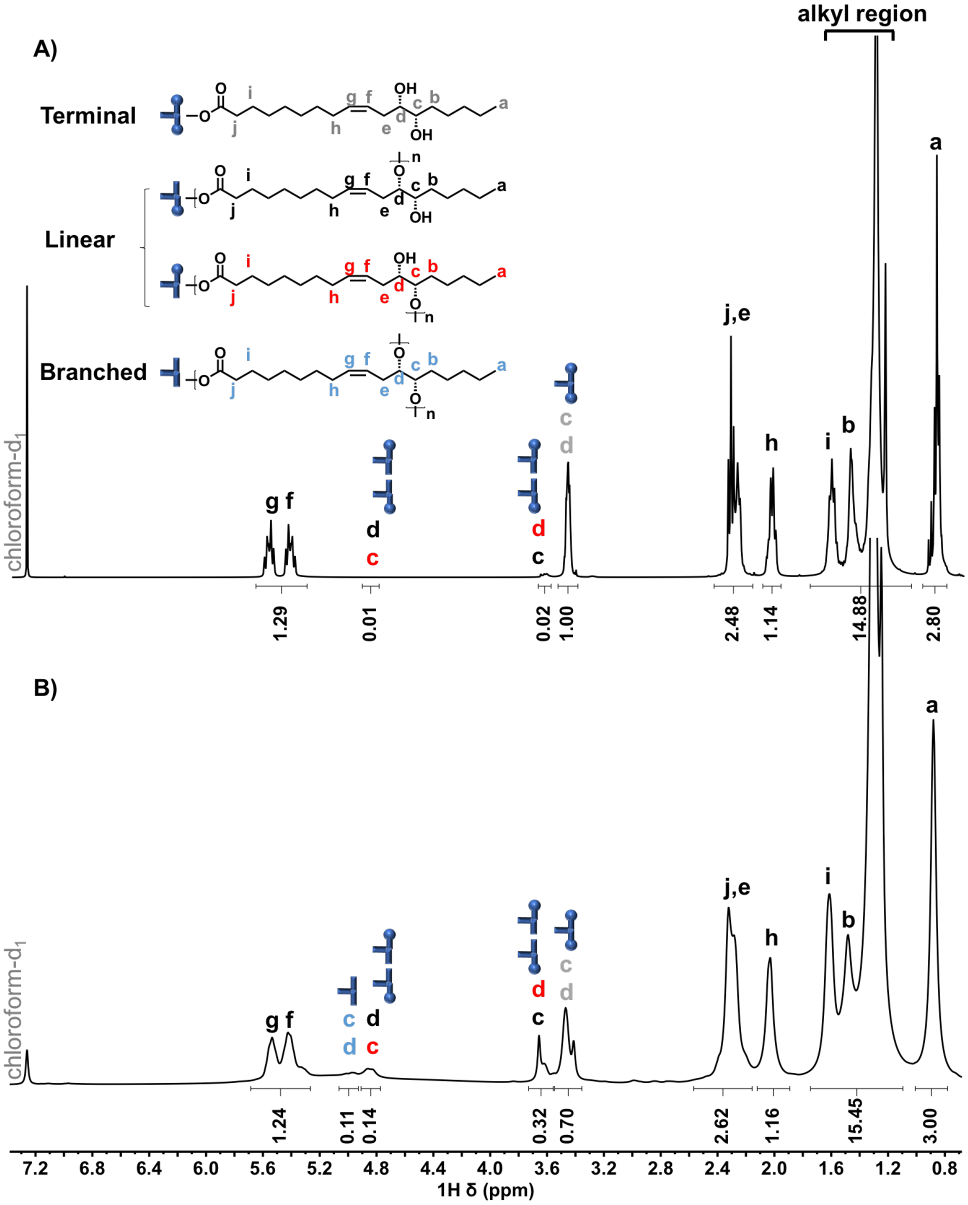

Figure 6.23 – ^{1}H-NMR spectra of DHA polymers catalysed with $Sn(Oct)_2$, at 95 ºC and 200 bar for A) 6h and B) 24 hours (Table 6.15). The solvent used was chloroform-d_1.

Table 6.15 – Synthesis of DHA polymers in $scCO_2$ at 275 bar and 95 ºC. [a] the overlapping of the chemical shifts of protons H_d and H_c as a monomer and a terminal group of the polymeric chain makes impossible to measure the conversion; [b] these M_n values corresponds to the peaks with higher molecular weights, other peaks were detected in the GPC trace, due to the presence of oligomers; [c] determined by Frey's equation ($DB_{Frey}=\frac{2\times B_0}{2\times B_0+B_1}\times 100$, B_0 = branched structure, B_1 = linear structure). *Note*: nd. = not defined.

Entry	**Time**	**Conversion**[a]	M_n^{GPC} **(Da)**[b]	$Đ$	**DB**[c]	T_g
25	3 h	nd.[a]	800	1.9	0%	-37 ºC
26	6 h		800	1.9	0%	-32 ºC
27	24 h		5,900	> 2	24%	-30 ºC

The degree of branching was calculated by integrating the ^{1}H-NMR resonances corresponding to protons H_c and H_d from B_0 (⊣) and B_1 (⊣and⊣) structures, and applying Frey's equation (Equation 6.1). The chemical shifts used were the same as described previously for the polymerisation of DHA in the melt (see above).

The formation of a branched polymer was only detected after a reaction time of 24 hours with a DB of 24% (Figure 6.23 B)), whilst the other products obtained after shorter reaction times, only oligomers were obtained with no branching pattern.

The thermal properties of the DHA oligomers and polymer were determined by DMA (Figure 6.24). After 3h, 6h and 24h polycondensation, low T_g's of -37, -32 and -30 ºC were obtained. A higher T_g was expected to obtain after 24h reactions, not only due to higher M_n (5,900 Da) but also because of DB (24%). This low T_g, obtained after 24h reaction, could be a result of the presence of oligomeric chains.

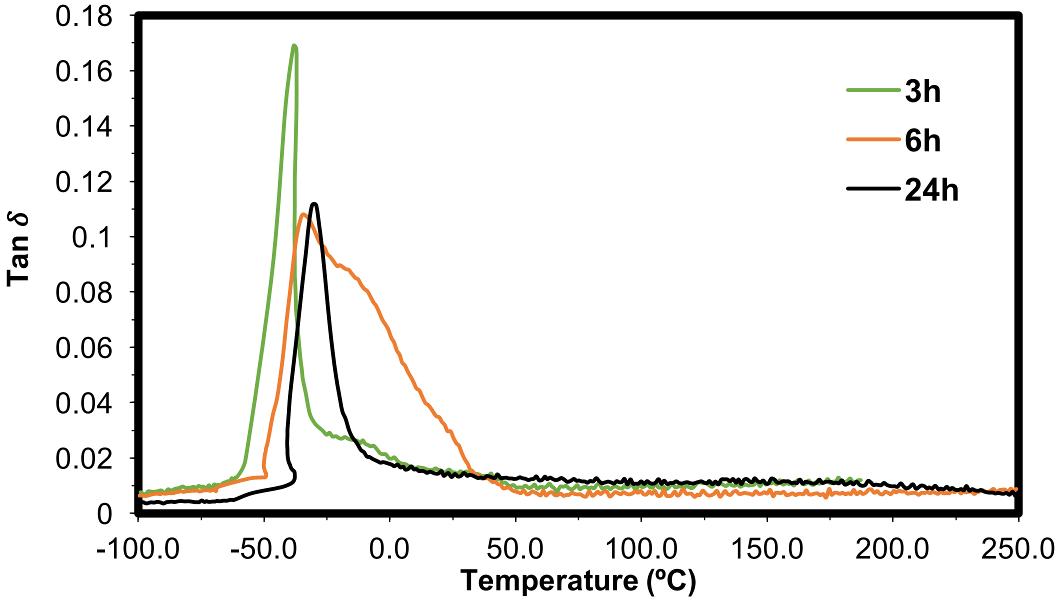

Figure 6.24 – DMA trace showing the T_g's of the DHA polymers obtained after 3 (green line), 6 (orange line) and 24 (black line) hours of polycondensation (Table 6.15).

6.5.2.2. Polycondensation of dodec-2-ene-1,12-diol and azelaic acid

The polycondensation of dodec-2-ene-1,12-diol (DED) with azelaic acid (AZ) was performed in $scCO_2$, using 25 wt.%[‡‡‡] CaLB in the presence of 25 wt.% molecular sieves at 35 ºC and 275 bar (Table 6.16). In contrast to the polycondensation in toluene (two-step procedure), the polymerisation using $scCO_2$ is a one-pot reaction at a lower reaction temperature. In addition, the DED monomer used for the polycondensation reaction is pure, confirmed by the integration of proton Hf (Figure 6.26). The integration of proton Hf (4.09-4.01 ppm) is 2.15, which corresponds to 2 protons. If there was a mixture, this peak would detect the presence of 6 protons and hence, the integration would be 6, as seen previously (Figure 6.17 and Figure 6.25).

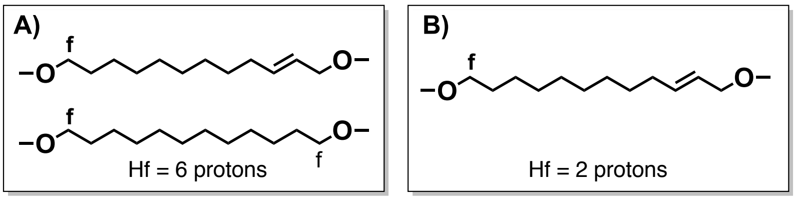

Figure 6.25 – Representation of the number of Hf protons of DED in the polymer backbone when in the presence of A) DED as mixture and B) DED pure.

[‡‡‡] including support

After 24 hours, a polymer with 88% monomer conversion and a molecular weight of 2,300 Da ($Đ > 2$) was obtained. This corresponds to only half of the molecular weight obtained through melt condensation but may be the result of the lower temperatures of system, 35 °C compared to the 100 °C used previously. It is well known that increasing the reaction temperature will favour the synthesis of polymers with high molecular weight (in polycondensation reactions).[409-412] Therefore, using a lower reaction temperature, obtaining a polymer with lower M_n was expected.

Table 6.16 – Polycondensation of dodec-2-ene-1,12-diol (DED) with azelaic acid (AZ) in $scCO_2$, at 275 bar and 35 °C. [a] The conversion was calculated through NMR, using the integration of proton H_f (of the monomer) against the integration of protons H_b and H_c; [b] these M_n values corresponds to the peaks with higher molecular weights, other peaks were detected in the GPC trace, due to the presence of oligomers.

Entry	Time	Conversion[a]	M_n^{GPC} (Da)[b]	$Đ$	T_g
28	24 h	88%	2,300	> 2	-11 °C

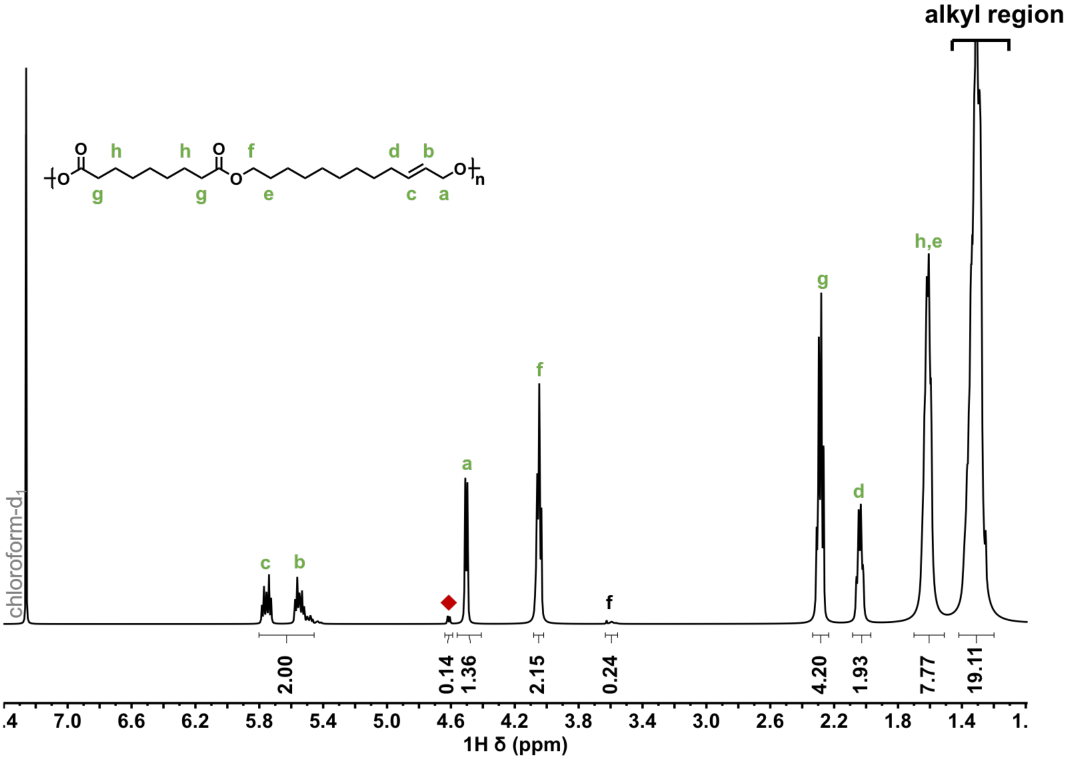

Figure 6.26 – ^{1}H-NMR spectra of the linear DED-AZ polymer (Table 6.16), catalysed with CaLB at 35 °C and 275 bar (24h reaction time). The solvent used was chloroform-d_1. *Note*: ◆ it is an unknown doublet peak. *Note*: the black protons letters are assigned to the monomer structures, and the green to the polymers.

There are limited examples on the literature showing the synthesis of polyesters, *via* the polycondensation of a dicarboxylic acid and diol, at temperatures below 40 °C. As an example, Iglesias, *et al.* [204] performed the enzymatic (CaLB) polycondensation of glycerol and adipic acid (in dioxane) at 30 ºC yielding a linear polyester after 72 hours with a molecular weight of 1,400 Da (DP = 5). In this work, after 24 hours reaction under supercritical conditions, at 35 ºC, a polymer with 2,300 Da (DP = 7) was obtained. This corresponds to polymer with ~1,000 Da more in M_n than the one obtained by Iglesias*, et al.* [204], after 72 hours. Therefore, $scCO_2$ plays a crucial role in the polymerisation of dicarboxylic acid and diols, *via* polycondensation.

The thermal properties of the DED-AZ polymer were evaluated by DMA and a T_g of -11 ºC was determined, which is a similar result to the polymer obtained by the condensation in the presence of toluene (-5 ºC). Nevertheless, two other broad peaks were detected at around -40 ºC and at 93 ºC. The former one might be due to the presence of a small portion of low-molecular weight molecules which might act as plasticizers. The later one, might be a result of polymer degradation or the presence of an impurity in the sample. Additional analysis, such as TGA and optimisation of the DMA parameters, are required to understand the thermal properties of this polymer.

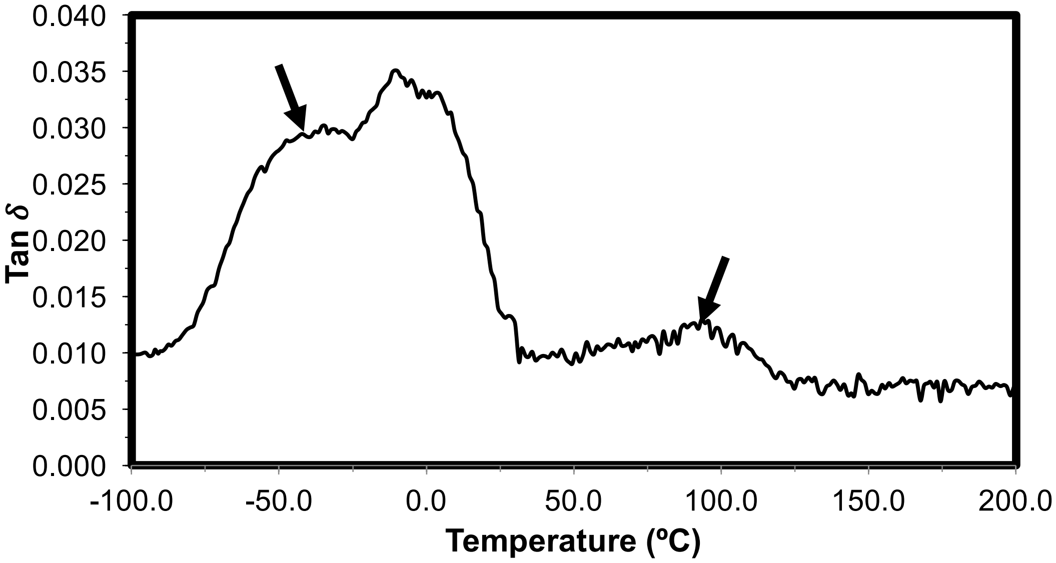

Figure 6.27 – DMA trace showing the T_g of the DED-AZ polymer obtained from Table 6.16.

6.6. Conclusions

This chapter demonstrates the polymerisation of the monomers synthesised from vernolic acid, which was isolated from the oil extracted from the *Vernonia galamensis* sp. seeds (Chapter 5). The main aim of this project was to establish the green synthesis of vernonia-based monomers to use as building blocks: (S,9Z,11E)-13-hydroxyoctadeca-9,11-dienoic acid (HA), (12S,13S,Z)-12,13-dihydroxyoctadec-9-enoic acid (DHA), dodec-2-ene-1,12-diol (DED) and the commercially available azelaic acid (AZ). Therefore, two different approaches were used:

a) The polymerisation reactions of HA and DHA monomers were conducted *via* melt condensation in the presence of $Sn(Oct)_2$ (at 140 ºC, for 19h30m) and $Sc(OTf)_3$ (at 60 ºC, for 5h). The polymerisation of DED and AZ was accomplished *via* enzymatic (CaLB) polycondensation, in toluene (at 100 ºC, for 48h).
b) Using $scCO_2$, the polycondensation of HA and DHA was accomplished using $Sn(Oct)_2$ at 95 ºC (for 3, 6 and 24h) and the enzymatic (CaLB) polycondensation between DED and AZ was accomplished at 35 ºC, for 24h.

The HA melt polycondensation using the Stannous catalyst showed better results in comparison with the Scandium. Using $Sn(Oct)_2$, after 4h30m, a polymer with 99% conversion and a molecular weight of 11,600 Da was obtained. Whilst with $Sc(OTf)_3$, after 4h, a polymer with 90% conversion and a M_n of 7,800 Da was accomplished. The thermal properties of both polymers were similar (-23 and -27 ºC) although, due to the presence of oligomers in the polymeric samples, they may act as plasticisers lowering the T_g of the polymer.

The same conclusions were obtained with regards the melt condensation of the DHA polymer using $Sn(Oct)_2$ and $Sc(OTf)_3$. After 4h30m, the former catalyst yielded a polymer with a molecular weight of 5,100 Da and with the later one, after 5h, a polymer with a M_n of 2,900 was obtained. In addition, having into consideration that DHA is a AB_2-type monomer, a branched polymer was expected to obtain. Nevertheless, using the Scandium catalyst, after 5h reaction no branching was detected while using the Stannous catalyst, after 4h30m reaction time, a DB of 40% was obtained. With regards the melt properties of these polymers, there are a few factors that might influence the T_g. If, from one hand, the presence of the alkyl chain would decrease the entanglement between the polymer chains (leading to a low glass transition), as a branched material, the entanglement should be high (leading to a higher glass transition). After DMA analysis, the polymer catalysed by $Sn(Oct)_2$ obtained a Tg of -23 ºC and the one catalysed by $Sc(OTf)_3$, -38 ºC. Testud*, et al.* [389] studied the polycondensation of a similar monomer (DB = 41%, 7,600 Da, *Đ* > 12) and a T_g of -22 ºC was obtained, which is in accordance with what was obtained in this Thesis. Therefore, the influence of the DB is visible since the polymer catalysed with the Scandium catalyst, where no branching was detected, a T_g of -38 ºC was obtained.

The polycondensation between DED and AZ was achieved by using CaLB as a bio-catalyst, at 100 ºC in toluene. It was observed a possible deactivation of the enzyme, triggered by the reaction temperature since after 20 and 48h reaction (82 and 87% monomer conversion), polymers with a molecular weight of 4,800 and 5,500 Da were obtained, respectively. It is important to emphasised that this polymer had a mixture of two different diols. As mentioned in Chapter 5, the synthesis of DED monomer resulted in a mixture of dodecane-1,12-diol and dodec-2-ene-1,12-diol. Through NMR analysis it was possible to detected the presence of these two monomers in the polymer structure. Considering the thermal analysis, a higher T_g was predicted to obtain than HA and DHA because in the DED-AZ polymer, there is no presence of the pendant alkyl chain. A glass transition of -5 ºC was obtained, which confirmed our hypothesis.

When using $scCO_2$, the polycondensations of HA and DHA were catalysed using $Sn(Oct)_2$ at 95 ºC and 200 bar, for 3, 6 and 24h. It was noticed that with increase of the reaction time there was an increase of the polymer M_n, which was expected. After 24 hours, a HA-polymer with a molecular weight of 63,000 Da, with high dispersity (*Đ* > 3) was obtained. In addition, a DHA-polymer with

5,9000 Da was obtained after 24 hours. The thermal properties (T_g) of HA and DHA polymers synthesised in $scCO_2$ agreed with the polymers synthesised in melt conditions.

The $scCO_2$ polycondensation of DED (pure) and AZ was accomplished at 35 ºC and 275 bar. A polymer with 88% conversion and a molecular weight of 2,300 Da ($Đ > 2$) was obtained after 24 hours' reaction. Although a lower M_n was obtained in $scCO_2$ than in toluene (5,100 Da, after 25 hours' reaction), the reaction temperature in $scCO_2$ was 35 ºC while in the solvent was at 100 ºC. Using a lower reaction temperature might lead to lower molecular weight polymer. With regards to the thermal properties, a T_g of -11 ºC was obtained.

Using $scCO_2$ as reaction medium was revealed to be a good approach to polymerise vernonia-based monomers since lower temperatures were used. Dropping the polymerisation temperatures from 140 ºC to 95 ºC (for the synthesis of HA and DHA polymers) and 100 ºC to 35 ºC (for the synthesis of DED-AZ polymers) has a dramatic effect. Using lower temperatures would be more energetically sustainable than the melt synthesis or in toluene. Nevertheless, the major drawback of this process, is the need to use toxic solvent (THF), although in a small amount, to separate the polymer from the molecular sieves and/or the enzyme beads.

CHAPTER 7. CONCLUSIONS AND FUTURE WORK

7.1. Overview

The final chapter reviews the general conclusions obtained from the research presented in this Thesis. Additionally, this chapter also discusses the possible future research that could be carried out for the continuation of the work.

7.2. Conclusions

The main focus of this Thesis has been to synthesise polyesters using renewable resources and green methodologies, targeting mild conditions and energy saving approaches that exploit supercritical carbon dioxide ($scCO_2$).

7.2.1. The glycerol opportunity

Generally, the synthesis of linear polyesters from multifunctional monomers (*e.g.* polyols, A_n-type monomers, where $n > 2$) is achieved by applying elaborate protection-deprotection steps, to avoid undesirable reaction of hydroxy functional groups. In addition, the synthesis of polymers from glycerol and diacid, e.g. poly(glycerol succinate) (PGLSA), would be normally conducted at high temperatures (> 150 ºC) due to the high melting points of diacids and the increase in viscosity during polymerisation. In this Thesis, the synthesis of linear PGLSA was surprisingly accomplished by using CaLB as the biocatalyst at low temperatures (Chapter 3). Several techniques were employed to determine and confirm the structure of PGLSA, such as MALDI-TOF and 2D-NMR. When synthesising PGLSA in the melt, at 120-140 ºC, in the absence of a catalyst or in the presence of a stannous(II) octanoate ($Sn(Oct)_2$), branched polymers with degrees of branching (DB) in the range 17% to 87%, and molecular weights (M_n) in the range of 3,900 Da < M_n < 11,400 Da were obtained. The topology of PGLSA can be controlled by the monomers ratios but normally an excess of succinic acid results in a polymer with a higher DB. To avoid branching/crosslinking, CaLB was used as biocatalyst. The enzymatic polycondensations in the bulk and in toluene, at high temperatures (110 ºC) and with an excess of succinic acid utilised the ability of CaLB to be regioselective to primary alcohols. Therefore, PGLSA with low DBs in the range 9% to 13% with a range of molecular weights of 1,800 < M_n < 14,500 Da were obtained.

However, enzymatic polycondensations in the melt, or in toluene, still require high temperatures. Therefore, the unique properties of $scCO_2$ were exploited to accomplish enzymatic polycondensations of glycerol and succinic acid at much milder conditions. Linear PGLSA was obtained at temperatures as low as 40 ºC at 275 bar, with a range of molecular weights of 1,100 Da < M_n < 3,500 Da and a range of DBs of 3% < DB < 13%. These results highlight the substantial advantages of using $scCO_2$ as the reaction medium, to synthesise linear PGLSA in the presence of CaLB. The decrease in polymerisation temperature from 140 ºC to 40 ºC is energetically more sustainable than a conventional melt synthesis and the production of linear polymers could open up new applications.

This methodology was then used to synthesise bio-based surfactants based on glycerol and succinic acid, which were end-capped with lauric acid (LA) or poly(ethylene glycol) (PEG), under mild reaction conditions (Chapter 4). The enzymatic polymerisations were carried out at 275 bar at a range of temperatures 40-60 ºC. For the synthesis of PGLSA end-capped with LA (LA-PGLSA), polymers with a M_n of 1,800 Da were obtained (DB < 12%), whilst PGLSA end-capped with PEG (PEG-PGLSA) showed M_n of ~ 2,000 Da (DB < 13%). These water soluble polyesters were evaluated against commercially available surfactants (Tween^{TM} 20 and NatraGem^{TM} E145). The PGLSA-based compounds reduced the surface tension of water to as low as 23 mN/m. In addition, these compounds self-assemble and form aggregates in the size range 178-621 nm, at low concentrations (0.02-0.08 wt.%). These results are comparable with the Tween^{TM} 20 and NatraGem^{TM} E145 revealing that these new PGLSA-based surfactants show promise as potential surfactants in cosmetic applications. The synthesis of biodegradable and biorenewable PGLSA-based surfactants (Figure 7.1) at mild conditions, could open up possibilities for promising surface-active agents for the next generation of bio-based products.

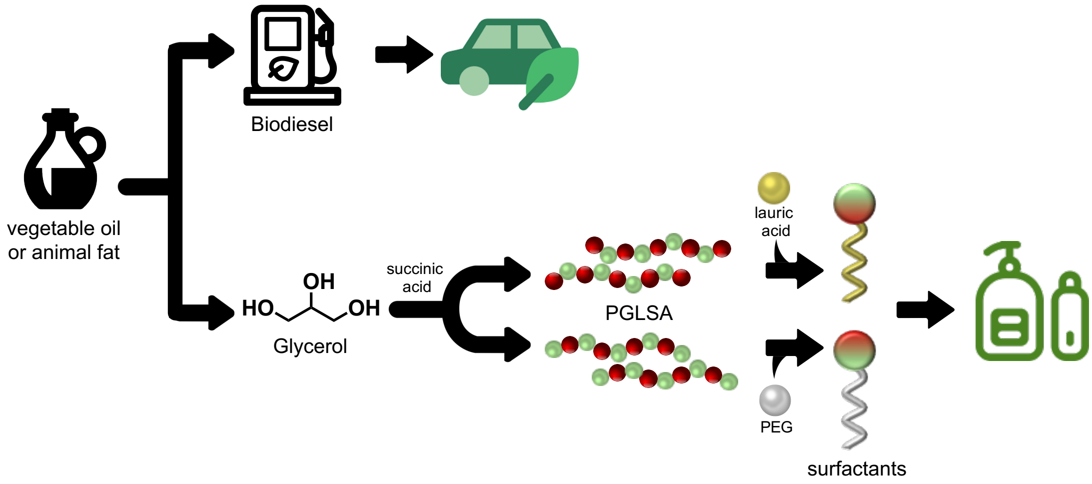

Figure 7.1 – Schematic representation of the glycerol opportunity to synthesise biorenewable and biodegradable surfactants for use in personal care products. *Note*: ● = glycerol, ● = succinic acid, ● = lauric acid and ● = poly(ethylene glycol).

7.2.2. The ironweed opportunity

The second part of this Thesis focussed upon the potential use of the naturally occurring epoxidised oil from the non-commercial Ethiopian ironweed (*Vernonia galamensis* sp.). The main aim was to convert these seed oil into new polyesters, using alternative and green methodologies (Figure 7.2).

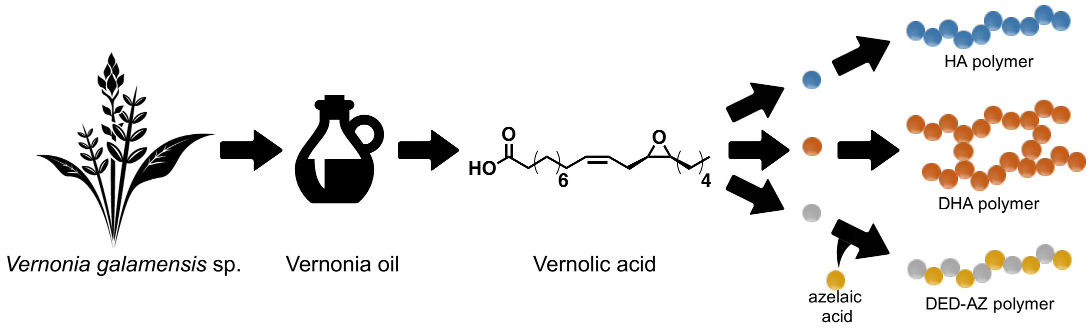

Figure 7.2 – Schematic representation of ironweed (*Vernonia galamensis* sp.) opportunity to synthesised biorenewable polyesters. *Note*: ● = 13-hydroxyoctadeca-9,11-dienoic acid monomer (HA, allylic alcohol), ● = 12,13-dihydroxyoctadec-9-enoic acid monomer (DHA, dihydroxy acid), ● = dodec-2-ene-1,12-diol (DED, diol) and ● = azelaic acid (AZ).

The extraction of the vernonia oil (VO) from ironweed seeds, was accomplished by using $scCO_2$ (Chapter 5). The extraction of VO using $scCO_2$

was compared to the extraction using *n*-hexane. An extraction efficiency of 80% was obtained at 450 bar and 60 ºC, after ~ 4 hours, in $scCO_2$ and the extracted oil had fewer impurities as compared to the oil extracted with *n*-hexane (at 80 ºC, after ~ 9 hours). Therefore, no additional oil treatment steps were required after extraction with $scCO_2$. The extraction with *n*-hexane, required several additional steps, such as bleaching, degumming and neutralisation to obtain pure VO.

The hydrolysis of VO, and the subsequent VA isolation, yielded 90% pure VA. The epoxy groups and double bonds from this fatty acid offer great opportunities for modification into new building blocks. Hence, taking the advantage of these functional groups, VA was converted into four monomers. From the synthesised monomers, hydroxy acid (HA), dihydroxy acid (DHA) and diol (DED) were used to synthesise new polyesters (Chapter 6). Firstly, the polycondensation reactions of HA and DHA were conducted *via* melt polymerisation, at 140 ºC using 1 wt.% $Sn(Oct)_2$ as catalyst. Polymers with M_n up to 34,400 and 7,900 Da, respectively, were obtained. It is important to note that DHA is a AB_2-type monomer, and its polymerisation can result in branched polymers. Indeed, a polymer with a degree of branching (DB) of 49% was obtained after 20 hours reaction. The polymerisation of DED with azelaic acid, which is a commercially available diacid, was performed in the presence of toluene at 100 ºC, using CaLB as biocatalyst. After 48 hours reaction, a polyester with a molecular weight of 5,500 Da was obtained. These methods all required high temperatures. However, when using $scCO_2$ as the reaction medium, a decrease in reaction temperature was possible for all the monomers. The polycondensation of HA and DHA was achieved at 95 ºC and 200 bar. Polymers with M_n up to 63,000 and 5,900 Da were obtained after 24 hours reaction. For DED-AZ, a polymer with a molecular weight of 2,300 Da was accomplished at 35 ºC and 275 bar, after 24 hours reaction.

Using $scCO_2$ as an extraction medium and then a reaction medium to synthesise new polyesters has been showed to be beneficial. Reducing the extraction temperatures from ~ 80 º to 60 ºC and the polymerisation temperatures from 140 º to 95 ºC or from 100 º to 35 ºC could have a strong effect on the energy efficiency of a future process. The potential financial and sustainable outcome could make vernonia-based polyester interesting candidates for the next generation of bio-based polymers.

7.3. Future work

Throughout this Thesis, green methodologies to synthesise biorenewable polyesters were described. However, there are a few areas in which further work is required, such as additional investigations of the polymer properties using more characterisation techniques and the optimisation of the polycondensation procedures.

With respect to the PGLSA synthesis in $scCO_2$ (Chapter 3), further investigations to fully understand the effect of monomer ratios (Gly:SA) and the reaction temperature on molecular weight in the polymer synthesis are needed. From the enzymatic polycondensation of PGLSA in $scCO_2$, using different temperatures (40 º – 60 ºC) and monomers ratio (1:1, 1:2 and 2:1), polymers with molecular weights from 1,100 to 3,500 Da were obtained. However, the effect of monomers ratio and temperature on the M_n was not clear. Hence, these reactions require further exploration to validate the effect of temperature and monomers ratio on the M_n of the synthesised polyesters. Furthermore, different diacids could be investigated (such as azelaic acid which is potentially bio-based), to understand if the length of the diacid would lead to the formation of polymers with different thermal properties and hence, different applications. Although PGLSA polymers have been demonstrated to be biodegradable by other authors,[154] it would of great interest to determine the rate of biodegradability of the PGLSA synthesised in $scCO_2$.

The green synthesis of linear PGLSA was employed to create surface active compounds (Chapter 4). Further investigations are required to fully understand the effect of the polymerisation temperature.

An in-depth investigation into the self-assembly of PGLSA-based surfactants would be desirable. For example, TEM analysis could be used to determine the shape of the self-assembled structures and the influence of concentration on the size/shape of the self-assembled structure.

The use of *Vernonia galamensis* sp. to synthesise green polymers, especially in $scCO_2$, showed promising results (Chapter 6). The presence of the double bond and epoxy group in vernolic acid (VA) offers great opportunities for the synthesis of new building blocks for polycondensation reactions. Some potential structures are outlined below (Figure 7.3).

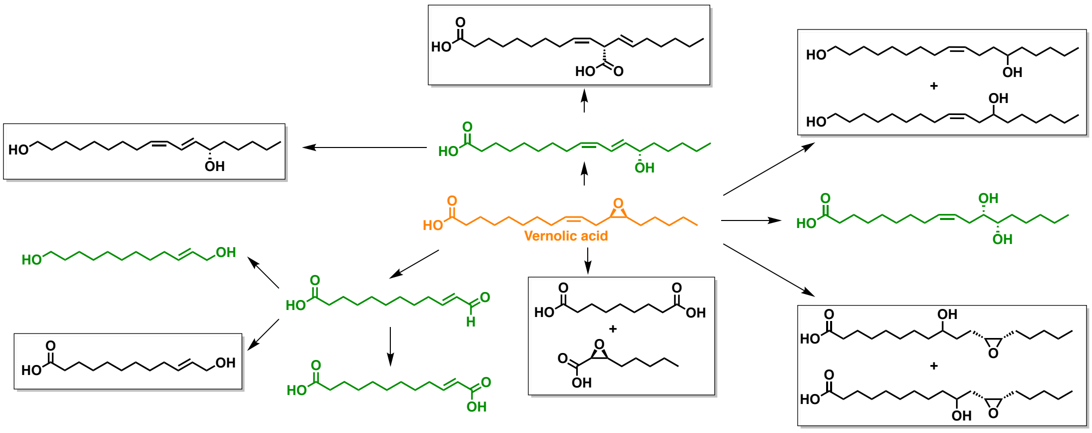

Figure 7.3 – Schematic representation of possible new building blocks, synthesised from vernolic acid. *Note*: the green building blocks are the ones already synthesised in this Thesis, whilst the black boxes are the proposed new monomers.

In this Thesis, the assessment of the vernonia-based polymers by MALDI technique was not possible, due to poor ionisation of the samples. Hence, it would be ideal optimise the MALDI parameters. From these results, it could then be determined whether the formation of cyclic structures had occurred; an undesirable, yet common, side-reaction in polycondensations. It would be also possible to confirm the presence of branched structures of DHA-polymer. In addition, the degradation of these polymers should be investigated to determine the environmental impact of these polyesters.

Another important aspect to consider is the general synthesis of polyesters in $scCO_2$ in Chapter 3, 4 and 6. As mentioned previously, water is a by-product from the polycondensation of diols with diacids, or from the self-condensation of hydroxy and dihydroxy acids. Hence, molecular sieves were required to trap the by-product and separation of molecular sieves (and enzyme beads) from the polymer could only be accomplished through the use of a small amount of THF. Ideally, a route should be developed using only $scCO_2$ to enable separations of the polymeric products, molecular sieves, enzyme beads and recycling of the enzyme.

To sum up, this Thesis has open up significant potential for the extraction of oil and synthesis of new polyesters at lower temperatures, combined with CaLB and all achieved using $scCO_2$. The key question now is to determine if this might lead to a commercially viable process.

CHAPTER 8. REFERENCES

1. Sheldon, R. A., Metrics of Green Chemistry and Sustainability: Past, Present, and Future. *Acs Sustainable Chemistry & Engineering* **2018,** *6* (1), 32-48.

2. Shafiee, S.; Topal, E., When will fossil fuel reserves be diminished? *Energy Policy* **2009,** *37* (1), 181-189.

3. Miller, R. G.; Sorrell, S. R., The future of oil supply Introduction. *Philosophical Transactions of the Royal Society a-Mathematical Physical and Engineering Sciences* **2014,** *372* (2006).

4. Lang, D. J.; Wiek, A.; Bergmann, M.; Stauffacher, M.; Martens, P.; Moll, P.; Swilling, M.; Thomas, C. J., Transdisciplinary research in sustainability science: practice, principles, and challenges. *Sustainability Science* **2012,** *7* (1), 25-43.

5. Mitchell, J. W., Alternative starting materials for industrial processes. *Proceedings of the National Academy of Sciences of the United States of America* **1992,** *89* (3), 821-826.

6. Sheldon, R. A., Organic synthesis. Past, present and future. *Chemistry and Insdustry* **1992,** (23), 903-906.

7. Trost, B., The atom economy - A search for synthetic efficiency. *Science* **1991,** *254* (5037), 1471-1477.

8. Anastas, P. T.; Warner, J. C., *Green chemistry: theory and practice*. Oxford University Press: Oxford, 1998.

9. Sheldon, R. A., Atom utilisation, *E* factors and the catalytic solution. *Comptes Rendus de l'Académie des Sciences - Series IIC - Chemistry* **2000,** *3* (7), 541-551.

10. Azapagic, A.; Perdan, S., Indicators of sustainable development for industry. *Process Safety and Environmental Protection* **2000,** *78* (4), 243-261.

11. Azapagic, A.; Millington, A.; Collett, A., A methodology for integrating sustainability considerations into process design. *Chemical Engineering Research and Design* **2006,** *84* (6), 439-452.

12. Sikdar, S. K., Sustainable development and sustainability metrics. *Aiche Journal* **2003,** *49* (8), 1928-1932.

13. Brudtland, C. G., The World Commission on Environmental Development. In *Our Common Future*, Oxford Univeristy Press: Oxford, 1987; pp 1-26.

14. Pollet, P.; Davey, E. A.; Ureña-Benavides, E. E.; Eckert, C. A.; Liotta, C. L., Solvents for sustainable chemical processes. *Green Chemistry* **2014,** *16*, 1034-1055.

15. Chia, S. R.; Chew, K. W.; Show, P. L.; Ong, H. C.; Phang, S. M.; Ling, T. C.; Nagarajan, D.; Lee, D.-J.; Chang, J.-S., Sustainable approaches for algae utilization in bioenergy production. *Renewable Energy* **2018,** *129*, 838-852.

16. IEA Statistics, O. I. Alternative and nuclear energy (% of total energy use). https://data.worldbank.org/indicator/EG.USE.COMM.CL.ZS (accessed 17th September 2018).

17. IEA Statistics, O. I. Fossil fuel energy consumption (% of total). https://data.worldbank.org/indicator/eg.use.comm.fo.zs (accessed 17th September 2018).

18. Corma, A.; Corresa, E.; Mathieu, Y.; Sauvanaud, L.; Al-Bogami, S.; Al-Ghrami, M. S.; Bourane, A., Crude oil to chemicals: light olefins from crude oil. *Catalysis Science & Technology* **2017,** *7*, 12-46.

19. Levi, P. G.; Cullen, J. M., Mapping global flows of chemicals: from fossil fuel feedstocks to chemical products. *Environmental Science & Technology* **2018,** *52* (4), 1725-1734.

20. Thompson, R. C.; Swan, S. H.; Moore, C. J.; Saal, F. S. v., Our plastic age. *Philosophical Transactions of the Royal Society B* **2009,** *364* (1526), 1973-1976.

21. Yarsley, V. E.; Couzens, E. G., *Plastics*. Pelican: UK, 1945.

22. Statista Global plastic production from 1950 to 2016 (in million metric tons). https://www.statista.com/statistics/282732/global-production-of-plastics-since-1950/ (accessed 14th September 2018).

23. Rivero, C. P.; Hu, Y.; Kwan, T. H.; Webb, C.; Theodoropoulos, C.; Daoud, W.; Lin, C. S. K., Bioplastics From Solid Waste. *Current Developments in Biotechnology and Bioengineering: Solid Waste Management* **2017**, 1-26.

24. World Economic Forum; Foundation, E. M. *The new plastics economy: Rethinking the future of plastics & catalysing action*; Ellen MacArthur Foundation: Barcelone, 2017.

25. Kobayashi, S., *Green polymer chemistry: Recent developments*. Springer-Verlag: Berlin, 2013; Vol. 262.

26. Ross, G.; Ross, S.; Tighe, B. J., Bioplastics: New Routes, New Products. In *Brydson's Plastics Materials*, Gilbert, M., Ed. Matthew Deans: Oxford, United Kingdom, 2017; pp 631-652.

27. Plastics Europe Plastics - the Facts 2017, An analysis of European plastics production, demand and waste data. https://www.plasticseurope.org/application/files/5715/1717/4180/Plastics_the_facts_2017_FINAL_for_website_one_page.pdf (accessed 27th August 2018).

28. European Commision A European strategy for plastics in a circular economy. http://ec.europa.eu/environment/circular-economy/pdf/plastics-strategy-brochure.pdf (accessed 27th August 2018).

29. Reillon, V., EU framework programmes for research and innovation - Evolution and key data from FP1 to Horizon 2020 in view of FP9. European Parliamentary Research Service, E., Ed. European Union, 2017; pp 1-35.

30. Popa, V. I., Biomass for Fuels and Biomaterials. In *Biomass as Renewable Raw Material to Obtain Bioproducts of High-Tech Value*, John Fedor: Oxford, United Kingdom, 2018; pp 1-37.

31. Kamm, B.; Kamm, M.; Gruber, P. R.; Kromus, S., Biorefinery Systems – An Overview. In *Biorefineries – Industrial Processes and Products. Status Quo and Future Directions.* , Kamm, B.; Gruber, P. R.; Kamm, M., Eds. WILEY-VCH Verlag GmbH & Co. KGaA: Weinheim, 2006; Vol. Vol. 1, pp 3-41.

32. Bohlmann, G. M., Biodegradable packaging life-cycle assessment. *Environmental Progress* **2004,** *23* (4), 342-347.

33. Hillmyer, M. A.; Tolman, W. B., Aliphatic polyester block polymers: Renewable, degradable, and sustainable. *Accounts of Chemical Research* **2014,** *47* (8), 2390–2396.

34. Yao, K.; Tang, C., Controlled polymerization of next-generation renewable monomers and beyond. *Macromolecules* **2013,** *46* (5), 1689-1712.

35. Berg, J. M.; Tymoczko, J. L.; Stryer, L., The Citric Acid Cycle. In *Biochemistry*, 5th edition ed.; W.H.Freeman & Co Ltd: New York, 2002.

36. Bechthold, I.; Bretz, K.; Kabasci, S.; Kopitzky, R.; Springer, A., Succinic acid: a new platform chemical for biobased polymers from renewable resources. *Chemical and Engineering Technology* **2008,** *31* (5), 647–654.

37. Mitsubishi Chemical Corporation Biodegradable Polymer – BioPBS™. https://www.m-chemical.co.jp/en/products/departments/mcc/sustainable/product/1201025_7964.html (accessed 31st August 2018).

38. Showa Denko Europe Bionolle® - The pioneer in biodegradable. https://www.showa-denko.com/news/bionolle-the-pioneer-in-biodegradable/ (accessed 31st August 2018).

39. Fujimaki, T., Processability and properties of aliphatic polyesters, ‘BIONOLLE’, synthesized by polycondensation reaction. *Polymer Degradation and Stability* **1998,** *59* (1-3), 209-214.

40. Showa Denko Europe SDK to Terminate Production and Sale of Biodegradable Plastic. http://www.sdk.co.jp/english/news/15030/16250.html (accessed 31st August 2018).

41. Pagliaro, M., Properties, applications, history, and market. In *Glycerol - the renewable platform chemical*, John Fedor: Oxford, UK, 2017; pp 1-21.

42. Hosseinzadeh-Bandbafha, H.; Tabatabaei, M.; Aghbashlo, M.; Khanali, M.; Demirbas, A., A comprehensive review on the environmental impacts of diesel/biodiesel additives. *Energy Conversion and Management* **2018,** *174*, 579-614.

43. Quispe, C. A. G.; Coronado, C. J. R.; Carvalho, J. A., Jr., Glycerol: Production, consumption, prices, characterization and new trends in combustion. *Renewable & Sustainable Energy Reviews* **2013,** *27*, 475-493.

44. Benefuel Novel biodiesel process expands applications. http://www.benefuel.net/news/novel-biodeiesel-process-expands-applications.php (accessed 31st August 2018).

45. Agach, M.; Marinkovic, S.; Estrine, B.; Nardello-Rataj, V., Acyl Poly(Glycerol-Succinic Acid) Oligoesters: Synthesis, Physicochemical and Functional Properties, and Biodegradability. *Journal of Surfactants and Detergents* **2016,** *19* (5), 933-941.

46. Khongphow, C.; Theerakul, J.; Puttamat, S.; Singkhonrat, J., Characterisation of poly(glycerol-succinate) oligomers as bio-based non-ionic surfactants by nuclear magnetic resonance and mass spectrometry. *Colloids and Surfaces a-Physicochemical and Engineering Aspects* **2015,** *468*, 301-308.

47. Wyatt, V. T.; Strahan, G. D., Degree of Branching in Hyperbranched Poly(glycerol-co-diacid)s Synthesized in Toluene. *Polymers* **2012,** *4* (1), 396-407.

48. Lin, D.; Yang, K.; Tang, W.; Liu, Y. T.; Yuan, Y.; Liu, C. S., A poly(glycerol sebacate)-coated mesoporous bioactive glass scaffold with adjustable mechanical strength, degradation rate, controlled-release and cell behavior for bone tissue engineering. *Colloids and Surfaces B-Biointerfaces* **2015,** *131*, 1-11.

49. Somisetti, V.; Allauddin, S.; Narayan, R.; Raju, K. V. S. N., Synthesis of a novel glycerol based B_3-type monomer and its application in hyperbranched polyester urethane-urea coatings. *Rsc Advances* **2015,** *5* (90), 74003-74011.

50. Wyatt, V. T.; Nunez, A.; Foglia, T. A.; Marmer, W. N., Synthesis of hyperbranched poly(glycerol-diacid) oligomers. *Journal of the American Oil Chemists Society* **2006,** *83* (12), 1033-1039.

51. Zhu, Y.; Romain, C.; Williams, C. K., Sustainable polymers from renewable resources. *Nature* **2016,** *540* (7633), 354-362.

52. Oil World Data Base. https://www.oilworld.biz/t/publications/data-base (accessed 1st May 2018).

53. Nor, N. M.; Derawi, D.; Salimon, J., The optimization of rbd palm oil epoxidation process using d-optimal design. *Sains Malaysiana* **2018,** *47* (7), 1359-1367.

54. Petrović, Z. S., Polyurethanes from vegetable oils. *Polymer Reviews* **2008,** *48* (1), 109-155.

55. Choe, E.; Min, D. B., Mechanisms and factors for edible oil oxidation. *Comprehensive Reviews in Food Science and Food Safety* **2006,** *5* (4), 169-186.

56. Schneider, C., An update on products and mechanisms of lipid peroxidation. *Molecular Nutrition & Food Research* **2009,** *53* (3), 315-321.

57. Carlson, K. D.; Schneider, W. J.; Chang, S. P.; Princen, L. H., Vernonia galamensis seed oil - a new source for epoxy coatings. *American Oil Chemists Society Monograph* **1981,** *9*, 297-318.

58. Maisonneuve, L.; Lebarbé, T.; Grauab, E.; Cramail, H., Structure-properties relationship of fatty acid-based thermoplastics as synthetic polymer mimics. *Polymer Chemistry* **2013,** *4* (22), 5465-5604.

59. Desalegn, T.; Garcia, I. J. V.; Titman, J.; Licence, P.; Diaz, I.; Chebude, Y., Enzymatic synthesis of epoxy fatty acid starch ester in ionic liquid–organic solvent mixture from vernonia oil. *Starch* **2014,** *66* (3-4), 385-392.

60. Grinberg, S.; Kolot, V.; Mills, D., New chemical derivatives based on Vernonia galamensis oil. *Industrial Crops and Products* **1994,** *3* (1-2), 113-119.

61. Holmberg, A. L.; Reno, K. H.; Wool, R. P.; Epps, T. H., Biobased building blocks for the rational design of renewable block polymers. *Soft Matter* **2014,** *10*, 7405-7424.

62. Nair, L. S.; Laurencin, C. T., Biodegradable polymers as biomaterials. *Progress in Polymer Science* **2007,** *32* (8-9), 762-798.

63. Obuchi, S.; Ogawa, S., Packaging and Other Commercial Applications. In *Poly(Lactic Acid): Synthesis, Structures, Properties, Processing, and Applications*, Auras, R.; Lim, L. T.; Selke, S. E. M.; Tsuji, H., Eds. John Wiley & Sons, Inc.: Hoboken, New Jersey, 2010; pp 457-468.

64. Yu, B.; Meng, L.; Fu, S.; Zhao, Z.; Liu, Y.; Wang, K.; Fu, Q., Morphology and internal structure control over PLA microspheres by compounding PLLA and PDLA and effects on drug release behavior. *Colloids and Surfaces B: Biointerfaces* **2018,** *172* (1), 105-112.

65. Suzuki, S.; Ikada, Y., Medical Applications. In *Poly(Lactic Acid): Synthesis, Structures, Properties, Processing, and Applications*, Auras, R.; Lim, L. T.; Selke, S. E. M.; Tsuji, H., Eds. John Wiley & Sons, Inc.: Hoboken, New Jersey, 2010; pp 443-456.

66. Castro-Aguirre, E.; Iñiguez-Franco, F.; Samsudin, H.; Fang, X.; Auras, R., Poly(lactic acid)—Mass production, processing, industrial applications, and end of life. *Advanced Drug Delivery Reviews* **2016,** *107*, 333-366.

67. Sathya, A. B.; Sivasubramanian, V.; Santhiagu, A.; Sebastian, C.; Sivashankar, R., Production of Polyhydroxyalkanoates from Renewable Sources Using Bacteria. *Journal of Polymers and the Environment* **2018,** *26* (9), 3995-4012.

68. Chen, G. Q.; Jiang, X. R., Engineering microorganisms for improving polyhydroxyalkanoate biosynthesis. *Current Opinion in Biotechnology* **2018,** *53*, 20-25.

69. Pakalapati, H.; Chang, C. K.; Show, P. L.; Arumugasamy, S. K.; Lan, J. C. W., Development of polyhydroxyalkanoates production from waste feedstocks and applications. *Journal of Bioscience and Bioengineering* **2018,** *126* (3), 282-292.

70. Numata, K.; Abe, H.; Iwata, T., Biodegradability of poly(hydroxyalkanoate) materials. *Materials* **2009,** *2* (3), 1104-1126.

71. Garrison, T. F.; Murawski, A.; Quirino, R. L., Bio-based polymers with potential for biodegradability. *Polymers* **2016,** *8* (263), 1-22.

72. Rudnik, E., Compostable polymer materials - definitions, structures and methods of preparation. In *Compostable Polymer Materials*, Elsevier: Hungary, 2008; pp 11-38.

73. Raza, Z. A.; Abid, S.; Banat, I. M., Polyhydroxyalkanoates: Characteristics, production, recent developmentsand applications. *International Biodeterioration & Biodegradation* **2018,** *126*, 45-56.

74. Bhaw-Luximon, A.; Jhurry, D.; Motala-Timol, S.; Lochee, Y., Polymerization of ε-Caprolactone and its Copolymerization with γ-Butyrolactone using Metal Complexes. *Macromolecular Symposia* **2006,** *231* (1), 60-68.

75. Mahapatro, A.; Kumar, A.; Gross, R. A., Mild, Solvent-Free ω-Hydroxy Acid Polycondensations Catalyzed by Candida antarctica Lipase B. *Biomacromolecules* **2004,** *5* (1), 62-68.

76. Labet, M.; Thielemans, W., Synthesis of polycaprolactone: a review. *Chemical Society Reviews* **2009,** *38*, 3484-3504.

77. Guarino, V.; Gentile, G.; Sorrentino, L.; Ambrosio, L., Polycaprolactone: Synthesis, Properties, and Applications. In *Encyclopedia of Polymer Science and Technology*, 2017.

78. Zumstein, M. T.; Rechsteiner, D.; Roduner, N.; Perz, V.; Ribitsch, D.; Guebitz, G. M.; Kohler, H.-P. E.; McNeill, K.; Sander, M., Enzymatic Hydrolysis of Polyester Thin Films at the Nanoscale: Effects of Polyester Structure and Enzyme Active-Site Accessibility. *Environmental Science & Technology* **2017,** *51* (13), 7476-7485.

79. Díaz, A. I.; Katsarava, R.; Puiggalí, J., Synthesis, Properties and Applications of Biodegradable Polymers Derived from Diols and Dicarboxylic Acids: From Polyesters to Poly(ester amide)s. *Molecular Sciences* **2014,** *15*, 7064-7123.

80. Mueller, R.-J., Biological degradation of synthetic polyesters—Enzymes as potential catalysts for polyester recycling. *Process Biochemistry* **2006,** *41* (10), 2124-2128.

81. Muller, R.-J.; Marten, E.; Deckwer, W.-D., Structure-Biodegradability Relationship of Polyesters. In *Biorelated Polymers: Sustainable Polymer Science and Technology*, Chiellini, E.; Gil, H.; Braunegg, G.; Buchert, J.; Gatenholm, P.; Zee, M. v. d., Eds. Kluwer Academic / Plenum Publishers: USA, 2001.

82. Jacobsen, L. L.; Ray, W. H., Analysis and Design of Melt and Solution Polycondensation Processes. *Aiche Journal* **1992,** *38* (6), 911-925.

83. Saunders, J. H.; Dobinson, F., The Kinetics of Polycondensation Reactions. In *Non-Radical Polymerisation - Comprehensive Chemical Kinetics 15*, Bamford, C. H.; Tipper, C. F. H., Eds. Elsevier Scientific publishing: Amsterdam, 1976; Vol. Volume 15, pp 473-581.

84. Velmathi, S.; Nagahata, R.; Takeuchi, K., Extremely Rapid Synthesis of Aliphatic Polyesters by Direct Polycondensation of 1:1 Mixtures of Dicarboxylic Acids and Diols Using Microwaves. *Polymer Journal* **2007,** *39* (8), 841-844.

85. Behera, G. C.; Ramakrishnan, S., Transetherification polycondensation: The roles of the catalyst, monomer structure, and polymerization conditions. *Journal of Polymer Science Part a-Polymer Chemistry* **2003,** *42* (1), 102-111.

86. Debuissy, T.; Pollet, E.; Avérous, L., Synthesis and Characterization of Fully Biobased Poly(propylene succinate-ran-propylene adipate). Analysis of the

Architecture-Dependent Physicochemical Behavior. *Journal of Polymer Science* **2017,** *55* (17), 2738-2748.

87. Su, W.-F., *Principles of Polymer Design and Synthesis*. Springer-Verlag: Berlin, 2013.

88. Flory, P. J., Fundamental principles of condensation polymerization. *Chem Rev* **1946,** *39*, 137-97.

89. Jarvie, A. W. P.; Overton, N.; Pourçain, C. B. S., Enzyme catalysed modification of synthetic polymers. *Journal of the Chemical Society, Perkin Transactions 1* **1999,** *15* (0), 2171-2176.

90. Douka, A.; Vouyiouka, S.; Papaspyridi, L.-M.; Papaspyrides, C. D., A review on enzymatic polymerization to produce polycondensation polymers: the case of aliphatic polyesters, polyamides and polyesteramides. *Progress in Polymer Science* **2018,** *79*, 1-25.

91. Faber, K., Commom prejudices against enzymes. In *Biotransformations in organic chemistry – A textbook*, 6th edition ed.; Springer Heidelberg Dordrech: New York, 2011.

92. Palmer, T.; Bonner, P. L., An Introduction to enzymes. In *Enzymes*, 2nd edition ed.; Woodhead Publishing, Limited: Cambridge, 2007.

93. McDonald, A. G.; Tipton, K., Fifty-five years of enzyme classification: advances and difficulties. *The FEBS Journal* **2014,** *281* (2), 583-592.

94. Kundys, A.; Białecka-Florjańczyk, E.; Fabiszewska, A.; Małajowicz, J., Candida antarctica Lipase B as catalyst for cyclic esters synthesis, their polymerization and degradation of aliphatic polyesters. *Journal of Polymer and the Environment* **2018,** *26* (1), 396-407.

95. Miletić, N.; Loos, K.; Gross, R. A., Enzymatic polymerisation of polyester. In *Biocatalysis in polymer chemistry*, Loos, K., Ed. Wiley-VCH Verlag & Co. KGaA: Germany, 2010; pp 83-129.

96. Li, C.; Tan, T.; Zhang, H.; Feng, W., Analysis of the conformational stability and activity of Candida antarctica Lipase B in organic solvents. *The Journal of Biological Chemistry* **2010,** *285* (37), 28434–28441.

97. Kulschewski, T.; Sasso, F.; Secundo, F.; Lotti, M.; Pleiss, J. r., Molecular mechanism of deactivation of C. antarctica lipase B by methanol. *Journal of Biotechnology* **2013,** *168*, 462-469.

98. Eriksson, M. Lipase-catalyzed syntheses of telechelic polyesters. PhD thesis, Royal Institute of Technology, Stocholm, 2010.

99. Pettersen, E. F.; Goddard, T. D.; Huang, C. C.; Couch, G. S.; Greenblatt, D. M.; Meng, E. C.; Ferrin, T. E., UCSF Chimera—A Visualization System for Exploratory Research and Analysis. *Journal of Computational Chemistry* **2004,** *25* (13), 1605-1612.

100. Mei, Y.; Kumar, A.; Gross, R. A., Probing water-temperature relationships for lipase-catalyzed lactone ring-opening polymerizations. *Macromolecules* **2002,** *35* (14), 5444-5448.

101. Poojari, Y.; Clarson, S. J., Thermal stability of Candida antarctica lipase B immobilized on macroporous acrylic resin particles in organic media. *Biocatalysis and Agricultural Biotechnology* **2013,** *2*, 7-11.

102. Uyama, H.; Inada, K.; Kobayashi, S., Lipase-catalyzed synthesis of aliphatic polyesters by polycondensation of dicarboxylic acids and glycols in solvent-free system. *Polymer Journal* **2000,** *32* (5), 440-443.

103. Veld, M. A. J.; Palmans, A. R. A., Hydrolases part I: enzyme mechanism, selectivity and control in the synthesis of well-defined polymers. In *Enzymatic polymerisation*, Palmans, A. R. A.; Heise, A., Eds. Springer: Berlin, 2010; pp 55-78.

104. Sahena, F.; Zaidul, I. S. M.; Jinap, S.; Karim, A. A.; Abbas, K. A.; Norulaini, N. A. N.; Omar, A. K. M., Application of supercritical CO_2 in lipid extraction – A review. *Journal of Food Engineering* **2009,** *95* (2), 240-253.

105. Loeker, F. C.; Duxbury, C. J.; Kumar, R.; Gao, W.; Gross, R. A.; Howdle, S. M., Enzyme-catalyzed ring-opening polymerization of ε-caprolactone in supercritical carbon dioxide. *Macromolecules* **2004,** *37*, 2450-2453.

106. Curia, S.; Barclay, A. F.; Torron, S.; Johansson, M.; Howdle, S. M., Green process for green materials: viable low-temperature lipase-catalysed synthesis of renewable telechelics in supercritical CO_2. *Philosophical Transactions of the Royal Society a-Mathematical Physical and Engineering Sciences* **2015,** *373* (2057), 1-16.

107. De Marco, I.; Riemma, S.; Iannone, R., Life cycle assessment of supercritical CO_2 extraction of caffeine from coffee beans. *Journal of Supercritical Fluids* **2018,** *133*, 393-400.

108. Kazarian, S. G., Polymer processing with supercritical fluids *Polymer Science, Series C* **2000,** *42* (1), 78-101.

109. Erdmenger, T.; Guerrero-Sanchez, C.; Vitz, J.; Hoogenboom, R.; Schubert, U. S., Recent developments in the utilization of green solvents in polymer chemistry. *Chemical Society Reviews* **2010,** *39* (8), 3317-3333.

110. Gameiro, M.; Lisboa, P.; Paiva, A.; Barreiros, S.; Simões, P., Supercritical carbon dioxide-based integrated continuous extraction of oil from chicken feather meal, and its conversion to biodiesel in a packed-bed enzymatic reactor, at pilot scale. *Fuel* **2015,** *153* (1), 135-142.

111. Kemmere, M. J., Supercritical Carbon Dioxide for Sustainable Polymer Processes. In *Supercritical Carbon Dioxide: in Polymer Reaction Engineering*, Kemmere, M. J.; Meyer, T., Eds. Wiley-VCH Verlag GmbH & Co. KGaA: 2005; pp 1-14.

112. Goddard, A. R.; Perez-Nieto, S.; Passos, T. M.; Quilty, B.; Carmichael, K.; Irvine, D. J.; Howdle, S. M., Controlled polymerisation and purification of branched poly(lactic acid) surfactants in supercritical carbon dioxide. *Green Chemistry* **2016,** *18* (17), 4772-4786.

113. NIST Chemistry WebBook – Thermophysical Properties of Fluid Systems. https://webbook.nist.gov/chemistry/fluid/ (accessed 28th August 2018).

114. Wimmer, Z.; Zarevúcka, M., A Review on the Effects of Supercritical Carbon Dioxide on Enzyme Activity. *International Journal of Molecular Sciences* **2010,** *11* (1), 233-253.

115. Beckman, E. J., Supercritical and near-critical CO_2 in green chemical synthesis and processing. *Journal of Supercritical Fluids* **2004,** *28* (2-3), 121-191.

116. Bockisch, M., The importance of fats. In *Fats and Oils Hanbook*, AOCS Press: Hamburg, Germany, 1998; pp 1-52.

117. Anderson, S., Soxtec: Its principles and applications. In *Oil Extraction and Analysis – Critical Issues and Comparative Studies*, Luthria, D. L., Ed. AOCS Press: Illinois, USA, 2004; pp 10-24.

118. Temelli, F.; Saldaña, M. D. A.; Moquin, P. H.; Sun, M., Supercritical fluid extraction of specialty oils. In *Supercritical Fluid Extraction of Nutraceuticals and Bioactive Compounds*, Martínez, J. L., Ed. CRC Press: Broken Sound Parkway NW, 2007; pp 51-102.

119. Park, H. S.; Lee, H. J.; Shin, M. H.; Lee, K.-W.; Lee, H.; Kim, Y.-S.; Kim, K. O.; Kim, K. H., Effects of cosolvents on the decaffeination of green tea by supercritical carbon dioxide. *Food Chemistry* **2007,** *105* (3), 1011-1017.

120. Mira, B.; Blasco, M.; Berna, A.; Subirats, S., Supercritical CO_2 extraction of essential oil from orange peel. Effect of operation conditions on the extract composition. *The Journal of Supercritical Fluids* **1999,** *14* (2), 95-104.

121. Ghafoor, K.; AL-Juhaimi, F. Y.; Choi, Y. H., Supercritical fluid extraction of phenolic compounds and antioxidants from grape (Vitis labrusca B.) seeds. *Plants Foods for Human Nutrition* **2012,** *67* (4), 407-414.

122. Vetter, G., Introduction. In *High Pressure Process Technology: Fundamentals and Applications*, 1st Edition ed.; Bertucco, A.; Vetter, G., Eds. Elsevier Science: Amsterdam, 2001; Vol. Volume 9, pp 1-16.

123. García, A.; Lucas, A. d.; Rincón, J.; Alvarez, A.; Gracia, I.; García, M. A., Supercritical carbon dioxide extraction of fatty and waxy material from rice bran. *Journal of the American Oil Chemists Society* **1996,** *73* (9), 1127-1131.

124. Maheshwari, P.; Nikolov, Z. L.; White, T. M.; Hartel, R., Solubility of fatty acids in supercritical carbon dioxide. *Journal of the American Oil Chemists Society* **1992,** *69* (11), 1069-1077.

125. Kendall, J. L.; Canelas, D. A.; Young, J. L.; DeSimone, J. M., Polymerisations in supercritical carbon dioxide. *Chemical Review* **1999,** *99* (2), 543-563.

126. Nalawade, S. P.; Picchioni, F.; Janssen, L. P. B. M., Supercritical carbon dioxide as a green solvent for processing polymer melts: Processing aspects and applications. *Progress in Polymer Science* **2006,** *31*, 19-43.

127. Cooper, A. I., Polymer synthesis and processing using supercritical carbon dioxide. *Journal of Materials Chemistry* **2000,** *10* (2), 207-234.

128. Santos, R. D.; Comim, S. R. R.; Oliveira, D. d.; Treichel, H.; Luccio, M. D.; Ferreira, S. R. S.; Oliveira, J. V., Lipase-catalyzed synthesis of poly(e-caprolactone) in supercritical carbon dioxide. *Biocatalysis and Agricultural Biotechnology* **2012,** *1* (4), 280-283.

129. Dua, L.; Kellya, J. Y.; Roberts, G. W.; Simone, J. M. D., Fluoropolymer synthesis in supercritical carbon dioxide. *The Journal of Supercritical Fluids* **2009,** *47* (3), 447-457.

130. Birkin, N. A.; Arrowsmith, N. J.; Park, E. J.; Richez, A. P.; Howdle, S. M., Synthesis and application of new CO_2-soluble vinyl pivalate hydrocarbon stabilisers via RAFT polymerisation. *Polymer Chemistry* **2011,** *6* (2), 1293-1299.

131. Picchioni, F., Supercritical carbon dioxide and polymers: an interplay of science and technology. *Polymer International* **2013,** *63* (8), 1394-1399.

132. Kajiya, D.; Imanishi, M.; Saitow, K.-i., Solvation of esters and ketones in supercritical CO_2. *The Journal of Physical Chemistry B* **2016,** *120* (4), 785-792.

133. Kelly, C. A.; Howdle, S. M.; Shakesheff, K. M.; Jenkins, M. J.; Leeke, G. A., Viscosity studies of poly(DL-lactic acid) in supercritical CO_2. *Journal of Polymer Science Part B - Polymer Physics* **2012,** *50* (19), 1383-1393.

134. Varma, I. K.; Albertsson, A.-C.; Rajkhowa, R.; Srivastava, R. K., Enzyme catalyzed synthesis of polyesters. *Progress in Polymer Science* **2005,** *30* (10), 949-981.

135. Lopez-Luna, A.; Gallegos, J. L.; Gimeno, M.; Vivaldo-Lima, E.; Barzana, E., Lipase-catalyzed syntheses of linear and hyperbranched polyesters using compressed fluids as solvent media. *Journal of Molecular Catalysis B: Enzymatic* **2010,** *67* (1-2), 143-149.

136. Bovey, F. A.; Mirau, P. A., Fundamentals of nuclear magnetic resonance. In *NMR of polymers*, Academic Press, Inc.: San Diego, California, 1996; pp 1-115.

137. Jr., C. E. C., Introduction of Polymers. In *Carraher's Polymer Chemistry*, 9th edition ed.; CRC Press: Florida, US, 2013; pp 1-26.

138. GmbH, K. Wilhelmy plate method. https://www.kruss-scientific.com/services/education-theory/glossary/wilhelmy-plate-method/ (accessed 30th July 2018).

139. Shümann, D., Controlled Cleaning by Measuring Surfactant Concentration. *Metal Finishing* **2009,** *107*, 25-30.

140. Solutions, S. P. SITA Science line t100. https://www.sita-process.com/products/tensiometer/sita-science-line-t100/ (accessed 31st July 2018).

141. Marion, P.; Bernela, B.; Piccirilli, A.; Estrine, B.; Patouillard, N.; Guilbot, J.; Jérôme, F., Sustainable chemistry: how to produce better and more from less? *Green Chemistry* **2017,** *19* (21), 4973-4989.

142. Tuck, C. O.; Pérez, E.; Horváth, I. n. T.; Sheldon, R. A.; Poliakoff, M., Valorization of Biomass: Deriving More Value from Waste. *Science* **2012,** *337* (6095), 695-699.

143. Beach, E. S.; Cui, Z.; Anastas, P. T., Green Chemistry: A design framework for sustainability. *Energy & Environmental Science* **2009,** *2* (10), 1038–1049.

144. Clark, J. H., From waste to wealth using green chemistry: The way to long term stability. *Current Opinion in Green and Sustainable Chemistry* **2017,** *8*, 10-13.

145. Pleissner, D., Green chemistry and the leisure industry: New business models for sustainability. *Current Opinion in Green and Sustainable Chemistry* **2017,** *8*, 1-4.

146. Fasciotti, M., Perspectives for the use of biotechnology in green chemistry applied to biopolymers, fuels and organic synthesis: from concepts to a critical point of view. *Sustainable Chemistry and Pharmacy* **2017,** *6*, 82-89.

147. Agach, M.; Marinkovic, S.; Estrine, B.; Nardello-Rataj, V., Biosourced lauroyl poly(glycerol-succinate) oligoesters modified by copolymerizable solvents: A wasteless and eco-friendly surfactants properties enhancement. *Colloids and Surfaces a-Physicochemical and Engineering Aspects* **2018,** *536*, 88-95.

148. Kobayashi, S., Green polymer chemistry: new methods of polymer synthesis using renewable starting materials. *Structural Chemistry* **2017,** *28* (2), 461-474.

149. Wongthongdee, N.; Durand, A.; Pongtharangkul, T.; Sunintaboon, P.; Inprakhoe, P., Green Formulation Strategy for Preparing Oil-in-Water Emulsions via Lipase-Catalyzed Transesterification. *Acs Sustainable Chemistry & Engineering* **2017,** *5* (2), 1948-1956.

150. Kumar, A.; Kulshrestha, A. S.; Gao, W.; Gross, R. A., Versatile route to polyol polyesters by lipase catalysis. *Macromolecules* **2003,** *36* (22), 8219-8221.

151. Victor T. Wyatt, A. N. e., Thomas A. Foglia, and William N. Marmer, Synthesis of Hyperbranched Poly(glycerol-diacid) Oligomers. *Journal of the American Oil Chemists' Society* **2006,** *83* (12), 1033-1039.

152. Kafouris, D.; Kossivas, F.; Constantinides, C.; Nguyen, N. Q.; Wesdemiotis, C.; Patrickios, C. S., Biosourced Amphiphilic Degradable Elastomers of Poly(glycerol sebacate): Synthesis and Network and Oligomer Characterization. *Macromolecules* **2013,** *46* (3), 622-630.

153. Baharu, M. N.; Kadhum, A. A. H.; Al-Amiery, A. A.; Mohamad, A. B., Synthesis and characterization of polyesters derived from glycerol, azelaic acid, and succinic acid. *Green Chemistry Letters and Reviews* **2014,** *8* (1), 31-38.

154. Agach, M.; Delbaere, S.; Marinkovic, S.; Estrine, B.; Nardello-Rataj, V., Synthesis, characterization, biodegradability and surfactant properties of bio-sourced lauroyl poly(glycerol-succinate) oligoesters. *Colloids and Surfaces a-Physicochemical and Engineering Aspects* **2013,** *419*, 263-273.

155. Soyler, Z.; Meier, M. A. R., Catalytic Transesterification of Starch with Plant Oils: A Sustainable and Efficient Route to Fatty Acid Starch Esters. *Chemsuschem* **2017,** *10* (1), 182-188.

156. Vilela, C.; Silvestre, A. J. D.; Meier, M. A. R., Plant Oil-Based Long-Chain C-26 Monomers and Their Polymers. *Macromolecular Chemistry and Physics* **2012,** *213* (21), 2220-2227.

157. Llevot, A.; Dannecker, P. K.; von Czapiewski, M.; Over, L. C.; Soyler, Z.; Meier, M. A. R., Renewability is not Enough: Recent Advances in the Sustainable Synthesis of Biomass-Derived Monomers and Polymers. *Chemistry-a European Journal* **2016,** *22* (33), 11509-11520.

158. Firdaus, M.; Meier, M. A. R., Renewable co-polymers derived from vanillin and fatty acid derivatives. *European Polymer Journal* **2013,** *49* (1), 156-166.

159. Chakraborty, S.; Ju, L.; Galuska, A. A.; Moore, R. B.; Turner, S. R., Suspension polymerization of itaconic acid diesters. *Journal of Applied Polymer Science* **2018,** *46417*.

160. Rodygin, K. S.; Werner, I.; Ananikov, V. P., A Green and Sustainable Route to Carbohydrate Vinyl Ethers for Accessing Bioinspired Materials with a Unique Microspherical Morphology. *Chemsuschem* **2018,** *11* (1), 292-298.

161. Jiang, Y.; Loos, K., Enzymatic Synthesis of Biobased Polyesters and Polyamides. *Polymers* **2016,** *8* (7).

162. Eurostat Infrastructure - biofuel production capacities - annual data. http://appsso.eurostat.ec.europa.eu/nui/submitViewTableAction.do (accessed 21st March 2018).

163. Ayoub, M.; Abdullah, A. Z., Critical review on the current scenario and significance of crude glycerol resulting from biodiesel industry towards more sustainable renewable energy industry. *Renewable & Sustainable Energy Reviews* **2012,** *16* (5), 2671-2686.

164. Wang, Z. X.; Zhuge, J.; Fang, H. Y.; Prior, B. A., Glycerol production by microbial fermentation: A review. *Biotechnology Advances* **2001,** *19* (3), 201-223.

165. Eudes, A.; Berthomieu, R.; Hao, Z.; Zhao, N.; Benites, V. T.; Baidoo, E. E. K.; Loqué, D., Production of muconic acid in plants. *Metabolic Engineering* **2018,** *46*, 13-19.

166. Maziere, A.; Prinsen, P.; Garcia, A.; Luque, R.; Len, C., A review of progress in (bio)catalytic routes from/to renewable succinic acid. *Biofuels Bioproducts & Biorefining-Biofpr* **2017,** *11* (5), 908-931.

167. McKinlay, J. B.; Vieille, C.; Zeikus, J. G., Prospects for a bio-based succinate industry. *Applied Microbiology and Biotechnology* **2007,** *76* (4), 727-740.

168. Li, X. Z.; Zhang, W. M.; Wu, M. K.; Xin, F. X.; Dong, W. L.; Wu, H.; Zhang, M.; Ma, J. F.; Jiang, M., Performance and mechanism analysis of succinate production under different transporters in Escherichia coli. *Biotechnology and Bioprocess Engineering* **2017,** *22* (5), 529-538.

169. Li, C.; Gao, S.; Yang, X. F.; Lin, C. S. K., Green and sustainable succinic acid production from crude glycerol by engineered Yarrowia lipolytica via agricultural residue based in situ fibrous bed bioreactor. *Bioresource Technology* **2018,** *249*, 612-619.

170. Considine, G. D., Dicarboxylic acid. In *Van Nostrand's Scientific Encyclopedia*, Considine, G. D., Ed. John Wiley & Sons Inc.: New York, 2006.

171. Agach, M.; Delbaere, S.; Marinkovic, S.; Estrine, B.; Nardello-Rataj, V., Characterization, stability and ecotoxic properties of readily biodegradable branched oligoesters based on bio-sourced succinic acid and glycerol. *Polymer Degradation and Stability* **2012,** *97* (10), 1956-1963.

172. Wyatt, V. T.; Strahan, G. D.; Nunez, A., The Lewis Acid-Catalyzed Synthesis of Hyperbranched Oligo(glycerol-diacid)s in Aprotic Polar Media. *Journal of the American Oil Chemists Society* **2010,** *87* (11), 1359-1369.

173. Tsutsumi, C.; Hayase, N.; Nakagawa, K.; Tanaka, S.; Miyahara, Y., The enzymatic degradation of commercial biodegradable polymers by some lipases and chemical degradation of them. *Macromolecular Symposia* **2003,** *197*, 431-442.

174. Ding, M. L.; Zhang, M.; Yang, J. M.; Qiu, J. H., Study on the enzymatic degradation of PBS and its alcohol acid modified copolymer. *Biodegradation* **2012,** *23* (1), 127-132.

175. Tokiwa, Y.; Ando, T.; Suzuki, T., Degradation of Polycaprolactone by a Fungus. *Journal of Fermentation Technology* **1976,** *54* (8), 603-608.

176. Chua, T. K.; Tseng, M.; Yang, M. K., Degradation of Poly(epsilon-caprolactone) by thermophilic Streptomyces thermoviolaceus subsp. thermoviolaceus 76T-2. *Amb Express* **2013,** *3*.

177. Tokiwa, Y.; Calabia, B. P.; Ugwu, C. U.; Aiba, S., Biodegradability of Plastics. *International Journal of Molecular Sciences* **2009,** *10* (9), 3722-3742.

178. Carothers, W. H., Polymers and polyfunctionality. *Transactions of the Faraday Society* **1936,** *32*, 39-49.

179. Billmeyer, F. W. J., Step-reaction (Condensation) Polymerisation. D. Polyfunctional step-reaction polymerisation. In *Textbook of Polymer Science*, John Wiley & Sons, Inc: United States of America, 1984.

180. Hovey, A. G.; Kienle, R. H., The polyhydric alcohol-polybasic acid reaction. I. Glycerol-phthalic anhydride. *Journal of the American Chemical Society* **1929,** *51* (2), 509-519.

181. Flory, P. J., Molecular Size Distribution in Three Dimensional Polymers. I. Tetrafunctional Branching Units. *Journal of the American Chemical Society* **1941,** *63*, 3091.

182. Flory, P. J., Molecular Size Distribution in Three Dimensional Polymers. II. Tetrafunctional Branching Units. *Journal of the American Chemical Society* **1941,** *63*, 3091.

183. Flory, P. J., Molecular Size Distribution in Three Dimensional Polymers. III. Tetrafunctional Branching Units. *Journal of the American Chemical Society* **1941,** *63*, 3096.

184. Odian, G. G., *Principles of polymerization*. 4th ed.; Wiley: New York, 1991; p xxii, 768 p.

185. Flory, P. J., Molecular Size Distribution in Three Dimensional Polymers. VI. Branched Polymers Containing A-R-Bf-1 Type Units. *Journal of the American Chemical Society* **1952,** *74* (11), 2718-2723.

186. Chen, H.; Kong, J., Hyperbranched polymers from A_2 + B_3 strategy: recent advances in description and control of fine topology. *Polymer Chemistry* **2016,** *7* (22), 3643-3663.

187. Kricheldorf, H. R.; Fritsch, D.; Vakhtangishvili, L.; Schwarz, G., Multicyclic Poly(ether sulfone)s of Phloroglucinol Forming Branched and Cross-Linked Architectures. *Macromolecules* **2003,** *36* (12), 4337-4344.

188. Hawker, C. J.; Lee, R.; Fréchet, J. M. J., One-Step Synthesis of Hyperbranced Dendritic Polyesters. *Journal of the American Chemical Society* **1991,** *113* (12), 4583-4588.

189. Hölter, D.; Burgath, A.; Frey, H., Degree of branching in hyperbranched polymers. *Acta Polymer* **1997,** *48*, 30-35.

190. Frey, H.; Hölter, D., Degree of branching in hyperbranched polymers. 3. Copolymerization of AB_m-monomers with AB and AB_n-monomers. *Acta Polymer* **1999,** *50*, 67-76.

191. Hawker, C. J.; Lee, R.; Fréchet, J. M. J., One-step synthesis of hyperbranched dendritic polyesters. *Journal of the American Chemical Society* **1991,** *113* (12), 4583-4588.

192. Zhou, Z.; Jia, Z.; Yan, D., Theoretical investigation on the polyaddition of A_2 and CB_2 monomers with non-equal reactivity. *Polymer Journal* **2009,** *50*, 5608-5612.

193. Schoon, I.; Kluge, M.; Eschig, S.; Robert, T., Catalyst influence on undesired side reactions in the polycondensation of fully bio-based polyester itaconates. *Polymers* **2017,** *9*, 693-704.

194. Parcheta, P.; Datta, J., Structure-rheology relationship of fully bio-based linear polyester polyols for polyurethanes - synthesis and investigation. *Polymer testing* **2018,** *67*, 110-121.

195. Kolb, N.; Meier, M. A. R., Monomers and their polymers derived from saturated fatty acid methyl esters and dimethyl carbonate. *Green Chemistry* **2012,** *14*, 2429-2435.

196. Terzopoulou, Z.; Karakatsianopoulou, E.; Kasmi, N.; Tsanaktsis, V.; Nikolaidis, N.; Kostoglou, M.; Papageorgiou, G. Z.; Lambropouloud, D. A.; Bikiaris, D. N., Effect of catalyst type on molecular weight increase and coloration of poly(ethylene furanoate) biobased polyester during melt polycondensation. *Polymer Chemistry* **2017,** *8*, 6895-6908.

197. Wyatt, V. T., Lewis Acid-Catalyzed Synthesis of Hyperbranched Polymers Based on Glycerol and Diacids in Toluene. *Journal of the American Oil Chemists Society* **2012,** *89* (2), 313-319.

198. Stumbé, J.-F.; Bruchmann, B., Hyperbranched polyesters based on adipic acid and glycerol. *Macromolecular Rapid Communications* **2004,** *25*, 921-924.

199. Gustini, L.; Lavilla, C.; Janssen, W. W. T. J.; Ilarduya, A. M. n. d.; Muñoz-Guerra, S.; Koning, C. E., Green and selective polycondensation methods toward linear sorbitol-based polyesters: enzymatic versus organic and metal-based catalysis. *Chemsuschem* **2016,** *9*, 2250-2262.

200. Shibata, Y.; Takasu, A., Synthesis of polyester having pendent hydroxyl groups via regioselective dehydration polycondensations of dicarboxylic acids and diols by low temperature polycondensation. *Journal of Polymer Science Part A: Polymer Chemistry* **2009,** *47*, 5747-5759.

201. Takasu, A.; Shibata, Y.; Narukawa, Y.; Hirabayashi, T., Chemoselective dehydration polycondensations of dicarboxylic acids and diols having pendant hydroxyl groups using the room temperature polycondensation eechnique. *Macromolecules* **2006,** *40* (2), 151-153.

202. Hahn, C.; Keul, H.; Möller, M., Hydroxyl-functional polyurethanes and polyesters: synthesis, properties and potential biomedical application. *Polymer International* **2012,** *61* (7), 1048-1060.

203. Okumura, S.; Iwai, M.; Tominaga, Y., Synthesis of ester oligomer by *Aspergillius-niger* lipase. *Agricultural and Biological Chemistry* **1984,** *48* (11), 2805-2808.

204. Iglesias, L. E.; Fukuyama, Y.; Nonami, H.; Erra-Balsells, R.; Baldessari, A., A simple enzymatic procedure for the synthesis of a hydroxylated polyester from glycerol and adipic acid. *Biotechnology Techniques* **1999,** *13*, 923-926.

205. Pessagno, R. C.; Baldessari, A., Lipase-catalyzed polymerization of glycerol and dicarboxylic acids in an organic medium. *Macromolecules* **2000,** *5*, 372-373.

206. Gustini, L.; Noordover, B. A. J.; Gehrels, C.; Dietz, C.; Koning, C. E., Enzymatic synthesis and preliminary evaluation as coating of sorbitol-based, hydroxy-functional polyesters with controlled molecular weights. *European Polymer Journal* **2015,** *67*, 459-475.

207. Hu, J.; Gao, W.; Kulshrestha, A. S.; Gross, R. A., “Sweet polyesters”: Lipase-catalyzed condensation-polymerizations of alditols. *Macromolecules* **2006,** *39*, 6789-6792.

208. Kulshrestha, A. S.; Gao, W.; Gross, R. A., Glycerol copolyesters: control of branching and molecular weight using a lipase catalyst. *Macromolecules* **2005,** *38*, 3193-3204.

209. Nguyen, H. D.; Löf, D.; Hvilsted, S.; Daugaard, A. E., Highly branched bio-based unsaturated polyesters by enzymatic polymerization. *Polymers* **2016,** *8* (10), 363-375.

210. Pin, J.-M.; Valerio, O.; Misra, M.; Mohanty, A., Impact of butyl glycidyl ether comonomer on poly(glycerol−succinate) architecture and dynamics for multifunctional hyperbranched polymer design. *Macromolecules* **2017,** *50* (3), 732-745.

211. Valerio, O.; Pin, J.-M.; Misra, M.; Mohanty, A. K., Synthesis of glycerol-based biopolyesters as toughness enhancers for polylactic acid bioplastic through reactive extrusion. *ACS Omega* **2016,** *1* (6), 1284-1295.

212. Weidner, S. M.; Falkenhagen, J., *MALDI mass spectroscopy for synthetic polymer analysis*. John Wiley & Sons, Inc. : Canada, 2010.

213. Fox, T. G.; Flory, P. J., The glass temperature and related properties of polystyrene. Influence of molecular weight. *Journal of Polymer Science Part A: General Papers* **1954,** *14* (75), 315-319.

214. Sunder, A.; Bauer, T.; Mülhaupt, R.; Frey, H., Synthesis and thermal behavior of esterified aliphatic hyperbranched polyether polyols. *Macromolecules* **2000,** *33* (4), 1330-1337.

215. Zhu, Q.; Wu, J.; Tu, C.; Shi, Y.; He, L.; Wang, R.; Zhu, X.; Yan, D., Role of branching architecture on the glass transition of hyperbranched polyethers. *The Journal of Physical Chemistry B* **2009,** *113* (17), 5777-5780.

216. Khalyavina, A.; Häußler, L.; Lederer, A., Effect of the degree of branching on the glass transition temperature of polyesters. *Polymer* **2012,** *53* (5), 1049-1053.

217. Winkler, M.; Lacerda, T. M.; Mack, F.; Meier, M. A. R., Renewable polymers from itaconic acid by polycondensation and ring-opening-metathesis polymerization. *Macromolecules* **2015,** *48* (5), 1398-1403.

218. Gubbels, E.; Jasinska-Walc, L.; Koning, C. E., Synthesis and characterization of novel renewable polyesters based on 2,5-furandicarboxylic acid and 2,3-butanediol. *Journal of Polymer Science Part a-Polymer Chemistry* **2012,** *51* (4), 890-898.

219. Kumar, R.; Gao, W.; Gross, R. A., Functionalized polylactides: preparation and characterization of [L]-lactide-co-pentofuranose. *Macromolecules* **2002,** *35* (18), 6835-6844.

220. Shen, Y.; Chen, X.; Gross, R. A., Polycarbonates from sugars: ring-opening polymerization of 1,2-*O*-isopropylidene-D-xylofuranose-3,5-cyclic carbonate (IPXTC). *Macromolecules* **1999,** *32* (8), 2799–2802.

221. Patil, D. P.; Rethwisch, D. G.; S., D. J., Enzymatic synthesis of a sucrose-containing linear polyester in nearly anhydrous organic media. *Biotechnology and Bioengineering* **1991,** *37* (7), 639-646.

222. Taresco, V.; Creasey, R. G.; Kennon, J.; Mantovani, G.; Alexander, C.; Burley, J. C.; Garnett, M. C., Variation in structure and properties of poly(glycerol adipate) via control of chain branching during enzymatic synthesis. *Polymer* **2016,** *89*, 41-49.

223. Yang, Y.; Lu, W.; Cai, J.; Hou, Y.; Ouyang, S.; Xie, W.; Gross, R. A., Poly(oleic diacid-co-glycerol): comparison of polymer structure resulting from chemical and lipase catalysis. *Macromolecules* **2011,** *44* (7), 1977-1985.

224. Yoon, K. R.; Hong, S.-P.; Kong, B.; Choi, I. S., Polycondensation of sebacic acid with primary and secondary hydroxyl groups containing diols catalyzed by *Candida antarctica* lipase B. *Synthetic Communications* **2012,** *42* (23), 3504-3512.

225. Brännström, S.; Finnveden, M.; Johansson, M.; Martinelle, M.; Malmström, E., Itaconate based polyesters: Selectivity and performance of esterification catalysts. *European Polymer Journal* **2018,** *103*, 370-377.

226. Lu, J.; Wu, L.; Li, B.-G., High Molecular Weight Polyesters Derived from Biobased 1,5-Pentanediol and a Variety of Aliphatic Diacids: Synthesis, Characterization, and Thermo-Mechanical Properties. *Acs Sustainable Chemistry & Engineering* **2017,** *5* (7), 6159-6166.

227. Henczka, M.; Djas, M., Reactive extraction of succinic acid using supercritical carbon dioxide. *Separation Science and Technology* **2017,** *53* (4), 655-661.

228. Medina-Gonzalez, Y.; Tassaing, T.; Camy, S.; Condoret, J. S., Phase equilibrium of the CO_2/glycerol system: experimental data by in situ FT-IR spectroscopy and thermodynamic modeling. *Supercritical Fluids* **2013,** *73*, 97-107.

229. Foley, P.; Kermanshahi-pour, A.; Beach, E. S.; Zimmerman, J. B., Derivation and synthesis of renewable surfactants. *Chemical Society Reviews* **2012,** *41* (4), 1499-1518.

230. Wood, L. Global market for surfactants report 2017: Segmented by material type, origin, application & geography - research and markets. https://www.businesswire.com/news/home/20170915005310/en/Global-Market-Surfactants-Report-2017-Segmented-Material (accessed 29th May 2018).

231. Pacwa-Płociniczak, M.; Płaza, G. y. A.; Piotrowska-Seget, Z.; Cameotra, S. S., Environmental Applications of Biosurfactants: Recent Advances. *International Journal of Molecular Sciences* **2011,** *12*, 633-654.

232. Curia, S.; Howdle, S. M., Towards sustainable polymeric nano-carriers and surfactants: facile low temperature enzymatic synthesis of bio-based amphiphilic copolymers in $scCO_2$. *Polymer Chemistry* **2016,** *7* (11), 2130-2142.

233. Myers, D., An Overview of Surfactant Science and Technology. In *Surfactant Science and Technology*, 3rd edition ed.; John Wiley & Sons, Inc.: New Jersey, 2006.

234. Baker, I. J. A.; Drummong, C. J.; Furlong, D. N.; Grieser, F., Surfactant Biodegradation: Sugar-based surfactants compared to other surfactants. In *Handbook of Detergents. Part D: Formulation*, Showell, M. S., Ed. Marcel Dekker, Inc.: Basel, Switzerland, 2008; Vol. Volume 128.

235. Raffa, P.; Wever, D. A. Z.; Picchioni, F.; Broekhuis, A. A., Polymeric surfactants: synthesis, properties, and links to applications. *Chemical Reviews* **2015,** *115* (16), 8504-8563.

236. Farn, R. J., *Chemistry and technology of surfactants*. Blackwell Publishing Ltd: United Kingdom 2006.

237. Scheibell, J. J., The evolution of anionic surfactant technology to meet the requirements of the laundry detergent industry. *Journal of Surfactants and Detergents* **2004,** *7* (4), 319-328.

238. Kronberg, B.; Holmberg, K.; Lindman, B., Types of surfactants, their synthesis and applications. In *Surface Chemistry of Surfactants and Polymers*, John Wiley & Sons, Ltd: United Kingdom, 2014.

239. Borse, M. S.; Devi, S., Importance of head group polarity in controlling aggregation properties of cationic gemini surfactants. *Advances in Colloid and Interface Science* **2006,** *123-126* (16), 387-399.

240. Boos, A. G. D.; Finnimore, E., The effects of cationinc surfactants on the bending properties of woven wool fabric. *Journal of the Textile Institute* **1984,** *75* (2), 81-91.

241. Souza, A. V.; Mendes, M. T.; Souza, S. T. S.; Palermo, L. C. M.; Oliveira, P. F.; Mansur, C. R. E., Synthesis of additives based on polyethylenimine modified with nonionic surfactants for application in phase separation of water-in-oil emulsions. *Energy and Fuels* **2017,** *31* (10), 10612-10619.

242. Tsubone, K.; Uchida, N.; Mimura, K., New amphoteric surfactants containing a phosphoric acid group: II. Binary system of amphoteric/anionic surfactant of sodium 2-(N-2-hydroxytetradecyl-N-methylamino)ethyl hydrogen phosphate. *Journal of the American Oil Chemists Society* **1990,** *67* (7), 455-458.

243. Rosen, M. J.; Kunjappu, J. T., Characteristic features of surfactants. In *Surfactants and Interfacial phenomena* 4th edition ed.; John Wiley & Sons, Inc: New Jersey, 2012.

244. Gecol, H., The basic theory. In *Chemistry and technology of surfactants*, Farn, R. J., Ed. Blackwell Publishing Ltd: United Kingdom 2006.

245. Company, A.-H. Polyethylene Glycol (PEG) 200. http://www.acme-hardesty.com/product/polyethylene-glycol-peg-200/ (accessed 30th May 2018).

246. Company, A.-H. Polyethylene Glycol (PEG) 300. http://www.acme-hardesty.com/product/polyethylene-glycol-300/ (accessed 30th May 2018).

247. Company, A.-H. Polyethylene Glycol (PEG) 400. http://www.acme-hardesty.com/product/polyethylene-glycol-peg-400/ (accessed 30th May 2018).

248. Company, A.-H. Polyethylene Glycol (PEG) 600. http://www.acme-hardesty.com/product/polyethylene-glycol-peg-600/ (accessed 30th May 2018).

249. BASF Pluronic®. https://worldaccount.basf.com/wa/NAFTA~en_US/Catalog/ChemicalsNAFTA/pi/BASF/Brand/pluronic (accessed 30th May 2018).

250. CRODA Synperonic PE/F68. https://www.crodaindustrialchemicals.com/en-gb/products-and-applications/product-finder/product/663/Synperonic_1_PE_2_F68 (accessed 30th May 2018).

251. Akash, M. S. H.; Rehman, K., Recent progress in biomedical applications of Pluronic (PF127): Pharmaceutical perspectives. *Journal of Controlled Release* **2015,** *209*, 120-138.

252. Usha, H. S.; Maitra, S., Synthesis characterization and application of polyglycerol esters of fatty acids: biodegradable surfactants. *Journal of Dispersion Science and Technology* **2015,** *37* (1), 41-47.

253. Thompson, R. C.; Moore, C. J.; Saal, F. S. v.; Swan, S. H., Plastics, the environment and human health: current consensus and future trends. *Philosophical Transactions of the Royal Society B* **2009,** *364* (1526), 2153-2166.

254. Dornburg, V.; Lewandowski, I.; Patel, M., Comparing theland requirements, energy savings, and greenhouse gas emissions reduction of biobased polymers and bioenergy. *Journal of Industrial Ecology* **2004,** *7* (3-4), 93-116.

255. Cheng, J.; Teply, B. A.; Sherifi, I.; Sung, J.; Luther, G.; Gu, F. X.; Levy-Nissenbaum, E.; Radovic-Moreno, A. F.; Langer, R.; Farokhzad, O. C., Formulation of functionalized PLGA–PEG nanoparticles for in vivo targeted drug delivery. *Biomaterials* **2007,** *28* (5), 869-876.

256. Jeong, B.; Han Bae, Y.; Wan Kim, S., Biodegradable thermosensitive micelles of PEG-PLGA-PEG triblock copolymers. *Colloids and Surfaces B-Biointerfaces* **1999,** *16* (1-4), 185-193.

257. Guo, J.; Gao, X.; Su, L.; Xia, H.; Gu, G.; Pang, Z.; Jiang, X.; Yao, L.; Chen, J.; Chen, H., Aptamer-functionalized PEG-PLGA nanoparticles for enhanced anti-glioma drug delivery. *Biomaterials* **2011,** *32* (31), 8010-8020.

258. Matsumoto, J.; Nakada, Y.; Sakurai, K.; Nakamura, T.; Takahashi, Y., Preparation of nanoparticles consisted of poly(L-lactide)–poly(ethylene glycol)–poly(L-lactide) and their evaluation in vitro. *International Journal of Pharmaceutics* **1999,** *185* (1), 93-101.

259. Nagasaki, Y.; Yasugi, K.; Yamamoto, Y.; Harada, A.; Kataoka, K., Sugar-installed block copolymer micelles: their preparation and specific interaction with lectin molecules. *Biomacromolecules* **2001,** *2* (4), 1067-1070.

260. Yasugi, K.; Nakamura, T.; Nagasaki, Y.; Kato, M.; Kataoka, K., Sugar-installed polymer micelles: synthesis and micellization of poly(ethylene glycol)-poly(D,L-lactide) block copolymers having sugar groups at the PEG chain end. *Macromolecules* **1999,** *32* (24), 8024-8032.

261. Ghahremankhani, A. A.; Dorkoosh, F., PLGA-PEG-PLGA tri-block copolymers as in situ gel-forming peptide delivery system: effect of formulation properties on peptide release. *Pharmaceutical Development and Technology* **2008,** *13* (1), 49-55.

262. Yamada, T.; Imamura, Y., Relation between characteristics and melting point of oligomers in poly(ethylene terephthalate) manufacturing. *Polymer Engineering and Science* **1988,** *28* (6), 381-392.

263. Ashman, P. C.; Booth, C., Melting of low molecular weight poly(ethylene oxide) with acetoxy- and trimethylsiloxy-end-groups. *Polymer* **1973,** *14* (7), 300-302.

264. Jr., J. A.; Blachechen, L. S.; Petri, D. F. S., Effect of sorbitan-based surfactants on glass transition temperature of cellulose esters. *Journal of Thermal Analysis and Calorimetry* **2012,** *107* (3), 1259-1265.

265. Fang, S. W.; Caro, P. D.; Pennarun, P.-Y.; Vaca-Garcia, C.; Thiebaud-Roux, S., Synthesis and characterization of new polyesters based on renewable resources. *Industrial Crops and Products* **2013,** *43* (1), 398–404.

266. Acme-Hardesty Company Polyethylene Glycol (PEG) 300. http://www.acme-hardesty.com/product/polyethylene-glycol-300/ (accessed 30th May 2018).

267. Kobayashi, S.; Ohmae, M., Polymer synthesis and modification by enzymatic catalysis. In *Macromolecular Engineering – Precise Synthesis, Materials Properties, Applications*, Matyjaszewski, K.; Gnanou, Y.; Leibler, L., Eds. WILEY-VCH Verlag GmbH & Co.: Germany, 2007; Vol. Volume 1 - Synthetic Techniques, pp 401-478.

268. Vassiliou, A. A.; Papadimitriou, S. A.; Bikiaris, D. N.; Mattheolabakis, G.; Avgoustakis, K., Facile synthesis of polyester-PEG triblock copolymers and preparation of amphiphilic nanoparticles as drug carriers. *Journal of Controlled Release* **2010,** *148* (3), 388-395.

269. Baiardo, M.; Frisoni, G.; Scandola, M.; Rimelen, M.; Lips, D.; Ruffieux, K.; Wintermantel, E., Thermal and mechanical properties of plasticized poly(L-lactic acid). *Journal of Applied Polymer Science* **2003,** *90* (7), 1731-1738.

270. Pivsa-Art, W.; Fujii, K.; Nomura, K.; Aso, Y.; Ohara, H.; Yamane, H., The effect of poly(ethylene glycol) as plasticizer in blends of poly(lactic acid) and poly(butylene succinate). *Journal of Applied Polymer Science* **2015,** *133* (8), 43044-43054.

271. Roberto, A.; Rachele, C.; Gennaro, G.; Veronica, A.; Stefano, F.; Maurizio, A.; Mariacristina, C.; Emanuela, E. M., Plasticization of poly(lactic acid) through blending with oligomers of lactic acid: Effect of the physical aging on properties. *European Polymer Journal* **2014,** *66*, 533-542.

272. Ljungberg, N.; Wesslén, B., Tributyl citrate oligomers as plasticizers for poly (lactic acid): thermo-mechanical film properties and aging. *Polymer* **2003,** *44* (25), 7679-7688.

273. Ljungberg, N.; Colombini, D.; Wesslén, B., Plasticization of poly(lactic acid) with oligomeric malonate esteramides: Dynamic mechanical and thermal film properties. *Journal of Applied Polymer Science* **2005,** *96* (4), 992-1002.

274. Ljungberg, N.; Wesslén, B., Preparation and properties of plasticized poly(lactic acid) films. *Biomacromolecules* **2005,** *6* (3), 1789-1796.

275. Santa Cruz Biotechnology Inc. Methoxypolyethylene glycol 350 (CAS 9004-74-4). https://www.scbt.com/scbt/product/methoxypolyethylene-glycol-350-9004-74-4 (accessed 5th July 2018).

276. Stempfle, F.; Ortmann, P.; Mecking, S., Long-chain aliphatic polymers to bridge the gap between semicrystalline polyolefins and traditional polycondensates. *Chemical Reviews* **2016,** *116* (7), 4597-4641.

277. Lewis, J. J., An introduction to surfactants. In *Preservation of Surfactant Formulations*, Morpeth, F., Ed. Springer: Netherlands, 1995; pp 53-82.

278. Kronberg, B.; Holmberg, K.; Lindman, B., Surfactant self-assembly: General aspects and spherical micelles. In *Surface Chemistry of Surfactants and Polymers*, John Wiley & Sons, Ltd: United Kingdom, 2014; pp 75-94.

279. Chemical-Distribution, B. Nonionic surfactants – for detergents and cleaning agents. https://www.btc-europe.com/en/AL/solution-finder/industry/detergents-cleaners-industry/detergents-and-cleaning-agents/nonionic-surfactants/nonionic-surfactants-for-detergents-and-cleaning-agents/ (accessed 6th July 2018).

280. Kumar, N.; Tyagi, R., Dimeric surfactants: promising ingredients of cosmetics and toiletries. *Cosmetics* **2013,** *1* (1), 3-13.

281. Somasundaran, P.; Wines, T. H.; Mehta, S. C.; Garti, N.; Farinato, R., Emulsions and their behaviour. In *Surfactants in Personal care Products and decorative cosmetics*, 3rd edition ed.; Rhein, L. D.; Schlossman, M.; O'Lenick, A.; Somasundaran, P., Eds. Taylor & Francis, LLC: New York, 2007; Vol. 135.

282. Glavas, L.; Olsén, P.; Odelius, K.; Albertsson, A.-C., Achieving Micelle Control through Core Crystallinity. *Biomacromolecules* **2013,** *14* (11), 4150-4156.

283. Cabral, H.; Matsumoto, Y.; Mizuno, K.; Chen, Q.; Murakami, M.; Kimura, M.; Terada, Y.; Kano, M. R.; Miyazono, K.; Uesaka, M.; NishiyamaGarti, N.; Kataoka, K., Accumulation of sub-100 nm polymeric micelles in poorly permeable tumours depends on size. *Nature Nanotechnology* **2011,** *6*, 815-823.

284. Jong, W. H. D.; Borm, P. J. A., Drug delivery and nanoparticles: Applications and hazards. *International Journal of Nanomedicine* **2008,** *3* (2), 133-149.

285. Bansal, K. K.; Kakde, D.; Purdie, L.; Irvine, D. J.; Howdle, S. M.; Mantovani, G.; Alexander, C., New biomaterials from renewable resources – amphiphilic block copolymers from δ-decalactone. *Polymer Chemistry* **2015,** *6* (40), 7196-7210.

286. Ahmad, Z.; Shah, A.; Siddiq, M.; Kraatz, H.-B., Polymeric micelles as drug delivery vehicles. *Rsc Advances* **2014,** *4* (33), 17028-17038.

287. Kislenko, V. N.; Zaichenko, A.; Mitina, N., Topochemistry and kinetics of functional particle formation at water dispersion polymerization. In *Encyclopedia of Surface and Colloid Science*, 2nd Edition ed.; Somasundaran, P., Ed. CRC Press: Florida, UA, 2004; Vol. Vol. 6, pp 632-648.

288. Ogino, K.; Kubota, T.; Uchiyama, H.; Abe, M., Micelle formation and micellar size by a light scattering technique. *Journal of the Japan Oil Chemists' Society* **1988,** *37* (8), 588-591.

289. Lee, T. R.; Yuan, Y., Contact angle and wetting properties. In *Surface Science Techniques*, Bracco, G.; Holst, B., Eds. Springer-Verlag Berlin, 2013; Vol. 51, pp 3-34.

290. Balasuwatthi, P.; Dechabumphen, N.; Saiwan, C.; Scamehorn, J. F., Contact angle of surfactant solutions on precipitated surfactant surfaces. II. Effects of surfactant structure, presence of a subsaturated surfactant, pH, and counterion/surfactant ratio. *Journal of Surfactants and Detergents* **2003,** *7* (1), 31-40.

291. Luepakdeesakoon, B.; Saiwan, C.; Scamehorn, J. F., Contact angle of surfactant solutions on precipitated surfactant surfaces. III. Effects of subsaturated anionic and nonionic surfactants and NaCl. *Journal of Surfactants and Detergents* **2006,** *9* (2), 125-136.

292. Shimelis, H.; Mashela, P. W.; Hugo, A., Performance of Vernonia as an alternative industrial oil crop in Limpopo province of South Africa. *Crop Science* **2008,** *48*, 236-242.

293. Shimelis, H. A.; Labuschagne, M. T.; Hugo, A., Variation of oil content and fatty acid composition in selected lines of vernonia (Vernonia galamensis variety ethiopica). *South African Journal of Plant and Soil* **2006,** *23* (1), 62-63.

294. Ayorinde, F. O.; Powers, F. T.; Streete, L. D.; Shepard, R. L.; Tabi, D. N., Synthesis of dodecanedioic acid from *Vernonia galamensis* oil. *Journal of the American Oil Chemists Society* **1989,** *66* (5), 690-692.

295. Gunstone, F. D., Fatty acids. Part II. The nature of the oxygenated acid present in *Vernonia anthelmintica* (Willd.) seed oil. *Journal of the Chemical Society* **1954,** (0), 1611-1616.

296. Sharmin, E.; Zafar, F.; Akram, D.; Alam, M.; Ahmad, S., Recent advances in vegetable oils based environment friendly coatings: A review. *Industrial Crops and Products* **2015,** *76* (15), 215-229.

297. Tripathy, D. B.; Mishra, A., Renewable Plant-Based Raw Materials for Industry. *Encyclopedia of Inorganic and Bioinorganic Chemistry* **2016**, 1-16.

298. Farmer, T. J.; Mascal, M., The biorefinery concept: an integrated approach. In *Introduction to Chemicals from Biomass*, 2nd edition ed.; Clark, J.; Deswarte, F., Eds. West Sussex, UK, 2015.

299. Bianchi, C., Renewable Energy Technology Roadmap: 20% RES by 2020. In *Advances in Global change Research – Local Governments and Climate Change*, Staden, M. v.; Musco, F., Eds. Springer Dordrecht Heidelberg: Brussels, 2010; pp 131-162.

300. Nilsson, H.; Olsson, A.; Lindström, M.; Iversen, T., Bark suberin as a renewable source of long-chain w-hydroxyalkanoic acids. *Macromolecular Symposia* **2008,** *272* (1), 104-106.

301. Lligadas, G.; Ronda, J. C.; Galià, M.; Cádiz, V., Renewable polymeric materials from vegetable oils: a perspective. *Materials Today* **2013,** *16* (9), 337-343.

302. Semlitsch, S.; Torron, S.; Johansson, M.; Martinelle, M., Enzymatic catalysis as a versatile tool for the synthesis of multifunctional, bio-based oligoester resins. *Green Chemistry* **2015,** *18* (7), 1923-1929.

303. Torron, S.; Semlitsch, S.; Martinelle, M.; Johansson, M., Polymer thermosets from multifunctional polyester resins based on renewable monomers. *Macromolecular Chemistry and Physics* **2014,** *215* (22), 2198-2206.

304. Biswas, A.; Cheng, H. N.; Klasson, K. T.; Liu, Z.; Berfield, J.; Ayorinde, F. O., Direct polymerization of vernonia oil through cationic means. *Journal of the American Oil Chemists Society* **2014,** *91* (12), 2111-2116.

305. Sharma, V.; Kundu, P. P., Condensation polymers from natural oils. *Progress in Polymer Science* **2008,** *33* (12), 1199-1215.

306. Meier, M. A. R.; Metzger, J. O.; Schubert, U. S., Plant oil renewable resources as green alternatives in polymer science. *Chemical Society Reviews* **2007,** *36* (11), 1788-1802.

307. Afolabi, O. A.; Aluko, M. E.; Wang, G. C.; Anderson, W. A.; Ayorinde, F. O., Synthesis of toughened elastomer from *Vernonia galamensis* seed oil. *Journal of the American Oil Chemists Society* **1989,** *66* (7), 983-985.

308. Nydick, D. Tall Ironweed. https://www.inaturalist.org/observations/1906657 (accessed 9th July 2018).

309. Richard, R. The garden path art photography and other stuff. https://roserichard.wordpress.com/tag/butterfly/ - jp-carousel-386 (accessed 9th July 2018).

310. Aminia, M.; Haghdoost, M. M.; Bagherzadeh, M., Monomeric and dimeric oxido–peroxido tungsten(VI) complexes in catalytic and stoichiometric epoxidation. *Coordination Chemistry Reviews* **2014,** *268* (1), 83-100.

311. Gelalcha, F. G., Biomimetic iron-catalyzed asymmetric epoxidations: fundamental concepts, challenges andopportunities. *Advanced Synthesis & Catalysis* **2014,** *356* (2-3), 261-299.

312. Teacă, C.-A.; Roşu, D.; Tanasă, F.; Zănoagă, M. d. I.; Mustaţă, F. n., Epoxidized Vegetable Oils for Thermosetting Resins and Their Potential Applications. In *Functional Biopolymers*, Thakur, V. K.; Thakur, M. K., Eds. Springer International Publishing Bedfordshire, UK, 2018; pp 217-238.

313. Hosney, H.; Nadiem, B.; Ashour, I.; Mustafa, I.; El-Shibiny, A., Epoxidized vegetable oil and bio-based materials as PVC plasticizer. *Journal of Applied Polymer Science* **2018,** *135* (20), 46270.

314. Prileschajew, N., Oxydation ungesättigter Verbindungen mittels organischer Superoxyde. *Chemische Berichte* **1909,** *42* (4), 4811-4815.

315. Goud, V. V.; Pradhan, N. C.; Patwardhan, A. V., Epoxidation of Karanja (*Pongamia glabra*) Oil by H_2O_2. *Journal of the American Oil Chemists Society* **2006,** *83* (7), 635-640.

316. Petrović, Z. S.; Zlatanić, A.; Lava, C. C.; Sinadinović-Fišer, S., Epoxidation of soybean oil in toluene with peroxoacetic and peroxoformic acids – kinetics and side reactions. *European Journal of Lipid Science and Technology* **2002,** *104* (5), 293-299.

317. Okieimen, F. E.; Bakare, O. I.; Okieimen, C. O., Studies on the epoxidation of rubber seed oil. *Industrial Crops and Products* **2002,** *15* (2), 139-144.

318. Campanella, A.; Baltanás, M. A.; Capel-Sánchez, M. C.; Campos-Martín, J. M.; Fierro, J. L. G., Soybean oil epoxidation with hydrogen peroxide using an amorphous Ti/SiO_2 catalyst. *Green Chemistry* **2004,** *6* (7), 330-334.

319. Epoxy-Europe Social & Economic Benefits. https://epoxy-europe.eu/en/social-economic-benefits/ (accessed 10th July 2018).

320. Xia, Q. H.; Ge, H. Q.; Ye, C. P.; Liu, Z. M.; Su, K. X., Advances in homogeneous and heterogeneous catalytic asymmetric epoxidation. *Chemical Reviews* **2005,** *105* (5), 1603-1662.

321. Vlček, T. š.; Petrović, Z. S., Optimization of the chemoenzymatic epoxidation of soybean oil. *Journal of the American Oil Chemists Society* **2006,** *83* (3), 247-252.

322. Goud, V. V.; Patwardhan, A. V.; Pradhan, N. C., Studies on the epoxidation of mahua oil (Madhumica indica) by hydrogen peroxide. *Bioresource Technology* **2006,** *97* (12), 1365-1371.

323. Swern, D., Organic peracids. *Chemical Reviews* **1949,** *45* (1), 1-68.

324. Biermann, U.; Friedt, W.; Lang, S.; Lühs, W.; Machmüller, G.; Metzger, J. r. O.; Klaas, M. R. s. g.; Schäfer, H. J.; Schneider, M. P., New syntheses with oils and fats asrenewable raw materials for the chemical industry. *Angewwandte Chemie International* **2000,** *39* (13), 2206-2224.

325. Ankudey, E. G.; Olivo, H. F.; Peeplesa, T. L., Lipase-mediated epoxidation utilizing urea–hydrogen peroxide in ethyl acetate. *8* **2006,** *10* (923-926).

326. Earle, F. R., Epoxy oils from plant seeds. *Journal of the American Oil Chemists Society* **1970,** *47* (12), 510-513.

327. Manson, M. M., Epoxides – is there a human health problem? *British Journal of Industrial Medicine* **1980,** *37* (4), 317-336.

328. Krewson, C. F., Naturally occuring epoxy oils. *Journal of the American Oil Chemists Society* **1968,** *45* (4), 250-256.

329. Morris, L. J.; Holman, R. T., Naturally occurring epoxy acids. II. Detection and measurement of long-chain epoxy acids by near infrared spectrophotometry. *Journal of Lipid Research* **1961,** *2* (1), 77-82.

330. Earle, F. R.; Jones, Q., Analyses of seed samples from 113 plant families. *Economic Botany* **1962,** *16* (4), 221-250.

331. Jones, Q.; Earle, F. R., Chemical analyses of seeds II: Oil and protein content of 759 species. *Economic Botany* **1966,** *20* (2), 127-155.

332. Gunstone, F. D.; Morris, L. J., Fatty acids. Part VI. The oxygenated acid present in *Camelina sativa* (Crantz.) seed oil. *Journal of the Chemical Society* **1959,** *0*, 2127-2132.

333. Tallent, W. H.; Cope, D. G.; Hagemann, J. W.; Earle, F. R.; Wolff, I. A., Identification and distribution of epoxyacyl groups in new, natural epoxy oils. *Lipids* **1966,** *1* (5), 335-340.

334. Bharucha, K. E.; Gunstone, F. D., Vegetable oils. V – The component acids of *Cephalocroton cordofanus* seed oil. *Journal of the Science of Food and Agriculture* **1956,** *7* (9), 606-609.

335. Kleiman, R.; Jr., C. R. S.; Yates, S. G.; Jones, Q., Search for new industrial oils. XII – Fifty-eight euphorbiaceae oils, including one rich in vernolic acid. *Journal of the American Oil Chemists Society* **1965,** *42* (3), 169-172.

336. Gunstone, F. D.; Sykes, P. J., Vegetable oils. IX – Application of reversed-phase chromatography to the analysis of seed oils. *Journal of the Science of Food and Agriculture* **1961,** *12* (2), 115-123.

337. Morris, L. J.; Holman, R. T.; Fontell, K., Naturally occurring epoxy acids. I. Detection and evaluation of epoxy fatty acids by paper, thin-layer, and gas-liquid chromatography. *Journal of Lipid Research* **1961,** *2* (1), 68-76.

338. Hopkins, C. Y.; Chisholm, M. J., Epoxy acid in seed oils of *Malvaceae* and preparation of (+)threo-12,13-Dihydroxyoleic acid. *Journal of the American Oil Chemists Society* **1960,** *37* (12), 682-684.

339. Hopkins, C. Y.; Chisholm, M. J., Fatty acids of Kenaf seed oil. *Journal of the American Oil Chemists Society* **1959,** *36* (3), 95-96.

340. Morris, L. J., The oxygenated acids of Isano (Boleko) oil. *Journal of the Chemical Society* **1963,** *0*, 5779-5781.

341. Jr., C. R. S.; Bagby, M. O.; Lohmar, R. L.; Glass, C. A.; Wolff, I. A., The epoxy acids of *Chrysanthemum coronarium* and *Clarkia elegans* seed oils. *The Journal of Organic Chemistry* **1960,** *25* (2), 218-222.

342. Tulloch, A. P.; Craig, B. M.; Ledingham, G. A., The oil of wheat stem rust uredospores. II. The isolation of *cis*-9,10-epoxyoctadecanoic acid, and the fatty acid composition of the oil. *Canadian Journal of Microbiology* **1959,** *5* (5), 485-491.

343. Vioque, E.; Morris, L. J.; Holman, R. T., Minor components of olive oils. II. *trans*-9,10-epoxystearic acid in orujo oil. *Journal of the American Oil Chemists Society* **1961,** *38* (489-492).

344. Gunstone, F. D., Fatty acids. Part II. The nature of the oxygenated acid present in *Vernonia anthelmintica* (Willd.) seed oil. *Journal of the Chemical Society* **1954,** *0*, 1611-1616.

345. Jr., C. R. S.; Koch, K. F.; Wolff, I. A., Isolation of vernolic acid from *Vernonia anthelmintica* oil. *Journal of the American Oil Chemists Society* **1959,** *36* (5), 219-220.

346. Thompson, A. E.; Dierig, D. A.; Kleiman, R., Variation in Vemonia galamensis flowering characteristics, seed oil and vernolic acid contents. *Industrial Crops and Products* **1994,** *3* (3), 175-183.

347. Dirlikov, S.; Frischinger, I.; Islam, M. S.; Lepkowski, T. J., Vernonia oil: A new reactive monomer. In *Biotechnology and polymers*, 1st Edition ed.; Gebelein, C. G., Ed. Springer Science+Business Media, LLC: Boston, Massachusetts, 1991.

348. Kolot, V.; Grinberg, S., Vernonia oil–based acrylate and methacrylate polymers and interpenetrating polymer *Journal of Applied Polymer Science* **2003,** *91* (6), 3835–3843.

349. Ncube, I.; Gitlesen, T.; Adlercreutz, P.; Read, J. S.; Mattiasson, B., Fatty acid selectivity of a lipase purified from *Vernonia galamensis* seed. *Biochimica et Biophysica Acta* **1995,** *1257* (2), 149-156.

350. Arthur, M. W. Extraction and characterization of vernonia oil and synthesis of n-(aminoalkyl)vernolamides and n,n-polymethylene bis(vernolamides). University of Nairobi, Nairobi, Kenya, 1996.

351. Bhardwaj, H. L.; Hamama, A. A.; Dierig, D., Fatty acids in vernonia produced in the mid-Atlantic region of the United States. *Journal of the American Oil Chemists Society* **2007,** *84* (4), 393-397.

352. Al-Hamimi, S.; Mayoral, A. A.; Cunico, L. P.; Turner, C., Carbon dioxide expanded ethanol extraction: solubility and extraction kinetics of α-pinene and cis-verbenol. *Analytical Chemistry* **2016,** *88* (8), 4336-4345.

353. King, J. W.; Mohamed, A.; Taylor, S. L.; Mebrahtu, T.; Paul, C., Supercritical fluid extraction of *Vernonia galamensis* seeds. *Industrial Crops and Products* **2001,** *14* (3), 241-249.

354. Montanari, L.; Fantozzi, P.; Snyder, J. M.; King, J. W., Selective extraction of phospholipids with supercritical carbon dioxide and ethanol. *Journal of Supercritical Fluids* **1999,** *14* (2), 87-93.

355. Kato, T.; Yamaguchi, Y.; Namai, T.; Hirukawa, T., Oxygenated Fatty Acids with Anti-rice Blast Fungus Activity in Rice Plants. *Bioscience, Biotechnology and Biochemistry* **1993,** *57* (2), 283-287.

356. Hou, C. T., Biotechnology for fats and oils: new oxygenated fatty acids. *New Biotechnology* **2009,** *26* (1-2), 2-10.

357. Kraus, G. A.; Frazier, K., Preparation of allylic alcohols from epoxides using iodotrimethylsilane. *The Journal of Organic Chemistry* **1980,** *45* (13), 2579-2581.

358. Nagarkatti, J. P.; Ashley, K. R., Periodic acid cleavage of epoxides in aqueous medium. *Tetrahedron Letters* **1973,** (46), 4599-4600.

359. Kim, J.; Matsuyama, S.; Suzuki, T., Deuterated analogues of 4,8-dimethyldecanal, the aggregation pheromone of *Tribolium castaneum*: synthesis and pheromonal activity. *Journal of Labelled Compounds and Radiopharmaceuticals* **2004,** *47* (13), 921-934.

360. Sankaranarayanan, S.; Chattopadhyay, S., Enantiospecific synthesis of 6-methylheptadec-(9*E*)-enoic acid enantiomers, the antimicrobial principles of Sporothrix species. *Tetrahedron: Asymmetry* **1998,** *9* (15), 2627-2633.

361. Binder, C. M.; Dixon, D. D.; Almaraz, E.; Tius, M. A.; Singaram, B., A Simple Procedure for C-C Bond Cleavage of Aromatic and Aliphatic Epoxides with Aqueous Sodium Periodate Under Ambient Conditions. *Tetrahedron Letters* **2008,** *49* (17), 2764-2767.

362. Concellón, J. M.; Concellón, C., Direct reaction of dibromoacetic acid with aldehydes promoted by samarium diiodide: an easy, efficient, and rapid synthesis of (E)-α,β-unsaturated carboxylic acids with total stereoselectivity. *The Journal of Organic Chemistry* **2006,** *71* (4), 1728-1731.

363. Augustine, J. K.; Naik, Y. A.; Mandal, A. B.; Chowdappa, N.; Praveen, V. B., *gem*-Dibromomethylarenes: A Convenient Substitute for Noncommercial Aldehydes

in the Knoevenagel−Doebner Reaction for the Synthesis of α,β-Unsaturated Carboxylic Acids. *The Journal of Organic Chemistry* **2007,** *72* (25), 9854-9856.

364. Bahrami, K.; Khodaei, M. M.; Kamali, S., Selective and efficient oxidation of aldehydes to their corresponding carboxylic acids using H_2O_2/HCl in the presence of hydroxylamine hydrochloride. *Chinese Journal of Chemistry* **2008,** *26* (6), 1119-1121.

365. Kon, Y.; Imao, D.; Nakashima, T.; Sato, K., Palladium(II)-catalyzed selective oxidation of α,β-unsaturated aldehydes to α,β-unsaturated carboxylic acids with hydrogen peroxide. *Chemistry Letters* **2009,** *38* (5), 430-431.

366. Tanaka, S.; Kon, Y.; Uesaka, Y.; Morioka, R.; Tamura, M.; Sato, K., Iron-catalyzed Selective Oxidation of α,β-Unsaturated Aldehydes to α,β-Unsaturated Carboxylic Acids by Molecular Oxygen. *Chemistry Letters* **2016,** *45* (2), 188-190.

367. Nystrom, R. F.; Brown, W. G., Reduction of organic compounds by lithium aluminum hydride. I. Aldehydes, ketones, esters, acid chlorides and acid anhydrides. *Journal of the American Chemical Society* **1947,** *69* (5), 1197-1199.

368. Chapuis, C., Enantioselective access to (−)-Ambrox® starting from β-farnesene. *Helvetica Chimica Acta* **2014,** *97* (2), 197-214.

369. Brandsma, L.; Verkruijsse, H. D., Organometallic Reagents, Solvents and Laboratory Equipment. In *Preparative Polar Organometallic Chemistry*, Springer-Verlag: Berlin, 1987; pp 19-20.

370. Sun, M.; Temelli, F., Supercritical carbon dioxide extraction of carotenoids from carrot using canola oil as a continuous co-solvent. *The Journal of Biological Chemistry* **2006,** *37* (3), 397-408.

371. Cheung, P. C. K.; Leung, A. Y. H.; Ang, P. O., Comparison of Supercritical Carbon Dioxide and Soxhlet Extraction of Lipids from a Brown Seaweed, *Sargassum hemiphyllum* (Turn.) C. Ag. *Journal of Agricultural and Food Chemistry* **1998,** *46* (10), 4228-4232.

372. Piras, A.; Rosa, A.; Falconieri, D.; Porcedda, S.; Dessì, M. A.; Marongiu, B., Extraction of Oil from Wheat Germ by Supercritical CO_2. *Molecules* **2009,** *14*, 2573-2581.

373. Li, Y.; Naghdi, F. G.; Garg, S.; Vega, T. C. A.-.; Thurecht, K. J.; Ghafor, W. A.; Tannock, S.; Schenk, P. M., A comparative study: the impact of different lipid extraction methods on current microalgal lipid research. *Microbial cell factories* **2014,** *13* (14), 1-9.

374. Smith, J. G., Synthetically useful reactions of epoxides. *Synthesis* **1984,** *8* (8), 629-656.

375. Clayden, J.; Greeves, N.; Warren, S., Nucleophile substitution at the carbonyl group. In *Organic Chemistry*, 2nd edition ed.; Oxford University Press: Oxford, UK, 2012; pp 197-221.

376. Blunt, J. W.; Hartshorn, M. P.; Soong, L. T.; Munro, M. H. G., Reactions of propargyl alcohols. V. Lithium aluminium hydride reduction of some C 1-epimeric 4-t-butyl-1-prop-1'-ynylcyclohexanols. *Australian Journal of Chemistry* **1982,** *35* (12), 2519-2528.

377. Meyer, G. R., Conjugate and nonconjugate reduction with $LiAlH_4$ and $NaBH_4$. *Journal of Chemical Education* **1981,** *58* (8), 628-630.

378. Nameer, S.; Semlitsch, S.; Martinelle, M.; Johansson, M., One-pot enzyme-catalyzed synthesis of dual-functional polyester macromers towards surface active hydrophobic films. *Rsc Advances* **2017,** *7* (79), 50294–50299.

379. Gandini, A.; Belgacem, M. N., The state of the art. In *Monomers, Polymers and Composites from Renewable Resources*, Gandini, A.; Belgacem, M. N., Eds. Elsevier: Netherlands, 2008; pp 1-16.

380. Thomsett, M. R.; Storr, T. E.; Monaghan, O. R.; Stockman, R. A.; Howdle, S. M., Progress in the synthesis of sustainable polymers from terpenes and terpenoids. *Green Materials* **2016,** *4* (3), 115-134.

381. Rose, M.; Palkovits, R., Cellulose-based sustainable polymers: state of the art and future trends. *Macromolecular Rapid Communications* **2011,** *32* (17), 1299-1311.

382. Croisier, F.; Jérôme, C., Chitosan-based biomaterials for tissue engineering. *European Polymer Journal* **2013,** *49* (4), 780-792.

383. Guo, M.; Wang, G., Milk protein polymer and its application in environmentally safe adhesives. *Polymers* **2016,** *8* (9), 324-336.

384. Gandini, A.; Belgacem, M. N., Materials from vegeteble oils: Major sources, properties and applications. In *Monomers, Polymers and Composites from Renewable Resources*, Gandini, A.; Belgacem, M. N., Eds. Elsevier: Netherlands, 2008; pp 39-66.

385. Zhang, C.; Garrison, T. F.; Madbouly, S. A.; Kessler, M. R., Recent advances in vegetable oil-based polymers and their composites. *Progress in Polymer Science* **2017,** *71*, 91-143.

386. Sokolsky-Papkov, M.; Shikanov, A.; Ezra, A.; Vaisman, B.; Domb, A. J., Fatty acid-based biodegradable polymers: synthesis and applications. In *Polymer degradation and performance*, Celina, M. C.; Wiggins, J. S.; Billingham, N. C., Eds. American Chemical Society: Washington, DC, 2009; pp 60-69.

387. Jain, J. P.; Sokolsky, M.; Kumar, N.; Domb, A. J., Fatty acid based biodegradable polymer. *Polymer Reviews* **2008,** *48* (1), 156-191.

388. Slivniak, R.; Domb, A. J., Lactic Acid and Ricinoleic Acid Based Copolyesters. *Macromolecules* **2005,** *38* (13), 5545-5553.

389. Testud, B.; Pintori, D.; Grau, E.; Taton, D.; Cramail, H., Hyperbranched polyesters by polycondensation of fatty acid-based AB_n-type monomers. *Green Chemistry* **2017,** *19* (1), 259-269

390. Yan, D.; Zhou, Z., Molecular weight distribution of hyperbranched polymers generated from polycondensation of AB_2 type monomers in the presence of multifunctional core moieties. *Macromolecules* **1999,** *32* (3), 819-824.

391. Allen, A. D.; Ayorinde, F. O.; Eribo, B. E., Substrates for PHA biosynthesis. In *Polyhydroxyalkanoates (PHAs): Biosynthesis, industrial production and applications in medicine*, Wu, L.-P., Ed. Nova Science Publishers, Inc.: 2014; pp 89-98.

392. Li, Y.; Beisson, F., The biosynthesis of cutin and suberin as an alternative source of enzymes for the production of bio-based chemicals and materials. *Biochimie* **2009,** *91* (6), 685-691.

393. Kolot, V.; Grinberg, S., Vernonia oil-based acrylate and methacrylate polymers and interpenetrating polymer networks with epoxy resins. *Journal of Applied Polymer Science* **2004,** *91* (6), 3835-3843.

394. Samuelsson, J.; Sundell, P. E.; Johansson, M., Synthesis and polymerization of a radiation curable hyperbranched resin based on epoxy functional fatty acids. *Progress in Organic Coatings* **2004,** *50* (3), 193-198.

395. Fürmeier, S.; Metzger, J. O., Fat-derived aziridines and their N-substituted derivatives: Biologically active compounds based on renewable raw materials. *European Journal of Organic Chemistry* **2003,** (4), 649-659.

396. Balakrishnan, S.; Raghavan, D., Synthesis of 13(14)-hydroxy-cis-10-nonadecenyl amine hydrochloride. *Journal of the American Oil Chemists Society* **2003,** *80* (5), 503-508.

397. Trumbo, D. L.; Mote, B. E.; Rudelich, J. C., Soluble polymers from a multifunctional natural oil. *Journal of Macromolecular Science - Pure and Applied Chemistry* **2001,** *38A* (5-6), 503-512.

398. Bhardwaj, H. L.; Hamama, A. A.; Rangappa, M.; Dierig, D. A., Vernonia oil seed production in the mid-Atlantic region of the United States. *Industrial Crops and Products* **2000,** *12* (2), 119-124.

399. Nayak, P. L., Natural oil-based polymers: opportunities and challenges. *Journal of Macromolecular Science - Polymer Reviews* **2000,** *40* (1), 1-21.

400. Ayorinde, F. O.; Nana, E. Y.; Nicely, P. D.; Woods, A. S.; Price, E. O.; Nwaonicha, C. P., Syntheses of 12-aminododecanoic and 11-aminoundecanoic acids from vernolic acid. *Journal of the American Oil Chemists Society* **1997,** *74* (5), 531-538.

401. Barrett, L. W.; Sperling, L. H.; Murphy, C. J., Naturally functionalized triglyceride oils in interpenetrating polymer networks. *Journal of the American Oil Chemists' Society* **1993,** *70* (5), 523-534.

402. Barrett, L. W.; Shaffer, O. L.; Sperling, L. H., Semi-interpenetrating polymer networks composed of poly(ethylene terephthalate) and vernonia oil. *Journal of Applied Polymer Science* **1993,** *48* (6), 953-968.

403. Barrett, L. W.; Sperling, L. H., Vernonia oil based semi-IPN's with poly(ethylene terephthalate). *Polymeric Materials Science and Engineering* **1992,** *66*, 395-396.

404. Sperling, L. H.; Carraher, C. E., Interpenetrating polymer networks based on functional triglyceride oils and other not yet commercial renewable resources. *Polymeric Materials Science and Engineering* **1990,** *62*, 222-225.

405. Fernandez, A. M.; Manson, J. A.; Sperling, L. H., Simultaneous interpenetrating networks based on vernonia oil polyesters and polystyrene. Part 2: A comparison of the reactivities of vernonia oil and castor oil toward the formation of polyesters. *Polymeric Materials Science and Engineering* **1985,** *52*, 169-176.

406. Sperling, L. H.; Manson, J. A., Interpenetrating polymer networks from triglyceride oils containing special functional groups: a brief review. *Journal of the American Oil Chemists' Society* **1983,** *60* (11), 1887-1892.

407. Fernandez, A. M.; Murphy, C. J.; Decosta, M. T.; Manson, J. A.; Sperling, L. H., Vernonia oil characterization and polymerization, and simultaneous interpenetrating polymer networks based on vernonia oil-sebacic acid/polystyrene-DVB compositions. *Polymer Science and Technology* **1983,** *17*, 273-288.

408. Takasu, A.; Makino, T.; Yamada, S., Polyestersynthesis at moderate temperatures via the direct polycondensation of dicarboxylic acids and diols catalyzed by rare-earth perfluoroalkanesulfonates and bis(perfluoroalkanesulfonyl)imides. *Macromolecules* **2010,** *43* (1), 144-149.

409. Laonuad, P.; Chaiyut, N.; Ksapabutr, B., Poly(lactic acid) preparation by polycondensation method. *Optoelectronics and Advanced Materials – Rapid Communications* **2010,** *4* (8), 1200-1202.

410. Takasu, A.; Iio, Y.; Mimura, T.; Hirabayashi, T., Room-temperature polycondensation of dicarboxylic acids and diols catalyzed by water-stable lewis acids. *Polymer Journal* **2005,** *37* (12), 946-953.

411. Sokolsky-Papkov, M.; Langer, R.; Domb, A. J., Synthesis of aliphatic polyesters by polycondensation using inorganic acid as catalyst. *Polymers for Advanced Technologies* **2011,** *22* (5), 502-511.

412. Ahn, B. D.; Kim, S. H.; Kim, Y. H.; Yang, J. S., Synthesis and characterization of the biodegradable copolymers from succinic scid and adipic acid with 1,4-butanediol. *Journal of Applied Polymer Science* **2001,** *82* (11), 2808-2826.

413. Seymour, R. B.; Jr., C. E. C., Thermal Properties of Polymers. In *Structure - Property Relationships in Polymers*, Springer: Boston, MA, 1984; pp 83-93.

414. Kunal, K. Influence of chemical structure and molecular weight on fragility in polymers. Electronic Thesis or Dissertation, University of Akron, Polymer Science, Ohio, US, 2009.

415. Boonme, P.; Junyaprasert, V. B.; Suksawad, N.; Songkro, S., Microemulsions and nanoemulsions: Novel vehicles for whitening cosmeceuticals. *Journal of Biomedical Nanotechnology* **2009,** *5* (4), 373-383.

416. Yu, J. S.; Kim, A. K., Effect of combination of taurine and azelaic acid on antimelanogenesis in murine melanoma cells. *Journal of Biomedical Science* **2010,** *17*, 1-5.

417. Ebata, H.; Toshima, K.; Matsumura, S., Lipase-catalyzed synthesis and curing of high-molecular-weight polyricinoleate. *Macromolecular Bioscience* **2007,** *7* (6), 798-803.

418. Ebata, H.; Toshima, K.; Matsumura, S., Lipase-catalyzed synthesis and properties of poly[(12-hydroxydodecanoate)-co-(12-hydroxystearate)] directed towards novel green and sustainable elastomers. *Macromolecular Bioscience* **2008,** *8* (1), 38-45.

CHAPTER 9. APPENDIX

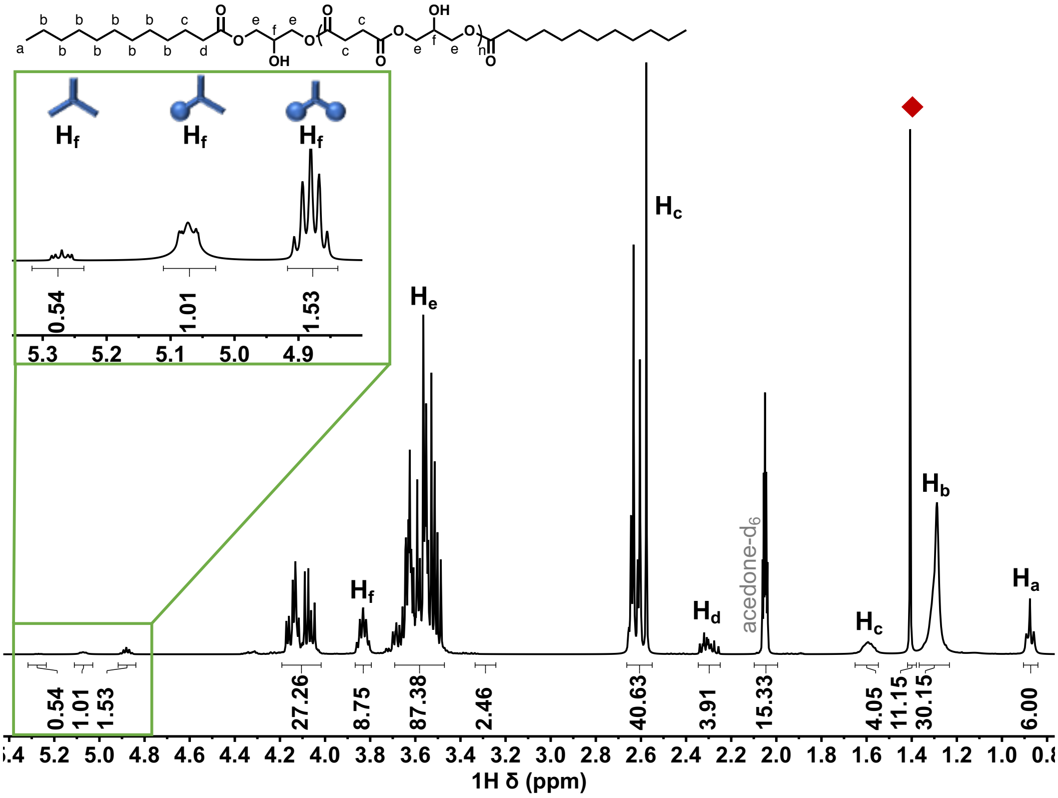

Figure A 1 – ^{1}H-NMR spectrum of LA-PGLSA from entries 2 of Table 4.3 and Table 4.4. The solvent used was acetone-*d*$_6$. Integrals of the peaks of H$_a$ (0.88 ppm, terminal methyl group from LA), and H$_e$ (3.50-3.72 ppm), H$_f$ (3.83 ppm) and H$_c$ (2.58-2.69 ppm) (backbone of PGLSA) can be used to estimate the average molecular weight of the polymer. The peak at 1.29ppm, H$_b$, is assigned to the –CH$_2$– in the LA chain, while peaks at 1.59 and 2.31 ppm, H$_c$ and H$_d$, are assigned to the –CH$_2$– close to the carboxy group of LA (–**CH$_2$**–**CH$_2$**–COO–). *Note*: ◆ is an unknown peak; the schematic representations shown in the highlighted region (5.4-4.8 ppm) corresponds to the branched, linear and terminal glycerol units as follow: ●⅄ = linear glycerol unit; in this case, the polymerisation occurred in positions e, ●⅄ = linear glycerol unit; in this case, the polymerisation occurred in positions e (right) and f, ●⅄● = terminal glycerol in the polymer backbone, leaving the hydroxy groups e free, ⅄ = trisubstituted glycerol unit in the branched polymer backbone.

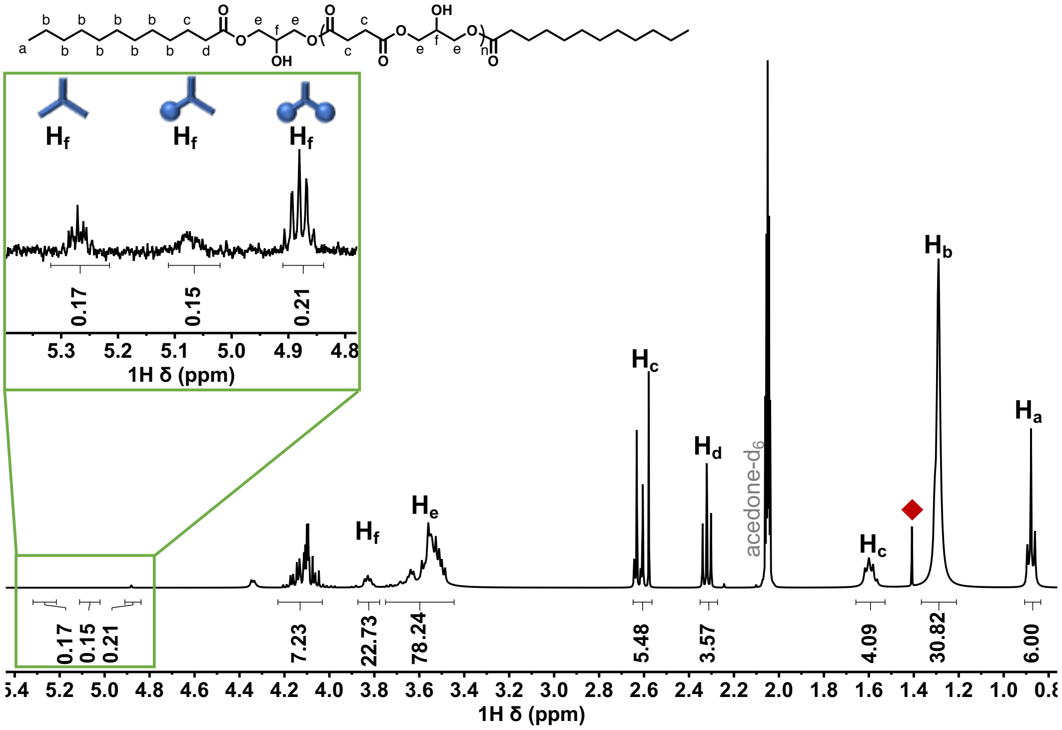

Figure A 2 – ^{1}H-NMR spectrum of LA-PGLSA from entries 3 of Table 4.3 and Table 4.4. The solvent used was acetone-*d*$_6$. Integrals of the peaks of H$_a$ (0.88 ppm, terminal methyl group from LA), and H$_e$ (3.50-3.72 ppm), H$_f$ (3.83 ppm) and H$_c$ (2.58-2.69 ppm) (backbone of PGLSA) can be used to estimate the average molecular weight of the polymer. The peak at 1.29ppm, H$_b$, is assigned to the –CH$_2$– in the LA chain, while peaks at 1.59 and 2.31 ppm, H$_c$ and H$_d$, are assigned to the –CH$_2$– close to the carboxy group of LA (–C**H$_2$**–C**H$_2$**–COO–). *Note*: ◆ is an unknown peak; the schematic representations shown in the highlighted region (5.4-4.8 ppm) corresponds to the branched, linear and terminal glycerol units as follow: ⅄ = linear glycerol unit; in this case, the polymerisation occurred in positions e, ⅄ = linear glycerol unit; in this case, the polymerisation occurred in positions e (right) and f, ⅄ = terminal glycerol in the polymer backbone, leaving the hydroxy groups e free, ⅄ = trisubstituted glycerol unit in the branched polymer backbone.

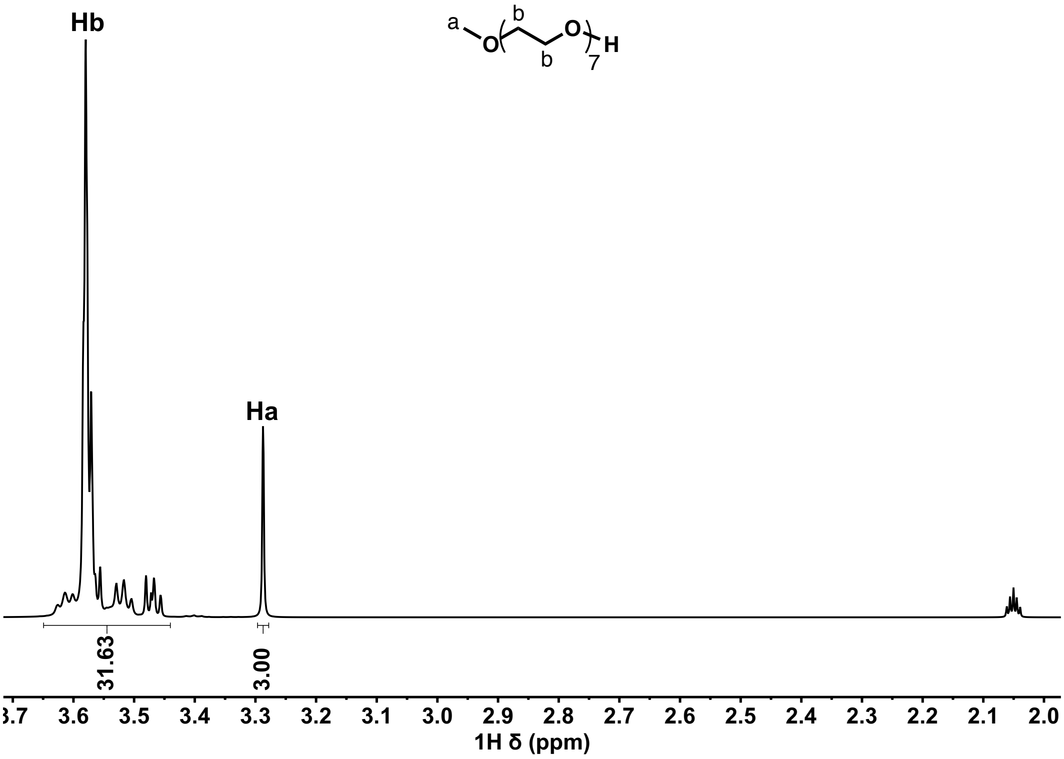

Figure A 3 – ^{1}H-NMR spectrum of M-PEG with a molecular weight of 350 Da. The solvent used was acetone-*d*$_6$.

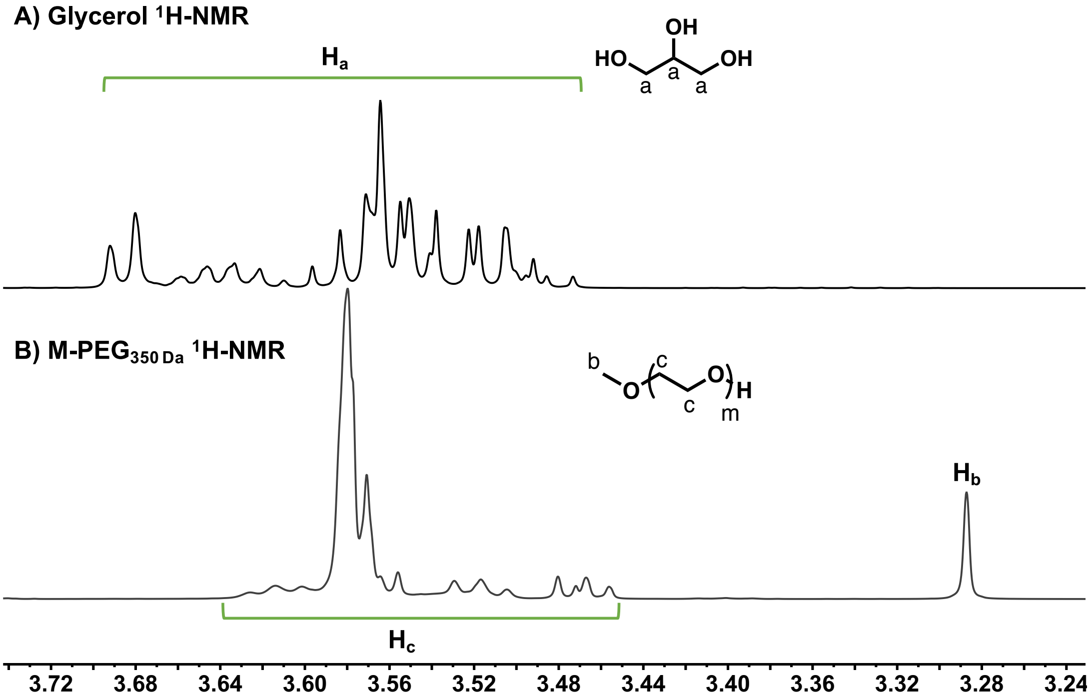

Figure A 4 – Section of the ^{1}H-NMR spectrum of M-PEG$_{350\ Da}$ and glycerol. The solvent used was acetone-*d*$_6$.

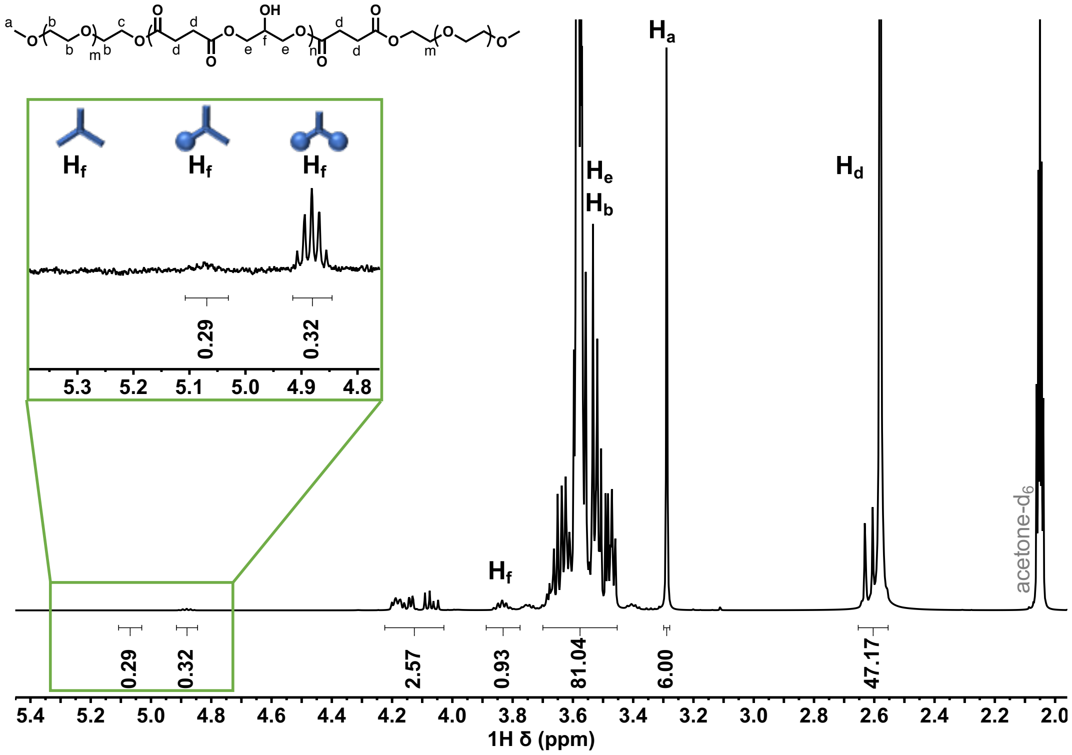

Figure A 5 – ^{1}H-NMR spectrum of PEG-PGLSA from entries 5 of Table 4.3 and Table 4.4. The solvent used was acetone-d_6. Integrals of the peaks of H$_a$ (3.29 ppm, terminal methyl group from M-PEG), and H$_e$ (3.50-3.72 ppm), H$_f$ (3.83 ppm) and H$_d$ (2.58-2.69 ppm) (backbone of PGLSA) can be used to estimate the average molecular weight of the polymer. The protons H$_b$, from the M-PEG backbone, are overlapped with the –CH$_2$– protons from the glycerol unit. *Note:* the schematic representations shown in the highlighted region (5.4-4.8 ppm) correspond to the branched, linear and terminal glycerol units as follows: ⅄ = linear glycerol unit; in this case, the polymerisation occurred in positions e, ⅄ = linear glycerol unit; in this case, the polymerisation occurred in positions e (right) and f, ⅄ = terminal glycerol in the polymer backbone, leaving the hydroxy groups e free, ⅄ = trisubstituted glycerol unit in the branched polymer backbone;

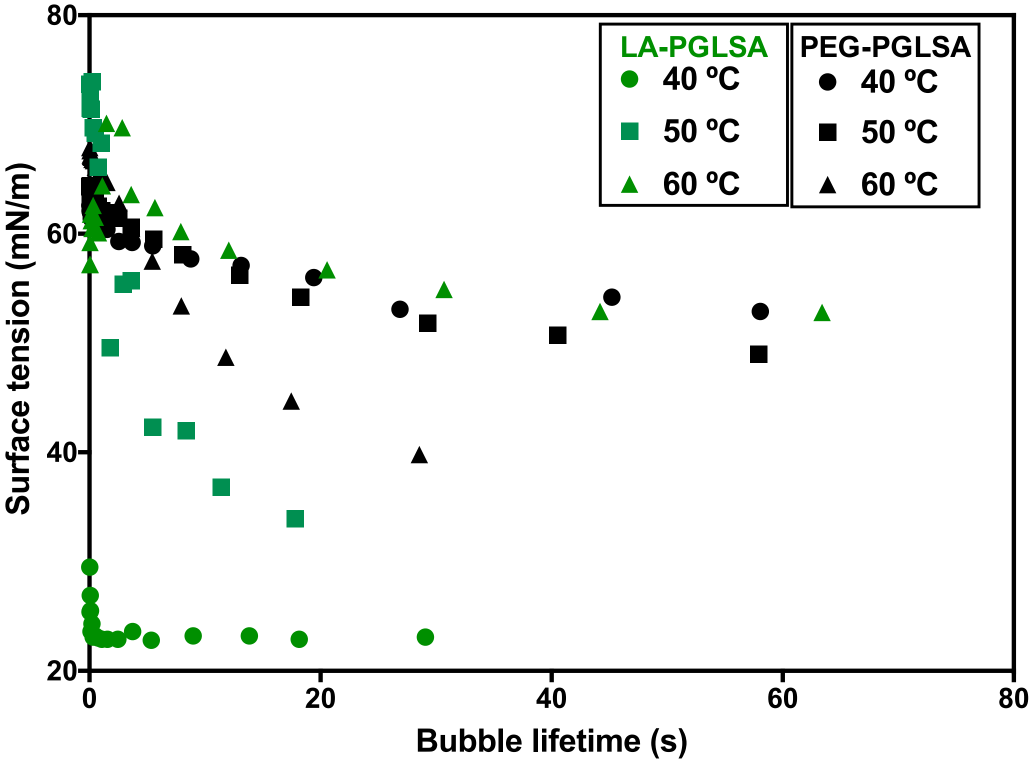

Figure A 6 – Bubble Tensiometer determination of dynamic surface tension at increasing bubble lifetimes for LA-PGLSA (0.5 wt.%) synthesised at different temperatures (40, 50 and 60 ºC, green symbols) and PEG-PGLSA (0.5 wt.%) synthesised at different temperatures (40, 50 and 60 ºC, black symbols).

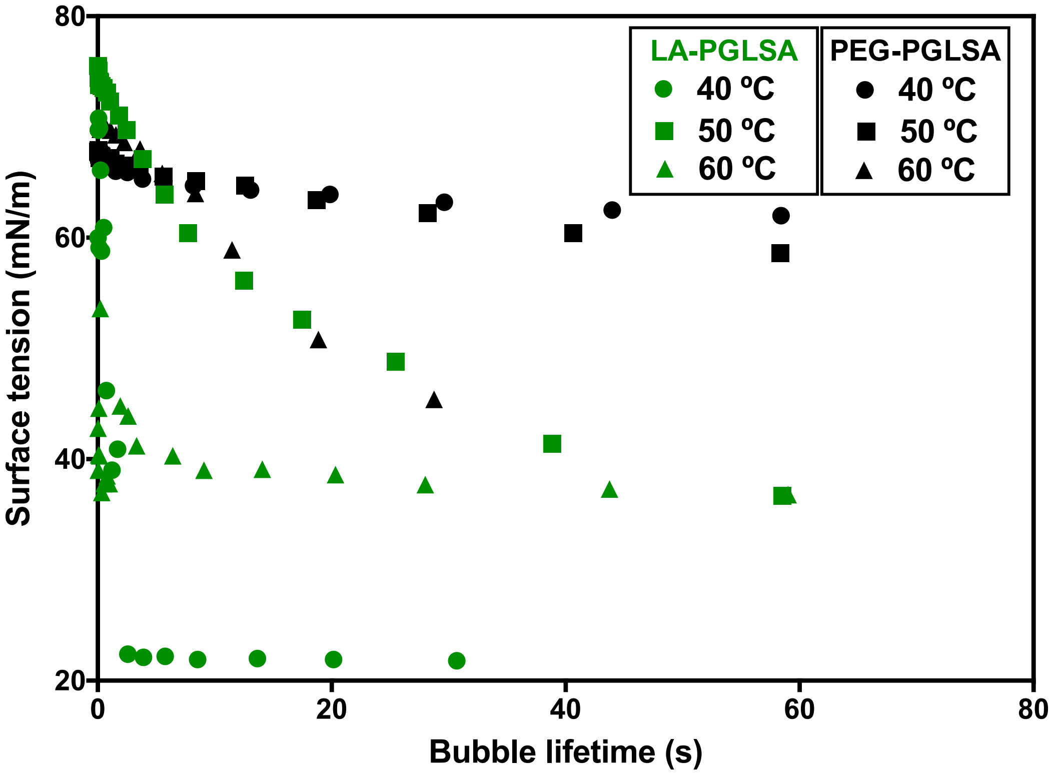

Figure A 7 – Bubble Tensiometer determination of dynamic surface tension at increasing bubble lifetimes for LA-PGLSA (0.1 wt.%) synthesised at different temperatures (40, 50 and 60 ºC, green symbols) and PEG-PGLSA (0.1 wt.%) synthesised at different temperatures (40, 50 and 60 ºC, black symbols).

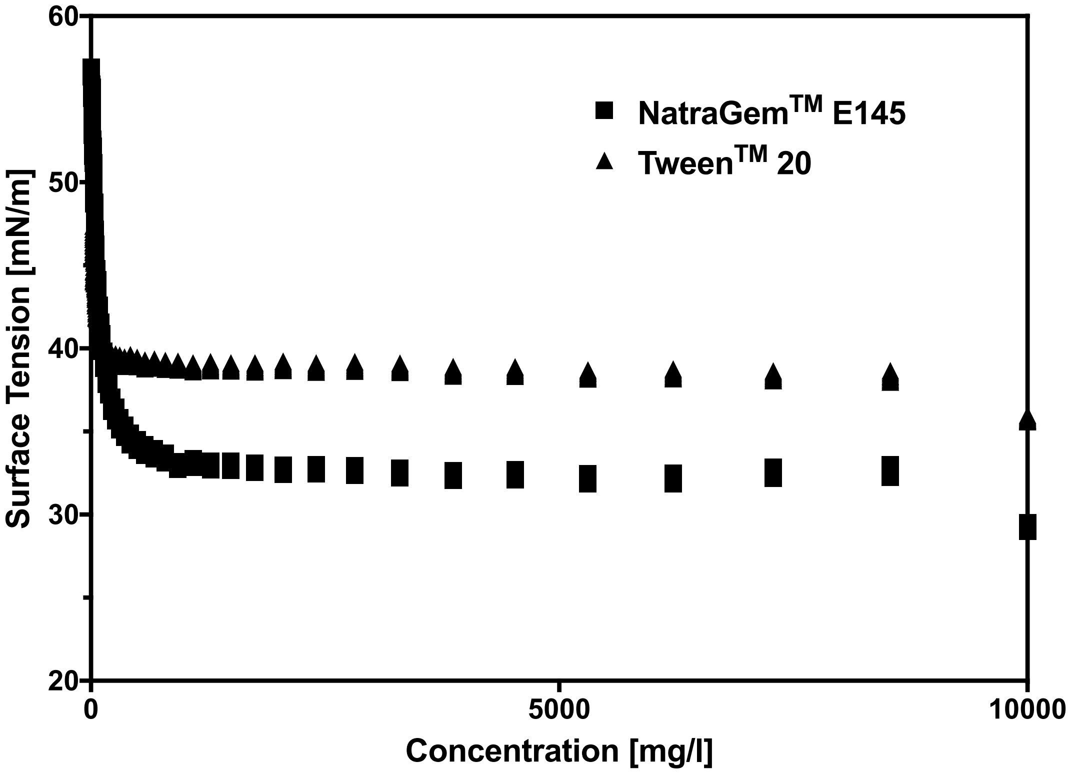

Figure A 8 – Surface tension measurements of NatraGem^{TM} E145 and Tween^{TM} 20 at several concentrations.

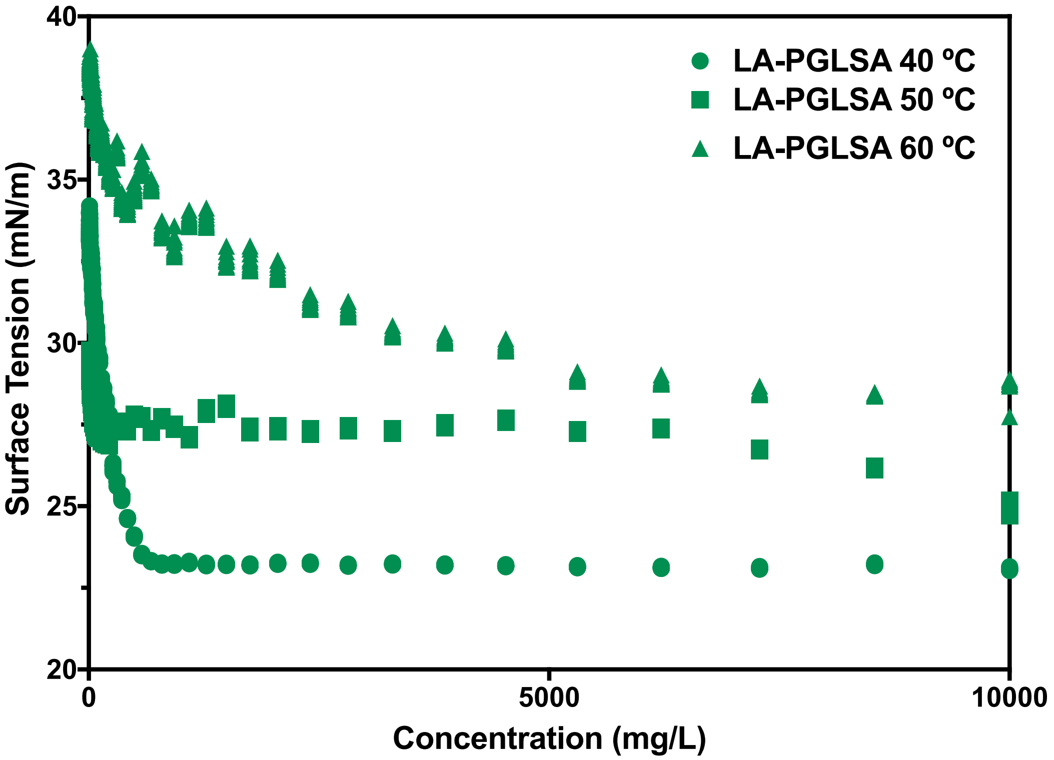

Figure A 9 – Surface tension measurements of LA-PEG synthesised at 40, 50 and 60 ºC at several concentrations.

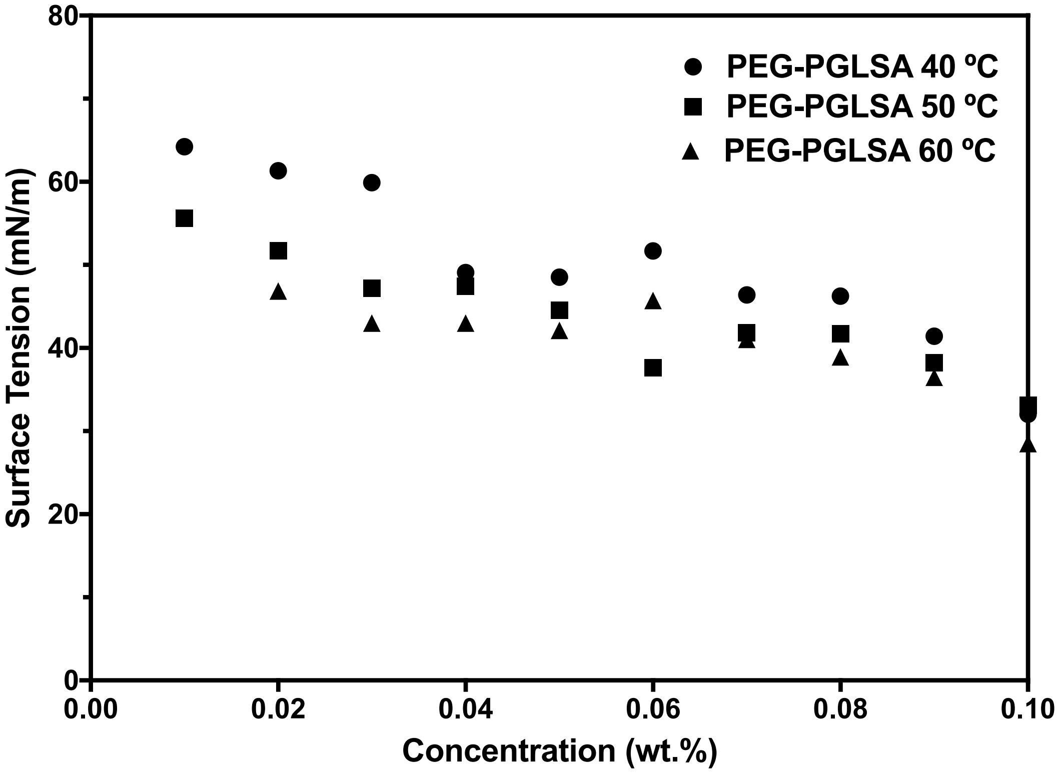

Figure A 10 – Surface tension measurements of PEG-PEG synthesised at 40, 50 and 60 ºC at several concentrations.

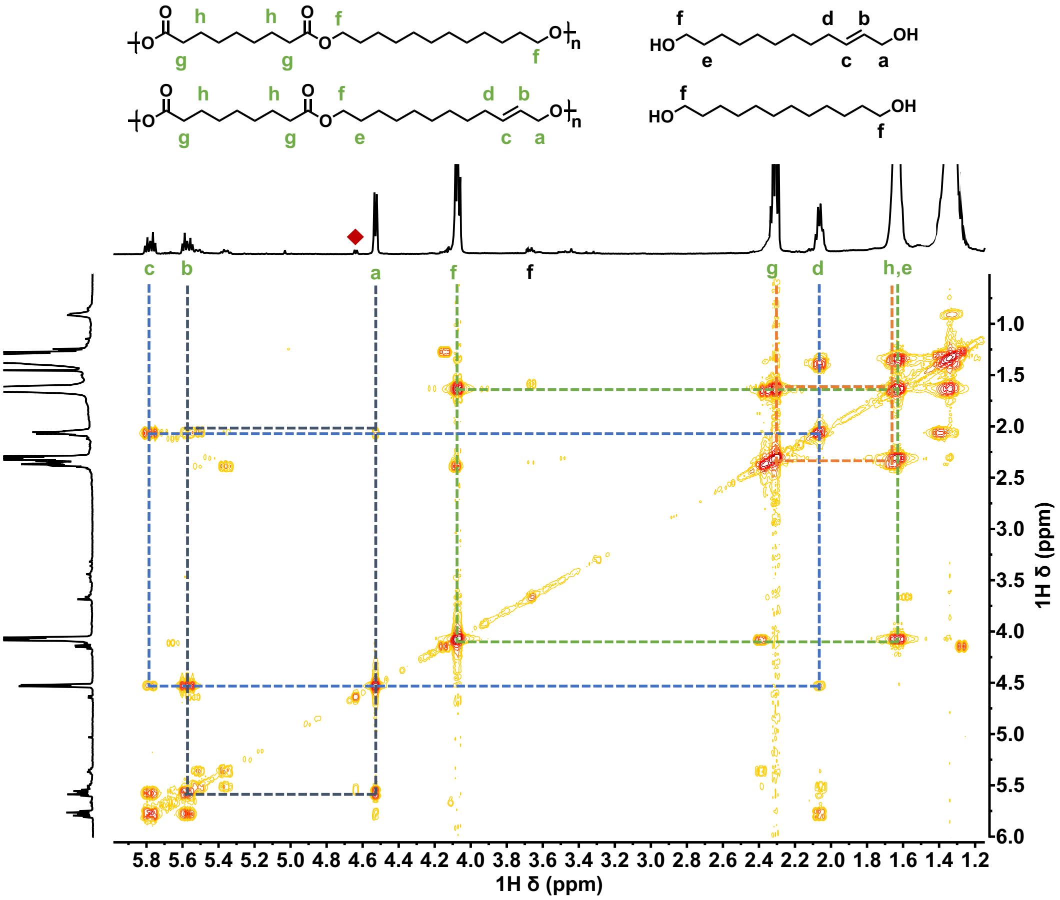

Figure A 11 – Section of the COSY-NMR spectrum of linear DED-AZ polymer (entries 21 from Table 6.13), catalysed with CaLB at 100 ºC (48h reaction time). The solvent used was chloroform-d$_1$. *Note*: ◆ it is an unknown doublet peak; the black protons letters are assigned to the monomer structures, and the green to the polymers.

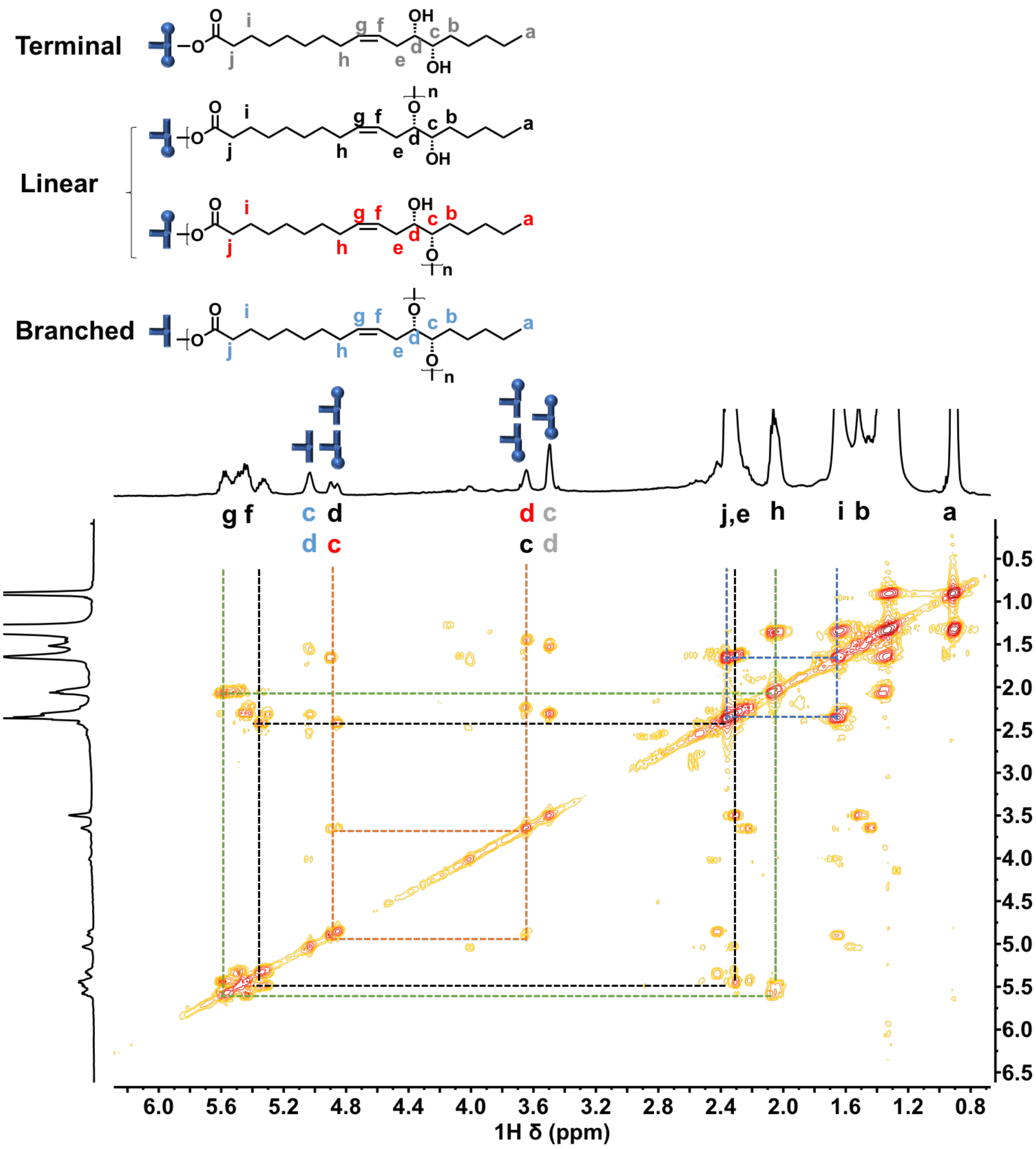

Figure A 12 – Section of the COSY-NMR spectrum showing the assignments for the DHA polymer. The solvent used was chloroform-d_1. *Note*: ┤ this symbol denotes that proton H_c and H_d is present in a branched structure; ┤ this symbol denotes for a linear structure and the polymerisation occurred in the positions H_c; ┤ this symbol denotes for a linear structure and the polymerisation occurred in the positions H_d; ┤ this symbol denotes a terminal unit of the dihydroxy acid; the blue dot represents an unreacted hydroxy group.